frontiers | Research Topics

Advancements in antibody-based immunotherapy and cancer vaccines for hepatocellular carcinoma

Edited by
Ashraf A. Tabll, Sherif El-Kafrawy and Anwaar Saeed

Published in
Frontiers in Immunology
Frontiers in Oncology

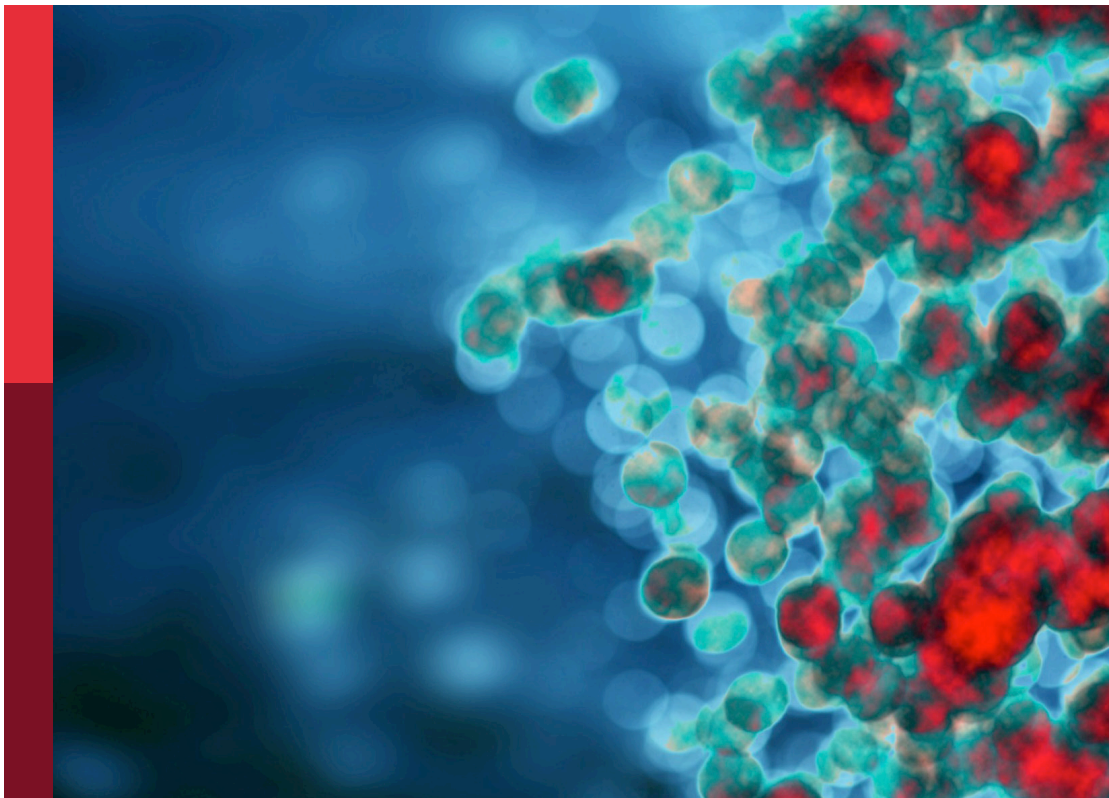

ISSN 1664-8714
ISBN 978-2-8325-7334-1
DOI 10.3389/978-2-8325-7334-1

Generative AI statement
Any alternative text (Alt text) provided alongside figures in the articles in this ebook has been generated by Frontiers with the support of artificial intelligence and reasonable efforts have been made to ensure accuracy, including review by the authors wherever possible. If you identify any issues, please contact us.

About Frontiers

Frontiers is more than just an open access publisher of scholarly articles: it is a pioneering approach to the world of academia, radically improving the way scholarly research is managed. The grand vision of Frontiers is a world where all people have an equal opportunity to seek, share and generate knowledge. Frontiers provides immediate and permanent online open access to all its publications, but this alone is not enough to realize our grand goals.

Frontiers journal series

The Frontiers journal series is a multi-tier and interdisciplinary set of open-access, online journals, promising a paradigm shift from the current review, selection and dissemination processes in academic publishing. All Frontiers journals are driven by researchers for researchers; therefore, they constitute a service to the scholarly community. At the same time, the *Frontiers journal series* operates on a revolutionary invention, the tiered publishing system, initially addressing specific communities of scholars, and gradually climbing up to broader public understanding, thus serving the interests of the lay society, too.

Dedication to quality

Each Frontiers article is a landmark of the highest quality, thanks to genuinely collaborative interactions between authors and review editors, who include some of the world's best academicians. Research must be certified by peers before entering a stream of knowledge that may eventually reach the public - and shape society; therefore, Frontiers only applies the most rigorous and unbiased reviews. Frontiers revolutionizes research publishing by freely delivering the most outstanding research, evaluated with no bias from both the academic and social point of view. By applying the most advanced information technologies, Frontiers is catapulting scholarly publishing into a new generation.

What are Frontiers Research Topics?

Frontiers Research Topics are very popular trademarks of the *Frontiers journals series*: they are collections of at least ten articles, all centered on a particular subject. With their unique mix of varied contributions from Original Research to Review Articles, Frontiers Research Topics unify the most influential researchers, the latest key findings and historical advances in a hot research area.

Find out more on how to host your own Frontiers Research Topic or contribute to one as an author by contacting the Frontiers editorial office: frontiersin.org/about/contact

Advancements in antibody-based immunotherapy and cancer vaccines for hepatocellular carcinoma

Topic editors

Ashraf A. Tabll — National Research Centre, Egypt

Sherif El-Kafrawy — King Abdulaziz University, Saudi Arabia

Anwaar Saeed — University of Pittsburgh, United States

Citation

Tabll, A. A., El-Kafrawy, S., Saeed, A., eds. (2026). *Advancements in antibody-based immunotherapy and cancer vaccines for hepatocellular carcinoma*. Lausanne: Frontiers Media SA. doi: 10.3389/978-2-8325-7334-1

Topic editor Anwaar Saeed reports a leadership role with Autem therapeutics, Exelixis, KAHR medical and Bristol-Myers Squibb; consulting or advisory board role with AstraZeneca, Bristol-Myers Squibb, Merck, Exelixis, Pfizer, Xilio therapeutics, Taiho, Amgen, Autem therapeutics, KAHR medical, and Daiichi Sankyo; institutional research funding from AstraZeneca, Bristol-Myers Squibb, Merck, Clovis, Exelixis, Actuate therapeutics, Incyte Corporation, Daiichi Sankyo, Five prime therapeutics, Amgen, Innovent biologics, Dragonfly therapeutics, Oxford Biotherapeutics, Arcus therapeutics, and KAHR medical; and participation as a data safety monitoring board chair for Arcus therapeutics. All other Topic Editors declare no competing interests with regards to the Research Topic subject.

Table of contents

frontiers | Frontiers in Immunology

TYPE Editorial
PUBLISHED 16 December 2025
DOI 10.3389/fimmu.2025.1759881

OPEN ACCESS

EDITED AND REVIEWED BY
Peter Brossart,
University of Bonn, Germany

*CORRESPONDENCE
Ashraf A. Tabll
aa.tabll@nrc.sci.eg
Sherif A. El-Kafrawy
saelkfrawy@kau.edu.sa

†These authors have contributed equally to this work

RECEIVED 03 December 2025
ACCEPTED 09 December 2025
PUBLISHED 16 December 2025

CITATION
Tabll AA, Saeed A, Elkafrawy MS and El-Kafrawy SA (2025) Editorial: Advancements in antibody-based immunotherapy and cancer vaccines for hepatocellular carcinoma. *Front. Immunol.* 16:1759881. doi: 10.3389/fimmu.2025.1759881

Editorial: Advancements in antibody-based immunotherapy and cancer vaccines for hepatocellular carcinoma

Ashraf A. Tabll[1*†], Anwaar Saeed[2], Mostafa S. Elkafrawy[3] and Sherif A. El-Kafrawy[4,5*†]

[1]Immunology Department, Egypt Center for Research and Regenerative Medicine (ECRRM), Cairo, Egypt, [2]Department of Medicine, Division of Hematology and Oncology, University of Pittsburgh Medical Center, Pittsburgh, PA, United States, [3]Faculty of Medicine, Menoufia University, Shebin El-Koam, Egypt, [4]Special Infectious Agents Unit–BioSafety Level 3 (BSL3), King Fahd Medical Research Center, King Abdulaziz University, Jeddah, Saudi Arabia, [5]Department of Medical Laboratory Sciences, Faculty of Applied Medical Sciences, King Abdulaziz University, Jeddah, Saudi Arabia

KEYWORDS

antibody-based immunotherapy, cancer vaccine, checkpoint inhibitors, hepatocellular carcinoma, priority research gaps

Editorial on the Research Topic
Advancements in antibody-based immunotherapy and cancer vaccines for hepatocellular carcinoma

Introduction

Hepatocellular carcinoma (HCC) is a highly lethal malignancy with limited benefit from traditional therapies, especially in advanced disease. This Research Topic highlights recent advances in antibody-based immunotherapy and cancer vaccine development, addressing key challenges in biomarkers, combination strategies, safety, and mechanisms of response. Together, these studies advance precision immunotherapy for HCC while underscoring ongoing obstacles posed by tumor heterogeneity, immune suppression, and therapeutic resistance.

Highlights from the Research Topic

Additional clinical case reports: safety and toxicity signals

Quiles et al. describe a rare but severe case of atezolizumab-induced vanishing bile duct syndrome (VBDS) in a 63-year-old man who developed progressive cholestatic injury after three cycles of therapy. Biopsy showed loss of intrahepatic bile ducts in over half of portal tracts, and liver function failed to recover despite immunosuppression. This case highlights the need for early recognition of atypical immune-related adverse events, particularly cholestatic or bile-duct–centered injury patterns, and the importance of biopsy when biochemical abnormalities persist or do not respond to steroids.

Zhang et al. report fatal hepatorenal failure four days after starting tislelizumab plus anlotinib in a 72-year-old patient, likely reflecting synergistic toxicity, possibly exacerbated by

concurrent infection. Together, these reports underscore the potential severity of ICI- and ICI/TKI-associated toxicity, emphasizing careful patient selection, vigilant monitoring, early histological assessment, and the urgent need for predictive biomarkers and more conservative escalation strategies in complex immunotherapy regimens.

PD-L1 expression as a prognostic biomarker

Lee et al. examined PD-L1 expression in both malignant cells and tumor-infiltrating cells among 72 HCC patients treated with atezolizumab plus bevacizumab. Using Combined Positive Score (CPS) thresholds (CPS ≥10, 1–10, <1), they demonstrated that patients with CPS ≥10 had significantly improved overall survival (median OS 14.8 vs. 8.3 months; P = 0.046) and progression-free survival (median PFS 11 months; P = 0.044). Objective response rates were also highest in the CPS ≥10 group (53.3% vs. 27.3% and 16.7%). In multivariate analysis, PD-L1 expression ≥1 and ≥10 were independently associated with favorable prognosis.

Huai et al. explored the role of TEA domain transcription factor 1 (TEAD1) in liver hepatocellular carcinoma (LIHC). Their multi-omics analysis suggested that TEAD1 may serve as both a prognostic biomarker and an immunotherapeutic target, as it influences proliferation, invasion, and tumor immunology.

Beyond single biomarker validation, understanding the full spectrum of available antibody-based therapeutic modalities is essential for contextualizing these predictive findings within the broader treatment landscape.

Antibody modalities in HCC immunotherapy

El-Kafrawy et al. contributed a thorough review of current and emerging antibody-based strategies for HCC, including monoclonal antibodies, bispecific antibodies, and antibody–drug conjugates, detailing mechanisms such as immune modulation, angiogenesis inhibition, and targeted cytotoxicity. They highlight breakthroughs like anti-PD-1/PD-L1 and CTLA-4 ICIs, along with approaches targeting glypican-3 (GPC3). The review emphasizes challenges, including tumor heterogeneity, resistance mechanisms, and immune-related adverse events, and advocates for strategic combination regimens and biomarker-driven selection to maximize therapeutic outcomes.

Translating this expanding therapeutic repertoire into evidence-based clinical practice requires systematic evaluation of comparative efficacy across treatment strategies, particularly for intermediate-stage HCC, where both locoregional and systemic approaches may be considered.

Viral reactivation and immunotherapy

Xu et al. investigated hepatitis B virus (HBV) reactivation in patients with HBV-related HCC undergoing conversion therapy, which included hepatic artery infusion chemotherapy (HAIC), transarterial chemoembolization (TACE), tyrosine kinase inhibitors (TKIs), and ICIs. Their findings demonstrated that HBV reactivation was associated with reduced progression-free survival, emphasizing the importance of prophylactic antiviral therapy and rigorous HBV DNA monitoring in this clinical setting.

Having established the importance of safety monitoring in viral hepatitis contexts, several contributions in this Research Topic demonstrate how integrating locoregional interventions with systemic immunotherapy may enhance efficacy while managing treatment-related complications.

Integration of locoregional and systemic therapies

Locoregional therapies continue to play an important role in HCC. Fang et al. systematically reviewed TACE combined with immune-targeted therapy in unresectable HCC. Their analysis showed that combination therapy offered superior local control and survival compared to ICIs alone, though at the expense of increased liver-related adverse events.

Chen et al. reported improved outcomes when TACE was combined with lenvatinib and tislelizumab in intermediate-stage HCC patients exceeding the up-to-11 criteria. Similarly, Li et al. compared PD-1 and PD-L1 inhibitors in combination with HAIC and lenvatinib, finding that PD-L1–based regimens yielded higher response rates with fewer severe adverse events.

While these clinical combination strategies demonstrate incremental benefits, breakthrough therapeutic advances may require more innovative high-order combinations that address multiple resistance mechanisms simultaneously.

High-order combinatorial approaches

Dong et al. introduced an innovative high-order combination strategy integrating oncolytic herpes simplex virus (OHSV2-DSTEFAP5/CD3), glypican-3 (GPC3)-targeted CAR-T cells, and immunotoxins in preclinical models. This approach promoted immune activation and tumor microenvironment remodeling, leading to notable tumor regression and a 40% complete response rate in experimental models. These studies provide compelling evidence for combination strategies that exploit non-overlapping resistance mechanisms to enhance efficacy.

Priority research gaps and future directions

Despite major progress, two research gaps require urgent attention. First, predictive biomarkers for immunotherapy response remain insufficient. Although candidates such as PD-L1 CPS ≥10, TEAD1, and HBV reactivation show promise, no validated markers reliably distinguish responders from patients with primary resistance driven by factors like Wnt/β-catenin signaling. Multimodal

approaches integrating molecular profiling, liquid biopsies, radiomics, and immune-microenvironment analysis are essential for true precision immunotherapy. Second, HCC therapeutic vaccines remain early in development. Major challenges include identifying tumor-specific antigens, overcoming the liver's highly immunosuppressive environment, and generating strong, durable $CD8^+$ T-cell responses in patients with cirrhosis or chronic viral infection.

Call to action

We urge clinicians to prioritize systematic biospecimen collection (tumor tissue, normal liver, serial blood, and archival samples) with standardized annotation and longitudinal follow-up to strengthen real-world evidence. Researchers should focus on three priorities: developing composite biomarker panels through multicenter collaboration; defining resistance mechanisms such as Wnt/β-catenin, metabolic rewiring, and myeloid checkpoints to guide rational combinations; and advancing therapeutic vaccine platforms using organoids and humanized models to identify HCC-specific neoantigens and optimize strategies targeting antigens such as GPC3. Progress will require global cooperation, data sharing, translationally oriented studies, and adaptive trial designs to accelerate breakthroughs toward curative immunotherapy.

Author contributions

AT: Writing – original draft, Conceptualization, Writing – review & editing. AS: Writing – original draft, Writing – review & editing. ME: Writing – original draft, Writing – review & editing. SE: Conceptualization, Writing – original draft, Writing – review & editing.

Conflict of interest

The author(s) declared that this work was conducted in the absence of any commercial or financial relationships that could be construed as a potential conflict of interest.

Generative AI statement

The author(s) declared that generative AI was not used in the creation of this manuscript.

Any alternative text (alt text) provided alongside figures in this article has been generated by Frontiers with the support of artificial intelligence and reasonable efforts have been made to ensure accuracy, including review by the authors wherever possible. If you identify any issues, please contact us.

Publisher's note

frontiers | Frontiers in Immunology

TYPE Original Research
PUBLISHED 26 July 2024
DOI 10.3389/fimmu.2024.1430571

OPEN ACCESS

EDITED BY
Hongwei Cheng,
University of Macau, China

REVIEWED BY
Hu Chen,
The First Affiliated Hospital of Xi'an Jiaotong University, China
Bin-Yan Zhong,
The First Affiliated Hospital of Soochow University, China

*CORRESPONDENCE
Wenbo Guo
guowenbo@mail.sysu.edu.cn

†These authors have contributed equally to this work

RECEIVED 10 May 2024
ACCEPTED 10 July 2024
PUBLISHED 26 July 2024

CITATION
Chen S, Shuangyan T, Shi F, Cai H, Wu Z, Wang L, Ma P, Zhou Y, Mai Q, Wang F, Lai J, Chen X, Chen H and Guo W (2024) TACE plus lenvatinib and tislelizumab for intermediate-stage hepatocellular carcinoma beyond up-to-11 criteria: a multicenter cohort study. *Front. Immunol.* 15:1430571. doi: 10.3389/fimmu.2024.1430571

TACE plus lenvatinib and tislelizumab for intermediate-stage hepatocellular carcinoma beyond up-to-11 criteria: a multicenter cohort study

Song Chen[1†], Tang Shuangyan[2†], Feng Shi[3], Hongjie Cai[2], Zhiqiang Wu[2], Liguang Wang[4], Ping Ma[5], Yuanmin Zhou[6], Qicong Mai[3], Fan Wang[2], Jiaming Lai[6], Xiaoming Chen[3], Huanwei Chen[4] and Wenbo Guo[2*]

[1]Department of Minimally Invasive Interventional Therapy, State Key Laboratory of Oncology in South China, Guangdong Provincial Clinical Research Center for Cancer, Sun Yat-sen University Cancer Center, Guangzhou, China, [2]Department of Interventional Radiology, The First Affiliated Hospital of Sun Yat-sen University, Guangzhou, China, [3]Department of Interventional Radiology, Guangdong Provincial People's Hospital, Guangzhou, China, [4]Department of Hepatopancreatic Surgery, The First People's Hospital of Foshan, Foshan, China, [5]Department of Oncology, The Twelfth People's Hospital of Guangzhou, Guangzhou, China, [6]Center of Hepato-Pancreato-Biliary Surgery, The First Affiliated Hospital of Sun Yat-sen University, Guangzhou, China

Background: Intermediate-stage (BCLC-B) hepatocellular carcinoma (HCC) beyond the up-to-11 criteria represent a significant therapeutic challenge due to high and heterogeneous tumor burden. This study evaluated the effectiveness and safety of transarterial chemoembolization (TACE) in combination with lenvatinib and tislelizumab for these patients.

Methods: In this retrospective cohort study, patients with unresectable intermediate-stage HCC beyond the up-to-11 criteria were enrolled and divided into TACE monotherapy (T), TACE combined with lenvatinib (TL), or TACE plus lenvatinib and tislelizumab (TLT) group based on the first-line treatment, respectively. The primary endpoint was overall survival (OS). The secondary outcomes included progression-free survival (PFS), tumor response according to RESIST1.1 and modified RECIST, and adverse events (AEs).

Results: There were 38, 45, and 66 patients in the T, TL, and TLT groups, respectively. The TLT group exhibited significantly higher ORR and DCR than the other two groups, as assessed by either mRECIST or RECIST 1.1 (all $P<0.05$). Median PFS and OS were significantly longer in the TLT group compared with the T group (PFS: 8.5 vs. 4.4 months; OS: 31.5 vs. 18.5 months; all $P<0.001$) and TL group (PFS: 8.5 vs. 5.5 months; OS: 31.5 vs. 20.5 months; all $P<0.05$). The incidence of TRAEs was slightly higher in the TLT and TL groups than in the T group, while all the toxicities were tolerable. No treatment-related death occurred in all groups.

Conclusions: TACE combined with lenvatinib and tislelizumab significantly improved the survival benefit compared with TACE monotherapy and TACE plus lenvatinib in patients with intermediate-stage HCC beyond the up-to-11 criteria, with an acceptable safety profile.

KEYWORDS

hepatocellular carcinoma, intermediate-stage, up-to-eleven criteria, transartrial chemoembolization, combination therapy

1 Introduction

Hepatocellular carcinoma (HCC) stands as the sixth most common malignancy and the third leading cause of cancer-related deaths worldwide (1). Ablation, liver resection, and liver transplantation are curative options for patients with HCC, but approximately 80% of the patients are diagnosed at the intermediate or advanced stage, and these curative strategies are unsuitable (2, 3). Transarterial chemoembolization (TACE) is the recommended standard of care for intermediate HCC, defined as Barcelona Clinic Liver Cancer (BCLC) stage B disease (4, 5). However, BCLC-B stage HCC is a very heterogeneous disease with a wide range of tumor burden and liver function, and not all patients can benefit from TACE (5, 6). It is worth noting that high tumor burden is an important component used by various subclassification or prediction models to select patients unsuitable for TACE (7).

In order to optimize prognosis and optimal treatment strategies, some studies have been conducted to develop a tailored subgroup stratification for BCLC-B stage HCC (8–11). For instance, Bolondi et al. (9) proposed the first subclassification for BCLC-B HCC based on the up-to-7 criteria in 2012, combining the number of tumors and the size of the largest tumor, with the sum being no more than 7. Subsequent studies have shown that the up-to-11 criteria (combining the number of tumors and the size of the largest tumor, with the sum being no more than 11) (12) may be more discriminative than the up-to-7 criteria for predicting survival after TACE. Still, the efficacy of TACE is limited in patients with high tumor burden, particularly those beyond the up-to-11 criteria (12, 13). The 7-11 criteria were also proposed, combining the number of tumors and the size of the largest tumor, with >11 being a heavy tumor burden, 7-11 an intermediate burden, and <7 a low burden (14). Moreover, there is a growing apprehension regarding the deleterious effects on hepatic function following repeated TACE procedures due to tumor progression or residual disease. Given these challenges, there is a pressing demand to explore TACE combination therapies that aim to improve therapeutic outcomes and reduce the number of TACE sessions. The theoretical synergy of TACE plus molecular targeted agents (MTAs) boasting anti-VEGF activity, such as sorafenib and lenvatinib, offers hope for improved prognosis. Regrettably, several early clinical randomized controlled trials (RCTs) comparing patient survival with combination therapy vs. TACE monotherapy have yielded negative results (15–17). None of the combination therapies are currently recommended, underscoring the great unmet need to explore novel combination strategies.

Recently, immune checkpoint inhibitors (ICIs) have shown promising efficacy and safety for advanced HCC. The phase III RATIONALE 301 trial demonstrated a clinically meaningful benefit in overall survival (OS) with tislelizumab monotherapy compared with sorafenib (18). In addition, the LEAP-002 trial examined the combination of lenvatinib plus pembrolizumab vs. lenvatinib alone in patients with unresectable HCC; although the trial did not reach a positive result, the OS and progression-free survival (PFS) were significantly longer in the combination group than in the monotherapy group (19). The CARES-310 trial showed that camrelizumab plus rivoceranib showed benefits in PFS and OS compared with sorafenib for patients with unresectable HCC (20). In addition, several RCTs confirmed the efficacy and safety of combining programmed death 1 (PD-1) or programmed death-ligand 1 (PD-L1) inhibitors with anti-VEGF antibodies or tyrosine kinase inhibitors (TKIs) in advanced HCC (21–23). As TACE is a locoregional inducer of immunogenic cell death in HCC, it can transform an immunosuppressive microenvironment into an immunostimulatory one, thereby promoting tumor-specific immune response and improving the response to ICIs (24). Besides, TACE combined with targeted therapy and immunotherapy has been gradually become a significant treatment strategy for HCC conversion (25). Nevertheless, few data are available regarding the triple combination therapy in patients with BCLC-B HCC beyond the up-to-11 criteria in clinical practice, who will have a heavier tumor burden (9, 12, 14) than the patients included in the previous RCTs that were mostly based on the up-to-7 criteria.

Therefore, this study aimed to evaluate the first-line treatment outcomes of TACE plus lenvatinib and tislelizumab in patients with BCLC-B HCC beyond the up-to-11 criteria compared with TACE monotherapy and TACE combined with lenvatinib. The results could contribute to developing effective treatment options for intermediate-stage HCC and provide a basis for future clinical trials.

2 Methods

2.1 Study design and patients

This multicenter retrospective cohort study included patients with unresectable BCLC-B HCC beyond the up-to-11 criteria. These patients underwent TACE between January 2016 and December 2022 at one of the four participating centers in China. The study was conducted in accordance with the Declaration of Helsinki (as revised in 2013). The study was approved by the ethics committee of the First Affiliated Hospital of Sun Yat-sen University (#2021-782), and individual consent for this retrospective analysis was waived. The study was reported according to the STROCSS criteria.

The inclusion criteria were 1) age between 18-75 years, 2) radiologically or pathologically diagnosed with HCC according to the practice guidelines of the American Association for the Study of Liver Diseases (26), 3) classified as BCLC-B or C stage beyond the up-to-11 criteria, with the sum of the diameter of the largest tumor (in cm) and the total number of tumors exceeding 11, 4) unresectable HCC according to the evaluation by a multidisciplinary team, 5) received TACE monotherapy, TACE plus lenvatinib, or TACE plus lenvatinib and tislelizumab as first-line treatment, 6) classified as Child-Pugh A or B before the first TACE procedure.

Patients were excluded if they had 1) other malignancies within 5 years before HCC diagnosis, 2) insufficient organ function or inadequate hematologic function, or 3) incomplete key medical data. Laboratory tests and imaging evaluations, including enhanced computed tomography (CT) and magnetic resonance imaging (MRI), were obtained within 1 week before the initial treatment.

2.2 Grouping

The patients were stratified into three distinct groups based on their first-line treatment regimen: T (TACE monotherapy), TL (TACE combined with lenvatinib), and TLT (TACE combined with lenvatinib and tislelizumab). The treatment strategy selection was determined based on the physician's recommendation, the patient's financial condition, and the accessibility of the targeted and immune drugs.

2.3 Standardized TACE procedure

The tip of the catheter was inserted into the tumor-feeding arterial branches according to tumor size, location, and vascular supply. Chemoembolization was performed utilizing an emulsion of doxorubicin and lipiodol, followed by introducing microspheres or an absorbable gelatin sponge. The embolization endpoint was classified according to the previously established subjective angiographic chemoembolization endpoint scale (SACE). Generally, the embolization endpoint corresponded to SACE levels III or IV, indicating diminished or absent antegrade arterial flow without tumor blush (27). All interventions were handled by the same physicians at each participating center with at least 10 years of experience in interventional radiology. Subsequent TACE sessions were administered as deemed necessary by the treating clinicians.

2.4 Lenvatinib treatment

Lenvatinib was initiated 3 to 5 days after the first TACE session, with dosage tailored to patient weight: 12 mg for those weighing above 60 kg and 8 mg for those below 60 kg. The dose was maintained in case of grade 1-2 adverse events (AEs), and supportive treatments were promptly introduced to manage the AEs. If grade 3-4 AEs occurred, the dose was reduced to 8 mg and 4 mg, respectively, or the frequency was reduced to once every other day until the AEs were resolved or alleviated. Persistent AEs led to dose suspension until they were alleviated or disappeared.

2.5 Tislelizumab treatment

For patients in the TLT group, tislelizumab was administered intravenously once every 3 weeks starting on the second day after TACE. Symptomatic treatment was provided to manage grade 1-2 AEs. If grade 3-4 AEs occurred, tislelizumab was suspended until they were resolved or alleviated. If grade 3-4 AEs recurred, tislelizumab was permanently discontinued. Dose adjustment for tislelizumab was not allowed.

2.6 Assessment and outcomes

A contrast-enhanced CT or MRI was performed every 4-6 weeks after TACE by two independent, experienced radiologists, and the interval was prolonged to 2-3 months if systemic maintenance therapy was given. The primary outcome was overall survival (OS). The secondary outcomes included progression-free survival (PFS), tumor response, and adverse events (AEs). Treatment response, objective response rates (ORRs), and disease control rates (DCRs) were determined according to the modified response evaluation criteria in solid tumors (mRECIST) and RECIST version 1.1. ORR was defined as the proportion of patients who achieved complete response (CR) or partial response (PR). DCR was defined as the proportion of patients who achieved CR, PR, or stable disease (SD). PFS was defined as the time from admission to disease progression (as per mRECIST) or death from any cause, whichever came first. OS was defined as the time from admission to death from any cause. Treatment-related AEs (TRAEs) were recorded and graded according to CTCAE version 5.0.

2.7 Theory/calculation

All statistical analyses were performed using R 4.0.3 (R Foundation Inc., Vienna, Austria) and SPSS 25.0 (IBM, Armon,

NY, USA). Continuous variables were expressed as means ± standard deviations or medians (interquartile range [IQR]) and compared using Student's t-test or the Mann-Whitney U-test. Categorical variables were presented as numbers and percentages and compared using the chi-squared test or Fisher's exact test. The Kaplan-Meier method was used to analyze time-to-event variables, and the differences were examined using the log-rank test. Univariable and multivariable Cox regression analyses were performed to identify the factors associated with PFS and OS. Variables with $P \leq 0.10$ in the univariable analyses were included in the multivariable analysis. Subgroup analyses of PFS and OS were performed to analyze the superiority of TLT versus TL. Two-sided $P<0.05$ was considered statistically significant.

3 Results

3.1 Baseline characteristics of patients

A total of 256 patients were assessed for eligibility, and 107 were excluded. Finally, 149 patients were included: 38 in the T group, 45 in the TL group, and 66 in the TLT group (Figure 1). As it was a multicenter study, the numbers of patients provided by each participating center were 19/10/5/4 for the T group, 21/16/3/5 for the TL group, and 34/14/12/6 for the TLT group. There were no significant differences in baseline characteristics among the three groups (all $P>0.05$) (Table 1). The patients were 56.5 ± 13.0, 56.6 ± 12.1, and 55.8 ± 11.2 years, respectively, and 138 (92.6%) were males. Among the 149 patients, 124 (83.2%) patients had hepatitis B virus infection, and 120 (80.5%) had cirrhosis. The median number of TACE sessions was six (range, four to 11), four (range, one to eight), and three (range, one to six) in the T, TL, and TLT groups, respectively.

3.2 Treatment response

According to mRECIST, the CR rates for the T, TL, and TLT groups were 0, 8.9%, and 16.7%, respectively ($P=0.024$). The ORRs were 31.6%, 53.3%, and 80.3% ($P<0.001$), and DCRs were 73.7%, 80.0%, and 93.9% ($P=0.014$) for the T, TL, and TLT groups, respectively. According to RECIST 1.1, the ORRs were 13.2%, 28.9%, and 45.5% ($P=0.003$), and DCRs were 65.8%, 80.0%, and 92.5% ($P=0.003$) in the T, TL, and TLT groups, respectively (Table 2).

3.3 Survival outcomes and associated factors

As of the last follow-up on December 31, 2023, the median follow-up for all patients was 29.8 (range, 12.0-49.4) months. PFS was significantly longer in the TLT group (median, 8.5 [95% CI, 5.7-12.1] months) compared with the T (median, 4.4 [95% CI, 3.6-5.9] months; $P<0.001$) and TL (median, 5.5 [95% CI, 4.7-8.3] months; $P=0.009$) groups (Figure 2A; Supplementary Figures 1A-C). By the end of the follow-up, 112 deaths occurred: 38 in the T group, 44 in the TL group, and 30 in the TLT group. The TLT group showed a significantly longer OS (median, 31.5 [95% CI, 27.8-NA] months) compared with the T (median, 18.5 [95% CI, 10.6-23.0] months; $P<0.001$) and TL (median, 20.5 [95% CI, 15.7-30.2] months; $P=0.013$) groups (Figure 2B; Supplementary Figures 1D-F).

After adjusting for the baseline patient characteristics, multivariable Cox regression analyses revealed that the treatment regimen was independently associated with PFS and OS. Specifically, for PFS, the adjusted hazard ratios (HRs) were 0.60 (95% CI, 0.37-0.96; $P=0.034$) for the TL group and 0.35 (95% CI,

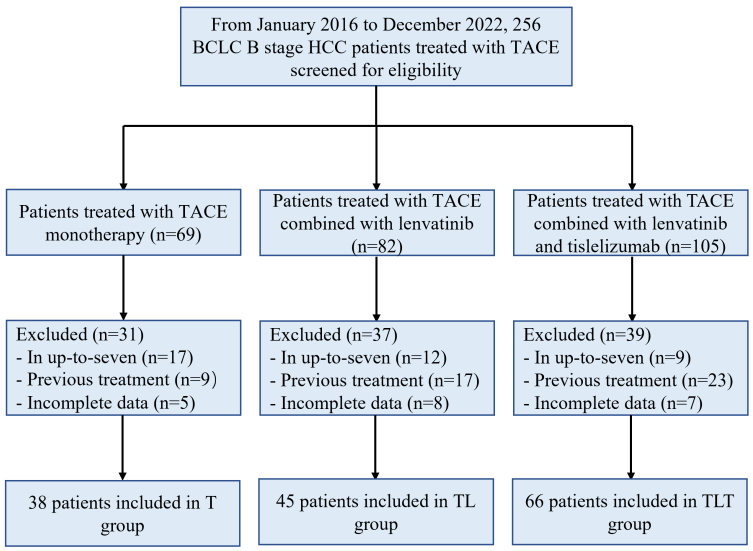

FIGURE 1
Study flowchart. T, TACE, transarterial chemoembolization; TL, TACE combined with lenvatinib; TLT, TACE combined with lenvatinib and tislelizumab; BCLC, Barcelona Clinic Liver Cancer.

TABLE 1 Baseline characteristics of the patients.

Characteristics	T (n=38)	TL (n=45)	TLT (n=66)	*P*
Age (years)	56.5 ± 13.0	56.6 ± 12.1	55.8 ± 11.2	0.940
Sex				0.974
Male	35 (92.1)	42 (93.3)	61 (92.4)	
Female	3 (7.9)	3 (6.7)	5 (7.6)	
Etiology				0.474
Hepatitis B virus	34 (89.5)	36 (80.0)	54 (81.8)	
Others	4 (10.5)	9 (20.0)	12 (18.2)	
Child-Pugh class				0.716
A	32 (84.2)	40 (88.9)	59 (89.4)	
B	6 (15.8)	5 (11.1)	7 (10.6)	
Cirrhosis				0.982
Yes	31 (81.6)	36 (80.0)	53 (80.3)	
No	7 (18.4)	9 (20.0)	13 (19.7)	
Tumor size (cm)	5.9 (4.9-8.1)	5.8 (3.1-8.0)	6.0 (3.9-8.4)	0.613
>7	23 (60.5)	27 (60.0)	41 (62.1)	0.972
≤7	15 (39.5)	18 (40.0)	25 (37.9)	
Number of lesions				0.967
>3	34 (89.5)	40 (88.9)	58 (87.9)	
2-3	4 (10.5)	5 (11.1)	8 (12.1)	
AFP (ng/mL)				0.257
<400	22 (57.9)	28 (62.2)	48 (72.7)	
≥400	16 (42.1)	17 (37.8)	18 (27.3)	
Sessions of TACE	6 (4-11)	4 (1-8)	3 (1-6)	0.059

T, TACE, transarterial chemoembolization; TL, TACE combined with lenvatinib; TLT, TACE combined with lenvatinib and tislelizumab; AFP, α-fetoprotein.

0.22-0.56; *P*<0.001) for the TLT group vs. TACE monotherapy. For OS, the HRs were 0.64 (95% CI, 0.41-1.00, *P*=0.051) for the TL group and 0.37 (95% CI, 0.23-0.60; *P*<0.001) for the TLT vs. TACE monotherapy (Supplementary Table 1). Subgroup analyses highlighted that the TLT group consistently demonstrated superior PFS and OS compared with the TL group in most subgroups defined by baseline patient characteristics, except for the Child-Pugh B subgroup (Figure 3).

TABLE 2 Tumor response rates according to mRECIST and RECIST 1.1.

Response, n (%)	T	TL	TLT	*P*	T	TL	TLT	*P*
	mRECIST				RECIST 1.1			
CR	0 (0)	4 (8.9)	11 (16.7)	0.024	0 (0)	0 (0)	0 (0)	
PR	12 (31.6)	20 (44.4)	42 (63.6)		5 (13.2)	13 (28.9)	30 (45.5)	
SD	16 (42.1)	12 (26.7)	9 (13.6)		20 (52.6)	23 (51.1)	31 (47.0)	
PD	10 (26.3)	9 (20.0)	4 (6.1)		13 (34.2)	9 (20.0)	5 (7.5)	
ORR	12 (31.6)	24 (53.3)	53 (80.3)	<0.001	5 (13.2)	13 (28.9)	30 (45.5)	0.003
DCR	28 (73.7)	36 (80.0)	62 (93.9)	0.014	25 (65.8)	36 (80.0)	61 (92.5)	0.003

mRECIST, modified Response Evaluation Criteria in Solid Tumors; RECIST 1.1, Response Evaluation Criteria in Solid Tumors 1.1; T, TACE, transarterial chemoembolization; TL, TACE combined with lenvatinib; TLT, TACE combined with lenvatinib and tislelizumab; CR, complete response; PR, partial response; SD, stable disease; PD, progressive disease; ORR, objective response rate; DCR, disease control rate; CI, confidence interval.

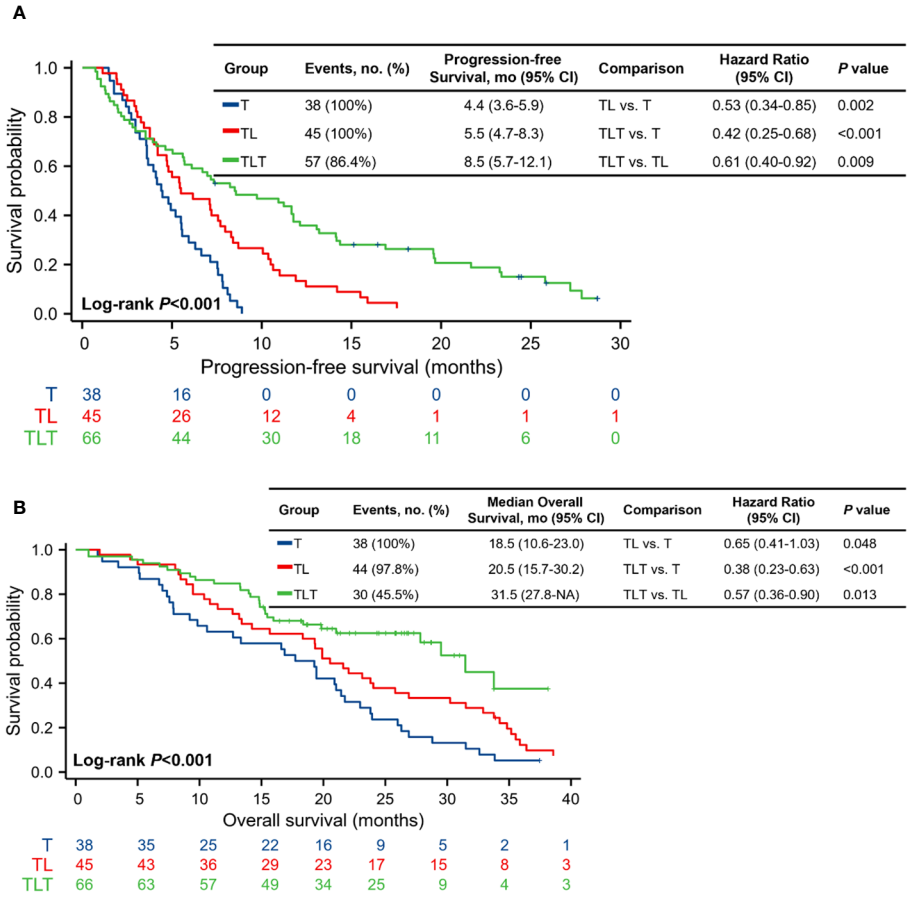

FIGURE 2
Kaplan-Meier analysis of progression-free survival. **(A)** and overall survival **(B)**. CI, confidence interval; T, TACE, transarterial chemoembolization; TL, TACE combined with lenvatinib; TLT, TACE combined with lenvatinib and tislelizumab.

3.4 Progression pattern and subsequent treatments

There were no statistically significant differences in the patterns of disease progression, including local lesion progression, intrahepatic metastasis, extrahepatic metastasis, or death, among the three groups (P=0.055). The T group had numerically higher proportions of local lesion progression (36.8% vs. 24.4% vs. 21.1%) and intrahepatic metastasis (42.1% vs. 31.1% vs. 22.8%) compared with the TL and TLT groups. The TLT group had the lowest local lesion progression and intrahepatic metastasis proportions among the three groups (Supplementary Table 2).

After tumor progression, most patients received subsequent antitumor treatment: 80.0% from the T group, 78.4% from the TL group, and 83.7% from the TLT group. A combination of TACE with TKIs was the most frequent subsequent treatment in the T group, accounting for 39.4%. In addition, the proportion of TACE combined with MTAs and ICIs was 14.3%, and no patients chose hepatic artery infusion chemotherapy (HAIC) combined with MTAs and ICIs or TACE combined with HAIC and MTAs and ICIs. The patients in the TL group predominantly favored a regimen of TACE in combination with MTAs and ICIs at 27.6%, and 20.7% opted for TACE plus HAIC in combination with MTAs and ICIs. Meanwhile, the patients in the TLT group mostly opted for TACE plus HAIC in combination with MTAs and ICIs and HAIC in combination with MTAs and ICIs, representing 27.8% and 22.2%, respectively (Supplementary Table 3).

3.5 TRAEs

The TRAEs were primarily related to the TACE procedure and are listed in Table 3. The most common TRAEs were aminotransferase increased, abdominal pain, fever, and nausea; most were moderate in severity. The incidence of grade 3 or 4 TRAEs was higher in the TLT and TL groups compared with the T group. AEs resulting in dose reduction or interruption of lenvatinib or tislelizumab were observed in eight (17.8%) patients in the TL group and 11 (16.7%) patients in the TLT group. These AEs were manageable, and no AEs leading to permanent treatment discontinuation or treatment-related death were reported during the study period at the four participating centers.

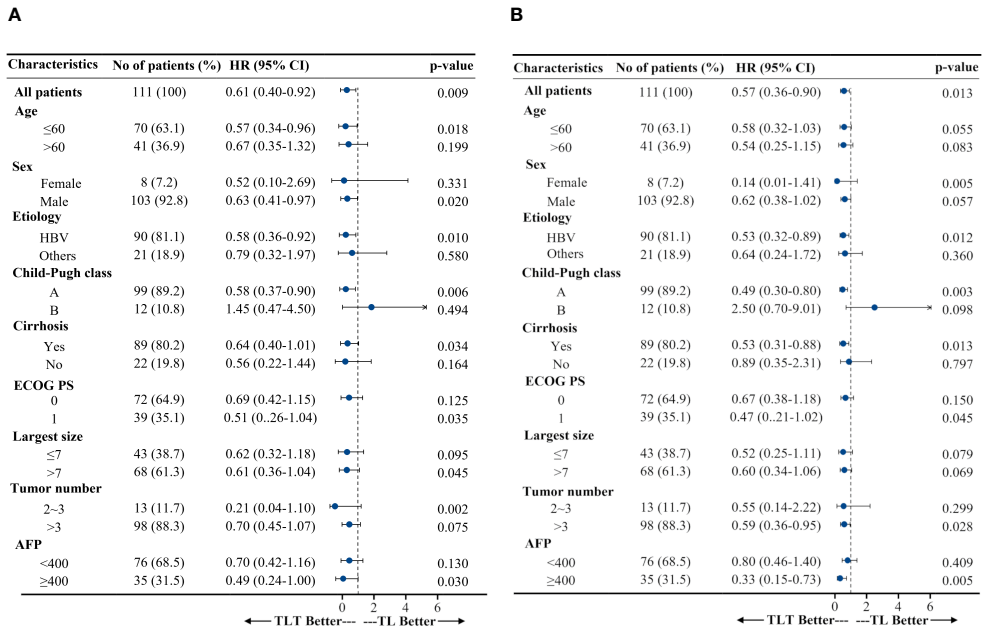

FIGURE 3
Subgroup analyses of progression-free survival **(A)** and overall survival **(B)**. HR, hazard ratio; CI, confidence interval; ECOG PS, Eastern Cooperative Oncology Group performance status; T, TACE, transarterial chemoembolization; TL, TACE combined with lenvatinib; TLT, TACE combined with lenvatinib and tislelizumab; AFP, α-fetoprotein.

4 Discussion

The present study was the first to evaluate the effectiveness and safety of TACE plus TKIs and PD-1 inhibitors for BCLC-B HCC beyond the up-to-11 criteria, compared with TACE plus TKIs and TACE monotherapy. The present study displays several innovative points, such as the high tumor burden (i.e., beyond the up-to-11 criteria), the inclusion of patients with intermediate-stage HCC (which display high heterogeneity), comparison among three treatments, all three treatments are first-line standard regimens for HCC. Significant ORR, PFS, and OS improvements were observed with TACE plus lenvatinib and tislelizumab. Subgroup analyses further echoed these findings, consistently indicating superior survival outcomes across the subgroups, all converging in favor of

TABLE 3 Treatment-related adverse events.

Event, n (%)	Any grade			*P*	Grade 3/4			*P*
	T (n=38)	TL (n=45)	TLT (n=66)		T (n=38)	TL (n=45)	TLT (n=66)	
Abdominal pain	15 (39.5)	21 (46.7)	30 (45.5)	0.812	2 (5.3)	4 (8.9)	5 (7.6)	0.363
Nausea	11 (28.9)	18 (40.0)	24 (36.4)	0.789	1 (2.6)	2 (4.4)	2 (3.0)	0.286
Diarrhea	5 (13.2)	17 (37.8)	29 (43.9)	0.339	0 (0)	5 (11.1)	8 (12.1)	–
Fever	15 (39.5)	18 (40.0)	28 (42.4)	0.636	0 (0)	1 (2.2)	2 (3.0)	–
Aminotransferase increased	30 (78.9)	38 (84.4)	55 (83.3)	0.685	5 (13.2)	15 (33.3)	21 (31.8)	0.809
Hypothyroidism	0 (0)	8 (17.8)	17 (25.8)	–	0 (0)	2 (4.4)	3 (4.5)	–
Platelet count decreased	3 (7.9)	11 (24.4)	19 (28.8)	0.809	0 (0)	3 (6.7)	5 (7.6)	–
Hypertension	0 (0)	6 (18.8)	8 (37.5)	–	0 (0)	0 (0)	0 (0)	–
Hand-foot syndrome	0 (0)	11 (24.4)	18 (27.3)	–	0 (0)	3 (6.7)	4 (6.1)	–
Proteinuria	0 (0)	9 (20.0)	13 (19.7)	–	0 (0)	3 (6.7)	3 (4.5)	–
Bleeding (gingiva)	0 (0)	4 (8.9)	6 (9.1)	–	0 (0)	1 (2.2)	1 (1.5)	–
Immune-related AEs	NA	NA	17 (25.8)	–	NA	NA	3 (4.5)	–

T, TACE, transarterial chemoembolization; TL, TACE combined with lenvatinib; TLT, TACE combined with lenvatinib and tislelizumab; NA, not applicable.

the triple combination therapy. Although the TLT group reported a slightly higher incidence of TRAEs than the T and TL groups, most of these events were mild-to-moderate and manageable.

For patients with intermediate-stage HCC, complete ORR and PFS data are lacking in the published literature for the subgroup of patients with HCC beyond the up-to-11 criteria. A recent retrospective study showed that the CR rate was 38.7% in patients with intermediate-stage HCC beyond up-to-11 criteria (28). Previous research reported that in patients with BCLC-B HCC beyond the up-to-7 criteria, TACE monotherapy induced an ORR of 33.3% and a median PFS of 3.0 months (29). These findings align well with the outcomes of the present study, where the T group showed an ORR of 31.6% and a median PFS of 4.4 months. The results strongly suggest that not all patients benefit from TACE; such patients are defined as "TACE-refractory" and "TACE-unsuitable" (30). New treatment strategies, such as early initiation of systemic therapies, have been recommended in such patients (31). In the present study, the survival benefit of the TL group was better than that of the T group (TL vs. T, median OS: 20.5 vs. 18.5 months; median PFS: 5.5 vs. 4.4 months). Beyond the up-to-11 criteria (HR=1.694, P<001) was reported to be an independent predictor of OS in BCLC-B HCC (13). In addition, a previous study showed that the median OS of TACE monotherapy was 11.3 months in patients with BCLC-B with HCC beyond the up-to-11 criteria (12). Studies by Kudo et al. (29) and Tada et al. (32) also revealed that in patients with unresectable BCLC-B HCC beyond the up-to-7 criteria, those who initially received lenvatinib had superior prognosis to those administered TACE monotherapy. It suggests that TACE in combination with lenvatinib may have a more pronounced beneficial effect than TACE monotherapy, particularly in patients bearing a high tumor burden.

Despite the potential of TACE in combination with lenvatinib, the prognosis of patients with unresectable BCLC-B HCC beyond the up-to-11 criteria may remain suboptimal due to high tumor burden. A previous investigation by the authors in patients with unresectable HCC highlighted the synergistic benefits of combining TACE with lenvatinib and pembrolizumab, leading to significant improvements in OS (median, 18.1 vs. 14.1 months) and PFS (median, 9.2 vs. 5.5 months) compared with TACE plus lenvatinib (33). The CHANCE001 trial reported the superior prognosis of TACE combined with PD-(L) 1 inhibitors and MTAs over TACE monotherapy (median OS: 19.2 vs. 15.7 months; median PFS: 9.5 vs. 8.0 months) in a cohort of patients (predominantly Chinese) with advanced HCC (34). The EMERALD-1 trial (BCLC-A, -B, and -C stages) showed that TACE combined with durvalumab and bevacizumab improved PFS compared with TACE in patients with unresectable HCC (15.0 vs. 8.2 months, P=0.032) (35). Previous trials also supported the use of tislelizumab in advanced HCC (18) and the use of lenvatinib in such patients (36, 37). The LEAP-002 trial supports the combination of lenvatinib plus pembrolizumab vs. lenvatinib alone (PFS of 8.2 vs. 8.0 months) (19), while the CARES-310 trial supports the use of an ICI with a TKI in advanced HCC (PFS of 5.6 months vs. 3.7 months with sorafenib) (20). Furthermore, recent retrospective analyses underscored the survival benefits of a TACE-lenvatinib-PD-(L)1 inhibitor regimen vs. the TACE-lenvatinib combination in patients with advanced or unresectable HCC (38, 39). Regarding the mechanism by which lenvatinib enhances the efficacy of immunotherapy, many basic studies have already explored and elucidated. Chen, et al. reported that lenvatinib inhibited the FGFR4 signaling pathway, downregulated the expression of PD-L1 on tumor cells, and limited the differentiation of Tregs, thereby modulating the tumor immune microenvironment to enhance the efficacy of PD-1 (40). Deng, et al. reported that both of vascular endothelial growth factor (VEGF) and fibroblast growth factor (FGF) increased in tumor and suppressed the immune microenvironment, lenvatinib can reduce the level of these two cytokines to improve the efficacy of PD-1 (41). Besides, as reported, TACE also has the function of remodeling the tumor immune microenvironment to improve the efficacy of PD-1 (42, 43). In total, TACE administrated in combination with systemic therapy-based treatment offers a new paradigm for unresectable HCC, including intermediate stage beyond up-to-11 criteria (44, 45). Notably, the present study suggested a numerically longer median OS with the triple combination therapy (31.5 months) compared with previous studies. This discrepancy can be attributed mainly to the patient pool; while earlier studies predominantly encompassed BCLC-C HCC patients, the present study targeted those in the BCLC-B stage. Moreover, the median PFS remained relatively consistent across different studies exploring the triple combination therapy, suggesting a more pronounced enhancement in OS than PFS across different HCC stages.

The advantages of combining TACE with lenvatinib and tislelizumab remained broadly consistent across a variety of clinical subgroups compared with the TACE-lenvatinib combination, including the subgroups relevant to HCC prognosis, such as age, sex, etiology, baseline tumor burden, and α-fetoprotein (AFP) levels. In addition, for BCLC-B HCC patients with Child-Pugh A, TACE with lenvatinib and tislelizumab resulted in better PFS and OS than TACE with lenvatinib. As is well known, the magnitude of tumor burden may be quite heterogeneous in the BCLC-B stage. The prognosis is also influenced by AFP concentration and the degree of liver function impairment, even if it still belongs to Child-Pugh class A (4, 46, 47). Elevated AFP values predict a higher risk of HCC recurrence and, thus, lower survival (4). Repeated TACE interventions may compromise liver function, consequently influencing patient survival (48). Of interest, the present study also found that for patients with AFP ≥400, TACE with lenvatinib and tislelizumab resulted in better PFS and OS than TACE-lenvatinib, and TACE with lenvatinib and tislelizumab was superior in PFS to TACE-lenvatinib for patients with tumors >7 cm in diameter. In addition, the combination therapy could reduce the number of TACE sessions in this study (six, four, and three in the T, TL, and TLT groups, respectively), probably contributing to better liver function reserve. It suggests a promising efficacy advantage for TACE with lenvatinib and tislelizumab. Further prospective studies are needed to confirm these findings.

Local lesion progression and intrahepatic metastasis can limit the survival benefit conferred by TACE (49). In the present study, the proportions of local lesion progression and intrahepatic metastasis were the highest in the T group and the lowest in the TLT group. After progression, over 75% of patients in each group received subsequent antitumor treatment. TACE or/and HAIC plus

MTAs and ICIs were administered to 66.7% of patients in the TLT group, compared with 55.2% in the TL group and 14.3% in the T group. PFS (8.5 vs. 5.5 vs. 4.4 months) and OS (31.5 vs. 20.5 vs. 18.5 months) were significantly longer in the TLT group compared with the TL group and T group. These results suggest that combining TACE with lenvatinib and tislelizumab could effectively control local disease progression and improve the survival benefit. It can be speculated that local therapies induce antigen and proinflammatory cytokine release, whereas VEGF inhibitors and tyrosine kinase inhibitors boost immunity and prime tumors for checkpoint inhibition (50). Hence, combining TACE with lenvatinib and tislelizumab could provide a synergistic antitumor effect.

Regarding safety, the TLT group exhibited a higher incidence of overall and grade 3-4 TRAEs, particularly immune-related AEs. This trend aligns with prior expectations, as previous clinical trials examining the combination of immunotherapy and targeted therapy have reported elevated incidences of grade ≥3 AEs, i.e., 61.6% in IMbrave 150 and 56% in ORIENT-32 (21, 51). In addition, the incidence of aminotransferase elevations in grade 3-4 TRAEs was higher in the TL group than in the TLT and T groups (33.3% vs. 31.8% vs. 13.2%), which is similar to the safety finding in the LAUNCH trial (52). Most AEs were mild-to-moderate in severity and either readily manageable or reversible in this study without affecting subsequent treatments.

Although favorable therapeutic responses and survival were observed in the present cohort, this study had limitations. First, the retrospective study nature may have induced biases. Second, although both lenvatinib monotherapy and tislelizumab monotherapy are recommended in guidelines for treating HCC, their combination remains outside standard recommendations and needs further investigation. Third, the sample size was relatively small, and the follow-up period was relatively short. Hence, future large-scale prospective studies are warranted to verify these findings.

Compared with TACE monotherapy and TACE plus lenvatinib, the combination of TACE, lenvatinib, and tislelizumab showed significantly improved ORR, PFS, and OS in patients with BCLC-B HCC beyond the up-to-11 criteria with an acceptable safety profile. Therefore, this triple combination therapy could be a potential superior treatment option for these patients. RCTs should be performed to confirm the results.

Data availability statement

The original contributions presented in the study are included in the article/Supplementary Material. Further inquiries can be directed to the corresponding author.

Ethics statement

The studies involving humans were approved by ethics committee of the First Affiliated Hospital of Sun Yat-sen University (#2021-782). The studies were conducted in accordance with the local legislation and institutional requirements. The participants provided their written informed consent to participate in this study.

Author contributions

SC: Conceptualization, Data curation, Formal Analysis, Methodology, Writing – original draft, Writing – review & editing. TS: Data curation, Formal Analysis, Writing – original draft, Writing – review & editing. FS: Data curation, Formal Analysis, Writing – original draft, Writing – review & editing. HJC: Data curation, Formal Analysis, Writing – original draft, Writing – review & editing. ZW: Data curation, Formal Analysis, Writing – original draft, Writing – review & editing. LW: Data curation, Formal Analysis, Writing – original draft, Writing – review & editing. PM: Data curation, Formal Analysis, Writing – original draft, Writing – review & editing. YZ: Conceptualization, Data curation, Formal Analysis, Methodology, Writing – original draft, Writing – review & editing. QM: Data curation, Formal Analysis, Writing – original draft, Writing – review & editing. FW: Data curation, Formal Analysis, Writing – original draft, Writing – review & editing. JL: Data curation, Formal Analysis, Writing – original draft, Writing – review & editing. XC: Conceptualization, Data curation, Formal Analysis, Methodology, Writing – original draft, Writing – review & editing. HWC: Conceptualization, Data curation, Formal Analysis, Methodology, Writing – original draft, Writing – review & editing. WG: Conceptualization, Data curation, Formal Analysis, Methodology, Writing – original draft, Writing – review & editing.

Funding

The author(s) declare financial support was received for the research, authorship, and/or publication of this article. The study was supported by grants from the National Natural Science Foundation of China (no. 82202271), Guangzhou Basic and Applied Basic Research Foundation (no. 202201011304).

Conflict of interest

The authors declare that the research was conducted in the absence of any commercial or financial relationships that could be construed as a potential conflict of interest.

Publisher's note

Supplementary material

The Supplementary Material for this article can be found online at: https://www.frontiersin.org/articles/10.3389/fimmu.2024.1430571/full#supplementary-material

References

1. Sung H, Ferlay J, Siegel RL, Laversanne M, Soerjomataram I, Jemal A, et al. Global cancer statistics 2020: GLOBOCAN estimates of incidence and mortality worldwide for 36 cancers in 185 countries. *CA Cancer J Clin*. (2021) 71:209–49. doi: 10.3322/caac.21660

2. Forner A, Reig M, Bruix J. Hepatocellular carcinoma. *Lancet*. (2018) 391:1301–14. doi: 10.1016/S0140-6736(18)30010-2

3. Llovet JM, Kelley RK, Villanueva A, Singal AG, Pikarsky E, Roayaie S, et al. Hepatocellular carcinoma. *Nat Rev Dis Primers*. (2021) 7:6. doi: 10.1038/s41572-020-00240-3

4. Reig M, Forner A, Rimola J, Ferrer-Fabrega J, Burrel M, Garcia-Criado A, et al. BCLC strategy for prognosis prediction and treatment recommendation: The 2022 update. *J Hepatol*. (2022) 76:681–93. doi: 10.1016/j.jhep.2021.11.018

5. Lu J, Zhao M, Arai Y, Zhong BY, Zhu HD, Qi XL, et al. Clinical practice of transarterial chemoembolization for hepatocellular carcinoma: consensus statement from an international expert panel of International Society of Multidisciplinary Interventional Oncology (ISMIO). *Hepatobil Surg Nutr*. (2021) 10:661–71. doi: 10.21037/hbsn

6. Piscaglia F, Ogasawara S. Patient selection for transarterial chemoembolization in hepatocellular carcinoma: importance of benefit/risk assessment. *Liver Cancer*. (2018) 7:104–19. doi: 10.1159/000485471

7. Koroki K, Ogasawara S, Ooka Y, Kanzaki H, Kanayama K, Maruta S, et al. Analyses of intermediate-stage hepatocellular carcinoma patients receiving transarterial chemoembolization prior to designing clinical trials. *Liver Cancer*. (2020) 9:596–612. doi: 10.1159/000508809

8. Yamakado K, Miyayama S, Hirota S, Mizunuma K, Nakamura K, Inaba Y, et al. Subgrouping of intermediate-stage (BCLC stage B) hepatocellular carcinoma based on tumor number and size and Child-Pugh grade correlated with prognosis after transarterial chemoembolization. *Jpn J Radiol*. (2014) 32:260–5. doi: 10.1007/s11604-014-0298-9

9. Bolondi L, Burroughs A, Dufour JF, Galle PR, Mazzaferro V, Piscaglia F, et al. Heterogeneity of patients with intermediate (BCLC B) Hepatocellular Carcinoma: proposal for a subclassification to facilitate treatment decisions. *Semin Liver Dis*. (2012) 32:348–59. doi: 10.1055/s-0032-1329906

10. Arizumi T, Ueshima K, Iwanishi M, Minami T, Chishina H, Kono M, et al. Validation of a modified substaging system (Kinki criteria) for patients with intermediate-stage hepatocellular carcinoma. *Oncology*. (2015) 89:47–52. doi: 10.1159/000440631

11. Wang JH, Kee KM, Lin CY, Hung CH, Chen CH, Lee CM, et al. Validation and modification of a proposed substaging system for patients with intermediate hepatocellular carcinoma. *J Gastroenterol Hepatol*. (2015) 30:358–63. doi: 10.1111/jgh.12686

12. Kim JH, Shim JH, Lee HC, Sung KB, Ko HK, Ko GY, et al. New intermediate-stage subclassification for patients with hepatocellular carcinoma treated with transarterial chemoembolization. *Liver Int*. (2017) 37:1861–8. doi: 10.1111/liv.13487

13. Lee IC, Hung YW, Liu CA, Lee RC, Su CW, Huo TI, et al. A new ALBI-based model to predict survival after transarterial chemoembolization for BCLC stage B hepatocellular carcinoma. *Liver Int*. (2019) 39:1704–12. doi: 10.1111/liv.14194

14. Hung YW, Lee IC, Chi CT, Lee RC, Liu CA, Chiu NC, et al. Redefining tumor burden in patients with intermediate-stage hepatocellular carcinoma: the seven-eleven criteria. *Liver Cancer*. (2021) 10:629–40. doi: 10.1159/000517393

15. Lencioni R, Llovet JM, Han G, Tak WY, Yang J, Guglielmi A, et al. Sorafenib or placebo plus TACE with doxorubicin-eluting beads for intermediate stage HCC: The SPACE trial. *J Hepatol*. (2016) 64:1090–8. doi: 10.1016/j.jhep.2016.01.012

16. Meyer T, Fox R, Ma YT, Ross PJ, James MW, Sturgess R, et al. Sorafenib in combination with transarterial chemoembolisation in patients with unresectable hepatocellular carcinoma (TACE 2): a randomised placebo-controlled, double-blind, phase 3 trial. *Lancet Gastroenterol Hepatol*. (2017) 2:565–75. doi: 10.1016/S2468-1253(17)30156-5

17. Kudo M, Cheng AL, Park JW, Park JH, Liang PC, Hidaka H, et al. Orantinib versus placebo combined with transcatheter arterial chemoembolisation in patients with unresectable hepatocellular carcinoma (ORIENTAL): a randomised, double-blind, placebo-controlled, multicentre, phase 3 study. *Lancet Gastroenterol Hepatol*. (2018) 3:37–46. doi: 10.1016/S2468-1253(17)30290-X

18. Qin S, Kudo M, Meyer T, Finn RS, Vogel A, Bai Y, et al. LBA36 Final analysis of RATIONALE-301: Randomized, phase III study of tislelizumab versus sorafenib as first-line treatment for unresectable hepatocellular carcinoma. *Ann Oncol*. (2022) 33:S1402–S3. doi: 10.1016/j.annonc.2022.08.033

19. Llovet JM, Kudo M, Merle P, Meyer T, Qin S, Ikeda M, et al. Lenvatinib plus pembrolizumab versus lenvatinib plus placebo for advanced hepatocellular carcinoma (LEAP-002): a randomised, double-blind, phase 3 trial. *Lancet Oncol*. (2023) 24:1399–410. doi: 10.1016/S1470-2045(23)00469-2

20. Qin S, Chan SL, Gu S, Bai Y, Ren Z, Lin X, et al. Camrelizumab plus rivoceranib versus sorafenib as first-line therapy for unresectable hepatocellular carcinoma (CARES-310): a randomised, open-label, international phase 3 study. *Lancet*. (2023) 402:1133–46. doi: 10.1016/S0140-6736(23)00961-3

21. Finn RS, Qin S, Ikeda M, Galle PR, Ducreux M, Kim TY, et al. Atezolizumab plus bevacizumab in unresectable hepatocellular carcinoma. *N Engl J Med*. (2020) 382:1894–905. doi: 10.1056/NEJMoa1915745

22. Finn RS, Ikeda M, Zhu AX, Sung MW, Baron AD, Kudo M, et al. Phase ib study of lenvatinib plus pembrolizumab in patients with unresectable hepatocellular carcinoma. *J Clin Oncol*. (2020) 38:2960–70. doi: 10.1200/JCO.20.00808

23. Xu J, Shen J, Gu S, Zhang Y, Wu L, Wu J, et al. Camrelizumab in combination with apatinib in patients with advanced hepatocellular carcinoma (RESCUE): A nonrandomized, open-label, phase II trial. *Clin Cancer Res*. (2021) 27:1003–11. doi: 10.1158/1078-0432.CCR-20-2571

24. Pinato DJ, Murray SM, Forner A, Kaneko T, Fessas P, Toniutto P, et al. Trans-arterial chemoembolization as a loco-regional inducer of immunogenic cell death in hepatocellular carcinoma: implications for immunotherapy. *J Immunother Cancer*. (2021) 9:e003311. doi: 10.1136/jitc-2021-003311

25. Li Z, Cheng H, Mao J, Liu G. Conversion therapy of intermediate and advanced hepatocellular carcinoma using superstable homogeneous iodinated formulation technology. *Sci China Life Sci*. (2022) 65:2114–7. doi: 10.1007/s11427-022-2142-3

26. Heimbach JK, Kulik LM, Finn RS, Sirlin CB, Abecassis MM, Roberts LR, et al. AASLD guidelines for the treatment of hepatocellular carcinoma. *Hepatology*. (2018) 67:358–80. doi: 10.1002/hep.29086

27. Lewandowski RJ, Wang D, Gehl J, Atassi B, Ryu RK, Sato K, et al. A comparison of chemoembolization endpoints using angiographic versus transcatheter intraarterial perfusion/MR imaging monitoring. *J Vasc Interv Radiol*. (2007) 18:1249–57. doi: 10.1016/j.jvir.2007.06.028

28. Saito N, Nishiofuku H, Sato T, Maeda S, Minamiguchi K, Taiji R, et al. Predictive factors of complete response to transarterial chemoembolization in intermediate stage hepatocellular carcinoma beyond up-to-7 criteria. *Cancers (Basel)*. (2023) 15:2609. doi: 10.3390/cancers15092609

29. Kudo M, Ueshima K, Chan S, Minami T, Chishina H, Aoki T, et al. Lenvatinib as an initial treatment in patients with intermediate-stage hepatocellular carcinoma beyond up-to-seven criteria and child-pugh A liver function: A proof-of-concept study. *Cancers (Basel)*. (2019) 11:1084. doi: 10.3390/cancers11081084

30. Kudo M, Matsui O, Izumi N, Iijima H, Kadoya M, Imai Y, et al. JSH consensus-based clinical practice guidelines for the management of hepatocellular carcinoma: 2014 update by the liver cancer study group of Japan. *Liver Cancer*. (2014) 3:458–68. doi: 10.1159/000343875

31. Kudo M, Kawamura Y, Hasegawa K, Tateishi R, Kariyama K, Shiina S, et al. Management of hepatocellular carcinoma in Japan: JSH consensus statements and recommendations 2021 update. *Liver Cancer*. (2021) 10:181–223. doi: 10.1159/000514174

32. Tada T, Kumada T, Hiraoka A, Michitaka K, Atsukawa M, Hirooka M, et al. Impact of early lenvatinib administration on survival in patients with intermediate-stage hepatocellular carcinoma: A multicenter, inverse probability weighting analysis. *Oncology*. (2021) 99:518–27. doi: 10.1159/000515896

33. Chen Y, Huang A, Yang Q, Yu J, Li G. Case report: A successful re-challenge report of GLS-010 (Zimberelimab), a novel fully humanized mAb to PD-1, in a case of recurrent endometrial cancer. *Front Immunol*. (2022) 13:987345. doi: 10.3389/fimmu.2022.987345

34. Wang K, Zhu H, Yu H, Cheng Y, Xiang Y, Cheng Z, et al. Early Experience of TACE Combined with Atezolizumab plus Bevacizumab for Patients with Intermediate-Stage Hepatocellular Carcinoma beyond Up-to-Seven Criteria: A Multicenter, Single-Arm Study. *J Oncol*. (2023) 2023:6353047. doi: 10.1155/2023/6353047

35. Lencioni R, Kudo M, Erinjeri J, Qin S, Ren Z, Chan S, et al. EMERALD-1: A phase 3, randomized, placebo-controlled study of transarterial chemoembolization combined with durvalumab with or without bevacizumab in participants with unresectable hepatocellular carcinoma eligible for embolization. *J Clin Oncol*. (2024) 42:LBA432–LBA. doi: 10.1200/JCO.2024.42.3_suppl.LBA432

36. Kudo M, Finn RS, Qin S, Han KH, Ikeda K, Piscaglia F, et al. Lenvatinib versus sorafenib in first-line treatment of patients with unresectable hepatocellular carcinoma: a randomised phase 3 non-inferiority trial. *Lancet*. (2018) 391:1163–73. doi: 10.1016/S0140-6736(18)30207-1

37. Ikeda M, Morizane C, Ueno M, Okusaka T, Ishii H, Furuse J. Chemotherapy for hepatocellular carcinoma: current status and future perspectives. *Jpn J Clin Oncol*. (2018) 48:103–14. doi: 10.1093/jjco/hyx180

38. Cai M, Huang W, Huang J, Shi W, Guo Y, Liang L, et al. Transarterial chemoembolization combined with lenvatinib plus PD-1 inhibitor for advanced hepatocellular carcinoma: A retrospective cohort study. *Front Immunol*. (2022) 13:848387. doi: 10.3389/fimmu.2022.848387

39. Zhu HD, Li HL, Huang MS, Yang WZ, Yin GW, Zhong BY, et al. Transarterial chemoembolization with PD-(L)1 inhibitors plus molecular targeted therapies for hepatocellular carcinoma (CHANCE001). *Signal Transduct Target Ther*. (2023) 8:58. doi: 10.1038/s41392-022-01235-0

40. Yi C, Chen L, Lin Z, Liu L, Shao W, Zhang R, et al. Lenvatinib targets FGF receptor 4 to enhance antitumor immune response of anti-programmed cell death-1 in HCC. *Hepatology*. (2021) 74:2544–60. doi: 10.1002/hep.31921

41. Deng H, Kan A, Lyu N, Mu L, Han Y, Liu L, et al. Dual vascular endothelial growth factor receptor and fibroblast growth factor receptor inhibition elicits antitumor immunity and enhances programmed cell death-1 checkpoint blockade in hepatocellular carcinoma. *Liver Cancer*. (2020) 9:338–57. doi: 10.1159/000505695

42. Liang X, Liu H, Chen H, Peng X, Li Z, Teng M, et al. Rhein-based Pickering emulsion for hepatocellular carcinoma: Shaping the metabolic signaling and immunoactivation in transarterial chemoembolization. *Aggregate* (2024) e552. doi: 10.1002/agt2.552

43. Cheng H, Fan X, Ye E, Chen H, Yang J, Ke L, et al. Dual tumor microenvironment remodeling by glucose-contained radical copolymer for MRI-guided photoimmunotherapy. *Adv Mater*. (2022) 34:e2107674. doi: 10.1002/adma.202107674

44. Zhong BY, Jin ZC, Chen JJ, Zhu HD, Zhu XL. Role of transarterial chemoembolization in the treatment of hepatocellular carcinoma. *J Clin Transl Hepatol*. (2023) 11:480–9. doi: 10.14218/JCTH.2022.00293

45. Zhong BY, Jiang JQ, Sun JH, Huang JT, Wang WD, Wang Q, et al. Prognostic performance of the China liver cancer staging system in hepatocellular carcinoma following transarterial chemoembolization. *J Clin Transl Hepatol*. (2023) 11:1321–8. doi: 10.14218/JCTH.2023.00099

46. Pinato DJ, Sharma R, Allara E, Yen C, Arizumi T, Kubota K, et al. The ALBI grade provides objective hepatic reserve estimation across each BCLC stage of hepatocellular carcinoma. *J Hepatol*. (2017) 66:338–46. doi: 10.1016/j.jhep.2016.09.008

47. Takayasu K, Arii S, Ikai I, Omata M, Okita K, Ichida T, et al. Prospective cohort study of transarterial chemoembolization for unresectable hepatocellular carcinoma in 8510 patients. *Gastroenterology*. (2006) 131:461–9. doi: 10.1053/j.gastro.2006.05.021

48. Park JW, Chen M, Colombo M, Roberts LR, Schwartz M, Chen PJ, et al. Global patterns of hepatocellular carcinoma management from diagnosis to death: the BRIDGE Study. *Liver Int*. (2015) 35:2155–66. doi: 10.1111/liv.12818

49. Sieghart W, Hucke F, Peck-Radosavljevic M. Transarterial chemoembolization: Modalities, indication, and patient selection. *J Hepatol*. (2015) 62:1187–95. doi: 10.1016/j.jhep.2015.02.010

50. Llovet JM, De Baere T, Kulik L, Haber PK, Greten TF, Meyer T, et al. Locoregional therapies in the era of molecular and immune treatments for hepatocellular carcinoma. *Nat Rev Gastroenterol Hepatol*. (2021) 18:293–313. doi: 10.1038/s41575-020-00395-0

51. Ren Z, Xu J, Bai Y, Xu A, Cang S, Du C, et al. Sintilimab plus a bevacizumab biosimilar (IBI305) versus sorafenib in unresectable hepatocellular carcinoma (ORIENT-32): a randomised, open-label, phase 2-3 study. *Lancet Oncol*. (2021) 22:977–90. doi: 10.1016/S1470-2045(21)00252-7

52. Peng Z, Fan W, Zhu B, Wang G, Sun J, Xiao C, et al. Lenvatinib combined with transarterial chemoembolization as first-line treatment for advanced hepatocellular carcinoma: A phase III, randomized clinical trial (LAUNCH). *J Clin Oncol*. (2023) 41:117–27. doi: 10.1200/JCO.22.00392

frontiers | Frontiers in Immunology

TYPE Systematic Review
PUBLISHED 02 August 2024
DOI 10.3389/fimmu.2024.1421520

OPEN ACCESS

EDITED BY
Sina Naserian,
Hôpital Paul Brousse, France

REVIEWED BY
Zhanjun Guo,
Fourth Hospital of Hebei Medical University, China
Bin-Yan Zhong,
The First Affiliated Hospital of Soochow University, China

*CORRESPONDENCE
Lei Wang
wangleiy001@126.com
Qiang Tu
jxchtuqiang@163.com

†These authors have contributed equally to this work and share first authorship

RECEIVED 22 April 2024
ACCEPTED 12 July 2024
PUBLISHED 02 August 2024

CITATION
Fang H, Ke Q, Wu S, Tu Q and Wang L (2024) Immune-targeted therapy with transarterial chemo(embolization) for unresectable HCC: a systematic review and meta-analysis. *Front. Immunol.* 15:1421520. doi: 10.3389/fimmu.2024.1421520

Immune-targeted therapy with transarterial chemo (embolization) for unresectable HCC: a systematic review and meta-analysis

Huipeng Fang[1,2†], Qiao Ke[3†], Shiji Wu[4†], Qiang Tu[5,6*] and Lei Wang[1*]

[1]Department of Radiation Oncology, Jiangxi Clinical Research Center for Cancer, Jiangxi Cancer Hospital, The Second Affiliated Hospital of Nanchang Medical College, Nanchang, Jiangxi, China, [2]Department of Hepatopancreatobiliary Surgery, Clinical Oncology School of Fujian Medical University, Fujian Cancer Hospital, Fuzhou, Fujian, China, [3]Department of Hepatobiliary Surgery, The First Affiliated Hospital, Fujian Medical University, Fuzhou, Fujian, China, [4]Department of Radiation Oncology, Clinical Oncology School of Fujian Medical University, Fujian Cancer Hospital, Fuzhou, Fujian, China, [5]Department of Hepatobiliary Tumor Surgery, Jiangxi Cancer Hospital, The Second Affiliated Hospital of Nanchang Medical College, Jiangxi Clinical Research Center for Cancer, Nanchang, Jiangxi, China, [6]Department of Interventional Therapy, Jiangxi Cancer Hospital, The Second Affiliated Hospital of Nanchang Medical College, Jiangxi Clinical Research Center for Cancer, Nanchang, Jiangxi, China

Background: Transarterial chemo(embolization) is preferred for treating unresectable hepatocellular carcinoma (uHCC); however, because of emerging immune-targeted therapies, its efficacy is at stake. This systematic review pioneers to evaluate the clinical efficacy and safety of transarterial chemo (embolization) combined with immune-targeted therapy for uHCC patients.

Methods: PubMed, Embase, and Cochrane Library were searched for studies comparing immune-targeted therapy with or without transarterial chemo (embolization) until 31 May 2024. The complete response (CR) rate, objective response rate (ORR), and disease control rate (DCR) were considered to be the primary outcomes calculated for the clinical outcomes of transarterial chemo (embolization) combined with immune-targeted therapy, along with progression-free survival (PFS) and overall survival (OS). The incidence of treatment-related severe adverse events was set as the major measure for the safety outcome.

Results: Sixteen studies, encompassing 1,789 patients receiving transarterial chemo(embolization) plus immune-targeted therapy and 1,215 patients receiving immune-targeted therapy alone, were considered eligible. The combination of transarterial chemo(embolization) and immune-targeted therapy demonstrated enhanced outcomes in CR (OR = 2.12, 95% CI = 1.35–3.31), ORR (OR = 2.78, 95% CI = 2.15–3.61), DCR (OR = 2.46, 95% CI = 1.72–3.52), PFS (HR = 0.59, 95% CI = 0.50–0.70), and OS (HR = 0.51, 95% CI = 0.44–0.59), albeit accompanied by a surge in ALT (OR = 2.17, 95% CI = 1.28–3.68) and AST (OR = 2.28, 95% CI = 1.42–3.65). The advantages of additional transarterial chemo(embolization) to immune-targeted therapy were also verified in subgroups of first-line treatment, intervention techniques, with or without

extrahepatic metastasis, Child–Pugh grade A or B, and with or without tumor thrombus.

Conclusion: The combination of transarterial chemo(embolization) and immune-targeted therapy seems to bolster local control and long-term efficacy in uHCC, albeit at the expense of hepatic complications.

Systematic review registration: http://www.crd.york.ac.uk/PROSPERO/, identifier 474669.

KEYWORDS

transarterial chemo(embolization), unresectable hepatocellular carcinoma, targeted agents, immunotherapy, systematic review

Introduction

In 2020, primary liver cancer was recognized as the sixth most prevalent malignant tumor globally, among which hepatocellular carcinoma (HCC) accounts for more than 90% of the cases (1). The majority of HCC cases have lost the chance of radical hepatectomy mainly because HCC generally progresses asymptomatically (2). It is diagnosed at an intermediate to advanced stage, also termed unresectable HCC (uHCC). The inception of the IMbrave150 trial heralded a new epoch in the utilization of targeted agents and immunotherapy for uHCC management, boasting an objective response rate (ORR) of 28% (3). This regimen, along with apatinib and camrelizumab (4) and lenvatinib and pembrolizumab (5), signifies a promising stride, albeit with an unsatisfactory median overall survival (OS).

Transcatheter arterial chemoembolization (TACE), as one of the classical transarterial therapies, is considered the standard treatment for uHCC (6). Conversely, hepatic artery infusion chemotherapy (HAIC), an emerging transarterial therapeutic modality, demonstrates non-inferior local control compared to TACE but superior long-term outcomes (7, 8). Despite these advancements, the advent of targeted agents and immunotherapy warrants re-evaluating the role of transarterial chemo(embolization) in HCC management. The IMbrave150 trial demonstrated the potential of integrating transarterial chemo(embolization) with targeted agents and immunotherapy (3, 9), hinting at a synergistic interaction. In theory, transarterial chemo(embolization) could enhance tumor antigen release and immunogenicity; bolster the infiltration of $CD4^+$ T, $CD8^+$ T, and NK cells; and elicit proinflammatory responses (10, 11), thereby fostering a conducive microenvironment for immune checkpoint inhibitors (ICIs). Concurrently, it can increase the expression of vascular endothelial growth factor (12, 13), hinting at a viable partnership with angiogenic blockers.

Preliminary studies have witnessed the promise of immune-targeted therapy with transarterial chemo(embolization) for uHCC in the recent three years (14–16), which was reiterated by a systematic review (17). However, most of the studies were retrospective, single-center, non-comparative analyses. In the recent two years, researchers have reported encouraging results upon comparing immune-targeted therapy with transarterial chemo(embolization) for uHCC (18–20); nonetheless, adding transarterial therapy to the targeted agents and immunotherapy appears debatable (21). Consequently, we embarked on this meta-analysis to juxtapose the efficacy and toxicity profiles of immune-targeted therapy with or without transarterial therapies for uHCC.

Materials and methods

Literature search

This meta-analysis was conducted according to the Preferred Reporting Items for Systematic Reviews and Meta-Analyses (PRISMA) guideline, which was also registered at http://www.crd.york.ac.uk/PROSPERO/ (Review registry 474669). An ethics statement was not required because this study was based exclusively on published research. A comprehensive search was executed in PubMed, Medline, Embase, the Cochrane Library, and Web of Science to identify publications concerning immune-targeted therapy with or without transarterial chemo (embolization) for uHCC. Supplementary Table S1 summarizes the search strategy. A supplementary search in gray literature was conducted by reviewing conference proceedings and reference lists of key articles. The publications were not confined to any specific language, provided that they had an abstract in English to ensure data reproducibility. The literature search was independently

conducted by two researchers from 1 February 2023 to 31 May 2024, based on predefined search strategies.

Literature screening and data acquisition

First, data collected through electronic or manual searches were imported to EndNote version X9 software (Clarivate) to detect duplicate records. Then, two reviewers (Huipeng Fang and Qiao Ke) conducted literature screening based on the inclusion and exclusion criteria (Supplementary Table S2). In case of any discrepancy between reviewers, a third-party reviewer was consulted to reach a final decision.

Information of the eligible studies was extracted directly by two independent researchers (Huipeng Fang and Qiao Ke) using a predefined format, encompassing data on publication, study design, baseline characteristics in each study, and endpoints. Data were cross-validated between researchers, and discrepancies were resolved through a multidisciplinary team (MDT) discussion, including at least one senior doctor.

Endpoints in this meta-analysis included the complete response (CR) rate, objective response rate (ORR), disease control rate (DCR), progression-free survival (PFS), overall survival (OS), and adverse events (AEs). Tumor response was evaluated based on the Modified Response Evaluation Criteria in Solid Tumors (mRECIST) or Response Evaluation Criteria in Solid Tumors (RECIST) version 1.1 (22). ORR was calculated as the proportion of patients with the best response of CR or partial response (PR). DCR was calculated as the proportion of patients with the best response of ORR or stable disease (SD). PFS was defined as the duration from the initiation of treatment to the onset of disease progression or mortality from any cause. OS was defined as the time from treatment initiation to cancer-related death. AEs were evaluated by the National Cancer Institute Common Terminology Criteria for Adverse Events version 4.0 or 5.0, with a grade ≥3 indicating severe AEs.

Quality assessment

Considering the retrospective nature of the included studies, the quality was evaluated using a modified Newcastle-Ottawa Scale (NOS) (23). The risk of bias was graphically represented for the following elements: i) clarity in the objective definition; ii) provision of a clear triple combination of TACE/HAIC, TKIs, and ICIs; iii) provision of response assessment criteria (i.e., RECIST or mRECIST); and iv) clear definition of outcomes including CR, ORR, DCR, and AEs.

Statistical analysis

Comparison analysis between two groups was conducted using RevMan Version 5.3. The odds ratio (OR) was calculated to compare the effect size of CR, ORR, DCR, and AEs with 95% confidence interval (CI), as well as the hazard ratio (HR) for OS and PFS. The χ^2 test and I^2 statistics were used to evaluate the heterogeneity among the included studies. P >0.10 and I^2 <50% suggested no apparent heterogeneity, and the fixed-effects model was used to estimate the effect size; otherwise, the random-effects model was used (24). Sensitivity analysis was carried out by removing each of the included studies sequentially to determine the reliability of the results. Additionally, subgroup analyses were also conducted to decrease the heterogeneity among the included studies. Publication bias was determined using the funnel plot with Egger's and Begg's tests (25, 26). In this study, a P-value <0.05 indicated statistical significance.

Results

Search results

Initially, 2,683 records were identified through electronic database search, apart from 11 records via manual searching. We excluded 108 duplicate studies, 2,586 studies upon screening titles and abstracts, and 92 studies after full-text review. Finally, 16 studies were considered eligible for this meta-analysis (Figure 1). Potential time and center crossover were noted among the studies, particularly between the studies of Mei et al. (27) and Fu et al. (28) from similar single-center and multicenter studies because of numerous participations by some centers.

All of the included studies originated from China; six were multicentered (16, 29–33) and five underwent PSM analysis (34–38) and one underwent sIPTW analysis (33). A total of 3,004 patients were included in this meta-analysis, encompassing 1,789 patients administered with transarterial chemo(embolization) plus immune-targeted therapy and 1,215 patients receiving immune-targeted therapy alone, respectively. Table 1 summarizes the baseline characteristics and quality assessment outcomes. Supplementary Table S3 summarizes the treatment regimens, considering no consensus on the transarterial chemo (embolization) plus immune-targeted therapy. Supplementary Figure S1 illustrates the quality of each study. Supplementary Table S4 summarizes the scoring rules of each study.

Short-term endpoints

CR was evaluated in 14 included trials (16, 19, 20, 27–29, 32, 34, 35, 37–41), without significant heterogeneity (I^2 = 0%, P = 0.45, Figure 2A). Using the fixed-effects model, the pooled CR rate was in favor of the experiment group over the control group (8.5% vs. 4.0%) with an OR of 2.12 (95% CI = 1.35–3.31, Figure 2A). Sensitivity analysis showed that the results did not change greatly after removing any included single study (Supplementary Figure S2A). Asymmetry was absent in the funnel plot (Supplementary Figure S3A), with P-values of 0.9756 and 0.6971 for Egger's test and Begg's test, respectively (Supplementary Table S5).

ORR was evaluated in 15 included trials (16, 19, 20, 27–29, 32–35, 37–41), among which significant heterogeneity was observed

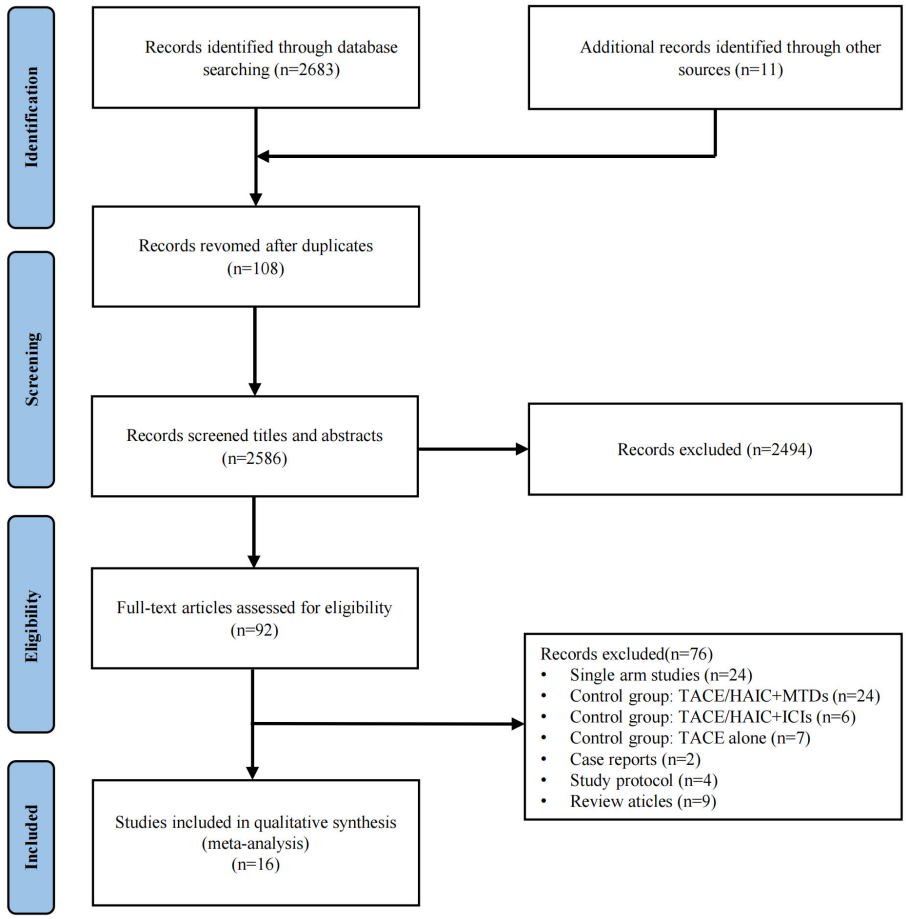

FIGURE 1
Flowchart of the study inclusion.

(I^2= 40%, P = 0.05, Figure 2B). Using the random-effects model, the pooled ORR rate was in favor of the experiment group over the control group (46.6% vs. 26.4%) with an OR of 2.78 (95% CI = 2.15–3.61, Figure 2B). The robustness of these results was confirmed by sensitivity analysis (Supplementary Figure S2B). Asymmetry was observed in the funnel plot (Supplementary Figure S3B), with P-values of 0.1017 and 0.2160 for Egger's test and Begg's test, respectively (Supplementary Table S5).

Similarly, DCR was evaluated in 14 studies (16, 19, 20, 27–29, 32, 34, 35, 37–41) with significant heterogeneity (I^2 = 47%, P = 0.03, Figure 2C). Using the random-effects model, the pooled DCR rate was in favor of the experiment group over the control group (82.9% vs. 69.4%) with an OR of 2.46 (95% CI = 1.72–3.52, Figure 2C). Sensitivity analysis validated the consistency of these findings (Supplementary Figure S2C). Asymmetry was observed by funnel plot (Supplementary Figure S3C), with P-values of 0.0195 and 0.0328 for Egger's test and Begg's test, respectively (Supplementary Table S5). The trim-and-fill method identified five additional publications, without any significant impact on the results (Supplementary Table S5).

Long-term endpoints

PFS was evaluated in 16 studies (16, 19, 20, 27–29, 31–35, 37–41), among which significant heterogeneity was observed (I^2 = 64%, P < 0.05, Figure 3A). Using the random-effects model, the pooled HR was in favor of the experiment group over the control group (HR = 0.59, 95% CI = 0.50–0.70, Figure 3A), a finding upheld by sensitivity analysis (Supplementary Figure S2D). Asymmetry was observed by funnel plot (Supplementary Figure S3D) with P-values of 0.0239 and 0.0581 for Egger's test and Begg's test, respectively (Supplementary Table S5). Six additional studies were identified through the trim-and-fill method, without substantial alteration in the results (Supplementary Table S5).

OS was evaluated in 16 studies (16, 19, 20, 27–29, 31–35, 37–41), with significant heterogeneity (I^2 = 36%, P = 0.07, Figure 3B). Using the random-effects model, the pooled HR was in favor of the experiment group over the control group (HR = 0.51, 95% CI = 0.44–0.59, Figure 3B), confirmed by sensitivity analysis (Supplementary Figure S2E). Funnel plot analysis showed asymmetry (Supplementary Figure S3E), with P-values of 0.0006

TABLE 1 Basic characteristics and quality assessment of the included studies.

Study	Design	Treatment	Patients	Age, years	Sex, M/F	HBV, P/N	Child–Pugh, A/B	AFP (ng/ml), <400/≥400	MVI, yes/no	Extrahepatic metastasis, yes/no	BCLC stage, A/B/C	CR, *N* (%)	ORR, *N* (%)	DCR, *N* (%)	Median PFS, months	Median OS, months	Quality
Dai 2021	R single center	TACE + Sor + sintilimab	35	56.5 ± 10.2	30/5	27/8	19/16	NA	17/18	6/29	0/14/21	6 (17)	10 (29)	28 (80)	5	13	H
		Sor + sintilimab	23	54.0 ± 15.0	21/2	18/5	12/11	NA	16/7	5/18	0/5/18	4 (17)	6 (26)	17 (74)	4	9	
Mei 2021	R single center	HAIC + Len+ ICIs	45	49.1 ± 10.6	38/7	37/8	44/1	4,106.0 (72.8–121,000.0)	36/9	15/30	0/5/40	0 (0)	18 (40)	38 (84)	8.8	15.9	H
		Len + ICIs	25	50.1 ± 12.3	18/7	19/6	22/3	767.6 (23.3–21,940.5)	18/7	13/12	0/3/22	0 (0)	4 (14)	11 (44)	5.4	8.6	
Chen 2021	R multi-center	HAIC + Len + pembrolizumab	84	52 (42–67)	72/12	45/39	71/13	3,984.0 (82.0–49,534.0)	49/35	20/64	0/22/62	13 (15)	50 (60)	74 (88)	10.9	17.7	H
		Len + pembrolizumab	86	53 (43–69)	71/15	48/38	75/11	4,022.0 (79.0–51,462.0)	55/31	24/62	0/21/65	8 (9)	36 (42)	71 (83)	6.8	12.6	
Guo 2022	R single center	cTACE+ MTDs + camrelizumab	31	24/7 <60/≥60	26/5	29/2	21/10	17/14	20/11	17/14	2/5/24	2 (6)	16 (52)	28 (90)	11.7	19.8	H
		MTDs + camrelizumab	23	12/11 <60/≥60	22/1	20/3	14/9	12/11	11/12	14/9	1/3/19	0 (0)	5 (22)	15 (65)	4	11.6	
Huang 2022 after PSM	R single center	TACE + immune-targeted therapy	24	58.0 ± 10.7	20/4	20/4	18/6	12/12	18/6	9/15	0/0/24	1 (4)	10 (42)	19 (79)	7.4	17.3	H
		Immune-targeted therapy	24	56.5 ± 14.0	21/3	20/4	14/10	9/15	18/6	13/11	0/0/24	0 (0)	3 (13)	12 (50)	6.7	11.8	
Dong 2022	R dual center	TACE/HAIC + immune-targeted therapy	66	52 (40–65)	57/9	54/12	50/16	39/27	25/41	29/37	0/0/66	2 (3)	40 (61)	56 (85)	8.4	11.6	H
		Immune-targeted therapy + TACE/HAIC	56	52 (41–64)	51/5	52/4	42/14	28/28	27/29	29/27	0/0/56	0 (0)	18 (32)	42 (75)	5.3	10.0	
		Immune-targeted therapy	41	57 (47–67)	34/7	36/5	31/10	20/21	16/25	24/17	0/0/41	0 (0)	9 (22)	33 (80)	6.3	11.3	

(Continued)

10.3389/fimmu.2024.1421520

TABLE 1 Continued

Study	Design	Treatment	Patients	Age, years	Sex, M/F	HBV, P/N	Child–Pugh, A/B	AFP (ng/ml), <400/≥400	MVI, yes/no	Extrahepatic metastasis, yes/no	BCLC stage, A/B/C	CR, *N* (%)	ORR, *N* (%)	DCR, *N* (%)	Median PFS, months	Median OS, months	Quality
Wang 2023 after PSM	R single center	TACE + Len + ICIs	43	57.07 ± 10.53	38/5	42/4	39/4	25/18	19/24	22/21	0/8/35	0 (0)	24 (56)	37 (86)	10.2	20.5	H
		Len + ICIs	43	58.00 ± 10.52	37/6	52/7	36/7	21/22	18/25	25/18	0/7/36	0 (0)	13 (30)	28 (65)	7.4	12.6	
Xin 2023	R single center	TACE + Len + ICIs	60	37/23 <60/≥60	54/6	56/4	60/0	32/28	28/32	18/42	0/ 21/39	10 (17)	46 (77)	58 (97)	16.2	29	H
		Len + ICIs	58	40/18 <60/≥60	51/7	51/7	58/0	28/30	17/41	26/32	0/ 23/35	3 (5)	26 (45)	44 (76)	10.2	17.8	
Yang 2023 after PSM	R single center	TACE + regorafenib + ICIs	23	53 (43.0–65.0)	20/3	19/4	22/1	15/8	8/15	11/12	0/ 19/14	0 (0)	8 (35)	16 (70)	5.8	13.6	H
		Regorafenib + ICIs	23	49 (45.0–56.0)	19/4	16/7	18/5	14/9	10/13	12/11	0/5/18	0 (0)	1 (4)	10 (44)	2.6	7.5	
Fu 2023	R single center	HAIC + Len + ICIs	89	51.9 ± 10.5	83/6	79/10	88/1	37/52	89/0	21/68	0/0/89	17 (19)	55 (62)	77 (87)	11.5	26.3	M
		Len + ICIs	53	53.5 ± 10.5	50/3	45/8	47/6	20/33	53/0	26/27	0/0/53	2 (4)	11 (21)	30 (57)	5.5	13.8	
Pan 2023 after PSM	R multicenter	TACE/HAIC + immune-targeted therapy	131	54.0 (48.5–61.0)	118/13	117/14	127/4	20,461.84 ± 36,365.99	102/29	48/83	0/ 19/112	2 (2)	48 (37)	112 (85)	NA	23.9	H
		Immune-targeted therapy	131	54.0 (47.5–60.5)	119/12	112/19	122/9	20,331.47 ± 85,642.76	83/48	48/83	0/ 19/112	6 (5)	43 (33)	109 (83)	NA	Not reached	
Lang 2023 after PSM	R single center	TACE + Len + sintilimab	75	57/18 ≤60/>60	66/9	69/6	59/16	45/30	23/52	26/49	0/ 32/43	2 (3)	33 (44)	47 (63)	11.1	Not reached	H
		Len+ sintilimab	39	29/10 ≤60/>60	34/5	35/4	30/9	23/16	9/30	19/20	0/ 14/25	0 (0)	9 (23)	17 (44)	5.1	14.0	
Li 2023	R multicenter	TACE + immune-targeted therapy	62	50/12 <65/≥65	55/7	46/16	48/13/1 A/B/C	24/38	28/34	14/48	6/9/46/1 A/B/C/D	NA	N	NA	7.4	20.3	M

(Continued)

10.3389/fimmu.2024.1421520

TABLE 1 Continued

Study	Design	Treatment	Patients	Age, years	Sex, M/F	HBV, P/N	Child–Pugh, A/B	AFP (ng/ml), <400/≥400	MVI, yes/no	Extrahepatic metastasis, yes/no	BCLC stage, A/B/C	CR, *N* (%)	ORR, *N* (%)	DCR, *N* (%)	Median PFS, months	Median OS, months	Quality
		Immune-targeted therapy	83	46/37 <65/≥65	71/12	58/35	65/17/1 A/B/C	43/40	43/40	32/51	6/8/68/1 A/B/C/D	NA	NA	NA	5.0	13.6	
Hu 2023	R single center	TACE + immune-targeted therapy	98	52 (42–62)	87/11	85/13	75/23	39/59 ≤200/>200	73/25	49/49	0/12/86	22 (22)	73 (74)	89 (91)	9.7	19.5	H
		Immune-targeted therapy	49	53 (47–63)	47/2	43/6	33/16	22/27 ≤200/>200	30/19	26/23	0/7/42	4 (8)	20 (41)	36 (73)	7.7	10.8	
Cao 2023	R dual center	TACE + Atez/Bev	62	55.8 ± 11.2	52/10	44/18	40/22	30/32	34/28	33/29	NA	1 (2)	24 (39)	43 (69)	10	14	H
		Atez/Bev	77	52.8 ± 11.0	65/12	59/18	51/26	41/36	43/34	45/32	NA	1 (1)	13 (17)	49 (64)	6	10	
Jin 2024 after sIPTW	R multicenter	TACE + immune-targeted therapy	805	54 (48–63)	693/112	681/124	659/146	394/354	570/235	471/334	NA	NA	332 (41.2)	NA	9.9	22.6	H
		Immune-targeted therapy	437	56 (47–62)	378/59	374/63	357/80	208/197	308/129	258/179	NA	NA	100 (22.9)	NA	7.4	15.9	

TACE, transcatheter arterial chemoembolization; HAIC, hepatic artery infusion chemotherapy; MTDs, molecularly targeted drugs; ICIs, immune checkpoint inhibitors; Len, lenvatinib; Sor, sorafenib; Atez, atezolizumab; Bev, bevacizumab; R, retrospective; M, male; F, female; HBV, hepatitis B virus; P, positive; N, negative; S, single; M, multiple; MVI, macrovascular invasion; BCLC, Barcelona Clinic Liver Cancer stage; CR, complete response; PR, partial response; ORR, objective response rate; DCR, disease control rate; OS, overall survival; PFS, progression-free survival; H, high; M, medium; NA, not available; PSM, propensity score matching; sIPTW, stabilized inverse probability of treatment weighting.

10.3389/fimmu.2024.1421520

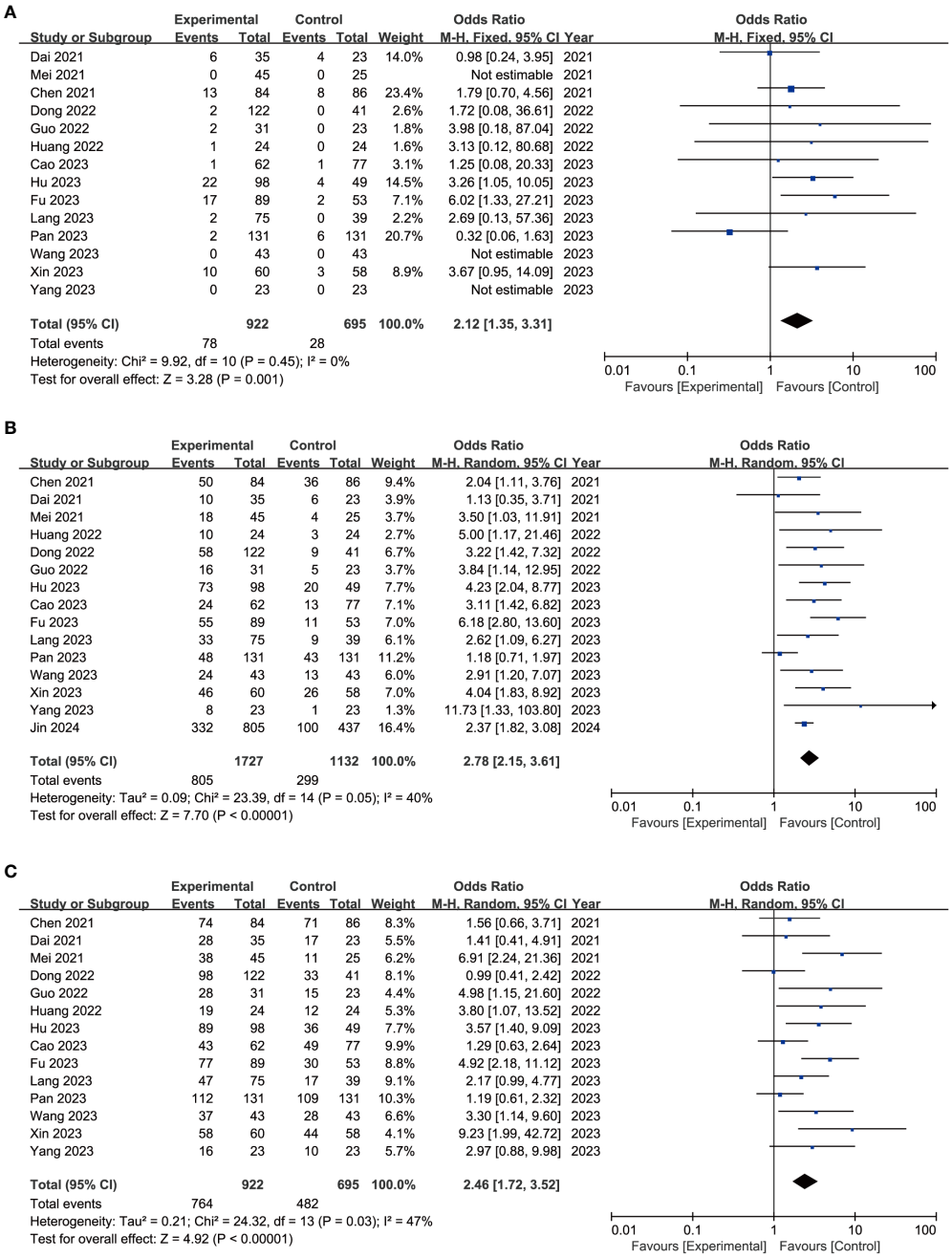

FIGURE 2
Forest plot of complete response **(A)**, disease control rate **(B)**, and objective response rate **(C)** of immune-targeted therapy with or without transarterial chemo(embolization).

and 0.0084 for Egger's test and Begg's test, respectively (Supplementary Table S5). The trim-and-fill method identified six more publications, with no significant change in the results (Supplementary Table S5).

Subgroup analysis

Ten of the included studies (16, 19, 20, 27, 29, 32, 33, 35, 39, 41) enrolled uHCC patients who did not receive prior treatment. Results revealed a superior outcome of combination therapy of transarterial chemo(embolization) and immune-targeted therapy in terms of CR (OR = 1.69, 95% CI = 1.05–2.73,Supplementary Table S6), ORR (OR = 2.34, 95% CI = 1.96–2.81, Supplementary Table S6), DCR (OR = 2.00, 95% CI = 1.29–3.10, Supplementary Table S6), median PFS (HR = 0.62, 95% CI = 0.50–0.77, Supplementary Table S6), and median OS (HR = 0.55, 95% CI = 0.46–0.66, Supplementary Table S6).

In China, TACE and HAIC are the two most common modalities of transarterial therapies (42). In this meta-analysis, TACE was adopted in 11 studies (19, 20, 31, 33–35, 37–41), whereas HAIC was adopted in

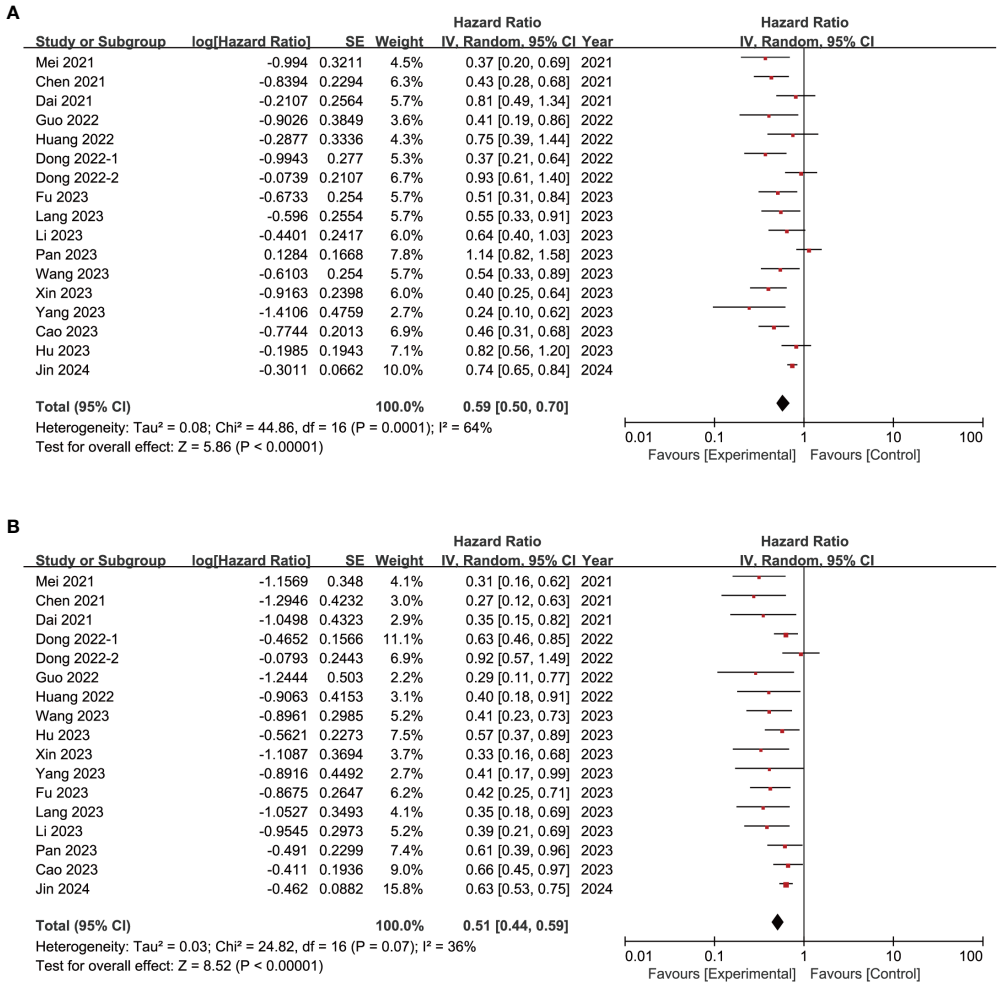

FIGURE 3
Forest plot of progression-free survival **(A)** and overall survival **(B)** of immune-targeted therapy with or without transarterial chemo(embolization).

three studies (16, 27, 28), respectively. Results confirmed the advantage of additional TACE to immune-targeted therapy in terms of CR (OR = 2.32, 95% CI = 1.26–4.26, Supplementary Table S6), ORR (OR = 2.72, 95% CI = 2.22–3.33, Supplementary Table S6), DCR (OR = 2.58, 95% CI = 1.84–3.61, Supplementary Table S6), median PFS (HR = 0.60, 95% CI = 0.49–0.72, Supplementary Table S6), and median OS (HR = 0.55, 95% CI = 0.48–0.63, Supplementary Table S6). Similarly, the advantage of additional HAIC to immune-targeted therapy was also verified in terms of CR, ORR, DCR, median PFS, and median OS (all $P < 0.05$, Supplementary Table S6).

Advanced HCC often coexists with extrahepatic metastasis (6, 42), making additional local treatment debatable. Herein, nine studies (27–29, 32–35, 37, 39) conducted subgroup analysis for patients with or without extrahepatic metastasis. Expectedly, in patients without extrahepatic metastasis, the experiment group outperformed the control group in median PFS and OS (HR = 0.67, 95% CI = 0.57–0.79; HR = 0.57, 95% CI = 0.47–0.68, respectively, Supplementary Table S6). Compared with the control group, the pooled HR for median PFS and OS favored the experiment in patients with extrahepatic metastasis (HR = 0.78, 95% CI = 0.68–0.89; HR = 0.66, 95% CI = 0.57–0.77, respectively, Supplementary Table S6).

Liver function is the bottleneck of additional transarterial chemo(embolization) to immune-targeted therapy (43). In this meta-analysis, seven studies (27, 28, 32–35, 37) compared patients with a Child–Pugh grade of A and B. Compared with the control group, the pooled HRs for both PFS and OS were in favor of the experiment group among patients with a Child–Pugh grade of A or B (all $P < 0.05$, Supplementary Table S6).

Transarterial chemo(embolization) improves the long-term prognosis of patients with tumor thrombus (44, 45), which is an aggressive characteristic of HCC (6, 42). Herein, eight studies (27, 28, 32–35, 37, 39) enrolled patients with tumor thrombus and seven studies (27, 32–35, 37, 39) enrolled patients without tumor thrombus. Compared with the control group, the pooled HRs for both PFS and OS were in favor of the experiment group among patients with or without tumor thrombus (all $P < 0.05$, Supplementary Table S6).

10.3389/fimmu.2024.1421520

Adverse events

Table 2 delineates treatment-related AEs. No treatment-related deaths were reported. The most prevalent all-grade AEs included fatigue, diarrhea, rash, and elevated alanine transaminase (ALT) and aspartate aminotransferase (AST). In aggregate, the addition of transarterial therapies heightened the risk of certain AEs including elevated ALT, AST, and gamma-glutamyl transpeptidase (GGT); fever; nausea; and vomiting (all $P < 0.05$, Table 2). Likewise, severe AEs mirrored those of all-grade AEs, with transarterial chemo (embolization) additionally elevating the risk of severe elevated ALT and AST (ALT: OR = 2.17, 95% CI = 1.28–3.68; AST: OR = 2.28, 95% CI = 1.42–3.65; both $P < 0.05$, Table 2).

Discussion

Traditionally, transarterial chemo(embolization) has been the preferred option for uHCC (6, 46, 47); however, its role is debatable in the era of immune-targeted therapy. To the best of our knowledge, this is the first meta-analysis to compare the clinical efficacy and safety of transarterial chemo(embolization) plus immune-targeted therapy versus immune-targeted therapy. This meta-analysis consisted of 16 studies, encompassing 1,789 patients who received transarterial chemo(embolization) plus immune-targeted therapy and 1,215 patients who received immune-targeted therapy. The results elucidated that transarterial chemo (embolization) plus immune-targeted therapy outperformed

TABLE 2 Treatment-related adverse events.

Events	All grade					Grade ≥3				
	Included studies	Participants	Effect model	OR (95 CI)	*P*-value	Included studies	Participants	Effect model	OR (95 CI)	*P*-value
Elevated ALT	12	2,316	Random	2.33 [1.48, 3.67]	<0.001	11	2,146	Fixed	2.17 [1.28, 3.68]	0.004
Elevated AST	12	2,316	Random	2.20 [1.41, 3.42]	<0.001	11	2,146	Fixed	2.28 [1.42, 3.65]	<0.001
Elevated GGT	2	172	Fixed	2.37 [1.09, 5.16]	0.03	2	172	Fixed	0.98 [0.24, 3.95]	0.98
Anemia	4	429	Random	2.03 [0.70, 5.86]	0.19	4	429	Fixed	0.98 [0.26, 3.65]	0.97
Neutropenia	3	302	Random	2.70 [0.74, 9.86]	0.13	3	302	Fixed	1.29 [0.34, 4.95]	0.71
Lymphopenia	2	172	Random	1.65 [0.52, 5.26]	0.4	2	172	Fixed	0.98 [0.24, 3.95]	0.98
Thrombocytopenia	11	2,373	Random	1.21 [0.71, 2.06]	0.47	11	2,492	Fixed	1.25 [0.75, 2.11]	0.39
Hypoleukemia	8	2,007	Random	1.38 [0.79, 2.44]	0.26	8	2,126	Fixed	1.38 [0.61, 3.10]	0.44
Hypoalbuminemia	4	500	Fixed	0.97 [0.62, 1.51]	0.89	3	330	Fixed	1.16 [0.41, 3.27]	0.78
Nausea and vomiting	9	1,077	Random	3.71 [1.48, 9.34]	0.005	8	1,054	Fixed	1.53 [0.61, 3.85]	0.37
Hand-foot syndrome	9	1,929	Fixed	1.07 [0.82, 1.41]	0.62	10	2,218	Fixed	1.02 [0.57, 1.82]	0.94
Hypertension	11	2,331	Fixed	0.94 [0.76, 1.15]	0.53	10	2,308	Fixed	0.97 [0.66, 1.41]	0.86

(Continued)

TABLE 2 Continued

Events	All grade					Grade ≥3				
	Included studies	Participants	Effect model	OR (95 CI)	*P*-value	Included studies	Participants	Effect model	OR (95 CI)	*P*-value
Hyperthyroidism	5	548	Fixed	1.11 [0.43, 2.86]	0.83	4	378	–	Not estimable	–
Hypothyroidism	10	2,160	Fixed	0.97 [0.70, 1.36]	0.88	9	1,990	Fixed	0.97 [0.40, 2.33]	0.94
Rash	13	2,479	Fixed	0.96 [0.74, 1.25]	0.76	12	2,309	Fixed	1.00 [0.51, 1.98]	1.00
RCCEP	5	1,510	Fixed	1.49 [0.90, 2.47]	0.12	5	1,510	Fixed	1.10 [0.33, 3.63]	0.88
Urine protein	9	2,052	Fixed	0.87 [0.64, 1.20]	0.40	8	1,910	Fixed	0.76 [0.33, 1.75]	0.52
Diarrhea	13	2,570	Fixed	1.03 [0.80, 1.33]	0.82	11	2,258	Fixed	0.88 [0.47, 1.66]	0.69
Fatigue	13	2,564	Fixed	0.95 [0.76, 1.19]	0.63	11	2,254	Fixed	1.33 [0.70, 2.53]	0.38
Decreased appetite	10	2,169	Fixed	0.98 [0.74, 1.30]	0.88	9	1,999	Fixed	0.87 [0.40, 1.90]	0.72
Fever	10	1,848	Random	4.23 [2.05, 8.71]	<0.001	9	1,978	Fixed	1.36 [0.65, 2.82]	0.42
Pain	4	1,532	Random	2.40 [0.62, 9.32]	0.21	3	1,362	Random	1.77 [0.41, 7.56]	0.44
Pruritus	6	1,798	Fixed	1.00 [0.57, 1.77]	1.00	5	1,628	Fixed	2.76 [0.13, 57.70]	0.51
Muscle soreness	2	168	Fixed	1.12 [0.31, 4.11]	0.86	2	168	Fixed	1.44 [0.20, 10.32]	0.72
Cough	3	298	Fixed	1.21 [0.48, 3.04]	0.69	2	128	–	Not estimable	–
Pneumonia	6	1,919	Fixed	0.85 [0.50, 1.46]	0.56	6	1,919	Fixed	0.85 [0.33, 2.18]	0.74

ALT, alanine aminotransferase; AST, aspartate aminotransferase; GGT, gamma-glutamyl transpeptidase; RCCEP, reactive cutaneous capillary endothelial proliferation; HR, hazard ratio; OR, odds ratio; CI, confidence interval.

immune-targeted therapy alone in terms of CR, ORR, DCR, PFS, and OS, albeit at the cost of escalated AEs concerning liver function.

Additional TACE has been introduced to amplify the local control effect, considering the promising results of immune-targeted therapy including IMbrave150 (3, 9). Since the first report by Liu et al. (48) in 2021, a plethora of pertinent studies regarding transarterial chemo(embolization) combined with immune-targeted therapy, both comparative (16, 19, 28, 29, 32, 34) and non-comparative (48, 49), have emerged. Supplementary Table S7 summarizes the ongoing trials (all from China). Notably, the application spectrum of transarterial chemo(embolization) in China diverges from Western practices (6, 50), extending to downstaging or bridge therapy for resectable HCC (51), conversion therapy for uHCC (52), adjuvant postoperative treatment for high-risk HCC

(8, 53), and salvage therapy for recurrence (54–56). Consistent with a 2022 systematic review (17), all studies originated from China.

A meta-analysis confirmed the superiority of transarterial chemo(embolization) combined with immune-targeted therapy over transarterial chemo(embolization) combined with TKIs regarding the short- and long-term outcomes (57). Unlike TACE combined with TKIs, immune-targeted therapy is preferred for uHCC management globally (6, 58). Our analysis demonstrated that a combination of TACE and immune-targeted therapy significantly bolstered the CR, ORR, and DCR and extended PFS and OS, compared with immune-targeted therapy alone. Noteworthy, the advantage of additional transarterial chemo (embolization) was also corroborated across various clinical scenarios (first-line treatment, TACE or HAIC, with or without extrahepatic metastasis, Child–Pugh A or B, and with or without tumor thrombus, Supplementary Table S6). These findings suggested that additional transarterial chemo(embolization) could potentially ameliorate the prognosis of uHCC, albeit necessitating higher-tier evidence from future studies.

CR and subsequent conversion hepatectomy have gained attention for uHCC (30, 59). Previous non-comparative studies have demonstrated a CR rate and conversion rate of 48% and 60%, respectively (60). However, in this meta-analysis, the CR rate was only reported in 14 studies and the conversion rate was reported in three studies (28, 29, 39), respectively. Moreover, the CR rate ranged from 0% to 22%, which was far beyond people's expectations. This paucity of data warrants a deeper exploration, particularly concerning whether a larger sample size may diminish the perceived benefits of additional transarterial chemo(embolization).

Researchers have underscored the potential of TACE to exacerbate liver damage (61, 62); hence, it is primarily recommended for patients with robust liver function (50, 63). Studies have demonstrated the tolerability of adjunctive TACE to immune-targeted therapy across both single-center (14, 31, 64) and multicenter settings (16, 30), consistent with systematic reviews (17, 57). However, a significant uptick in AEs was revealed in six studies (27, 28, 33, 37, 40, 41), predominantly centering on impaired liver function. Furthermore, we found that the pooled rates of elevated ALT and AST were significantly higher in the transarterial chemo (embolization) plus targeted immunotherapy group than in immune-targeted therapy alone (31.3% vs. 21.6%, 32.2% vs. 24.3%, $P < 0.05$, Table 2). The larger sample size in this analysis unveils these AEs, which are scarcely highlighted in single studies, underscoring the need for safety assessments in larger cohorts. However, other liver function-related indexes such as total bilirubin and prothrombin time and the occurring timepoint of AEs were rarely reported, which deserve more attention in ongoing RCTs. Considering that the safety profile of immune-targeted therapy has been fully inspected in both large RCTs and real-world studies, additional transarterial chemo(embolization) might be the choke point of safety.

Nonetheless, there were several limitations in this meta-analysis. First, the retrospective design of the included studies may have resulted in confounding bias, despite five studies (29, 34, 35, 37, 38) utilizing PSM. Second, reporting bias, notably regarding CR rate and conversion rate, was also inevitable. Third, the inherent heterogeneity within the uHCC patient population would potentially circumscribe the generalizability of our findings beyond this demographic, aside from the differences in the regimen of transarterial chemo(embolization) and immune-targeted therapy. Fourth, immune-targeted therapy is initiated immediately after transarterial chemo(embolization); therefore, the timing of AEs concerning liver function needs to be described. AST and ALT were possibly elevated after transarterial chemo(embolization), suggesting its therapeutic effect. Finally, all studies were from China, and the findings would be applicable only in China.

Conclusion

With the available data, the combination of transarterial chemo (embolization) and immune-targeted therapy surpasses immune-targeted therapy alone regarding local control and long-term efficacy. However, the adjunctive use of transarterial chemo (embolization) escalates the incidence of liver function-related AEs.

Data availability statement

The original contributions presented in the study are included in the article/Supplementary Material. Further inquiries can be directed to the corresponding authors.

Author contributions

HF: Data curation, Formal analysis, Investigation, Project administration, Writing – original draft, Writing – review & editing. QK: Conceptualization, Data curation, Investigation, Methodology, Project administration, Supervision, Validation, Writing – original draft, Writing – review & editing. SW: Data curation, Methodology, Supervision, Validation, Writing – review & editing. QT: Conceptualization, Resources, Writing – review & editing. LW: Conceptualization, Investigation, Project administration, Resources, Supervision, Validation, Writing – original draft, Writing – review & editing.

Funding

The author(s) declare financial support was received for the research, authorship, and/or publication of this article. This study was supported by the Jiangxi Province Natural Science Foundation (20234BAB206086).

Conflict of interest

The authors declare that the research was conducted in the absence of any commercial or financial relationships that could be construed as a potential conflict of interest.

Publisher's note

All claims expressed in this article are solely those of the authors and do not necessarily represent those of their affiliated organizations, or those of the publisher, the editors and the reviewers. Any product that may be evaluated in this article, or claim that may be made by its manufacturer, is not guaranteed or endorsed by the publisher.

Supplementary material

The Supplementary Material for this article can be found online at: https://www.frontiersin.org/articles/10.3389/fimmu.2024.1421520/full#supplementary-material

References

1. Sung H, Ferlay J, Siegel RL, Laversanne M, Soerjomataram I, Jemal A, et al. Global cancer statistics 2020: globocan estimates of incidence and mortality worldwide for 36 cancers in 185 countries. *CA: Cancer J Clin*. (2021) 71:209–49. doi: 10.3322/caac.21660

2. Vogel A, Meyer T, Sapisochin G, Salem R, Saborowski A. Hepatocellular carcinoma. *Lancet (London England)*. (2022) 400:1345–62. doi: 10.1016/s0140-6736(22)01200-4

3. Finn RS, Qin S, Ikeda M, Galle PR, Ducreux M, Kim TY, et al. Atezolizumab plus bevacizumab in unresectable hepatocellular carcinoma. *New Engl J Med*. (2020) 382:1894–905. doi: 10.1056/NEJMoa1915745

4. Xu J, Shen J, Gu S, Zhang Y, Wu L, Wu J, et al. Camrelizumab in combination with apatinib in patients with advanced hepatocellular carcinoma (Rescue): A nonrandomized, open-label, phase ii trial. *Clin Cancer Res an Off J Am Assoc Cancer Res*. (2021) 27:1003–11. doi: 10.1158/1078-0432.Ccr-20-2571

5. Finn RS, Ikeda M, Zhu AX, Sung MW, Baron AD, Kudo M, et al. Phase ib study of lenvatinib plus pembrolizumab in patients with unresectable hepatocellular carcinoma. *J Clin Oncol Off J Am Soc Clin Oncol*. (2020) 38:2960–70. doi: 10.1200/jco.20.00808

6. Reig M, Forner A, Rimola J, Ferrer-Fàbrega J, Burrel M, Garcia-Criado Á, et al. Bclc strategy for prognosis prediction and treatment recommendation: the 2022 update. *J Hepatol*. (2022) 76:681–93. doi: 10.1016/j.jhep.2021.11.018

7. Li S, Mei J, Wang Q, Shi F, Liu H, Zhao M, et al. Transarterial infusion chemotherapy with folfox for advanced hepatocellular carcinoma: A multi-center propensity score matched analysis of real-world practice. *Hepatobiliary Surg Nutr*. (2021) 10:631–45. doi: 10.21037/hbsn.2020.03.14

8. Li SH, Mei J, Cheng Y, Li Q, Wang QX, Fang CK, et al. Postoperative adjuvant hepatic arterial infusion chemotherapy with folfox in hepatocellular carcinoma with microvascular invasion: A multicenter, phase iii, randomized study. *J Clin Oncol Off J Am Soc Clin Oncol*. (2023) 41:1898–908. doi: 10.1200/jco.22.01142

9. Qin S, Ren Z, Feng YH, Yau T, Wang B, Zhao H, et al. Atezolizumab plus bevacizumab versus sorafenib in the chinese subpopulation with unresectable hepatocellular carcinoma: phase 3 randomized, open-label imbrave150 study. *Liver Cancer*. (2021) 10:296–308. doi: 10.1159/000513486

10. Singh P, Toom S, Avula A, Kumar V, Rahma OE. The immune modulation effect of locoregional therapies and its potential synergy with immunotherapy in hepatocellular carcinoma. *J hepatocellular carcinoma*. (2020) 7:11–7. doi: 10.2147/jhc.S187121

11. Pinato DJ, Murray SM, Forner A, Kaneko T, Fessas P, Toniutto P, et al. Trans-arterial chemoembolization as a loco-regional inducer of immunogenic cell death in hepatocellular carcinoma: implications for immunotherapy. *J immunotherapy Cancer*. (2021) 9(9):e003311. doi: 10.1136/jitc-2021-003311

12. Wang B, Xu H, Gao ZQ, Ning HF, Sun YQ, Cao GW. Increased expression of vascular endothelial growth factor in hepatocellular carcinoma after transcatheter arterial chemoembolization. *Acta radiologica (Stockholm Sweden 1987)*. (2008) 49:523–9. doi: 10.1080/02841850801958890

13. Abou-Alfa GK. Tace and sorafenib: A good marriage? *J Clin Oncol Off J Am Soc Clin Oncol*. (2011) 29:3949–52. doi: 10.1200/jco.2011.37.9651

14. Cao F, Yang Y, Si T, Luo J, Zeng H, Zhang Z, et al. The efficacy of tace combined with lenvatinib plus sintilimab in unresectable hepatocellular carcinoma: A multicenter retrospective study. *Front Oncol*. (2021) 11:783480. doi: 10.3389/fonc.2021.783480

15. Chen S, Wu Z, Shi F, Mai Q, Wang L, Wang F, et al. Lenvatinib plus tace with or without pembrolizumab for the treatment of initially unresectable hepatocellular carcinoma harbouring pd-L1 expression: A retrospective study. *J Cancer Res Clin Oncol*. (2022) 148:2115–25. doi: 10.1007/s00432-021-03767-4

16. Chen S, Xu B, Wu Z, Wang P, Yu W, Liu Z, et al. Pembrolizumab plus lenvatinib with or without hepatic arterial infusion chemotherapy in selected populations of patients with treatment-naive unresectable hepatocellular carcinoma exhibiting pd-L1 staining: A multicenter retrospective study. *BMC Cancer*. (2021) 21:1126. doi: 10.1186/s12885-021-08858-6

17. Ke Q, Xin F, Fang H, Zeng Y, Wang L, Liu J. The significance of transarterial chemo(Embolization) combined with tyrosine kinase inhibitors and immune checkpoint inhibitors for unresectable hepatocellular carcinoma in the era of systemic therapy: A systematic review. *Front Immunol*. (2022) 13:913464. doi: 10.3389/fimmu.2022.913464

18. Zhu HD, Li HL, Huang MS, Yang WZ, Yin GW, Zhong BY, et al. Transarterial chemoembolization with pd-(L)1 inhibitors plus molecular targeted therapies for hepatocellular carcinoma (Chance001). *Signal transduction targeted Ther*. (2023) 8:58. doi: 10.1038/s41392-022-01235-0

19. Cao F, Shi C, Zhang G, Luo J, Zheng J, Hao W. Improved clinical outcomes in advanced hepatocellular carcinoma treated with transarterial chemoembolization plus atezolizumab and bevacizumab: A bicentric retrospective study. *BMC Cancer*. (2023) 23:873. doi: 10.1186/s12885-023-11389-x

20. Xin Y, Zhang X, Liu N, Peng G, Huang X, Cao X, et al. Efficacy and safety of lenvatinib plus pd-1 inhibitor with or without transarterial chemoembolization in unresectable hepatocellular carcinoma. *Hepatol Int*. (2023) 17:753–64. doi: 10.1007/s12072-023-10502-3

21. Llovet JM, De Baere T, Kulik L, Haber PK, Greten TF, Meyer T, et al. Locoregional therapies in the era of molecular and immune treatments for hepatocellular carcinoma. *Nat Rev Gastroenterol Hepatol*. (2021) 18:293–313. doi: 10.1038/s41575-020-00395-0

22. Eisenhauer EA, Therasse P, Bogaerts J, Schwartz LH, Sargent D, Ford R, et al. New response evaluation criteria in solid tumours: revised recist guideline (Version 1.1). *Eur J Cancer (Oxford Engl 1990)*. (2009) 45:228–47. doi: 10.1016/j.ejca.2008.10.026

23. Stang A. Critical evaluation of the newcastle-ottawa scale for the assessment of the quality of nonrandomized studies in meta-analyses. *Eur J Epidemiol*. (2010) 25:603–5. doi: 10.1007/s10654-010-9491-z

24. Higgins JP, Thompson SG, Deeks JJ, Altman DG. Measuring inconsistency in meta-analyses. *BMJ (Clinical Res ed)*. (2003) 327:557–60. doi: 10.1136/bmj.327.7414.557

25. Egger M, Davey Smith G, Schneider M, Minder C. Bias in meta-analysis detected by a simple, graphical test. *BMJ (Clinical Res ed)*. (1997) 315:629–34. doi: 10.1136/bmj.315.7109.629

26. Begg CB, Mazumdar M. Operating characteristics of a rank correlation test for publication bias. *Biometrics*. (1994) 50:1088–101. doi: 10.2307/2533446

27. Mei J, Tang YH, Wei W, Shi M, Zheng L, Li SH, et al. Hepatic arterial infusion chemotherapy combined with pd-1 inhibitors plus lenvatinib versus pd-1 inhibitors plus lenvatinib for advanced hepatocellular carcinoma. *Front Oncol*. (2021) 11:618206. doi: 10.3389/fonc.2021.618206

28. Fu Y, Peng W, Zhang W, Yang Z, Hu Z, Pang Y, et al. Induction therapy with hepatic arterial infusion chemotherapy enhances the efficacy of lenvatinib and pd1 inhibitors in treating hepatocellular carcinoma patients with portal vein tumor thrombosis. *J Gastroenterol*. (2023) 58:413–24. doi: 10.1007/s00535-023-01976-x

29. Pan Y, Zhu X, Liu J, Zhong J, Zhang W, Shen S, et al. Systemic therapy with or without transcatheter intra-arterial therapies for unresectable hepatocellular carcinoma: A real-world, multi-center study. *Front Immunol*. (2023) 14:1138355. doi: 10.3389/fimmu.2023.1138355

30. Wu JY, Yin ZY, Bai YN, Chen YF, Zhou SQ, Wang SJ, et al. Lenvatinib combined with anti-pd-1 antibodies plus transcatheter arterial chemoembolization for unresectable hepatocellular carcinoma: A multicenter retrospective study. *J hepatocellular carcinoma*. (2021) 8:1233–40. doi: 10.2147/jhc.S332420

31. Li H, Su K, Guo L, Jiang Y, Xu K, Gu T, et al. Pd-1 inhibitors combined with antiangiogenic therapy with or without transarterial chemoembolization in the

treatment of hepatocellular carcinoma: A propensity matching analysis. *J hepatocellular carcinoma*. (2023) 10:1257–66. doi: 10.2147/jhc.S415843

32. Dong H, Jian Y, Wang M, Liu F, Zhang Q, Peng Z, et al. Hepatic artery intervention combined with immune-targeted therapy is superior to sequential therapy in bclc-C hepatocellular carcinoma. *J Cancer Res Clin Oncol*. (2023) 149:5405–16. doi: 10.1007/s00432-022-04386-3

33. Jin ZC, Chen JJ, Zhu XL, Duan XH, Xin YJ, Zhong BY, et al. Immune checkpoint inhibitors and anti-vascular endothelial growth factor antibody/tyrosine kinase inhibitors with or without transarterial chemoembolization as first-line treatment for advanced hepatocellular carcinoma (Chance2201): A target trial emulation study. *EClinicalMedicine*. (2024) 72:102622. doi: 10.1016/j.eclinm.2024.102622

34. Huang JT, Zhong BY, Jiang N, Li WC, Zhang S, Yin Y, et al. Transarterial chemoembolization combined with immune checkpoint inhibitors plus tyrosine kinase inhibitors versus immune checkpoint inhibitors plus tyrosine kinase inhibitors for advanced hepatocellular carcinoma. *J hepatocellular carcinoma*. (2022) 9:1217–28. doi: 10.2147/jhc.S386672

35. Lang M, Gan L, Ren S, Han R, Ma X, Li G, et al. Lenvatinib plus sintilimab with or without transarterial chemoembolization for intermediate or advanced stage hepatocellular carcinoma: A propensity score-matching cohort study. *Am J Cancer Res*. (2023) 13:2540–53.

36. Qin J, Huang Y, Zhou H, Yi S. Efficacy of sorafenib combined with immunotherapy following transarterial chemoembolization for advanced hepatocellular carcinoma: A propensity score analysis. *Front Oncol*. (2022) 12:807102. doi: 10.3389/fonc.2022.807102

37. Wang J, Zhao M, Han G, Han X, Shi J, Mi L, et al. Transarterial chemoembolization combined with pd-1 inhibitors plus lenvatinib showed improved efficacy for treatment of unresectable hepatocellular carcinoma compared with pd-1 inhibitors plus lenvatinib. *Technol Cancer Res Treat*. (2023) 22:15330338231166765. doi: 10.1177/15330338231166765

38. Yang X, Deng H, Sun Y, Zhang Y, Lu Y, Xu G, et al. Efficacy and safety of regorafenib plus immune checkpoint inhibitors with or without tace as a second-line treatment for advanced hepatocellular carcinoma: A propensity score matching analysis. *J hepatocellular carcinoma*. (2023) 10:303–13. doi: 10.2147/jhc.S399135

39. Hu Y, Pan T, Cai X, He QS, Zheng YB, Huang MS, et al. Addition of transarterial chemoembolization improves outcome of tyrosine kinase and immune checkpoint inhibitors regime in patients with unresectable hepatocellular carcinoma. *J gastrointestinal Oncol*. (2023) 14:1837–48. doi: 10.21037/jgo-23-486

40. Guo Z, Zhu H, Zhang X, Huang L, Wang X, Shi H, et al. The efficacy and safety of conventional transcatheter arterial chemoembolization combined with pd-1 inhibitor and anti-angiogenesis tyrosine kinase inhibitor treatment for patients with unresectable hepatocellular carcinoma: A real-world comparative study. *Front Oncol*. (2022) 12:941068. doi: 10.3389/fonc.2022.941068

41. Dai L, Cai X, Mugaanyi J, Liu Y, Mao S, Lu C, et al. Therapeutic effectiveness and safety of sintilimab-dominated triple therapy in unresectable hepatocellular carcinoma. *Sci Rep*. (2021) 11:19711. doi: 10.1038/s41598-021-98937-2

42. Zhou J, Sun H, Wang Z, Cong W, Wang J, Zeng M, et al. Guidelines for the diagnosis and treatment of hepatocellular carcinoma (2019 edition). *Liver Cancer*. (2020) 9:682–720. doi: 10.1159/000509424

43. Wong JK, Lim HJ, Tam VC, Burak KW, Dawson LA, Chaudhury P, et al. Clinical consensus statement: establishing the roles of locoregional and systemic therapies for the treatment of intermediate-stage hepatocellular carcinoma in Canada. *Cancer Treat Rev*. (2023) 115:102526. doi: 10.1016/j.ctrv.2023.102526

44. Lyu N, Wang X, Li JB, Lai JF, Chen QF, Li SL, et al. Arterial chemotherapy of oxaliplatin plus fluorouracil versus sorafenib in advanced hepatocellular carcinoma: A biomolecular exploratory, randomized, phase iii trial (Fohaic-1). *J Clin Oncol Off J Am Soc Clin Oncol*. (2022) 40:468–80. doi: 10.1200/jco.21.01963

45. Xiang X, Lau WY, Wu ZY, Zhao C, Ma YL, Xiang BD, et al. Transarterial chemoembolization versus best supportive care for patients with hepatocellular carcinoma with portal vein tumor thrombus: a multicenter study. *Eur J Surg Oncol J Eur Soc Surg Oncol Br Assoc Surg Oncol*. (2019) 45:1460–7. doi: 10.1016/j.ejso.2019.03.042

46. Li QJ, He MK, Chen HW, Fang WQ, Zhou YM, Xu L, et al. Hepatic arterial infusion of oxaliplatin, fluorouracil, and leucovorin versus transarterial chemoembolization for large hepatocellular carcinoma: A randomized phase iii trial. *J Clin Oncol Off J Am Soc Clin Oncol*. (2022) 40:150–60. doi: 10.1200/jco.21.00608

47. Zhong BY, Jin ZC, Chen JJ, Zhu HD, Zhu XL. Role of transarterial chemoembolization in the treatment of hepatocellular carcinoma. *J Clin Trans Hepatol*. (2023) 11:480–9. doi: 10.14218/jcth.2022.00293

48. Liu J, Li Z, Zhang W, Lu H, Sun Z, Wang G, et al. Comprehensive treatment of trans-arterial chemoembolization plus lenvatinib followed by camrelizumab for advanced hepatocellular carcinoma patients. *Front Pharmacol*. (2021) 12:709060. doi: 10.3389/fphar.2021.709060

49. Liu BJ, Gao S, Zhu X, Guo JH, Kou FX, Liu SX, et al. Real-world study of hepatic artery infusion chemotherapy combined with anti-pd-1 immunotherapy and tyrosine kinase inhibitors for advanced hepatocellular carcinoma. *Immunotherapy*. (2021) 13:1395–405. doi: 10.2217/imt-2021-0192

50. IBoCMDA SGoID. [Chinese expert consensus on intra-arterial drug and combined drug administration for primary hepatocellular carcinoma]. *Zhonghua nei ke za zhi*. (2023) 62:785–801. doi: 10.3760/cma.j.cn112138-20230202-00049

51. Kulik L, Heimbach JK, Zaiem F, Almasri J, Prokop LJ, Wang Z, et al. Therapies for patients with hepatocellular carcinoma awaiting liver transplantation: A systematic review and meta-analysis. *Hepatol (Baltimore Md)*. (2018) 67:381–400. doi: 10.1002/hep.29485

52. Hu Z, Yang Z, Wang J, Fu Y, Hu Z, Zhou Z, et al. Survival benefit of neoadjuvant hepatic arterial infusion chemotherapy followed by hepatectomy for hepatocellular carcinoma with portal vein tumor thrombus. *Front Pharmacol*. (2023) 14:1223632. doi: 10.3389/fphar.2023.1223632

53. Wang Z, Ren Z, Chen Y, Hu J, Yang G, Yu L, et al. Adjuvant transarterial chemoembolization for hbv-related hepatocellular carcinoma after resection: A randomized controlled study. *Clin Cancer Res an Off J Am Assoc Cancer Res*. (2018) 24:2074–81. doi: 10.1158/1078-0432.Ccr-17-2899

54. Peng Z, Wei M, Chen S, Lin M, Jiang C, Mei J, et al. Combined transcatheter arterial chemoembolization and radiofrequency ablation versus hepatectomy for recurrent hepatocellular carcinoma after initial surgery: A propensity score matching study. *Eur Radiol*. (2018) 28:3522–31. doi: 10.1007/s00330-017-5166-4

55. Peng Z, Chen S, Wei M, Lin M, Jiang C, Mei J, et al. Advanced recurrent hepatocellular carcinoma: treatment with sorafenib alone or in combination with transarterial chemoembolization and radiofrequency ablation. *Radiology*. (2018) 287:705–14. doi: 10.1148/radiol.2018171541

56. Lu J, Zhao M, Arai Y, Zhong BY, Zhu HD, Qi XL, et al. Clinical practice of transarterial chemoembolization for hepatocellular carcinoma: consensus statement from an international expert panel of international society of multidisciplinary interventional oncology (Ismio). *Hepatobiliary Surg Nutr*. (2021) 10:661–71. doi: 10.21037/hbsn-21-260

57. Liu J, Wang P, Shang L, Zhang Z, Tian Y, Chen X, et al. Tace plus tyrosine kinase inhibitors and immune checkpoint inhibitors versus tace plus tyrosine kinase inhibitors for the treatment of patients with hepatocellular carcinoma: A meta-analysis and trial sequential analysis. *Hepatol Int*. (2024) 18:595–609. doi: 10.1007/s12072-023-10591-0

58. Benson AB, D'Angelica MI, Abbott DE, Anaya DA, Anders R, Are C, et al. Hepatobiliary cancers, version 2.2021, nccn clinical practice guidelines in oncology. *J Natl Compr Cancer Network JNCCN*. (2021) 19:541–65. doi: 10.6004/jnccn.2021.0022

59. Wu JY, Zhang ZB, Zhou JY, Ke JP, Bai YN, Chen YF, et al. Outcomes of salvage surgery for initially unresectable hepatocellular carcinoma converted by transcatheter arterial chemoembolization combined with lenvatinib plus anti-pd-1 antibodies: A multicenter retrospective study. *Liver Cancer*. (2023) 12:229–37. doi: 10.1159/000528356

60. Zhang J, Zhang X, Mu H, Yu G, Xing W, Wang L, et al. Surgical conversion for initially unresectable locally advanced hepatocellular carcinoma using a triple combination of angiogenesis inhibitors, anti-pd-1 antibodies, and hepatic arterial infusion chemotherapy: A retrospective study. *Front Oncol*. (2021) 11:729764. doi: 10.3389/fonc.2021.729764

61. Lao XM, Wang D, Shi M, Liu G, Li S, Guo R, et al. Changes in hepatitis B virus DNA levels and liver function after transcatheter arterial chemoembolization of hepatocellular carcinoma. *Hepatol Res Off J Japan Soc Hepatol*. (2011) 41:553–63. doi: 10.1111/j.1872-034X.2011.00796.x

62. Miksad RA, Ogasawara S, Xia F, Fellous M, Piscaglia F. Liver function changes after transarterial chemoembolization in us hepatocellular carcinoma patients: the livert study. *BMC Cancer*. (2019) 19:795. doi: 10.1186/s12885-019-5989-2

63. Cho Y, Choi JW, Kwon H, Kim KY, Lee BC, Chu HH, et al. Transarterial chemoembolization for hepatocellular carcinoma: 2023 expert consensus-based practical recommendations of the korean liver cancer association. *Clin Mol Hepatol*. (2023) 29:521–41. doi: 10.3350/cmh.2023.0202

64. Zheng L, Fang S, Wu F, Chen W, Chen M, Weng Q, et al. Efficacy and safety of tace combined with sorafenib plus immune checkpoint inhibitors for the treatment of intermediate and advanced tace-refractory hepatocellular carcinoma: A retrospective study. *Front Mol Biosci*. (2020) 7:609322. doi: 10.3389/fmolb.2020.609322

frontiers | Frontiers in Immunology

TYPE Original Research
PUBLISHED 23 October 2024
DOI 10.3389/fimmu.2024.1491857

OPEN ACCESS

EDITED BY
Mithun Rudrapal,
Vignan's Foundation for Science, Technology and Research, India

REVIEWED BY
Koyel Kar,
BCDA College of Pharmacy and Technology, India
André Mauricio De Oliveira,
Federal Center for Technological Education of Minas Gerais, Brazil

*CORRESPONDENCE
Wei Wei
weiwei@sysucc.ogr.cn
Rongping Guo
guorp@sysucc.org.cn

†These authors have contributed equally to this work

RECEIVED 05 September 2024
ACCEPTED 30 September 2024
PUBLISHED 23 October 2024

CITATION
Li S, Mei J, Zhao R, Zhou J, Wang Q, Lu L, Li J, Zheng L, Wei W and Guo R (2024) Comparing PD-L1 with PD-1 antibodies combined with lenvatinib and hepatic arterial infusion chemotherapy for unresectable hepatocellular carcinoma.
Front. Immunol. 15:1491857.
doi: 10.3389/fimmu.2024.1491857

Comparing PD-L1 with PD-1 antibodies combined with lenvatinib and hepatic arterial infusion chemotherapy for unresectable hepatocellular carcinoma

Shaohua Li[1,2†], Jie Mei[1,2†], Rongce Zhao[1,2†], Jing Zhou[2,3†], Qiaoxuan Wang[2,4], Lianghe Lu[1,2], Jibin Li[2,5], Lie Zheng[2,6], Wei Wei[1,2*] and Rongping Guo[1,2*]

[1]Department of Liver Surgery, Sun Yat-sen University Cancer Center, Guangzhou, Guangdong, China, [2]State Key Laboratory of Oncology in South China, Guangdong Provincial Clinical Research Center for Cancer, Collaborative Innovation Center for Cancer Medicine, Guangzhou, Guangdong, China, [3]Department of Pathology, Sun Yat-sen University Cancer Center, Guangzhou, Guangdong, China, [4]Department of Radiation Oncology, Sun Yat-sen University Cancer Center, Guangzhou, Guangdong, China, [5]Department of Clinical Research Methodology, Sun Yat-sen University Cancer Center, Guangzhou, Guangdong, China, [6]Department of Radiology, Sun Yat-sen University Cancer Center, Guangzhou, Guangdong, China

Background: A combination of hepatic arterial infusion chemotherapy (HAIC), lenvatinib, and immune checkpoint inhibitors (ICIs) yields a high tumor response rate and survival benefit in unresectable hepatocellular carcinoma (uHCC). However, the selection criteria for different ICIs remain unclear. This study aims to compare the efficacy and safety of PD-1/PD-L1 antibodies combined with HAIC and lenvatinib.

Methods: This retrospective study included 184 patients with uHCC treated with HAIC+lenvatinib+PD-1/PD-L1 antibody from June 2019 to January 2022. We utilized propensity score matching (PSM) to select and match 60 patients treated with HAIC + durvalumab + lenvatinib (HDL) against 60 patients treated with HAIC + PD-1 antibodies + lenvatinib (HPL) to compare the efficacy and safety profiles of these two groups.

Results: After PSM, the baseline characteristics were well-balanced between the HDL and HPL groups. The overall survival (p = 0.293) and progression-free survival (p = 0.146) showed no significant difference. The objective response rate (ORR) was higher in the HDL group compared to the HPL group according to

modified RECIST (74.1% vs. 53.6%, p = 0.022) and RECIST 1.1 (60.3% vs. 41.1%, p = 0.040), respectively. The incidence of grade 3 or 4 adverse events (AEs) was 10.0% and 18.3% (p = 0.191) in the HDL and HPL groups, respectively.

Conclusions: PD-L1 antibody appears to be a preferable companion in the combination therapy of HAIC + ICIs + lenvatinib compared to PD-1 antibody, showing higher ORR and relatively lower incidence of severe AEs. Further prospective studies involving a larger patient population are warranted.

KEYWORDS

hepatocellular carcinoma, PD-1/PD-L1 antibodies, hepatic arterial infusion chemotherapy, lenvatinib, durvalumab, combination therapy, response rate

Introduction

Hepatocellular carcinoma (HCC) ranks as the sixth most common cancer globally and is the third leading cause of cancer-related deaths (1). In China alone, the burden of liver cancer is significant, with approximately 367.7 thousand new cases and 316.5 thousand related deaths reported in 2022 (2). Unfortunately, the 5-year overall survival rate for liver cancer in China remains low at only 14.1% (3). The onset of HCC is often insidious, and the disease progresses rapidly, frequently leading to diagnosis in advanced stages where curative treatments like resection or transplantation are no longer viable options. For many years, there was a dearth of effective systemic treatments for unresectable HCC (uHCC). However, the landscape has changed dramatically with the rapid development of immune and targeted therapies. Key trials such as Imbrave 150, RESCUE, and ORIENT-32 have demonstrated the efficacy of combining targeted therapies with immunotherapy in significantly improving the prognosis of uHCC patients (4, 5). This paradigm shift has offered new hope for patients previously facing limited treatment options.

Despite advancements in systemic therapies, local therapies such as interventional procedures continue to hold a crucial role in the comprehensive management of liver cancer. Clinicians frequently employ a combination of local and systemic therapies to treat uHCC patients, leveraging the benefits of both approaches. Previous studies have underscored the superiority of hepatic arterial infusion chemotherapy (HAIC) combined with immunotherapy and lenvatinib over systemic immunotherapy combined with lenvatinib (6).

In the phase III HIMALAYA study uHCC, STRIDE (Single Tremelimumab Regular Interval Durvalumab) significantly improved overall survival (OS) versus sorafenib, and durvalumab monotherapy was noninferior to sorafenib for OS (7). The recent HIMALAYA study has further bolstered the arsenal against uHCC, demonstrating positive outcomes, particularly in populations from Hong Kong and Taiwan, with notable long-term survival and high objective response rate (ORR) benefits (8). However, despite these advancements, challenges remain, particularly in the choice of immune checkpoint inhibitor (ICI) regimens. A variety of ICIs are currently available in the clinic, of which the most widely used are PD-1 and PD-L1 inhibitors. Nevertheless, there exists a paucity of robust evidence guiding the selection of different ICI regimens in combination therapy for uHCC. To address this gap, the present study aims to retrospectively analyze the impact of various types of immunotherapies on the prognosis of patients with advanced liver cancer. By elucidating the comparative effectiveness of different ICI regimens, this study seeks to provide valuable insights into optimizing treatment strategies for uHCC.

Patients and treatment

Patients

This study was conducted in accordance with the ethical principles outlined in the 1975 Declaration of Helsinki. The analysis of patient data underwent thorough review and received approval from both the Institutional Review Board and Human Ethics Committee at the Sun Yat-sen University Cancer Center (SYSUCC) in Guangzhou, China (Approval Number: B2020-190-01). The study retrospectively included patients diagnosed with uHCC who underwent initial treatment with a combination therapy consisting of HAIC, lenvatinib, and PD-1/PD-L1 antibody from June 2019 to January 2022 at the liver surgery department of Sun Yat-sen University Cancer Center. The inclusion criteria for the study were: (1) Confirmation of HCC diagnosis using either pathological examination or radiological imaging following the Asian Pacific Association for the Study of the Liver (APASL) practice guidelines (9); (2) Unresectable lesions confirmed by multidisciplinary teams; (3) Eastern Cooperative Oncology Group performance status (ECOG PS) of 0-1. (4) Child-Pugh class A liver function; (5) Initial treatment with HAIC + lenvatinib + PD-1/PD-

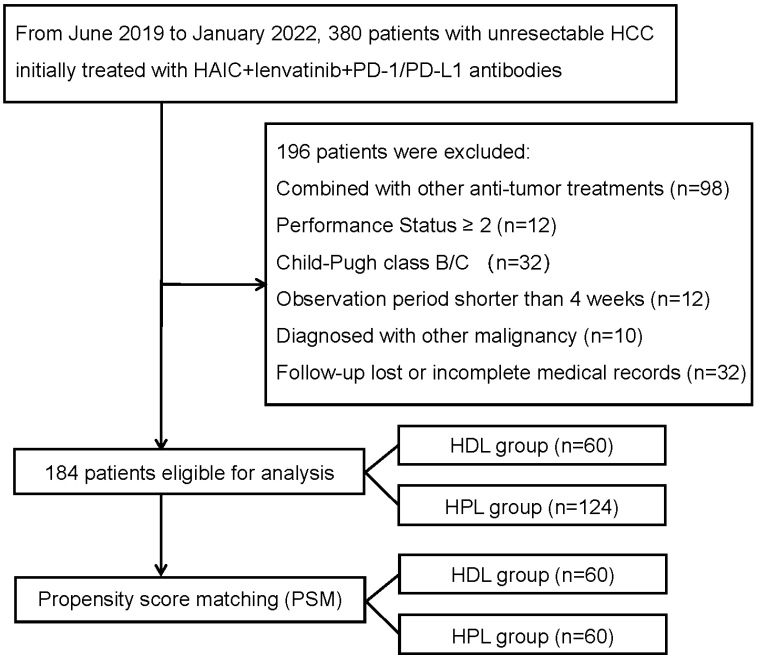

FIGURE 1
The flowchart of the study. HCC, hepatocellular carcinoma; HAIC, hepatic arterial infusion chemotherapy; HDL, HAIC+durvalumab+lenvatinib; HPL, HAIC+PD-1 antibodies+lenvatinib.

L1 antibody triple therapy. The exclusion criteria were: (1) Patients who received other primary anticancer therapy; (2) Patients who underwent other interventional therapies or received targeted or immune drugs during the triple therapy; (3) Patients diagnosed with other malignant tumors; (4) Observation period less than 4 weeks; (5) Patients with incomplete clinical data or loss to follow-up. The flowchart illustrating the progression of patient selection and inclusion is presumably depicted in Figure 1. This rigorous methodology ensures the reliability and validity of the findings while upholding ethical standards in medical research.

Treatment procedures

The procedure for HAIC described follows established protocols and previous studies (10, 11). Percutaneous hepatic artery puncture and catheterization are performed. Superior mesenteric arteriography and hepatic arteriography are conducted to visualize the blood supply to the tumor. A catheter is then inserted into the blood-supplying artery of the tumor. Patients with an indwelling catheter are shifted to the ward. No implanted port system is applied. The catheter is connected to the injection pump in the ward. Chemotherapeutic drugs are continuously pumped: Oxaliplatin: 135 mg/m^2 from 0 to 3 hours on day 1. Leucovorin: 400 mg/m^2 from 3 to 4.5 hours on day 1. Fluorouracil: 400 mg/m^2 from 4.5 to 6.5 hours on day 1. Fluorouracil: 2400 mg/m^2 over 46 hours from day 1 to day 3. Patients remain bedridden during chemotherapy. After completion of infusion chemotherapy, PD-1/PD-L1 antibody is injected the next morning and patients are observed for about 2 hours. If no adverse reactions are observed, discharge is arranged. Oral lenvatinib is started on the day of discharge. Dosages of PD-1/PD-L1 antibody and lenvatinib adhere to drug instructions. Patients in treatment cohorts were treated with HAIC + durvalumab + lenvatinib (HDL), while patients in control cohorts were treated with HAIC + PD-1 antibodies + Lenvatinib (HPL). Informed consent is obtained from all patients before treatment initiation.

Follow-up and assessment

Post-treatment follow-up aligns with routine diagnosis and treatment practices. Reexamination occurs after every two cycles of HAIC. Reexaminations include: enhanced CT/MR of the chest and upper abdomen, electrocardiogram, blood routine, urine routine, biochemistry, coagulation function, tumor markers, etc. Additional examinations such as gastroscopy, thyroid function, and cardiac function if necessary. During treatment, if there's an opportunity for radical treatment such as surgery, active communication with patients and families occurs, and surgery may be proposed after evaluating the risk/benefit ratio.

Patients received enhanced CT/MR of the upper abdomen within 3 days before the initial of treatment. Tumor response rate included objective response rate (ORR) and disease control rate (DCR). ORR was defined as the percentage of complete response (CR) and partial response (PR) which was maintained for at least 4 weeks from the first radiological confirmation, and DCR was defined as the percentage of patients with CR, PR and stable

disease (SD) (12). Tumor response was evaluated according to the modified Response Evaluation Criteria in Solid Tumors (mRECIST) criteria (13) and RECIST 1.1 criteria (14). Adverse events were graded according to the National Cancer Institute Common Terminology Criteria for Adverse Events (NCI-CTCAE) version 5.0. HAIC treatment can be performed up to 8 times. If the patient's treatment is effective but imaging shows no significant enhancement of the tumor artery, or if liver angiography shows that the tumor has been mostly de-vascularized, HAIC is terminated. Lenvatinib combined with PD-1/PD-L1 maintenance treatment will be used. If the tumor progresses, appropriate follow-up treatment will be decided by the supervising physician based on the individual patient's condition and response to therapy. In such cases, maintenance treatment with lenvatinib combined with PD-1/PD-L1 inhibitors may be initiated.

Statistical analysis

The statistical analysis conducted to compare baseline characteristics between the treatment and control groups utilized various tests depending on the nature of the variables. Here's a breakdown of the methods employed: The distribution of categorical variables was compared using either Pearson's $\chi 2$ test or Fisher's exact test. For normally distributed continuous variables, the mean and standard deviation were calculated to describe the variable distribution. Student's t-test was then used to assess the difference in means between the treatment and control groups. For non-normally distributed continuous variables, the median and range were used to describe the variable distribution. The Mann-Whitney test, a non-parametric test, was employed to compare the distributions of these variables between the groups. All statistical analyses were performed using the Statistical Package for the Social Sciences (SPSS) software, version 24.0, developed by SPSS Inc. located in Chicago, IL, USA. A significance level of $P < 0.05$ (two-tailed) was chosen to determine statistical significance. This threshold indicates that the observed differences between the groups are unlikely to have occurred due to random chance alone.

Results

Patient characteristics

This study included a retrospective analysis of 184 cases of uHCC patients who underwent HAIC combined with lenvatinib and either a PD-1 or PD-L1 antibody triple therapy at the Department of Liver Surgery, Sun Yat-sen University Cancer Center, from June 2019 to January 2022. The distribution of patients was 60 cases in the HAIC + lenvatinib + PD-L1 antibody combined therapy group (HDL group) and 124 cases in the HAIC + lenvatinib + PD-1 antibody combined therapy group (HPL group). Notably, all patients in the HDL group received durvalumab (AstraZeneca), while the specific PD-1 antibodies used in the

TABLE 1 Baseline characteristics of patients in the HDL group and the HPL group.

	HDL group (n=60)	HPL group (n=124)	p value
Age (yr)	51.2 ± 1.5	53.0 ± 1.1	0.321
Gender			0.149
Male,N.(%)	53 (88.3)	117 (94.4)	
Female,N,(%)	7 (11.7)	7 (5.6)	
WBC ($\times 10^9$/L)	6.47 (2.80-12.83)	6.87 (2.57-17.71)	0.066
NE ($\times 10^9$/L)	4.405 (1.11-10.47)	4.40 (1.33-13.69)	0.179
Hgb (g/L)	142.8 ± 2.8	144.0 ± 1.9	0.724
PLT ($\times 10^9$/L)	207 (69-714)	214 (59-662)	0.693
ALT (U/L)	42.45 (0.4-162.1)	48.1 (11.1-251.3)	0.152
ALB (g/L)	42.2 (28.3-51.4)	42.1 (29.6-50.5)	0.647
TBil (umol/L)	14.8 (5.9-55.2)	16.3 (6.0-62.8)	0.193
PT (s)	11.65 (10.2-15.1)	12.0 (9.7-17.1)	0.105
CRE (umol/L)	71.0 ± 1.7	73.2 ± 1.4	0.352
Cycles of HAIC	4 (1-6)	3 (1-7)	0.112
AFP (ng/ml)			0.984
≤400,N.(%)	27 (45.0)	56 (45.2)	
>400,N.(%)	33 (55.0)	68 (54.8)	
HBsAg			0.931
Negative,N.(%)	9 (15.0)	18 (14.5)	
Positive,N.(%)	51 (85.0)	106 (85.5)	
Anti-HCV			0.555
Negative,N.(%)	57 (95.0)	120 (96.8)	
Positive,N.(%)	3 (5.0)	4 (3.2)	
HBV-DNA			0.837
≤1×10^3 copies,N.(%)	30 (50.0)	60 (48.4)	
>1×10^3 copies,N.(%)	30 (50.0)	64 (51.6)	
Maximum diameter of tumor (cm)	10.55 (3.4-19.3)	10.0 (1.3-22.1)	0.141
Tumor numbers			0.012
Single,N.(%)	7 (11.7)	35 (28.2)	
Multiple,N.(%)	53 (88.3)	89 (71.8)	
Tumor distribution			0.010
Uni-lobe,N.(%)	18 (30.0)	62 (50.0)	
Bi-lobe,N.(%)	42 (70.0)	62 (50.0)	
Macrovascular invasion			0.955
Absent,N.(%)	23 (38.3)	47 (37.9)	
Present,N.(%)	37 (61.7)	77 (62.1)	

(Continued)

10.3389/fimmu.2024.1491857

TABLE 1 Continued

	HDL group (n=60)	HPL group (n=124)	p value
Distant metastasis			0.884
Absent,N.(%)	40 (66.7)	84 (67.7)	
Present,N.(%)	20 (33.3)	40 (32.3)	
Subsequent operation			0.323
Yes,N.(%)	6 (10.0)	19 (15.3)	
No,N.(%)	54 (90.0)	105 (84.7)	

HDL, HAIC+durvalumab+lenvatinib; HPL, HAIC+PD-1 antibodies+lenvatinib; WBC, white blood cell; NE, neutrophil; Hgb, hemoglobin; PLT, platelet; ALB, albumin; ALT, alanine aminotransferase; PT, prothrombin; TBIL, total bilirubin; CRE, Creatinine; AFP, alpha-fetoprotein; HAIC, hepatic arterial infusion chemotherapy.

TABLE 2 Baseline characteristics of patients in the HDL group and the HPL group after PSM.

	HDL group (n=60)	HPL group (n=60)	p value
Age (yr)	51.2 ± 1.5	53.5 ± 1.6	0.303
Gender			0.186
Male	53 (88.3%)	57 (95.0%)	
Female	7 (11.7%)	3 (5.0%)	
WBC ($\times10^9$/L)	6.47 (2.80-12.83)	6.90 (3.79-17.71)	0.142
NE ($\times10^9$/L)	4.405 (1.11-10.47)	4.475 (1.70-13.69)	0.352
Hgb (g/L)	142.8 ± 2.8	143.3 ± 2.6	0.907
PLT ($\times10^9$/L)	207 (69-714)	202.5 (91-662)	0.439
ALT (U/L)	42.45 (0.4-162.1)	49.8 (16.2-209.8)	0.078
ALB (g/L)	42.2 (28.3-51.4)	41.7 (31.0-50.5)	0.723
TBil (umol/L)	14.8 (5.9-55.2)	16.3 (7.0-36.0)	0.099
PT (s)	11.65 (10.2-15.1)	12.3 (10.2-16.3)	0.058
CRE (umol/L)	71.0 ± 1.7	72.2 ± 2.0	0.630
Cycles of HAIC	4 (1-6)	3.5 (1-7)	0.586
AFP (ng/ml)			1.000
≤400	27 (45.0%)	27 (45.0%)	
>400	33 (55.0%)	33 (55.0%)	
HBsAg			1.000
Negative	9 (15.0%)	9 (15.0%)	
Positive	51 (85.0%)	51 (85.0%)	
Anti-HCV			0.619
Negative	57 (95.0%)	59 (98.3%)	
Positive	3 (5.0%)	1 (1.7%)	
HBV-DNA			0.715
≤1×10^3 copies	30 (50.0%)	32 (53.3%)	
>1×10^3 copies	30 (50.0%)	28 (46.7%)	
Maximum diameter of tumor (cm)	10.55 (3.4-19.3)	9.95 (2.0-22.1)	0.153
Tumor numbers			0.037
Single	7 (11.7%)	16 (26.7%)	
Multiple	53 (88.3%)	44 (73.3%)	
Tumor distribution			0.130
Uni-lobe	18 (30.0%)	26 (43.3%)	
Bi-lobe	42 (70.0%)	34 (56.7%)	
Macrovascular invasion			0.245
Absent	23 (38.3%)	17 (28.3%)	
Present	37 (61.7%)	43 (71.7%)	
Distant metastasis			1.000
Absent	40 (66.7%)	40 (66.7%)	
Present	20 (33.3%)	20 (33.3%)	
Subsequent operation			0.408
Yes	6 (10.0%)	9 (15.0%)	
No	54 (90.0%)	51 (85.0%)	

PSM, propensity score matching; HDL, HAIC+durvalumab+ lenvatinib; HPL, HAIC+PD-1 antibodies+lenvatinib; WBC, white blood cell; NE, neutrophil; Hgb, hemoglobin; PLT, platelet; ALB, albumin; ALT, alanine aminotransferase; PT, prothrombin; TBIL, total bilirubin; CRE, Creatinine; AFP, alpha-fetoprotein; HAIC, hepatic arterial infusion chemotherapy.

HPL group were detailed in Supplementary Table 1. Our analysis revealed significant differences in the proportion of multiple tumors and lesions involving both livers between the HDL and HPL groups (p=0.012 and 0.010, respectively), as indicated in Table 1. To address potential biases inherent in retrospective analyses, we employed (PSM) to match and screen selected cases (15). The propensity-score model included gender, serum alpha-fetoprotein (AFP) levels before treatment (≤ or > 400 ng/ml), tumor numbers (single or multiple), liver involvement (unilateral or bilateral), macrovascular invasion (absent or present), and distant metastasis (absent or present). Patients in the HDL and HPL groups were matched in a 1:1 ratio, with a nearest neighbor caliper width of 0.2. This process resulted in a total of 120 patients included in the paired analysis, with 60 patients in each group. Following pairing, the baseline characteristics of the two groups were essentially similar, as summarized in Table 2.

Efficacy analysis

The median OS and PFS are not evaluated on the data cut-off date of Match 10, 2023. The provided data illustrates the outcomes of two treatment groups, HDL and HPL, in terms of overall survival

(OS) and progression-free survival (PFS) rates at various time intervals. For the HDL group, the OS rates at 6, 12, and 18 months were 94.5%, 89.5%, and 77.5%, respectively. In comparison, the HPL group exhibited OS rates of 97.4%, 86.8%, and 72.8% at the same intervals. Statistical analysis indicated no significant difference in OS between the two groups (p=0.607). In terms of PFS, the HDL group showed rates of 85.4%, 68.2%, and 51.2% at 6, 12, and 18 months, respectively. Contrastingly, the PFS rates for the HPL group were 81.4%, 46.3%, and 27.2% at the corresponding time points. Although the PFS rate of the HDL group suggested a trend of superiority over the HPL group, this difference was not statistically significant (p=0.078) (Figures 2A, B). Following PSM, the OS rates at 6, 12, and 18 months in the HDL group were 94.5%, 89.5%, and 77.5%, respectively, while those at 6, 12, and 18 months in the HPL group were 96.3%, 83.2%, and 71.1%, respectively, with no significant difference (p=0.293). The PFS rates at 6, 12, and 18 months in the HDL group were 85.4%, 68.2%, and 51.2%, respectively. The PFS rates at 6, 12, and 18 months in the HPL group were 82.1%, 43.4%, and 31.2%, respectively. There was no significant difference between the two groups (p=0.146) (Figures 2C, D). Subgroup analysis, as depicted in Figures 3A, B, highlighted similar OS benefits between the HDL and HPL groups across different subgroups. However, PFS benefits favored the HDL group in tumors with a maximum diameter ≤10 cm and involving both liver lobes.

The treatment response is summarized in Table 3. In matching paired population, the CR rate (17.2%) of the HDL group was still significantly higher than HPL group (5.4%, p=0.046), and the ORR was 74.1%, which was also significantly higher than that of the HPL group (53.6%, p=0.022) according to mRECIST; and according to RECIST 1.1, ORR in the HDL group (60.3%) was significantly better than the 41.1% in the HPL group (p=0.040) as well. The individual tumor response is shown in Figure 4.

Safety analysis

All adverse events (AEs) are listed in Table 4. The most common AEs happened were pain (48.33%), ALT level elevated (40%), Thrombocytopenia (30%), and anemia (23.33%) in the HDL group, and pain (41.67%), ALT level elevated (35%), vomiting (33.33%), and anemia (30%) in HPL group. The incidence rates of all grades of AEs were similar in the two groups, 93.3% in the HDL group and 96.67% in the HPL group (p=0.679). The HPL

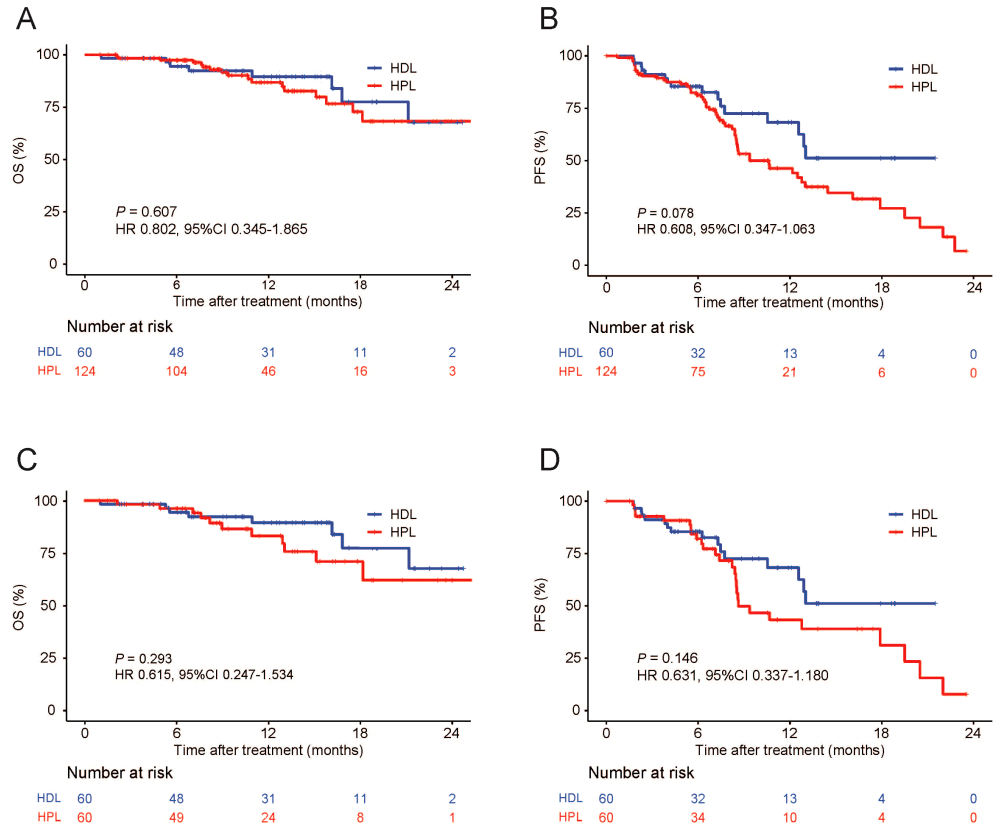

FIGURE 2
Kaplan–Meier curves for OS and PFS. Primary cohort **(A, B)**, PSM cohort **(C, D)**. OS, overall survival; PFS, progression-free survival; PSM, propensity score matching; HDL, HAIC+durvalumab+lenvatinib; HPL, HAIC+PD-1 antibodies+lenvatinib.

10.3389/fimmu.2024.1491857

group exhibited a reduced proportion of patients experiencing Grade 1-2 anorexia (8.3% vs. 28.3%, p=0.008) and Grade 1-2 hyperbilirubinemia (1.7% vs. 16.7%, p=0.008) compared to the HDL group. The incidence of Grade ≥3 AEs was lower in the HDL group at 10% compared to 18.3% in the HPL group, although this difference was not statistically significant (p= 0.191).

Discussion

The combination of local therapies with systemic treatments such as immunotherapy and targeted therapy has become a common approach in treating advanced liver cancer. This strategy aims to provide both localized control of the tumor and systemic

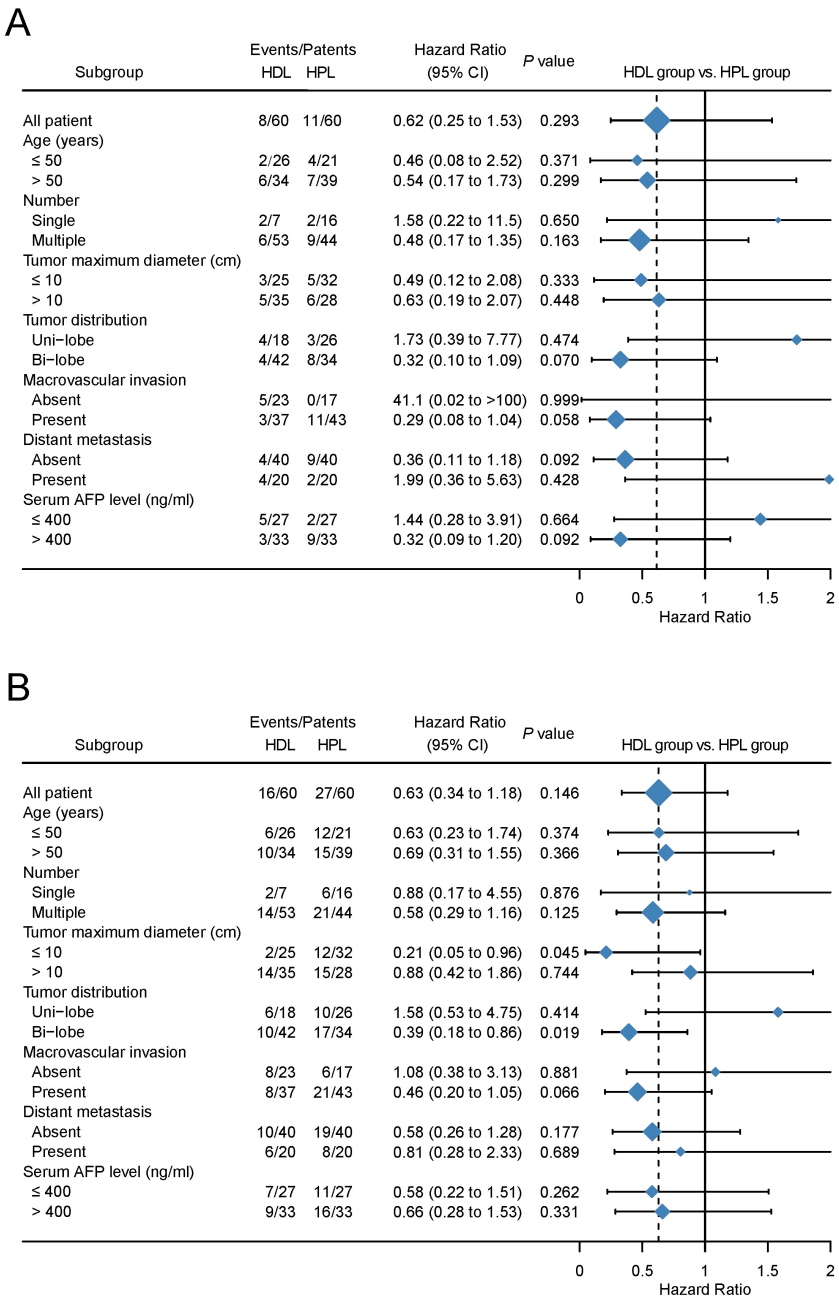

FIGURE 3
Forest plots by subgroup for OS **(A)** and PFS **(B)**.

10.3389/fimmu.2024.1491857

TABLE 3 Tumor response in patients in the HDL group and the HPL group after PSM.

	HDL group (n=58)	HPL group (n=56)	*P* value
mRECIST			
CR	10 (17.2%)	3 (5.4%)	0.046
PR	33 (56.9%)	27 (48.2%)	0.353
SD	11 (19.0%)	23 (41.1%)	0.010
PD	4 (6.9%)	3 (5.4%)	0.732
ORR	43 (74.1%)	30 (53.6%)	0.022
DCR	54 (93.1%)	53 (94.6%)	0.732
RECIST 1.1			
CR	0 (0.0%)	0 (0.0%)	1.000
PR	35 (60.3%)	23 (41.1%)	0.040
SD	19 (32.8%)	30 (53.6%)	0.025
PD	4 (6.9%)	3 (5.4%)	0.732
ORR	35 (60.3%)	23 (41.1%)	0.040
DCR	54 (93.1%)	53 (94.6%)	0.732

PSM, propensity score matching; HDL, HAIC+durvalumab+ lenvatinib; HPL, HAIC+PD-1 antibodies+lenvatinib; mRECIST, modified response evaluation criteria in solid tumors; RECIST, response evaluation criteria in solid tumors.

disease management. Studies have suggested that HAIC may offer advantages over transarterial chemoembolization (TACE) as a local treatment for advanced liver cancer patients (16, 17). Additionally, our research group's findings indicate that combining HAIC with lenvatinib and immunotherapy yields better efficacy compared to using lenvatinib and immunotherapy alone (6). The selection between PD-1 and PD-L1 inhibitors for immunotherapy has become crucial for clinicians. Understanding the differences in efficacy and safety profiles between these agents is essential for optimizing treatment outcomes.

In this study, The baseline is equilibrium between HDL and HPL groups after matching. In this retrospective study, the baseline clinical characteristics of patients showed a heavy tumor burden, with a maximum diameter of tumor in the HDL group of 10.55 (3.4-19.3) cm and in the HPL group of 9.95 (2.0-22.1) cm, with macroscopic invasion in more than 60% of patients and distance metastasis in more than 30% of patients. After PSM, There was no significant difference in OS rates between the HDL and HPL groups at 6, 12, and 18 months. After PSM, the PFS rates at 6, 12, and 18 months in the HDL group were 85.4%, 68.2%, and 51.2%, respectively. The PFS rates at 6, 12, and 18 months in the HPL group were 82.1%, 43.4%, and 31.2%, respectively, The PFS rate of the HDL group showed a trend of being superior to the HPL group, but there was still no statistically significant difference. We speculate that the reason why the benefit trend of PFS has not been translated into the benefit of OS may be due to the blurring of this difference by posterior treatment. The subgroup analysis of OS and PFS showed that the OS benefits of the two groups were similar, while the PFS benefits the HDL group in the tumors with a maximum diameter ≤ 10 cm and involving both livers. The lack of translation of PFS benefits into OS benefits could be attributed to subsequent treatments received by patients after the initial therapy, which might have confounded the survival outcomes. Subgroup analysis revealed similar OS benefits between the two treatment groups. However, the HDL group showed improved PFS in tumors with a maximum diameter of ≤10 cm and involving both liver lobes.

Results showed the ORR was higher in the HDL group than in the HPL group according to modified RECIST (mRECIST) (74.1% vs. 53.6%, p = 0.022) and RECIST 1.1 (60.3% vs. 41.1%, p = 0.040) respectively. The results of the HPL group ORR and retrospective study report on PD-1 combined with lenvatinib and HAIC in the treatment of HCC are similar (18). Harvard University's Manish J. Butte et al. found that in addition to binding to PD-1, PD-L1 can also bind to B7.1 molecules (19). B7.1 is a co-stimulatory molecule expressed on the surface of antigen-presenting dendritic cells, which can bind to CD28 molecules on T cells to activate them. Dendritic cells inherently express PD-L1 molecules and can interact

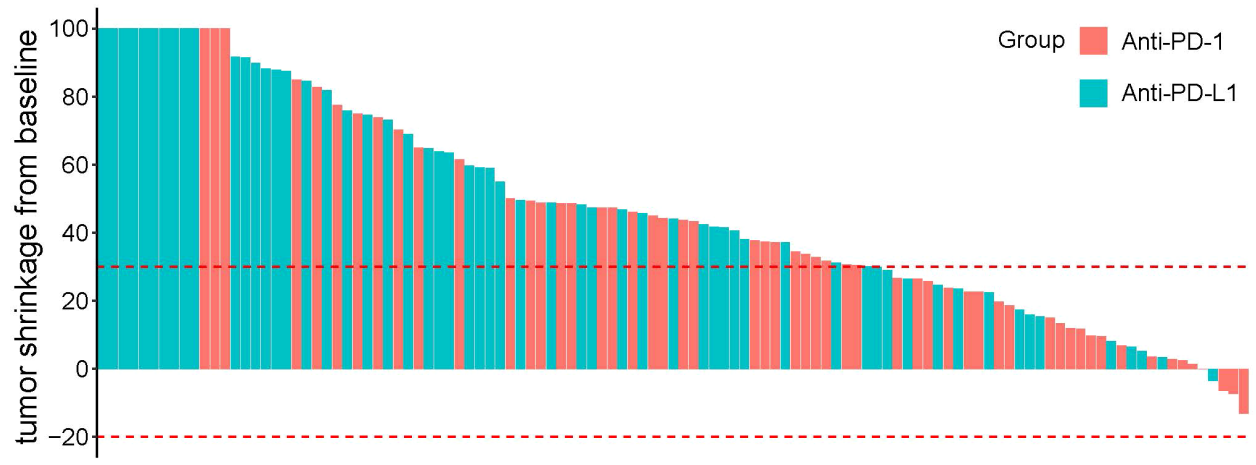

FIGURE 4
Chart of individual tumor response.

TABLE 4 Summary of treatment-related adverse events.

Adverse Events,N(%)		HDL group (n=60)	HPL group (n=60)	p-value
Overall	All grades	56 (93.3)	58 (96.7)	0.679
	≥3 grade	6 (10.0)	11 (18.3)	0.191
ALT level elevated	All grades	24 (40.0)	21 (35.0)	0.706
	≥3 grade	0 (0.0)	0 (0.0)	NA
Anorexia	All grades	5 (8.3)	17 (28.3)	0.008
	≥3 grade	0 (0.0)	0 (0.0)	NA
Diarrhea	All grades	11 (18.3)	10 (16.7)	1.000
	≥3 grade	0 (0.0)	0 (0.0)	NA
Anemia	All grades	14 (23.3)	18 (30.0)	0.536
	≥3 grade	0 (0.0)	0 (0.0)	NA
Constipation	All grades	9 (15.0)	5 (8.3)	0.394
	≥3 grade	0 (0.0)	0 (0.0)	NA
Pain	All grades	29 (48.3)	25 (41.7)	0.582
	≥3 grade	0 (0.0)	1 (1.6)	1.000
Vomiting	All grades	11 (18.3)	20 (33.3)	0.094
	≥3 grade	0 (0.0)	1 (1.6)	1.000
Rash	All grades	8 (13.3)	4 (6.7)	0.362
	≥3 grade	2 (3.3)	0 (0.0)	0.496
Leukocytopenia	All grades	7 (11.7)	14 (23.3)	0.148
	≥3 grade	0 (0.0)	3 (5.0)	0.244
Neutropenia	All grades	10 (16.7)	17 (28.3)	0.189
	≥3 grade	1 (1.7)	7 (11.7)	0.061
Hypertension	All grades	7 (11.7)	8 (13.3)	1.000
	≥3 grade	0 (0.0)	1 (1.7)	1.000
Hypoalbuminemia	All grades	11 (18.3)	7 (11.7)	0.444
	≥3 grade	0 (0.0)	0 (0.0)	NA
Thrombocytopenia	All grades	18 (30.0)	14 (23.3)	0.536
	≥3 grade	2 (3.3)	0 (0.0)	0.496
Edema	All grades	3 (5.0)	4 (6.7)	1.000
	≥3 grade	0 (0.0)	0 (0.0)	NA
PT prolong	All grades	1 (1.7)	0 (0.0)	1.000
	≥3 grade	0 (0.0)	0 (0.0)	NA
Fever	All grades	2 (3.3)	7 (11.7)	0.163
	≥3 grade	0 (0.0)	0 (0.0)	NA
Cough	All grades	2 (3.3)	1 (1.7)	1.000
	≥3 grade	0 (0.0)	0 (0.0)	NA
Dysuria	All grades	3 (5.0)	4 (6.7)	1.000
	≥3 grade	0 (0.0)	0 (0.0)	NA

(Continued)

TABLE 4 Continued

Adverse Events,N(%)		HDL group (n=60)	HPL group (n=60)	p-value
Insomnia	All grades	2 (3.3)	2 (3.3)	1.000
	≥3 grade	0 (0.0)	0 (0.0)	NA
pulmonary embolism	All grades	1 (1.7)	0 (0.0)	1.000
	≥3 grade	1 (1.7)	0 (0.0)	1.000
Hyperbilirubinemia	All grades	1 (1.7)	10 (16.7)	0.008
	≥3 grade	0 (0.0)	1 (1.7)	1.000
GI bleeding	All grades	0 (0.0)	1 (1.7)	1.000
	≥3 grade	0 (0.0)	1 (1.7)	1.000
Arrhythmia	All grades	0 (0.0)	1 (1.7)	1.000
	≥3 grade	0 (0.0)	0 (0.0)	NA
Infection	All grades	0 (0.0)	3 (5.0)	0.244
	≥3 grade	0 (0.0)	1 (1.7)	1.000
perianal abscess	All grades	0 (0.0)	1 (1.7)	1.000
	≥3 grade	0 (0.0)	1 (1.7)	1.000

HDL, HAIC+durvalumab+lenvatinib; HPL, HAIC+PD-1 antibodies+lenvatinib; ALT, alanine aminotransferase; GI, gastrointestinal; NA, not applicable.

with their own B7.1 (20). PD-L1 monoclonal antibody may actually rescue these dendritic cells that are inhibited by PD-L1. This suggests that PD-L1 may have a higher ORR in anti-tumor therapy.

PD-L1 inhibitors are noted for their ability to preserve immune balance by not blocking PD-L2. This characteristic reduces the risk of severe immune-related adverse events (irAEs) (21). A meta-analysis of non-small cell lung cancer (NSCLC) patient data suggests that compared to PD-L1 inhibitor treatment, PD-1 inhibitor treatment may increase the incidence of irAEs, both in terms of any grade and high-grade (3-4 grades) irAEs (22). Durvalumab, an engineered Ig1 antibody, does not induce antibody-dependent cell-mediated cytotoxicity (ADCC) effects (23). In the safety analysis mentioned, it was observed that the incidence of any level of hyperbilirubinemia and anorexia was lower in the HDL group compared to the HPL group.

The results of this study indicate that triple therapy with PD-L1 yields significantly better tumor reduction effects than triple therapy with PD-1, and it also has a lower incidence of severe adverse events (AEs). Further prospective studies involving a larger patient population are necessary. Given the promising efficacy and safety of HAIC combined with lenvatinib and PD-L1 in clinical practice, our group initiated a prospective study (HDL-001, NCT04961918) to further evaluate this treatment regimen and address the remaining questions from this paper.

Conclusion

In conclusion, PD-L1 antibody seems to be a better companion in the combination therapy of HAIC+ICIs+lenvatinib than PD-1 antibody for higher ORR and lower incidence of severe AEs. Further prospective study involving a larger population of patients is required.

Data availability statement

The original contributions presented in the study are included in the article/Supplementary Material. Further inquiries can be directed to the corresponding authors.

Ethics statement

The studies involving humans were approved by the Institutional Review Board and Human Ethics Committee at the Sun Yat-sen University Cancer Center (SYSUCC) in Guangzhou, China (Approval Number: B2020-190-01). The studies were conducted in accordance with the local legislation and institutional requirements. The ethics committee/institutional review board waived the requirement of written informed consent for participation from the participants or the participants' legal guardians/next of kin because this is a retrospective study, data are anonymized.

Author contributions

JM: Conceptualization, Data curation, Methodology, Software, Writing – original draft, Writing – review & editing. SL: Conceptualization, Data curation, Resources, Writing – original draft, Writing – review & editing. RZ: Data curation, Funding

acquisition, Software, Writing – review & editing. JZ: Methodology, Software, Writing – review & editing. QW: Resources, Software, Writing – review & editing. LL: Investigation, Software, Writing – review & editing. JL: Methodology, Writing – review & editing. LZ: Software, Writing – review & editing. WW: Conceptualization, Project administration, Supervision, Writing – review & editing. RG: Conceptualization, Project administration, Supervision, Validation, Writing – review & editing.

Funding

The author(s) declare financial support was received for the research, authorship, and/or publication of this article. This study was supported by the National Natural Science Foundation of China (No. 82172579, No.82303879, No.82303875, No.82203111); Science and Technology Planning Project of Guangzhou (No.2023A04J1777, No. 2023A04J1781, No.202206080016); Clinical Trials Project (5010 Project) of Sun Yat-sen University (No.5010-2017009, No. 5010-2023001). Guangdong Medical Science and Technology Research Fund Project (A2022366).

Acknowledgments

The authors acknowledge and express their deepest gratitude to the participants of this research.

Conflict of interest

The authors declare that the research was conducted in the absence of any commercial or financial relationships that could be construed as a potential conflict of interest.

Generative AI statement

The author(s) declare that no Generative AI was used in the creation of this manuscript.

Publisher's note

Supplementary material

The Supplementary Material for this article can be found online at: https://www.frontiersin.org/articles/10.3389/fimmu.2024.1491857/full#supplementary-material

References

1. Bray F, Laversanne M, Sung H, Ferlay J, Siegel RL, Soerjomataram I, et al. Global cancer statistics 2022: GLOBOCAN estimates of incidence and mortality worldwide for 36 cancers in 185 countries. *CA Cancer J Clin*. (2024) 74:229–63. doi: 10.3322/caac.21834

2. Han B, Zheng R, Zeng H, Wang S, Sun K, Chen R, et al. Cancer incidence and mortality in China, 2022. *J Natl Cancer Cent*. (2024) 4:47–53. doi: 10.1016/j.jncc.2024.01.006

3. Allemani C, Matsuda T, Di Carlo V, Harewood R, Matz M, Niksic M, et al. Global surveillance of trends in cancer survival 2000-14 (CONCORD-3): analysis of individual records for 37 513 025 patients diagnosed with one of 18 cancers from 322 population-based registries in 71 countries. *Lancet*. (2018) 391:1023–75. doi: 10.1016/S0140-6736(17)33326-3

4. Finn RS, Qin S, Ikeda M, Galle PR, Ducreux M, Kim TY, et al. Atezolizumab plus bevacizumab in unresectable hepatocellular carcinoma. *N Engl J Med*. (2020) 382:1894–905. doi: 10.1056/NEJMoa1915745

5. Ren Z, Xu J, Bai Y, Xu A, Cang S, Du C, et al. Sintilimab plus a bevacizumab biosimilar (IBI305) versus sorafenib in unresectable hepatocellular carcinoma (ORIENT-32): a randomised, open-label, phase 2-3 study. *Lancet Oncol*. (2021) 22:977–90. doi: 10.1016/S1470-2045(21)00252-7

6. Mei J, Tang YH, Wei W, Shi M, Zheng L, Li SH, et al. Hepatic arterial infusion chemotherapy combined with PD-1 inhibitors plus lenvatinib versus PD-1 inhibitors plus lenvatinib for advanced hepatocellular carcinoma. *Front Oncol*. (2021) 11:618206. doi: 10.3389/fonc.2021.618206

7. Abou-Alfa GK, Lau G, Kudo M, Chan SL, Kelley RK, Furuse J, et al. Tremelimumab plus durvalumab in unresectable hepatocellular carcinoma. *NEJM Evid*. (2022) 1:EVIDoa2100070. doi: 10.1056/EVIDoa2100070

8. Lau G, Abou-Alfa GK, Cheng AL, Sukeepaisarnjaroen W, Dao TV, Kang YK, et al. Outcomes in the Asian subgroup of the phase III randomised HIMALAYA study of tremelimumab plus durvalumab in unresectable hepatocellular carcinoma. *J Hepatol*. (2024). doi: 10.1016/j.jhep.2024.07.017

9. Shiina S, Gani RA, Yokosuka O, Maruyama H, Nagamatsu H, Payawal DA, et al. APASL practical recommendations for the management of hepatocellular carcinoma in the era of COVID-19. *Hepatol Int*. (2020) 14:920–9. doi: 10.1007/s12072-020-10103-4

10. He M, Li Q, Zou R, Shen J, Fang W, Tan G, et al. Sorafenib plus hepatic arterial infusion of oxaliplatin, fluorouracil, and leucovorin vs sorafenib alone for hepatocellular carcinoma with portal vein invasion: A randomized clinical trial. *JAMA Oncol*. (2019) 5:953–60. doi: 10.1001/jamaoncol.2019.0250

11. Li S, Mei J, Wang Q, Guo Z, Lu L, Ling Y, et al. Postoperative adjuvant transarterial infusion chemotherapy with FOLFOX could improve outcomes of hepatocellular carcinoma patients with microvascular invasion: A preliminary report of a phase III, randomized controlled clinical trial. *Ann Surg Oncol*. (2020) 27:5183–90. doi: 10.1245/s10434-020-08601-8

12. Wolchok JD, Hoos A, O'day S, Weber JS, Hamid O, Lebbe C, et al. Guidelines for the evaluation of immune therapy activity in solid tumors: immune-related response criteria. *Clin Cancer Res*. (2009) 15:7412–20. doi: 10.1158/1078-0432.CCR-09-1624

13. Lencioni R, Llovet JM. Modified RECIST (mRECIST) assessment for hepatocellular carcinoma. *Semin Liver Dis*. (2010) 30:52–60. doi: 10.1055/s-0030-1247132

14. Eisenhauer EA, Therasse P, Bogaerts J, Schwartz LH, Sargent D, Ford R, et al. New response evaluation criteria in solid tumours: revised RECIST guideline (version 1.1). . *Eur J Cancer*. (2009) 45:228–47. doi: 10.1016/j.ejca.2008.10.026

15. Chen JW, Maldonado DR, Kowalski BL, Miecznikowski KB, Kyin C, Gornbein JA, et al. Best practice guidelines for propensity score methods in medical research: consideration on theory, implementation, and reporting. A review. *Arthroscopy*. (2022) 38:632–42. doi: 10.1016/j.arthro.2021.06.037

16. Li S, Mei J, Wang Q, Shi F, Liu H, Zhao M, et al. Transarterial infusion chemotherapy with FOLFOX for advanced hepatocellular carcinoma: a multi-center propensity score matched analysis of real-world practice. *Hepatobiliary Surg Nutr*. (2021) 10:631–45. doi: 10.21037/hbsn

17. Li QJ, He MK, Chen HW, Fang WQ, Zhou YM, Xu L, et al. Hepatic arterial infusion of oxaliplatin, fluorouracil, and leucovorin versus transarterial chemoembolization for large hepatocellular carcinoma: A randomized phase III trial. *J Clin Oncol*. (2022) 40:150–60. doi: 10.1200/JCO.21.00608

18. Cao G, Wang X, Chen H, Gao S, Guo J, Liu P, et al. Hepatic arterial infusion chemotherapy plus regorafenib in advanced colorectal cancer: a real-world retrospective study. *BMC Gastroenterol*. (2022) 22:328. doi: 10.1186/s12876-022-02344-4

19. Butte MJ, Keir ME, Phamduy TB, Sharpe AH, Freeman GJ. Programmed death-1 ligand 1 interacts specifically with the B7-1 costimulatory molecule to inhibit T cell responses. *Immunity*. (2007) 27:111–22. doi: 10.1016/j.immuni.2007.05.016

20. Chaudhri A, Xiao Y, Klee AN, Wang X, Zhu B, Freeman GJ. PD-L1 binds to B7-1 only in cis on the same cell surface. *Cancer Immunol Res*. (2018) 6:921–9. doi: 10.1158/2326-6066.CIR-17-0316

21. Chen DS, Irving BA, Hodi FS. Molecular pathways: next-generation immunotherapy–inhibiting programmed death-ligand 1 and programmed death-1. *Clin Cancer Res*. (2012) 18:6580–7. doi: 10.1158/1078-0432.CCR-12-1362

22. Sun X, Roudi R, Dai T, Chen S, Fan B, Li H, et al. Immune-related adverse events associated with programmed cell death protein-1 and programmed cell death ligand 1 inhibitors for non-small cell lung cancer: a PRISMA systematic review and meta-analysis. *BMC Cancer*. (2019) 19:558. doi: 10.1186/s12885-019-5701-6

23. Stewart R, Morrow M, Hammond SA, Mulgrew K, Marcus D, Poon E, et al. Identification and characterization of MEDI4736, an antagonistic anti-PD-L1 monoclonal antibody. *Cancer Immunol Res*. (2015) 3:1052–62. doi: 10.1158/2326-6066.CIR-14-0191

frontiers | Frontiers in Immunology

TYPE Original Research
PUBLISHED 10 December 2024
DOI 10.3389/fimmu.2024.1506355

OPEN ACCESS

EDITED BY
Ashraf A. Tabll,
National Research Centre (Egypt), Egypt

REVIEWED BY
Roba M Talaat,
University of Sadat City, Egypt
Koyel Kar,
BCDA College of Pharmacy and Technology, India

*CORRESPONDENCE
Ji Won Han
tmznjf@catholic.ac.kr
Pil Soo Sung
pssung49@gmail.com

†These authors have contributed equally to this work

RECEIVED 05 October 2024
ACCEPTED 25 November 2024
PUBLISHED 10 December 2024

CITATION
Lee J, Yoo J-S, Kim JH, Lee DY, Yang K, Kim B, Choi J-I, Jang JW, Choi JY, Yoon SK, Han JW and Sung PS (2024) Prognostic significance of combined PD-L1 expression in malignant and infiltrating cells in hepatocellular carcinoma treated with atezolizumab and bevacizumab. *Front. Immunol.* 15:1506355. doi: 10.3389/fimmu.2024.1506355

Prognostic significance of combined PD-L1 expression in malignant and infiltrating cells in hepatocellular carcinoma treated with atezolizumab and bevacizumab

Jaejun Lee[1,2†], Jae-Sung Yoo[3†], Ji Hoon Kim[1,4], Dong Yeup Lee[2], Keungmo Yang[1,2], Bohyun Kim[5], Joon-Il Choi[5], Jeong Won Jang[1,2], Jong Young Choi[1,2], Seung Kew Yoon[1,2], Ji Won Han[1,2*] and Pil Soo Sung[1,2*]

[1]The Catholic University Liver Research Center, Department of Biomedicine & Health Sciences, College of Medicine, The Catholic University of Republic of Korea, Seoul, Republic of Korea, [2]Division of Hepatology, Department of Internal Medicine, Seoul St. Mary's Hospital, College of Medicine, The Catholic University of Republic of Korea, Seoul, Republic of Korea, [3]School of Medicine, Kyungpook National University, Daegu, Republic of Korea, [4]Division of Hepatology, Department of Internal Medicine, Uijeongbu St. Mary's Hospital, College of Medicine, The Catholic University of Republic of Korea, Seoul, Republic of Korea, [5]Departmend of Radiology, Seoul St. Mary's Hospital, College of Medicine, The Catholic University of Republc of Korea, Seoul, Republic of Korea

Background: Programmed death-ligand 1 (PD-L1) expression is abundant not only in malignant cells but also in infiltrating cells within the tumor microenvironment (TME) of hepatocellular carcinoma (HCC). This study explored the association between PD-L1 expression in TME and outcomes in HCC patients treated with atezolizumab plus bevacizumab (AB), emphasizing the implications of PD-L1 expression in both malignant and tumor-infiltrating cells.

Methods: This study included 72 patients with HCC who underwent percutaneous core needle liver biopsy before AB treatment between September 2020 and December 2023. PD-L1 expression on tumor tissues was assessed using the combined positive score (CPS) with cutoff values of 1 and 10, utilizing antibody clone 22C3 (Dako).

Results: The distribution of PD-L1 CPS included 24 patients with CPS <1, 33 patients with CPS 1–10, and 15 patients with CPS ≥10. Significant differences in overall survival (OS) were observed across the three groups, with CPS ≥10 showing the highest survival rates (p = 0.010). Patients with CPS ≥10 had better OS than those with CPS <10 (median OS 14.8 vs. 8.3 months, P = 0.046), and CPS ≥1 had better OS than CPS <1 (P = 0.021). For progression-free survival (mPFS), the CPS ≥10 group had the highest median PFS of 11.0 months among the three groups (P = 0.044). Objective response rates (ORR) were higher in the PD-L1 CPS ≥10 group than in the 1-10 and <1 group (53.3%, 27.3%, and 16.7%, respectively; *P* = .047). Multivariate analysis identified that PD-L1 expression ≥10 and ≥1 were associated with favorable outcomes regarding OS (hazard ratio [HR] 0.283, *P* = .027 and HR 0.303, *P* = .006, respectively).

Conclusions: Combined analysis of PD-L1 expression in malignant and tumor-infiltrating cells can be a promising biomarker for the prognosis of HCC patients treated with AB.

KEYWORDS

PD-L1, HCC, atezolizumab, overall survival, objective response

1 Introduction

Hepatocellular carcinoma (HCC) is the most common type of primary liver cancer and ranks as the fourth leading cause of cancer-related deaths globally (1, 2). For advanced HCC, treatment options were limited to tyrosine kinase inhibitors until the recent IMbrave150 trial, which reshaped the landscape of HCC treatment through immunotherapy (3). The introduction of atezolizumab, a programmed cell death-ligand 1 (PD-L1) inhibitor, combined with bevacizumab, an anti-vascular endothelial growth factor, has significantly improved survival outcomes in patients with advanced HCC (4). Additionally, other immune checkpoint inhibitors (ICIs), such as tremelimumab plus durvalumab and nivolumab plus ipilimumab, have also been approved for HCC as first-line and second-line systemic therapies, respectively, and they have expanded the therapeutic options for clinicians treating advanced HCC (5–8). However, the objective response rate (ORR) of these ICIs remains mostly under 30%, highlighting the need for promising biomarkers to identify patients who could benefit the most from these treatments (3, 5, 6).

The programmed cell death protein 1 (PD-1)/PD-L1 axis plays a crucial role in the immune evasion mechanisms of tumors. PD-L1 on tumor cells binds to PD-1 on T cells, leading to the inhibition of T cell function and allowing the tumor to evade the immune response (9). Moreover, recent studies have highlighted the role of PD-L1 expression not only on tumor cells but also on tumor-infiltrating cells such as tumor-associated macrophages (TAMs), which are pivotal in regulating anti-tumor immunity (10–12). Given that ICIs primarily target PD-1/PD-L1 axis, numerous studies have investigated the implications of PD-L1 expression levels across various malignancies when treating these patients with ICIs (13–15). For most of the studies, consistent results were observed regarding better treatment outcomes for those with higher PD-L1 expression than those with lower expression (16, 17).

Since the advent of atezolizumab plus bevacizumab (AB), which has significantly impacted the treatment landscape of HCC, many studies have been conducted to identify biomarkers that can predict the outcome of ICIs in advanced HCC. PD-L1 is one of the most promising candidates for predictive markers (18, 19). However, the role of PD-L1 as a predictive marker has not been clearly established in HCC. Clinical trials such as CheckMate 459, KEYNOTE-224, and CheckMate 040 have presented consistent results supporting PD-L1 expression as a favorable biomarker for ICI-treated HCC (6, 20, 21). In contrast, results from studies such as the HIMALAYA trial have shown that the efficacy of these drugs is independent of PD-L1 expression status (5, 22, 23).

While controversy exists over whether PD-L1 expression levels can serve as a biomarker for ICI-treated HCC, it is important to note that previous clinical trials have been conducted across various nations and institutions, resulting in inconsistent procedures for detecting PD-L1. Moreover, the majority of these studies used tumor proportion score (TPS), which counts PD-L1 expression only in tumor cells, thus providing a limited evaluation of the tumor microenvironment (TME). In this study, we aimed to address these concerns by comparing the outcomes of patients with advanced HCC treated with AB, stratified by diverse thresholds of PD-L1 expression levels in both malignant and tumor-infiltrating cells, using a reliable and uniform antibody clone for detecting PD-L1.

2 Methods

2.1 Patients

In this study, we retrospectively reviewed the medical records of patients with unresectable HCC who received AB treatment between September 2020 and December 2023. The diagnosis of HCC was based on either histological or radiological examinations such as computed tomography or, magnetic resonance imaging, or all three. The inclusion criteria were as follows: 1) patients diagnosed with unresectable HCC; 2) availability of histological data with immunohistochemical staining for PD-L1 in cells (malignant and tumor-infiltrating cells) obtained via liver biopsy prior to the initiation of AB treatment; 3) age ≥ 18 years; 4) Eastern

Abbreviations: AB, Atezolizumab plus bevacizumab; AUC-ROC, area under the curve of receiver operating characteristics; CI, confidence interval; CPS, combined positive score; CR, complete response; CT, computed tomography; DCR, disease control rate; ECOG, Eastern Cooperative Oncology Group; HCC, hepatocellular carcinoma; HR, hazard ratio; ICI, immune checkpoint inhibitor; mOS, median overall survival; mPFS, median progression-free survival; mRECIST, modified Response Evaluation Criteria in Solid Tumors; MRI, magnetic resonance imaging; ORR, objective response rate; OS, overall survival; PD-1, programmed cell death protein 1; PD-L1, programmed cell death ligand 1; PFS, progression-free survival; PR, partial response; TAMs, tumor-associated macrophages; TPS, tumor proportion score.

Cooperative Oncology Group (ECOG) performance status ≤ 1; and 5) patients who had at least one follow-up visit at the clinic after receiving AB treatment. Patients with concurrent extrahepatic malignancies or severe liver dysfunction classified as Child-Pugh class C were excluded from the study (Supplementary Table S1). This study was approved by the Institutional Review Board of the Catholic University of Korea (approval number: KC22EASI0342) and was performed in accordance with the Declaration of Helsinki. Informed consent was waived due to the retrospective nature of the study.

2.2 Treatment protocols and response evaluation

AB was administered following the standard dosing regimen outlined in the IMbrave 150 trial, which involved intravenous doses of 1200 mg of atezolizumab and 15 mg/kg of bevacizumab every three weeks. Tumor response was assessed approximately every three to four treatment cycles using the mRECIST (modified Response Evaluation Criteria in Solid Tumors) criteria (24). Treatment response was evaluated in all patients using follow-up liver dynamic computed tomography (CT) or dynamic magnetic resonance imaging (MRI) with liver-specific contrast agents. According to the mRECIST criteria, disease progression was defined as an increase in the diameter of the viable lesion by more than 20%. Treatment with AB was continued until disease progression, death, or the occurrence of intolerable adverse events.

2.3 Assessment of PD-L1 expression level

PD-L1 expression was assessed using the 22C3 antibody clone (1:50 dilution, Cat# M3653, Dako), which is used for the detection of the extracellular epitope (25). First, a tumor sample was obtained via core-needle liver biopsy. A 4-μm thick cross-section of the paraffin-embedded block was placed on a glass slide. Deparaffinization, rehydration, and antigen retrieval were performed using the CC1 antigen retrieval solution (Ventana Medical Systems) in an automated slide stainer (Ventana Medical Systems) for 64 minutes at 95-100°C. The sample was incubated with the 22C3 antibody for 32 minutes at 37°C and then washed with phosphate-buffered saline. After washing, the EnVision+ system HRP-labeled polymer (Dako) was applied to the slides at 24°C for 5 minutes. The slides were then treated with 3,3′-diaminobenzidine for 5 minutes and counterstained with hematoxylin. Finally, sections were dehydrated, cleared, and mounted for microscopic examination.

In the present study, a combined positive score (CPS) was used to quantify PD-L1 expression levels (26). CPS was determined by summing the number of viable PD-L1-positive tumor cells and the number of positive tumor-infiltrating cells, such as lymphocytes and macrophages, and then dividing that total by the overall number of viable tumor cells, with a maximum score of 100. Two different cut-off levels of CPS 1 and 10, based on previous studies, were employed to assess the outcomes of AB treatment in relation to PD-L1 expression levels (27).

2.4 Study endpoints

The primary endpoint of the study was overall survival (OS), defined as the duration between the start of AB treatment and death from any cause. Patients who were lost to follow-up or remained alive at the end of the study period were considered censored. Secondary endpoints were progression-free survival (PFS) and objective response rate (ORR). PFS was defined as the period from the start of the AB treatment until disease progression or death. ORR was defined as the proportion sum of complete response (CR) and partial response (PR), according to the mRECIST criteria.

2.5 Statistical analysis

All analyses were performed using the R statistical software (version 4.0.3; R Foundation Inc., Vienna, Austria; http://cran.r-project.org, accessed on June 10, 2024). Continuous variables are reported as mean values with standard deviations. Student t-test was performed when continuous variables for two independent group were compared while an analysis of variance was performed to compare among groups of three or more. Categorical variables were assessed with the chi-square test. Survival analyses were conducted via the Kaplan–Meier method, with differences evaluated using the log-rank test. Cox regression analyses were utilized to identify factors associated with survival outcomes, with those showing P <.20 in univariate analysis included in multivariate analysis. The time-dependent area under the curve of receiver operating characteristic (AUC-ROC) was utilized to assess the predictive performance of PD-L1 expression levels for survival outcomes. A restricted cubic spline was applied to estimate the trend of the dose-response relationship between PD-L1 expression levels and survival outcomes, such as OS and PFS. Statistical significance was determined at P <.05.

3 Results

3.1 Baseline characteristics

A total of 72 patients were included in the study. Table 1 shows the baseline characteristics of the study population. Males were predominant (84.7%), and the mean age of the study population was 62.1 years. The most common cause of HCC was Hepatitis B virus infection (56.9%) followed by alcoholic liver disease (27.8%). Regarding liver function, 61.1% had a Child-Pugh score of 5, 22.2% had a Child-Pugh score of 6, and 16.7% had a Child-Pugh score of 7. Additionally, 31.9% of the patients had a single tumor mass, and the mean tumor size was 7.6 cm. In terms of tumor stage, the majority of the study population had advanced HCC, with 54.2% and 93.1%

exhibiting mUICC stage IVB and BCLC stage C, respectively. The mean AFP level and PIVKA level were 628.0 ng/mL and 1298.0 mAU/mL, respectively.

The study population was categorized into three groups according to PD-L1 expression levels using CPS cutoff values of 1 and 10. The three groups had no differences in sex distribution; however, the high PD-L1 (CPS ≥10) group was older than the other groups (P = .042).

3.2 Representative immunohistochemical findings of the enrolled patients

Figure 1 displays the representative immunohistochemical findings for the enrolled patients, including samples with high or low PD-L1 expression and diverse prognoses. PD-L1 immunohistochemistry slides (Figures 1A–C) show varying PD-L1 expression levels (CPS <1, 5, 90) in biopsy samples from patients with different clinical

TABLE 1 Baseline characteristics of enrolled patients.

	Total (n=72)	PD-L1 (CPS<1) (n=24)	PD-L1 (CPS 1–10) (n=33)	PD-L1 (CPS≥10) (n=15)	P
Male sex	61 (84.7)	19 (79.2)	30 (90.9)	12 (80.0)	0.405
Age	62.1 ± 11.7	60.2 ± 9.1	60.4 ± 13.3	68.8 ± 9.6	0.042
Etiology					0.328
HBV	41 (56.9)	15 (62.5)	20 (60.6)	6 (40.0)	
HCV	5 (6.9)	1 (4.2)	3 (9.1)	1 (6.7)	
Alcohol	20 (27.8)	7 (29.2)	8 (24.2)	5 (33.3)	
Others	6 (8.3)	1 (4.2)	2 (6.1)	3 (20.0)	
PLT (10^9/ L)	176.0 ± 94.6	187.7 ± 115.5	176.4 ± 84.0	151.9 ± 80.1	0.513
AST (IU/L)	76.4 ± 84.8	109.0 ± 122.6	57.1 ± 52.2	66.5 ± 52.3	0.063
ALT (IU/L)	33.4 ± 21.9	40.0 ± 27.1	29.6 ± 16.5	31.2 ± 22.1	0.193
TB (mg/dL)	0.9 ± 0.6	0.9 ± 0.5	1.0 ± 0.7	0.8 ± 0.5	0.791
Albumin (mg/dL)	3.8 ± 0.4	3.7 ± 0.4	3.8 ± 0.5	3.8 ± 0.4	0.715
PT (INR)	1.1 ± 0.1	1.1 ± 0.1	1.1 ± 0.1	1.2 ± 0.2	0.981
Child-Pugh class					0.961
A5	44 (61.1)	14 (58.3)	20 (60.6)	10 (66.7)	
A6	16 (22.2)	5 (20.8)	8 (24.2)	3 (20.0)	
B7	12 (16.7)	5 (20.8)	5 (15.2)	2 (13.3)	
Tumor no.(single)	23 (31.9)	4 (16.7)	15 (45.5)	4 (26.7)	0.063
Tumor size (cm)	7.6 ± 5.5	8.5 ± 6.6	6.7 ± 4.7	8.0 ± 5.4	0.455
mUICC stage					0.710
II	2 (2.8)	1 (4.2)	1 (3.0)	0 (0.0)	
III	4 (5.6)	1 (4.2)	3 (9.1)	0 (0.0)	
IVa	27 (37.5)	8 (33.3)	11 (33.3)	8 (53.3)	
IVb	39 (54.2)	14 (58.3)	18 (54.5)	7 (46.7)	
BCLC stage					0.490
B/C	5 (6.9)/67 (93.1)	2 (8.3)/22 (91.7)	3 (9.1)/30 (90.9)	0 (0.0)/15 (100.0)	
AFP (ng/mL)	628.0 (18.6, 19259.5)	1171.5 (19.5, 23676.5)	887.0 (18.6, 18462.0)	457.0 (23.7, 3836.5)	0.858
PIVKA (mAU/mL)	1298.0 (175.0, 7783.0)	5193.0 (419.5, 19482.8)	1045.0 (123.0, 3264.0)	772.0 (113.0, 8046.0)	0.261

Values are presented as mean ± standard deviation or number (%). AFP, alpha fetoprotein; AST, aspartate aminotransferase; ALT, alanine aminotransferase; BCLC, Barcelona clinic liver cancer; CPS, combined positive score; HBV, hepatitis B virus; HCV, hepatitis C virus; mUICC, modified union for international cancer control; PIVKA, protein induced by vitamin K absence; PLT, platelet; PT, prothrombin time; TB, total bilirubin.

outcomes. In addition, PD-L1 expression in malignant cells versus tumor-infiltrating non-malignant cells is also presented in Figures 1D, E.

3.3 Treatment responses

Tumor response to AB treatment was assessed (Table 2). Overall, 21 patients achieved partial response, resulting in an ORR of 29.2%. Additionally, 21 patients achieved stable disease, resulting in a disease control rate (DCR) of 58.4%. Twenty-two patients exhibited progressive disease after AB treatment and radiologic assessments were not performed in eight patients during the treatment.

The three groups stratified by PD-L1 expression levels were compared with respect to treatment response (Table 2). For ORR, the high PD-L1 (CPS ≥10) group had the highest rate at 53.3% (n = 8), followed by the intermediate PD-L1 (CPS 1-10) group at 27.3% (n = 9), and the low PD-L1 (CPS <1) group at 16.7% (n = 4) (P = .047). Regarding DCR, the high PD-L1 group had the highest rate at 80.0% compared with the intermediate PD-L1 group (57.6%) and the low PD-L1 group (45.8%), although the difference was not statistically significant (P = .108). Next, CPS 1 and 10 were each applied as a sole cutoff value and assessed for tumor response rates. For ORR, the high PD-L1 group showed higher ORR compared to the low PD-L1 group (CPS ≥10: 53.3% vs. CPS <10: 22.8%, P = .021; CPS ≥1: 35.4% vs. CPS <1: 16.7%, P = .099). In terms of DCR, the high PD-L1 groups were higher than the low PD-L1 groups, although statistical significance

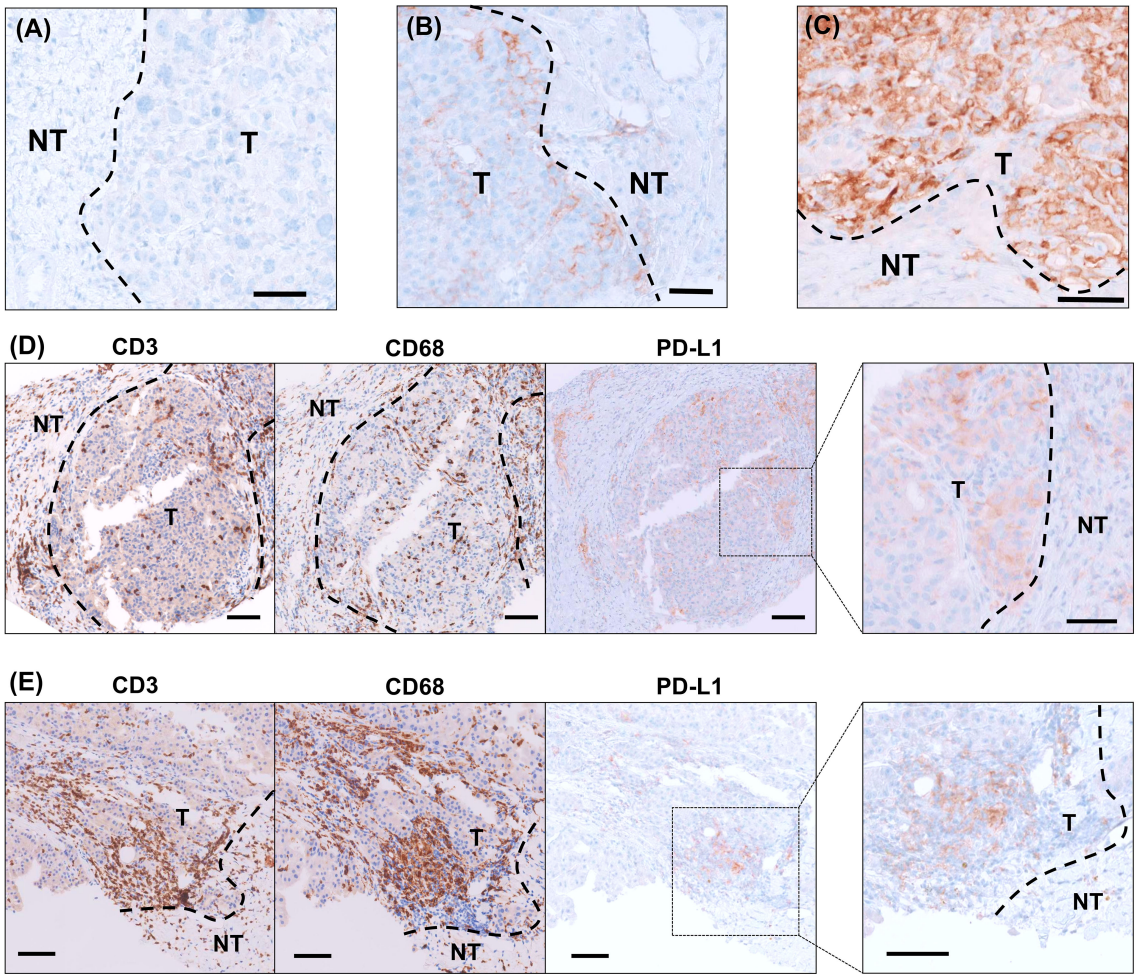

FIGURE 1
Representative images of PD-L1 immunohistochemistry in the biopsy samples. **(A)** PD-L1 immunohistochemical staining in a biopsy sample from a patient with low PD-L1 (CPS <1) expression, who experienced disease progression within 2 months. **(B)** PD-L1 immunohistochemical staining in a biopsy sample from a patient with a PD-L1 CPS of 5, who achieved progression-free survival for more than 12 months. **(C)** PD-L1 immunohistochemical staining in a biopsy sample from a patient with high PD-L1 expression (CPS 90), who achieved a partial response following treatment with atezolizumab plus bevacizumab. **(D)** Immunohistochemical staining of tumor tissues for CD3, CD68, and PD-L1, with PD-L1 staining predominantly positive in malignant cells. **(E)** Immunohistochemical staining for CD3, CD68, and PD-L1, with PD-L1 staining primarily positive in tumor-infiltrating non-malignant cells. Scale bar represents 100 μm; CPS, combined positive score; NT, non-tumor; T, tumor.

TABLE 2 Treatment responses by PD-L1 expression level.

	PD-L1<1 (n = 24)	PD-L1 1–10 (n = 33)	PD-L1≥10 (n = 15)	*P* value
Treatment responses				0.105
PR	4 (16.7)	9 (27.3)	8 (53.3)	
SD	7 (29.2)	10 (30.3)	4 (26.7)	
PD	11 (45.8)	8 (24.2)	3 (20.0)	
NA	2 (8.3)	6 (18.2)	0 (0.0)	
ORR	4 (16.7)	9 (27.3)	8 (53.3)	0.047
DCR	11 (45.8)	19 (57.6)	12 (80.0)	0.108

Values are presented as number (%). DCR, disease control rate; ORR, objective response rate; PD, progressive disease; PR, partial response; SD, stable disease, NA, not applicable.

was not reached (CPS ≥10: 80.0% vs. CPS <10: 52.6%, $P = .055$; CPS ≥1: 64.6% vs. CPS <1: 45.8%, $P = .128$).

3.4 Overall survival based on the PD-L1 expression levels

During the median follow-up period of 7.4 months, 26 mortality cases were documented. The median overall survival (mOS) for the entire cohort was 14.8 months (95% confidence interval [CI], 11.3 months–NA). First, using CPS values of 1 and 10 as cutoff points, patients were categorized into three groups and compared for OS (Figure 2A). The OS was significantly longer in the high PD-L1 (CPS ≥10) group, with 92.9% survival rates at six months and 77.4% survival rates at 12 months, compared to the intermediate PD-L1 (CPS 1-10) group (mOS 13.1 months) and the low PD-L1 (CPS <1) group (mOS 8.0 months) ($P = .010$). When comparing the two groups based on a single PD-L1 CPS cutoff of 10, the high PD-L1 (CPS ≥10) group again exhibited better OS than the low PD-L1 (CPS <10) group (mOS 11.9 months) ($P = .046$) (Figure 2B). Using a PD-L1 CPS of 1 as a cutoff value, the 6-month and 12-month survival rates of the high PD-L1 (CPS ≥1) group were 86.1% and 64.7%, respectively, which were higher than the 66.0% and 29.3% survival rates of the low PD-L1 (CPS <1) group ($P = .021$) (Figure 2C).

3.5 Progression-free survival based on the PD-L1 expression levels

The median progression-free survival (mPFS) for the entire cohort was 5.8 months (95% CI, 4.2–8.9 months). When the study populations were stratified into three groups using CPS values of 1 and 10 as cutoff points, the high PD-L1 group showed the longest mPFS of 11.0 months (95% CI, 5.8 months–NA) compared to the intermediate PD-L1 group (mPFS 5.9 months, 95% CI, 2.8 months–NA) and the low PD-L1 group (mPFS 4.0 months, 95% CI, 3.4–8.9 months) ($P = .044$) (Figure 3A). When CPS 10 was used as the sole cut-off value, the high PD-L1 group (mPFS not applicable (NA)) showed a tendency toward longer PFS than the low PD-L1 group (mPFS 5.43 months) ($P = .051$) (Figure 3B). When CPS 1 was employed as a cut-off value, the mPFS for the high PD-L1 and low PD-L1 groups were 4.6 months (95% CI, 2.1–7.1 months) and 2.8 months (95% CI, 2.2–6.6 months), respectively ($P = .188$) (Figure 3C).

Regarding dose-dependent correlation between PFS and PD-L1 expression level, the hazard ratio (HR) for progression or death

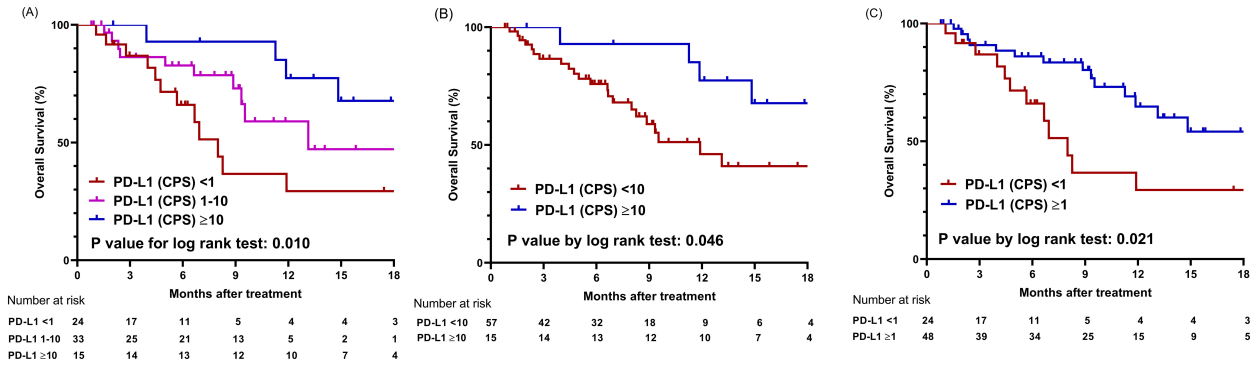

FIGURE 2
Comparison of overall survival based on PD-L1 expression levels using different cut-off values. **(A)** Graphs showing comparison of overall survival among three groups categorized by cutoff values of CPS 1 and 10. **(B)** Graphs showing comparison of overall survival between two groups categorized by cutoff value of CPS 10. **(C)** Graphs showing comparison of overall survival between two groups categorized by cutoff value of CPS 1; CPS, combined positive score.

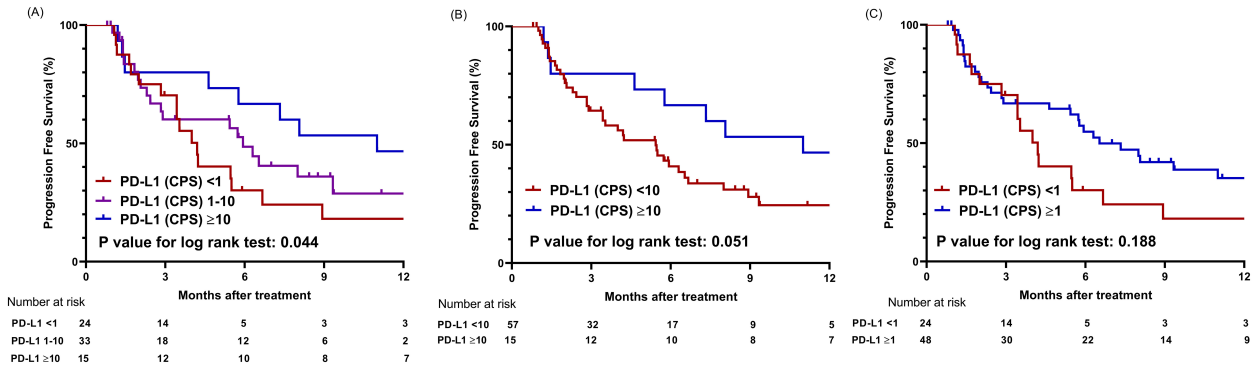

FIGURE 3
Comparison of progression-free survival based on PD-L1 expression levels using different cut-off values. **(A)** Graphs showing comparison of progression-free survival among three groups categorized by cutoff values of CPS 1 and 10. **(B)** Graphs showing comparison of progression-free survival between two groups categorized by cutoff value of CPS 10. **(C)** Graphs showing comparison of progression-free survival between two groups categorized by cutoff value of CPS 1; CPS, combined positive score.

tended to decline as the PD-L1 expression level increased, although this trend was not statistically significant ($P = .146$) (Supplementary Figure S1B). For PD-L1 CPS of 10, the HR for PFS was 0.77 (95% CI 0.58–1.02).

3.6 Factors contributing to survival outcomes

Various factors that could affect the survival outcomes were included in the analysis. In terms of OS, univariate analysis revealed that ECOG 1 and a Child-Pugh score of 5 were associated with the outcomes. Subsequently, factors with a P value of less than 0.2 in the univariate analysis were included in the multivariate analysis. Two models were assessed, each incorporating different cutoff values for CPS as a marker for PD-L1 expression. In Model 1, which used PD-L1 (CPS ≥10) as the biomarker, PD-L1 (CPS ≥10) was the only factor associated with OS (HR 0.283, 95% CI, 0.092–0.865; $P = .027$). In Model 2, which used PD-L1 (CPS ≥1) as the covariate, PD-L1 (CPS ≥1) remained the only significant factor favorably associated with OS (HR 0.303, 95% CI, 0.128–0.713; $P = .006$) (Table 3).

TABLE 3 Factors associated with survival outcomes.

	Univariate analysis		Multivariate analysis			
			Model 1		Model 2	
	HR (95% CI)	*P* value	HR (95% CI)	*P* value	HR (95% CI)	*P* value
PD-L1 ≥ 10 CPS	0.346 (0.117, 1.024)	0.055	0.283 (0.092, 0.865)	0.027	–	–
PD-L1 ≥ 1 CPS	0.409 (0.187, 0.893)	0.025	–	–	0.303 (0.128, 0.713)	0.006
Sex (Female)	1.397 (0.525, 3.715)	0.503				
Age≥65	1.147 (0.531, 2.481)	0.727				
ECOG 1 (vs. 0)	2.342 (1.078, 5.090)	0.032	2.162 (0.916, 5.101)	0.078	2.293 (0.959, 5.482)	0.062
Etiology-Viral (vs non-viral)	0.846 (0.383, 1.868)	0.678				
Child-Pugh score 5	0.449 (0.207, 0.974)	0.043	0.510 (0.224, 1.162)	0.109	0.522 (0.227, 1.201)	0.126
AFP>400ng/mL	1.619 (0.747, 3.508)	0.222				
Tumor size>5cm	2.101 (0.928, 4.756)	0.075	1.657 (0.687, 3.999)	0.261	1.820 (0.759, 4.367)	0.180
Number of tumors≥2	1.082 (0.482, 2.433)	0.848				
Vascular invasion	0.659 (0.305, 1.422)	0.287				
Extrahepatic metastasis	2.084 (0.925, 4.695)	0.076	1.465 (0.618, 3.475)	0.386	1.514 (0.633, 3.618)	0.351

Model 1 includes PD-L1 ≥ 10 CPS as a covariate, and Model 2 includes PD-L1 ≥ 1 CPS as a covariate. AFP, alpha fetoprotein; CI, confidence interval; ECOG, Eastern Cooperative Oncology Group; HR, hazard ratio.

Regarding PFS, only a Child-Pugh score of 5 remained significant in the univariate analysis. In multivariate analysis Model 1, which included PD-L1 (CPS ≥10), sex, ECOG score, Child-Pugh score, and extrahepatic metastasis as variables, PD-L1 (CPS ≥10) (HR 0.406, 95% CI 0.188–0.878, P = .022), female sex (HR 2.643, 95% CI 1.146–6.096, P = .023), and Child-Pugh score 5 (HR 0.503, 95% CI 0.269–0.941, P = .032) were significantly associated with PFS in the study cohort. In Model 2, female sex (HR 2.339, 95% CI 1.018–5.373, P = .045) and Child-Pugh score 5 (HR 0.525, 95% CI 0.282–0.977, P = .042) were associated with PFS (Table 4).

3.7 Predictive performance of PD-L1 on survival outcomes

To evaluate the predictive performance of PD-L1 on survival outcomes, the time-dependent AUC-ROC was calculated for 12-month OS (Figure 4). The AUC-ROC for 12-month OS in the study population was 0.703 (95% CI: 0.539–0.867). Using Youden's index, a CPS of 5 was identified as the optimal cutoff value for predicting survival outcomes, with a sensitivity of 84.3% and specificity of 52.7%. Furthermore, the HR for survival outcomes was assessed based on PD-L1 expression level. The HR tended to decline as PD-L1 expression level increased (P = .031) (Supplementary Figure S1A). Using a CPS of 5 as a reference, the HR was 0.60 (95% CI 0.38–0.94) for CPS 10 of the PD-L1 level.

3.8 Sensitivity analysis using different cutoff value for PD-L1 expression

A PD-L1 CPS of 5 was used as an alternative cutoff value to perform a sensitivity analysis on the impact of PD-L1 expression levels on survival outcomes. For OS, the high PD-L1 (CPS ≥5) group exhibited 6- and 12-month survival rates of 85.7% and 71.9%, respectively, which were significantly higher than the 76.6% and 43.0% survival rates of the low PD-L1 (CPS < 5) group (P = .044) (Supplementary Figure S2A). In terms of PFS, the high PD-L1 group (mPFS 6.5 months, 95% CI, 1.6 months–NA) tended towards prolonged PFS compared to the low PD-L1 group (mPFS 3.4 months, 95% CI, 2.2–5.3 months) (P = .069) (Supplementary Figure S2B).

3.9 Subgroup analysis in patients with viral etiologies

Survival outcomes were assessed in patients with viral etiologies (n = 46). For OS, patients with higher PD-L1 expression exhibited longer survival times, although the difference was not statistically significant (mOS: CPS ≥1 NA, CPS 1–10 13.1 months, and CPS <1 8.0 months, P = .095) (Supplementary Figure S3A). In terms of PFS (Supplementary Figure S3B), patients with PD-L1(CPS ≥10) exhibited a mPFS of 17.2 months, which was higher than CPS 1-10 (mPFS 5.9 months) and CPS<1 group (mPFS 3.4 months) (P = .173).

TABLE 4 Factors associated with progression-free survival.

	Univariate analysis		Multivariate analysis			
			Model 1		Model 2	
	HR (95% CI)	*P* value	HR (95% CI)	*P* value	HR (95% CI)	*P* value
PD-L1 ≥ 10 CPS	0.493 (0.240, 1.013)	0.054	0.406 (0.188, 0.878)	0.022	–	–
PD-L1 ≥ 1 CPS	0.675 (0.375, 1.214)	0.189	–	–	0.583 (0.317, 1.071)	0.082
Sex (Female)	1.697 (0.792, 3.635)	0.173	2.643 (1.146, 6.096)	0.023	2.339 (1.018, 5.373)	0.045
Age≥65	0.806 (0.457, 1.423)	0.458				
ECOG 1 (vs. 0)	1.532 (0.870, 2.696)	0.140	1.249 (0.683, 2.283)	0.470	1.201 (0.651, 2.215)	0.557
Etiology-Viral (vs non-viral)	1.251 (0.687, 2.278)	0.463				
Child-Pugh score 5	0.552 (0.311, 0.979)	0.042	0.503 (0.269, 0.941)	0.032	0.525 (0.282, 0.977)	0.042
AFP>400ng/mL	1.306 (0.743, 2.296)	0.354				
Tumor size>5cm	1.345 (0.757, 2.389)	0.312				
Number of tumors≥2	1.113 (0.612, 2.026)	0.726				
Vascular invasion	0.739 (0.415, 1.315)	0.303				
Extrahepatic metastasis	1.728 (0.968, 3.084)	0.064	1.401 (0.762, 2.573)	0.278	1.593 (0.867, 2.928)	0.134

Model 1 includes PD-L1 ≥ 10 CPS as a covariate, and Model 2 includes PD-L1 ≥ 1 CPS as a covariate. AFP, alpha fetoprotein; CI, confidence interval; ECOG, Eastern Cooperative Oncology Group; HR, hazard ratio.

10.3389/fimmu.2024.1506355

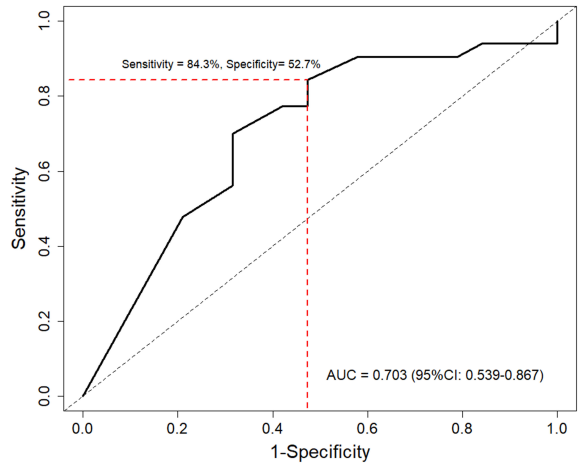

FIGURE 4
Time-dependent receiver operating characteristic curve of PD-L1 levels for predicting 12-month overall survival. Red line indicates optimal cutoff value determined by Youden's index. AUC, area under the curve.

4 Discussion

In patients with advanced HCC, AB treatment is considered first-line systemic therapy. However, as the IMbrave150 trial demonstrated, only about 30% of patients exhibit a tumor response to AB, highlighting the need for effective biomarkers to identify those who will benefit most from this treatment (28). Unfortunately, no specific biomarker for this identification has been established to date. Our study revealed that patients with high PD-L1 expression levels in malignant and tumor-infiltrating cells showed favorable outcomes in terms of both OS and PFS. Specifically, a PD-L1 level with a CPS of 10 or higher was identified as a good prognostic factor for these patients in terms of both OS and PFS. Moreover, the tumor response rate was higher in tumors with high PD-L1 expression than in those with intermediate or low PD-L1 expression. Overall, present study meticulously elucidated the impact of PD-L1 expression on survival outcomes in patients with HCC treated with AB.

The TME of HCC is characterized by a complex interplay between various cellular components, among which TAMs, cancer-associated fibroblasts, and other tumor-infiltrating immune cells play a crucial role in modulating antitumor immunity (29, 30). In addition, TAMs and other immune cells, such as dendritic cells and regulatory T cells, express PD-L1, contributing significantly to the immunosuppressive nature of the TME (31). By expressing PD-L1, these cells inhibit the cytotoxic functions of CD8+ T cells and enhance the activity of regulatory T cells, thus creating an environment favorable to tumor growth and progression. In this context, it has been proposed that patients with high PD-L1 expression in tumor-infiltrating cells might benefit more from ICIs than those with lower expression levels (32–34). While numerous studies on various types of malignancies have demonstrated a correlation between PD-L1 expression levels and treatment outcomes, relatively few studies have explored this correlation specifically in HCC (16, 17). Among these studies, different outcomes have been observed. Regarding ORR, a study using the CheckMate 459 trial demonstrated a superior outcome for tumors with TPS of PD-L1 ≥1% compared to those with PD-L1 <1% (28% vs 12%) (35). In terms of survival outcomes, such as OS, a study utilizing the CheckMate 040 cohort showed improved OS for tumors with PD-L1 ≥1% in tumor cells compared to those with PD-L1 <1%, which is consistent with the results from our study (36). However, other studies have shown insignificant differences in ORR and survival outcomes between PD-L1 positive and negative tumors, raising controversies regarding this issue (22, 37–39).

Several factors can explain these differences between the studies. First, the use of different PD-L1 immunohistochemistry assays between studies might result in inter-assay variation, causing heterogeneity in study results (40). To date, there are five Food and Drug Administration-approved diagnostic assays for PD-L1 detection, including 22C3, SP142 (Ventana), SP263 (Ventana), 28-8 (Dako), and 73-10 (Dako) (41). Among these diagnostic assays, 22C3 is utilized across a variety of tumor types with various cutoff values. Additionally, 22C3 is approved as a companion diagnostic assay for non-small cell lung cancer, gastric cancer, cervical cancer, urothelial carcinoma, and head and neck squamous cell carcinoma, whereas the other assays serve as complementary diagnostic tests (41, 42). Notably, 22C3 has demonstrated superior sensitivity compared to other assays and has been shown to correlate well with the tumor immune microenvironment in HCC, enhancing the reliability of results obtained using this method (43, 44). Our study's use of 22C3 exclusively may contribute to the robustness of our findings. Furthermore, previous studies have employed diverse treatment modalities, which might have contributed to the heterogeneity between the studies. In this context, the results derived from diverse settings cannot be directly applied to patients with HCC treated with AB. Thus, the results of our study hold the importance for the implication of PD-L1 expression in AB-treated HCC. Lastly, variations in counting methods for defining PD-L1 expression could account for discrepancies among studies. Our study carefully counted PD-L1 staining cells not only in malignant cells but also in tumor-infiltrating cells such as macrophages and lymphocytes. Given the critical role of TAMs and other tumor-infiltrating cells in the TME, including tumor-infiltrating cells expressing PD-L1 is essential for accurately reflecting the immunological context within tumors (45). This comprehensive approach provides a more integrated view of the tumor immune environment, which may lead to more accurate predictions of treatment response.

Our study focused on the predictive performance of PD-L1 levels for 12-month OS in HCC patients treated with AB. The results showed that the AUC-ROC was 0.703, indicating good performance of PD-L1 as a biomarker. We also assessed the dose-dependent relationship between PD-L1 expression and survival outcomes. In a restricted cubic spline curve analysis, a clear tendency of decreasing HR for survival outcomes with increasing PD-L1 level was observed. Moreover, consistent results favoring high PD-L1 expression for survival outcomes were observed in analyses using different cutoff values, namely 1, 5, and 10. In this context, our study results indicate that regardless of the definition of

PD-L1 positivity, PD-L1 expression is associated with a good prognosis in HCC patients treated with AB.

While our research provides valuable insights, it also has several limitations. First, the retrospective design necessitates further investigation using a prospective design to enhance the evidence level of our results. Another limitation is the relatively small sample size collected from a single center. Additionally, the lack of data on immune cell populations and cytokine profiles restricts the comprehensive understanding of the mechanisms underlying our findings. Future studies incorporating these profiles before and after AB treatment would improve our understanding of the pathophysiological implications of our analysis. Another limitation lies in the invasiveness of biopsy procedures, which may limit the practical accessibility of PD-L1 expression as a biomarker in real-world clinical settings. Lastly, the majority of our study population had hepatitis B virus infection as the etiology of HCC. Given the potential differences in immune contexture between viral and non-viral etiologies of HCC, validation including patients with non-viral HCC is warranted (46, 47).

Through meticulous analysis, PD-L1 expression levels in malignant and tumor-infiltrating cells were identified as prognostic factors in patients with HCC treated with AB. This finding highlights the potential of PD-L1 expression levels as a biomarker for these patients. As patients with high PD-L1 expression exhibited promising survival outcomes, those in this category may be particularly suitable candidates for AB treatment. Conversely, clinicians might consider alternative treatments for tumors with low or no PD-L1 expression (48). Additionally, performing immunohistochemistry on liver biopsy specimens before selecting a treatment modality could guide clinicians in making more informed choices, potentially leading to improved treatment outcomes.

Data availability statement

The raw data supporting the conclusions of this article will be made available by the authors, without undue reservation.

Ethics statement

The studies involving humans were approved by Institutional Review Board of the Catholic University of Korea. The studies were conducted in accordance with the local legislation and institutional requirements. The ethics committee/institutional review board waived the requirement of written informed consent for participation from the participants or the participants' legal guardians/next of kin because Informed consent was waived due to the retrospective nature of the study.

Author contributions

JL: Conceptualization, Data curation, Formal analysis, Methodology, Project administration, Validation, Visualization, Writing – original draft, Writing – review & editing. J-SY: Formal analysis, Investigation, Visualization, Writing – original draft, Writing – review & editing. JK: Conceptualization, Validation, Writing – review & editing. DL: Validation, Writing – review & editing. KY: Data curation, Validation, Writing – review & editing. BK: Formal analysis, Validation, Writing – review & editing. J-IC: Data curation, Validation, Writing – review & editing. JJ: Data curation, Supervision, Validation, Writing – review & editing. JC: Validation, Writing – review & editing. SY: Validation, Writing – review & editing. JH: Formal analysis, Supervision, Validation, Writing – review & editing. PS: Formal analysis, Supervision, Validation, Writing – review & editing.

Funding

The author(s) declare financial support was received for the research, authorship, and/or publication of this article. The Basic Science Research Program supported this research through a National Research Foundation of Korea (NRF) funded by the Korean government (MSIT) (grant RS–2024–00337298). This research was also supported by the Korea Health Technology R&D Project through the Korea Health Industry Development Institute (KHIDI), funded by the Ministry of Health & Welfare, Republic of Korea (grant number RS-2024-00406716 to JH).

Conflict of interest

The authors declare that the research was conducted in the absence of any commercial or financial relationships that could be construed as a potential conflict of interest.

Generative AI statement

The author(s) declare that no Generative AI was used in the creation of this manuscript.

Publisher's note

Supplementary material

The Supplementary Material for this article can be found online at: https://www.frontiersin.org/articles/10.3389/fimmu.2024.1506355/full#supplementary-material

References

1. Bray F, Laversanne M, Sung H, Ferlay J, Siegel RL, Soerjomataram I, et al. Global cancer statistics 2022: GLOBOCAN estimates of incidence and mortality worldwide for 36 cancers in 185 countries. *CA Cancer J Clin*. (2024) 74:229–63. doi: 10.3322/caac.21834

2. 2022 KLCA-NCC Korea practice guidelines for the management of hepatocellular carcinoma. *Clin Mol Hepatol*. (2022) 28:583–705. doi: 10.3350/cmh.2022.0294

3. Finn RS, Qin S, Ikeda M, Galle PR, Ducreux M, Kim TY, et al. Atezolizumab plus bevacizumab in unresectable hepatocellular carcinoma. *N Engl J Med*. (2020) 382:1894–905. doi: 10.1056/NEJMoa1915745

4. Kulkarni AV PK, Menon B, Sekaran A, Rambhatl A, Iyengar S, et al. Downstaging with atezolizumab-bevacizumab: A case series. *J Liver Cancer*. (2024) 24:224–33. doi: 10.17998/jlc.2024.05.12

5. Abou-Alfa GK, Lau G, Kudo M, Chan SL, Kelley RK, Furuse J, et al. Tremelimumab plus durvalumab in unresectable hepatocellular carcinoma. *NEJM Evid*. (2022) 1:EVIDoa2100070. doi: 10.1056/EVIDoa2100070

6. Yau T, Kang YK, Kim TY, El-Khoueiry AB, Santoro A, Sangro B, et al. Efficacy and safety of nivolumab plus ipilimumab in patients with advanced hepatocellular carcinoma previously treated with sorafenib: the checkMate 040 randomized clinical trial. *JAMA Oncol*. (2020) 6:e204564. doi: 10.1001/jamaoncol.2020.4564

7. Sankar K, Gong J, Osipov A, Miles SA, Kosari K, Nissen NN, et al. Recent advances in the management of hepatocellular carcinoma. *Clin Mol Hepatol*. (2024) 30:1–15. doi: 10.3350/cmh.2023.0125

8. Kim HJ, Hwang SY, Im JW, Jeon KJ, Jeon W. A case of nearly complete response in hepatocellular carcinoma with disseminated lung metastasis by combination therapy of nivolumab and ipilimumab after treatment failure of atezolizumab plus bevacizumab. *J Liver Cancer*. (2023) 23:213–8. doi: 10.17998/jlc.2023.02.23

9. Liu J, Chen Z, Li Y, Zhao W, Wu J, Zhang Z. PD-1/PD-L1 checkpoint inhibitors in tumor immunotherapy. *Front Pharmacol*. (2021) 12:731798. doi: 10.3389/fphar.2021.731798

10. Liu Y, Zugazagoitia J, Ahmed FS, Henick BS, Gettinger SN, Herbst RS, et al. Immune cell PD-L1 colocalizes with macrophages and is associated with outcome in PD-1 pathway blockade therapy. *Clin Cancer Res*. (2020) 26:970–7. doi: 10.1158/1078-0432.Ccr-19-1040

11. Wang L, Guo W, Guo Z, Yu J, Tan J, Simons DL, et al. PD-L1-expressing tumor-associated macrophages are immunostimulatory and associate with good clinical outcome in human breast cancer. *Cell Rep Med*. (2024) 5:101420. doi: 10.1016/j.xcrm.2024.101420

12. Zhang W, Liu Y, Yan Z, Yang H, Sun W, Yao Y, et al. IL-6 promotes PD-L1 expression in monocytes and macrophages by decreasing protein tyrosine phosphatase receptor type O expression in human hepatocellular carcinoma. *J Immunother Cancer*. (2020) 8:e000285. doi: 10.1136/jitc-2019-000285

13. Paz-Ares L, Spira A, Raben D, Planchard D, Cho BC, Özgüroğlu M, et al. Outcomes with durvalumab by tumour PD-L1 expression in unresectable, stage III non-small-cell lung cancer in the PACIFIC trial. *Ann Oncol*. (2020) 31:798–806. doi: 10.1016/j.annonc.2020.03.287

14. Mok TSK, Wu YL, Kudaba I, Kowalski DM, Cho BC, Turna HZ, et al. Pembrolizumab versus chemotherapy for previously untreated, PD-L1-expressing, locally advanced or metastatic non-small-cell lung cancer (KEYNOTE-042): a randomised, open-label, controlled, phase 3 trial. *Lancet*. (2019) 393:1819–30. doi: 10.1016/s0140-6736(18)32409-7

15. Nishio M, Barlesi F, West H, Ball S, Bordoni R, Cobo M, et al. Atezolizumab plus chemotherapy for first-line treatment of nonsquamous NSCLC: results from the randomized phase 3 IMpower132 trial. *J Thorac Oncol*. (2021) 16:653–64. doi: 10.1016/j.jtho.2020.11.025

16. Xu R, Wong CHL, Chan KSK, Chiang CL. PD-L1 expression as a potential predictor of immune checkpoint inhibitor efficacy and survival in patients with recurrent or metastatic nasopharyngeal cancer: a systematic review and meta-analysis of prospective trials. *Front Oncol*. (2024) 14:1386381. doi: 10.3389/fonc.2024.1386381

17. Maiorano BA, Di Maio M, Cerbone L, Maiello E, Procopio G, Roviello G. Significance of PD-L1 in metastatic urothelial carcinoma treated with immune checkpoint inhibitors: A systematic review and meta-analysis. *JAMA Netw Open*. (2024) 7:e241215. doi: 10.1001/jamanetworkopen.2024.1215

18. Lehrich BM, Zhang J, Monga SP, Dhanasekaran R. Battle of the biopsies: Role of tissue and liquid biopsy in hepatocellular carcinoma. *J Hepatol*. (2023) 80:515–30. doi: 10.1016/j.jhep.2023.11.030

19. Han JW, Jang JW. Predicting outcomes of atezolizumab and bevacizumab treatment in patients with hepatocellular carcinoma. *Int J Mol Sci*. (2023) 24:11799. doi: 10.3390/ijms241411799

20. Verset G, Borbath I, Karwal M, Verslype C, Van Vlierberghe H, Kardosh A, et al. Pembrolizumab monotherapy for previously untreated advanced hepatocellular carcinoma: data from the open-label, phase II KEYNOTE-224 trial. *Clin Cancer Res*. (2022) 28:2547–54. doi: 10.1158/1078-0432.Ccr-21-3807

21. Yau T, Park JW, Finn RS, Cheng AL, Mathurin P, Edeline J, et al. Nivolumab versus sorafenib in advanced hepatocellular carcinoma (CheckMate 459): a randomised, multicentre, open-label, phase 3 trial. *Lancet Oncol*. (2022) 23:77–90. doi: 10.1016/s1470-2045(21)00604-5

22. Lee DW, Cho EJ, Lee JH, Yu SJ, Kim YJ, Yoon JH, et al. Phase II study of avelumab in patients with advanced hepatocellular carcinoma previously treated with sorafenib. *Clin Cancer Res*. (2021) 27:713–8. doi: 10.1158/1078-0432.Ccr-20-3094

23. Yang Y, Chen D, Zhao B, Ren L, Huang R, Feng B, et al. The predictive value of PD-L1 expression in patients with advanced hepatocellular carcinoma treated with PD-1/PD-L1 inhibitors: A systematic review and meta-analysis. *Cancer Med*. (2023) 12:9282–92. doi: 10.1002/cam4.5676

24. Llovet JM, Lencioni R. mRECIST for HCC: Performance and novel refinements. *J Hepatol*. (2020) 72:288–306. doi: 10.1016/j.jhep.2019.09.026

25. Ilie M, Khambata-Ford S, Copie-Bergman C, Huang L, Juco J, Hofman V, et al. Use of the 22C3 anti-PD-L1 antibody to determine PD-L1 expression in multiple automated immunohistochemistry platforms. *PloS One*. (2017) 12:e0183023. doi: 10.1371/journal.pone.0183023

26. Paver EC, Cooper WA, Colebatch AJ, Ferguson PM, Hill SK, Lum T, et al. Programmed death ligand-1 (PD-L1) as a predictive marker for immunotherapy in solid tumours: a guide to immunohistochemistry implementation and interpretation. *Pathology*. (2021) 53:141–56. doi: 10.1016/j.pathol.2020.10.007

27. Zhu AX, Abbas AR, de Galarreta MR, Guan Y, Lu S, Koeppen H, et al. Molecular correlates of clinical response and resistance to atezolizumab in combination with bevacizumab in advanced hepatocellular carcinoma. *Nat Med*. (2022) 28:1599–611. doi: 10.1038/s41591-022-01868-2

28. Nam H, Lee J, Han JW, Lee SK, Yang H, Lee HL, et al. Analysis of immune-related adverse events of atezolizumab and bevacizumab in patients with hepatocellular carcinoma: A multicentre cohort study. *Liver Cancer*. (2023) 13:413–25. doi: 10.1159/000535839

29. Sung PS. Crosstalk between tumor-associated macrophages and neighboring cells in hepatocellular carcinoma. *Clin Mol Hepatol*. (2022) 28:333–50. doi: 10.3350/cmh.2021.0308

30. Mun K, Han J, Roh P, Park J, Kim G, Hur W, et al. Isolation and characterization of cancer-associated fibroblasts in the tumor microenvironment of hepatocellular carcinoma. *J Liver Cancer*. (2023) 23:341–9. doi: 10.17998/jlc.2023.04.30

31. Zhang H, Liu L, Liu J, Dang P, Hu S, Yuan W, et al. Roles of tumor-associated macrophages in anti-PD-1/PD-L1 immunotherapy for solid cancers. *Mol Cancer*. (2023) 22:58. doi: 10.1186/s12943-023-01725-x

32. Peng Q, Qiu X, Zhang Z, Zhang S, Zhang Y, Liang Y, et al. PD-L1 on dendritic cells attenuates T cell activation and regulates response to immune checkpoint blockade. *Nat Commun*. (2020) 11:4835. doi: 10.1038/s41467-020-18570-x

33. Chen J, Lin Z, Liu L, Zhang R, Geng Y, Fan M, et al. GOLM1 exacerbates CD8(+) T cell suppression in hepatocellular carcinoma by promoting exosomal PD-L1 transport into tumor-associated macrophages. *Signal Transduct Target Ther*. (2021) 6:397. doi: 10.1038/s41392-021-00784-0

34. Park DJ, Sung PS, Lee GW, Cho S, Kim SM, Kang BY, et al. Preferential expression of programmed death ligand 1 protein in tumor-associated macrophages and its potential role in immunotherapy for hepatocellular carcinoma. *Int J Mol Sci*. (2021) 22:4710. doi: 10.3390/ijms22094710

35. Yau T, Park JW, Finn RS, Cheng AL, Mathurin P, Edeline J, et al. LBA38_PR - CheckMate 459: A randomized, multi-center phase III study of nivolumab (NIVO) vs sorafenib (SOR) as first-line (1L) treatment in patients (pts) with advanced hepatocellular carcinoma (aHCC). *Ann Oncol*. (2019) 30:v874–v5. doi: 10.1093/annonc/mdz394.029

36. Sangro B, Melero I, Wadhawan S, Finn RS, Abou-Alfa GK, Cheng AL, et al. Association of inflammatory biomarkers with clinical outcomes in nivolumab-treated patients with advanced hepatocellular carcinoma. *J Hepatol*. (2020) 73:1460–9. doi: 10.1016/j.jhep.2020.07.026

37. Lee MS, Ryoo BY, Hsu CH, Numata K, Stein S, Verret W, et al. Atezolizumab with or without bevacizumab in unresectable hepatocellular carcinoma (GO30140): an open-label, multicentre, phase 1b study. *Lancet Oncol*. (2020) 21:808–20. doi: 10.1016/s1470-2045(20)30156-x

38. El-Khoueiry AB, Sangro B, Yau T, Crocenzi TS, Kudo M, Hsu C, et al. Nivolumab in patients with advanced hepatocellular carcinoma (CheckMate 040): an open-label, non-comparative, phase 1/2 dose escalation and expansion trial. *Lancet*. (2017) 389:2492–502. doi: 10.1016/s0140-6736(17)31046-2

39. Xu J, Shen J, Gu S, Zhang Y, Wu L, Wu J, et al. Camrelizumab in combination with apatinib in patients with advanced hepatocellular carcinoma (RESCUE): A nonrandomized, open-label, phase II trial. *Clin Cancer Res*. (2021) 27:1003–11. doi: 10.1158/1078-0432.Ccr-20-2571

40. Pinato DJ, Mauri FA, Spina P, Cain O, Siddique A, Goldin R, et al. Clinical implications of heterogeneity in PD-L1 immunohistochemical detection in hepatocellular carcinoma: the Blueprint-HCC study. *Br J Cancer*. (2019) 120:1033–6. doi: 10.1038/s41416-019-0466-x

41. Vranic S, Gatalica Z. PD-L1 testing by immunohistochemistry in immuno-oncology. *Biomol BioMed*. (2023) 23:15–25. doi: 10.17305/bjbms.2022.7953

42. Lea D, Zaharia C, Søreide K. Programmed death ligand-1 (PD-L1) clone 22C3 expression in resected colorectal cancer as companion diagnostics for immune checkpoint inhibitor therapy: A comparison study and inter-rater agreement evaluation across proposed cut-offs and predictive (TPS, CPS and IC) scores. *Cancer Treat Res Commun*. (2024) 38:100788. doi: 10.1016/j.ctarc.2023.100788

43. Maule JG, Clinton LK, Graf RP, Xiao J, Oxnard GR, Ross JS, et al. Comparison of PD-L1 tumor cell expression with 22C3, 28-8, and SP142 IHC assays across multiple tumor types. *J Immunother Cancer*. (2022) 10:e005573. doi: 10.1136/jitc-2022-005573

44. Shi L, Zhang SJ, Chen J, Lu SX, Fan XJ, Tong JH, et al. A comparability study of immunohistochemical assays for PD-L1 expression in hepatocellular carcinoma. *Mod Pathol*. (2019) 32:1646–56. doi: 10.1038/s41379-019-0307-8

45. Han JW, Kim JH, Kim DH, Jang JW, Bae SH, Choi JY, et al. Higher number of tumor-infiltrating PD-L1+ Cells is related to better response to multikinase inhibitors in hepatocellular carcinoma. *Diagnostics (Basel)*. (2023) 13:1453. doi: 10.3390/diagnostics13081453

46. Brown ZJ, Ruff SM, Pawlik TM. The effect of liver disease on hepatic microenvironment and implications for immune therapy. *Front Pharmacol*. (2023) 14:1225821. doi: 10.3389/fphar.2023.1225821

47. Pinter M, Pinato DJ, Ramadori P, Heikenwalder M. NASH and hepatocellular carcinoma: immunology and immunotherapy. *Clin Cancer Res*. (2023) 29:513–20. doi: 10.1158/1078-0432.Ccr-21-1258

48. Kim JH, Kim YH, Nam HC, Kim CW, Yoo JS, Han JW, et al. Consistent efficacy of hepatic artery infusion chemotherapy irrespective of PD−L1 positivity in unresectable hepatocellular carcinoma. *Oncol Lett*. (2024) 28:388. doi: 10.3892/ol.2024.14521

frontiers | Frontiers in Immunology

TYPE Original Research
PUBLISHED 08 May 2025
DOI 10.3389/fimmu.2025.1509087

OPEN ACCESS

EDITED BY
Ashraf A. Tabll,
National Research Centre (Egypt), Egypt

REVIEWED BY
Nashwa El-Khazragy,
Ain Shams University, Egypt
Mulu Tesfay,
University of Arkansas for Medical Sciences, United States

*CORRESPONDENCE
Sheng Hu
ehusmn@163.com
Binlei Liu
liubinlei@binhui-bio.com
Mingqian Feng
fengmingqian@mail.hzau.edu.cn

†These authors have contributed equally to this work

RECEIVED 10 October 2024
ACCEPTED 14 April 2025
PUBLISHED 08 May 2025

CITATION
Dong S, Chen X, Li X, Wang Y, Huang Q, Li Y, Jin J, Zhu X, Zhong Y, Cai Q, Xue C, Guo F, Huang L, Feng M, Liu B and Hu S (2025) A conceptual exploration on the synergistic anti-tumor effects of high-order combination of OHSV2-DSTE$^{FAP5/CD3}$, CAR-T cells, and immunotoxins in hepatocellular carcinoma. *Front. Immunol.* 16:1509087. doi: 10.3389/fimmu.2025.1509087

A conceptual exploration on the synergistic anti-tumor effects of high-order combination of OHSV2-DSTE$^{FAP5/CD3}$, CAR-T cells, and immunotoxins in hepatocellular carcinoma

Shuang Dong[1†], Xin Chen[2,3†], Xiaoyu Li[1†], Yang Wang[3], Qing Huang[1], Yuanxiang Li[1], Jing Jin[4], Xianmin Zhu[1], Yi Zhong[1], Qian Cai[1], Chang Xue[1], Fang Guo[5], Le Huang[2], Mingqian Feng[2*], Binlei Liu[3,4*] and Sheng Hu[1*]

[1]Department of Medical Oncology, Tongji Medical College, Hubei Cancer Hospital, Huazhong University of Science and Technology, Wuhan, China, [2]College of Life Science and Technology, Huazhong Agricultural University, Wuhan, China, [3]National "111" Center for Cellular Regulation and Molecular Pharmaceutics, Key Laboratory of Fermentation Engineering (Ministry of Education), Hubei Provincial Cooperative Innovation Center of Industrial Fermentation, Hubei Key Laboratory of Industrial Microbiology, Hubei University of Technology, Wuhan, Hubei, China, [4]Wuhan Binhui Biopharmaceutical Co., Ltd, Wuhan, China, [5]Department of Pathology, Tongji Medical College, Hubei Cancer Hospital, Huazhong University of Science and Technology, Wuhan, China

Background: Although the treatment landscape for advanced hepatocellular carcinoma (HCC) has seen significant advancements in the past decade with the introduction of immune checkpoint inhibitors and antiangiogenic drugs, progress has fallen short of expectations. Recently, a novel engineered oncolytic virus (OHSV2) that secretes dual-specific T-cell engagers (DSTEs) targeting the fibroblast activation protein (FAP) was developed and combined with GPC3-targeting CAR-T cells and immunotoxins to exert a synergistic antitumor effect.

Methods: OHSV2-DSTE$^{FAP5/CD3}$ was initially generated by transducing the DSTEs engaging FAP5 on fibroblasts into the backbone of our oncolytic virus OHSV2. An innovative high-order combination was devised in a xenograft mouse model to conceptually explore whether enhanced anti-tumor effects could be achieved. Additionally, the underlying mechanisms of synergistic effects and safety profiles were preliminarily investigated.

Results: OHSV2-DSTE$^{FAP5/CD3}$ effectively targeted and eliminated fibroblasts *in vitro* while maintaining cytotoxicity and inducing immune activation compared to parental OHSV2. *In vivo*, dose-adjusted combination therapy resulted in a remarkable antitumor effect compared to control treatments, leading to tumor regression in 40% of mice without significant toxicity to major organs. Mechanistically, rather than directly depleting fibroblasts, OHSV2-DSTE$^{FAP5/CD3}$ played an essential role in priming T-cell proliferation, infiltration, and activation, and inhibiting the supportive interaction between cancer cells and fibroblasts.

10.3389/fimmu.2025.1509087

Conclusions: This high-order combination represents a novel multiple-wave immunotherapeutic approach for HCC. Despite being a conceptual exploration, this strategy has demonstrated promising therapeutic efficacy and acceptable safety profiles.

KEYWORDS

immunotherapy, oncolytic virus, CAR-T, immunotoxins, dual-specific T cell engagers, FAP, GPC3, synergistic effect

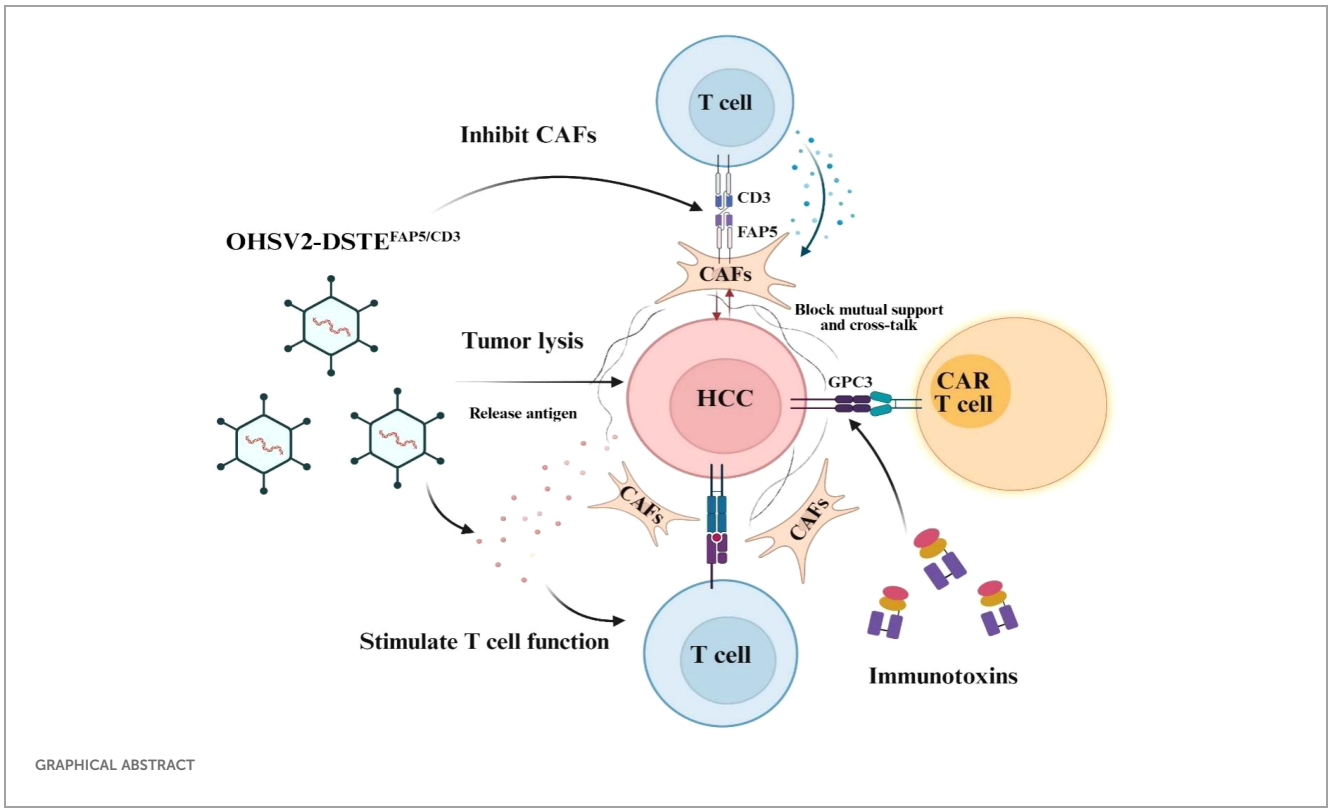

GRAPHICAL ABSTRACT

Background

Hepatocellular carcinoma (HCC) consistently ranks as the third leading cause of cancer-related mortality among all cancers worldwide, highlighting the urgent need for improved therapeutic strategies (1). Over the past decade, the treatment landscape for advanced HCC has undergone significant renovation with the introduction of immune checkpoint inhibitors (ICIs), either as monotherapies, in combination with each other, or plus antiangiogenic drugs. However, therapeutic progress remains suboptimal, as no more than 30% of patients achieve an objective response to the current standard-of-care treatments, with complete responses in fewer than 10% (2, 3). The mechanisms underlying resistance to immunotherapy are exceptionally complex (4), involving intricate interactions among cancer cells, various immune cells, and fibroblasts, which means that anti-cancer battle cannot be won with a single weapon. Nowadays, multiple strategies for combination therapy mechanistically are being explored in parallel, including directly double blocking of a single target on cancer cells, like HER-2, the combination of CAR T cells or ICIs with other drugs facilitating immune cells activation and infiltration or eliminating fibroblasts, such as oncolytic virus or BiTEs (bispecific T-cell engagers). Therefore, the conceptual design of a three-layered combination to overcome resistance and extend clinical response is particularly compelling in the field of HCC treatment, as a high-order combination of multiple immune-based therapies, mainly derived from clinical insights, holds great promise for success both in terms of efficacy and safety (5).

Oncolytic viruses (OVs), as a promising cancer therapeutic approach, not only can selectively replicate within cancer cells and

lyse them while sparing normal cells but also induce immunogenic death and subsequently trigger the immune stimulation *in situ* (6), endorsed by definite evidence from Talimogene laherparepvec (T-Vec), a herpes simplex virus type I (HSV-1) approved by the US Food and Drug Administration (FDA) for melanoma in 2015 (7), and our oncolytic herpes simplex virus type II (OHSV2), which has shown efficacy in melanoma and malignant ascites of colon cancer, and other OVs for diversified types of cancer in the preclinical and clinical studies (8–11). However, faced with the fact that the effectiveness of OVs is limited in the vast majority of cancers beyond melanoma, a widely adopted strategy is to fully leverage their function as expression platforms and immune stimulators, using them as a cornerstone for combination therapies, rather than solely focusing on enhancing their direct oncolytic effects.

In the tumor microenvironment (TME), the interaction between cytotoxic T cells (CTLs) and cancer cells resembles that of a predator–prey dynamic within an ecosystem, where predators kill another species (12). Therefore, a logical therapeutic strategy is to directly increase the number of "predators," such as CAR-T cells. Significant advances have been made in CAR-T cells for hematological malignancies (13, 14), with rapid progress in the context of solid tumors, including our GPC3-targeting CAR-T cells in HCC (15, 16). However, CAR-T cell therapy for solid tumors faces critical challenges, including safety concerns and generally limited antitumor efficacy, albeit with a few promising preclinical outcomes (17). The mechanisms of CAR-T cell resistance are multifaceted, with one major obstacle being the extracellular matrix (ECM) barriers (18) mainly derived from cancer-associated fibroblasts (CAFs), which highly express fibroblast activation protein (FAP) to impede infiltrating of T cells, thereby shaping an immune-suppressive tumor microenvironment, especially in virus-related HCC (19–21).

Accordingly, massive strategies to overcome CAR-T cell resistance and improve safety are currently being developed in preclinical settings (22, 23). Leveraging our extensive experience in OV development, we propose to engineer dual-specific T-cell engagers (DSTEs) into OHSV2, specifically targeting FAP to disrupt CAFs theoretically, which could address CAR-T cells resistance from two dimensions or layers mentioned above, thereby achieving a synergistic anti-tumor effect once combined with GPC3-targeting CAR-T cells for HCC. However, eliminating cancer cells remains a formidable challenge, just like the proverb "cunning rabbit with three holes" (24, 25). Moreover, we have discovered the positive synergy between immunotoxins and CAR-T cells targeting GPC3, consistent with previous findings on the multiple blockades of HER-2 or CD19 (NCT06063317) (26).

In this study, we initially developed OHSV2-DSTE$^{FAP5/CD3}$ and designed an innovative high-order combination by incorporating OHSV2-DSTE$^{FAP5/CD3}$, GPC3-targeting CAR-T cells, and immunotoxins (27) in a mouse HCC model. This approach, distinct from ICIs and anti-angiogenic inhibitors, aims to establish a synergistic process of immune activation and tumor microenvironment remodeling and conceptually explore whether more potent anti-tumor effects can be generated. Additionally, the underlying mechanisms of synergistic effects and safety profiles are preliminarily investigated.

Methods

Ethics statement

Peripheral blood was collected from healthy donors following written informed consent, and all animal experiments were conducted according to the institutional review board and research ethics committees of the Huazhong University of Science and Technology, PR China (2019-S1010 and 2019-IEC-S213) to ensure the ethical and welfare of human participants and animals involved in the research process.

Cell lines

Cell lines in this study, including A375 (human melanoma cell line), A549 (human lung carcinoma cell line), BGC823 (human gastric carcinoma cell line), Hep2 (human head and neck squamous cell carcinoma cell line), HuH-7 (human hepatocellular carcinoma cell line), LoVo (human colon carcinoma cell line), PANC-1 (human pancreatic carcinoma cell line), U87MG (human glioblastoma cell line), 5637 (human bladder carcinoma cell line), MRC-5 (human embryonic lung fibroblasts line), and HEK293 (human embryonic kidney cell line) were obtained from the Cell Bank of Chinese Academy of Sciences (SGST, Shanghai, China). The composition of the culture medium is DME/F12 (Invitrogen, Carlsbad, CA) medium supplemented with 10% fetal bovine serum (HyClone, Logan, UT), 1% L-glutamine (Invitrogen, Carlsbad, CA), and 1% penicillin-streptomycin (Invitrogen, Carlsbad, CA) in a CO_2 incubator at 37°C for most of these cell lines, while it will undergo appropriate modifications for the other lines. FAP5 cDNA was amplified using FAP-specific primers in 2× qPCR BIO SyGreen Blue Mix Hi-ROX Master Mix (PCR BioSystems) and then transduced into various cancer cells through the well-constructed plasmids to obtain the cancer cells with high expression of FAP5.

Peripheral blood mononuclear cells, CAR-T cells, and immunotoxins

Peripheral blood mononuclear cells (PBMCs) were isolated by Ficoll separation method (Stem Cell Technologies, Vancouver, BC, Canada). PBMCs were cultured in RPMI 1640 medium supplemented with 200 IU/ml human recombinant interleukin (IL)-2 and activated by Dynabeads™ CD3/CD28 Human T-activator (Cat. 11131D, Thermo Fisher, Waltham, MA) for 3 days according to the manufacturer's instruction. Alternatively, they can be directly isolated using a blood cell separator (Fresenius CEM TEC., Germany).

The activated PBMCs were directly used in various experiments *in vivo* or *in vitro* or transfected with the lentivirus expressing CARs

to obtain CAR-T^{HN3} targeting GPC3 by us (15). In addition, the immunotoxins (scFv fused with PE24, the 24-kDa cytotoxic domain of *Pseudomonas* exotoxin A) targeting the membrane-distal N-lobe of GPC3 previously developed by us, named as J80A-PE24, could suppress tumor growth much greater than naked HN3-PE24 in a xenograft mouse model (27).

Generation and purification of OHSV2-DSTE$^{FAP5/CD3}$

The DSTE$^{FAP5/CD3}$ was produced by fusing the single-chain variable fragments (scFvs) of anti-FAP 28H1 from patent EP3333194A1-1 and anti-CD3 OKT3 to construct the FAP5/CD3-DSTE expression fragment.

The final fragment VH_{FAP5}-VL_{FAP5}-VH_{CD3}-VL_{CD3} was constructed by Nanjing Kingsley Company and assembled into the pHG52d34.5-CMV shuttle vector (also referred to as pGFP) established in our laboratory for subsequent homologous recombination. The parental virus OHSV2-GFP and OHSV2-DSTE$^{CD19/CD3}$ derived from laboratory were utilized as controls. The genome of OHSV2-DSTE$^{FAP5/CD3}$ was obtained by recombineering and subsequently sequenced by the Tsingke Biotech (Beijing, China). The sequencing results were aligned to the original FAP/CD3-DSTE plasmid sequences by SnapGene software. OHSV2-DSTE$^{FAP5/CD3}$, OHSV2-DSTE$^{CD19/CD3}$, and OHSV2-GFP were used to infect Vero cells for 48–72 h, and the supernatant was collected after the addition of a virus-releasing solution. Afterwards, virus was purified and titrated.

OHSV2-DSTE$^{FAP5/CD3}$ was used to infect Vero cells for 48 h at multiplicity of infection (MOI) of 0.01. After infection, the viral supernatants were collected and purified using High-Affinity Ni-Charged Resin (GenScript). Subsequently, the DSTE$^{FAP5/CD3}$ protein released by infected cells was eluted with the appropriate buffer. The resultant protein solution was purified through 20K Slide-A-Lyzer Dialysis Cassettes according to the manufacturer's instructions (Thermo Fisher).

Flow cytometry to analyze cellular components and cytokine levels

Flow cytometry was performed on Accuri C6 cytometer (BD Biosciences, Franklin Lakes, NJ). Human-derived FAP expression was detected with anti-FAP antibody (phycoerythrin, accession number: MIH1, BD Biosciences). T cells were analyzed using the following antibodies: anti-CD3 (APC, accession number: HIT3a, BD Biosciences), anti-CD4 (FITC, accession number: RPA-T4, BD Biosciences), anti-CD8 (FITC, accession number: RPA-T8, BD Biosciences), anti-CD25 (PE, accession number: MA251, BD Biosciences), and anti-CD69 (APC, accession number: FN50, BD Biosciences). Cytokine, including IL2, IL4, IL6, IL10, TNF, and IFN-γ in culture supernatants or peripheral blood, was detected with BD^{TM} Cytometric Bead Array (CBA) Human Th1/Th2 Cytokine Kit II. All flow cytometry data were processed with FlowJo v7.6.5 and FCAP Array v3.0.

In vitro cytotoxicity assays

To investigate the cytotoxicity of free DSTE, oncolytic virus, and T-cell-mediated killing, an average of 1.5×10^4 cancer cells per well was seeded into E-Plate 16 (ACEA Biosciences Inc, San Diego, CA) and co-cultured with pre-activated PBMCs (cancer cells, PBMCs = 1:2) or/and fibroblasts treated by OHSV2-DSTE$^{FAP5/CD3}$ (MOI = 0.1) alone or the other agents and OHSV2 or OHSV2-DSTE$^{CD19/CD3}$ (MOI = 0.1) as control virus. Cellular vitality of cancer cells or others was continuously monitored by the xCELLigence Real-Time Cell Analyzer (ACEA Biosciences Inc, San Diego, CA), following the manufacturer's protocol. The half-maximal inhibitory concentration (IC50) was calculated by a dose–response inhibition (variable slope) curve with GraphPad Prism V8.0 (GraphPad Software, Inc, La Jolla, CA).

We selected engineering high-expressing FAP5 cancer cells, BGC823-GFP-FAP5 cell lines with three different levels of FAP5 expression to investigate free DSTE or OHSV2-DSTE$^{FAP5/CD3}$ impairment on the cell proliferation *in vitro* continuously in the above-mentioned cell proliferation experiment.

Reverse transcription quantitative polymerase chain reaction

RNA was extracted from cell lines, mouse tumor tissue, or rabbit spleen, or other components using RNA Simple Total RNA Kit (Tiangen Biotech, Beijing, China), and reverse transcription was carried out to detect levels of IL2RA, GZMB, and PRF1, which are T-cell activation markers by RT-qPCR using 5 × HiScript II QRTSuperMix II (Vazyme Biotech, Nanjing, China) and iTaq Universal SYBR Green Supermix (Bio-Rad, Redmond, WA). Specific primers were designed through the software of Invitrogen's Vector NTI® Advance 11.5.1. The RT-qPCR procedures briefly were as follows: pre-denaturation at 95°C for 1 min, followed by 40 cycles of 95°C for 5 s, 61°C for 31 s, 95°C for 15 s, and 60°C for 60 s, ending up with heating to 95°C. The relative expression level of the target gene was calculated by the $2^{-\triangle\triangle CT}$ method with glyceraldehyde 3-phosphate dehydrogenase (GAPDH) gene as an internal reference for three independent biological replicates.

Animal experiments

6-week-old female BALB/c nude mice were purchased from the Animal Center of Huazhong Agricultural University. Three million HuH-7 cells were subcutaneously injected into the right flank of nude mice feeding under specific pathogen-free conditions. After tumor mass reached the size of approximately 100–200 mm^3, mice

were randomized into seven groups listed in Table 1 for details. Tumor volume was calculated from the formula: tumor volume (mm^3) = (length × width × width)/2 by digital calipers. We first carried out dose-found research of OHSV2-DSTE$^{FAP5/CD3}$ *in vivo* in a HuH-7 subcutaneous mouse model intratumorally injected with three different doses of OHSV2-DSTE$^{FAP5/CD3}$ ($CCID_{50}$ = 1 × 10^6, 1 × 10^7, and 1 × 10^8, respectively) or control OHSV2-GFP, once a week, for a total of 4 weeks. Subsequently, formal high-order combination research will be conducted according to the specified schedule and dosages shown in Table 1. Mice in the control group and treatment groups were sacrificed for analysis at day 42 after tumor inoculation or at any time due to the oversized tumors.

Side-effect analysis in mouse tumor model

To examine whether the functions of major organs and systems such as liver, kidney, bone marrow, myocardium, and endocrine system have been impaired by different schedules of administration, we collected peripheral venous blood of mice at the end of the experiment and analyzed levels of various serum enzymes (such as alanine aminotransferase, ALT; aspartate aminotransferase, AST; and creatine kinase, CK), blood glucose, blood lipids, albumin, total bilirubin, creatinine, electrolytes, and cytokine.

Histopathology and immunohistochemistry analysis in mouse tumor model

Once the mice were sacrificed by cervical dislocation, major organs and partial tumor tissue were collected and immersed in 10% neutral-buffered formalin for fixation. Subsequently, the samples were embedded in paraffin, sectioned (5 μm), and hematoxylin–eosin stained. Additionally, the levels of FAP5 expression were detected by immunohistochemical staining, and grading was assessed by a digital camera (Leica ICC50 HD, Germany) to gather the area and density of the dyed region and calculate the integrated optical density (IOD) value, from five randomly selected fields (Image-Pro Plus 6.0).

These analyses are independently evaluated by two pathologists, and in case of inconsistency, a discussion will be held to make the decision.

Preliminary analysis of the mechanism by single-cell RNA sequencing

For the high-order combined therapy group, we conducted a preliminary analysis of the mechanism by single-cell RNA sequencing, in addition to T-cell activation characterization and cytokine levels. Tumor tissues were harvested from mice in different treatment groups at the end of the experiments for sample preparation and single-cell RNA sequencing. In short, after digested into cell suspension, they were filtered by a 40-μm strainer and resuspended in the PBS solution to obtain single cells for single-cell sequencing. Single-cell capture was performed by the BD Rhapsody Single-Cell Analysis System (BD Biosciences, Franklin Lakes, NJ) for library construction. Upon preparation of the libraries, they were quantified using the Agilent 2100 Bioanalyzer (Agilent Technologies, Palo Alto, CA) and the Qubit 4.0 (Thermo Fisher Scientific, USA). Finally, the libraries were sequenced on the Illumina NovaSeq 6000 (Illumina, USA), and 300-bp reads (including 150-bp paired-end reads) were generated. Single-cell RNA sequencing data were subjected to multiple analyses including quality control, alignment, clustering, marker gene identification, annotation of clusters, and other analyses.

The clustering results were visualized using t-distributed stochastic neighbor embedding (tSNE) and uniform manifold approximation and projection (UMAP). The marker genes for each cluster were identified using the default parameters through the "FindAllMarkers" function in Seurat. The original clusters were annotated based on the MouseRNAseqData dataset via SingleR (v.1.0.1). T-cell clusters were extracted for further sub-analysis using the subset function. To enhance the distinction between cell

TABLE 1 The specified schedule of dosages and administration.

Groups[a] (N=5)	Treatment schedules
Control group	PBS solution 100 μl, intraperitoneal administration once every other day, a total of 4 weeks.
Immunotoxin group	J80A-PE24, administered via the tail vein injection of 3 mg/kg, once a week, for a total of 4 times (27).
Lenvatinib plus anti-PD-1 antibody (pembrolizumab) group	Pembrolizumab, intraperitoneal injection, once every 2 weeks, with a concentration of 2 mg/kg, a total of 2 times. Lenvatinib, 5 mg/kg, was administered by gavage every other day, for a total of 4 weeks.
OHSV2-DSTE$^{FAP5/CD3}$	OHSV2-DSTE$^{FAP5/CD3}$, administered by local injection, once a week, for a total of 4 weeks[b].
OHSV2-DSTE$^{FAP5/CD3}$ plus J80A-PE24	J80A-PE24 and OHSV2-DSTE$^{FAP5/CD3}$ are administered by the same method above.
OHSV2-DSTE$^{FAP5/CD3}$ plus J80A-PE24 plus anti-PD-1 antibody	J80A-PE24, OHSV2-DSTE$^{FAP5/CD3}$ and anti-PD-1 are administered by the same method above.
OHSV2-DSTE$^{FAP5/CD3}$ plus J80A-PE24 plus CAR-T^{HN3}	CAR-T^{HN3} cells, 3 × 10^6, intravenous injection, once every 2 weeks, a total of 2 times (15, 28). J80A-PE24 and OHSV2-DSTE$^{FAP5/CD3}$ are administered by the same method above.

[a]PBMCs, 2.5 × 10^6 cells, were intravenously injected into all groups once every 2 weeks, a total of 2 times.
[b]The dose of OHSV2-DSTE$^{FAP5/CD3}$ was confirmed by initial dose-finding research.

types, the ImmGenData dataset was utilized for cluster annotation. Differentially expressed genes (DEGs) related to interleukin (IL) and interferon (IFN) family were screened from the T-cell cluster with |Log2-fold change| > 0.5 and p-value < 0.05 as thresholds and visualized through violin plot by Seurat. Furthermore, genes related to CAFs and T-cell exhaustion were also analyzed.

Statistical analysis

Quantitative data are usually displayed as mean ± SD from at least three biological replicates and related to the control. Two-tailed unpaired Student's t-tests were performed for comparisons of two independent data sets. Comparisons among three or more groups were performed using two-way ANOVA with Tukey's multiple comparison test. The statistical significance was denoted as follows: n.s, non-significant; *$p < 0.05$; **$p < 0.01$; ***$p < 0.001$; and ****$p < 0.0001$. Statistical analysis was conducted by GraphPad Prism 8.0.

Results

OHSV2-DSTE$^{FAP5/CD3}$ is successfully constructed

DSTE$^{FAP5/CD3}$ was constructed using the FAP5 monoclonal antibody 28H1, paired with the CD3 monoclonal antibody OKT3. In combination with peripheral blood mononuclear cells (PBMCs), DSTE$^{FAP5/CD3}$ significantly inhibited the proliferation of BGC823 cells overexpressing FAP5, and fibroblasts, in a time-dependent manner, with maximal effect at 60 h (95% tumor cell apoptosis) monitored by CellInsight CX5 high-content system (Figures 1A, B), compared with DSTE$^{CD19/CD3}$ (preserved in our laboratory only utilized as a control).

Mechanistically, our results showed a significant upregulation in the proliferation of both CD4+ and CD8+ T cells in the DSTEFAP5/CD3 plus PBMC group (2,557 ± 76.59 and 9,362 ± 101.8, respectively), compared to the control group (1,141 ± 79.23 and 6,215 ± 120.7, respectively, $p < 0.05$) (Figures 1C, D). In addition, the proliferation amplitude between CD4+ and CD8+ T cells was approximately similar in DSTE$^{FAP5/CD3}$ plus PBMC group. Furthermore, multiple cytokine levels in the supernatant were found to be significantly elevated, particularly IFN-γ, IL-6, and TNF (Figures 1E, F).

Next, DSTE$^{FAP5/CD3}$ was transduced into OHSV2 to generate a novel virus, named OHSV2-DSTE$^{FAP5/CD3}$ (Figure 2A), which was used to infect Vero cells. At 60 h post-infection, the concentration of DSTE$^{FAP5/CD3}$ reached 0.12 ng/ml, despite lower than that achieved by recombination methods, indicating that insertion of DSTE gene fragments did not impair replication of OHSV2 relative. Subsequently, we collected the supernatant and found that DSTE$^{FAP5/CD3}$ also exhibited killing activity (Figures 2B, C). Moreover, the levels of DSTE$^{FAP5/CD3}$-induced cytokines, including IL-2, IL-4, IL-6, IL-10, TNF, and IFN-γ were markedly elevated *in vitro*, indicating the activation of T cells and immune function enhancement in BGC823 cells overexpressing FAP5 cells and MRC-5 cells (Figures 2D–G), suggesting that OHSV2-DSTE$^{FAP5/CD3}$ is successfully constructed; thus, in-depth exploration is necessary to achieve our therapeutic objectives.

OHSV2-DSTE$^{FAP5/CD3}$ exhibits killing activity and simultaneously stimulates PBMCs *in vitro*

To further explore the lytic function of OHSV2-DSTE$^{FAP5/CD3}$, we initially examined human melanoma cells, which demonstrate relatively higher sensitivity to most immunotherapy drugs. Our findings showed that OHSV2-DSTE$^{FAP5/CD3}$ can exhibit uncompromising lytic activity compared to its parental virus (Figures 3A, B). Furthermore, the *in vitro* anti-tumor efficacy of OHSV2-DSTE$^{FAP5/CD3}$ against HuH-7 cells was significantly greater than that observed in CT-26, MC-38, 4T1, and BGC823 cell lines lacking FAP5 expression, and analogous to control virus, such as OHSV2-DSTE$^{CD19/CD3}$ or OHSV2, albeit weaker than its effect on melanoma cells (Table 2). These results imply that HuH-7 cells possess an inherent susceptibility to immune-mediated killing induced by OHSV2-DSTE$^{FAP5/CD3}$, accompanied by significant T-cell activation (Figures 3C, D), prompting our team to select this cell line for further investigation.

OHSV2 demonstrates limited replication capacity and consequently fails to directly eliminate fibroblasts or other nonepithelial stromal cells with normal antiviral pathways, such as interferon secretion. Furthermore, co-culturing cancer cells and fibroblasts may affect their respective survival rates, although these effects can vary depending on multiple factors. Hence, co-cultivation of HuH-7 and FAP-expressing stromal fibroblasts was lastly carried out. The results suggested that OHSV2-DSTE$^{FAP5/CD3}$ exhibited direct HuH-7 cell killing and T-cell-mediated fibroblast elimination (Figure 3E). However, the potential enhancement of oncolytic effects through CD3-induced T-cell clustering activation remains to be elucidated. Moreover, OHSV2-DSTE$^{FAP5/CD3}$ exhibits negligible cytotoxicity toward fibroblasts in the absence of cancer cells or PBMCs, indicating that its function is constrained by environmental conditions, which may confer potential safety advantages for further exploration and even clinical development.

Furthermore, the levels of multiple cytokines, including IL-2, IL-4, IL-6, IL-10, TNF, and IFN-γ in the supernatant of the OHSV2-DSTE$^{FAP5/CD3}$ group co-cultured with cancer cells and fibroblasts, showed a significant increase compared to groups with either cell type alone (Figure 3F). This suggests that T cells derived from PBMCs are primarily activated by OHSV2, with DSTE playing a secondary regulatory role. It should be noted that our interpretation is based solely on a correlation study and requires further validation.

Subsequently, the FAP5-targeted function of OHSV2-DSTE$^{FAP5/CD3}$ in high FAP5 expression setting was explored. Initial assessment of FAP5 expression levels across various tumor cell lines revealed that only MRC-5 and U87MG cell lines exhibited high expression levels of FAP5, with an expression of 45% and 18%,

10.3389/fimmu.2025.1509087

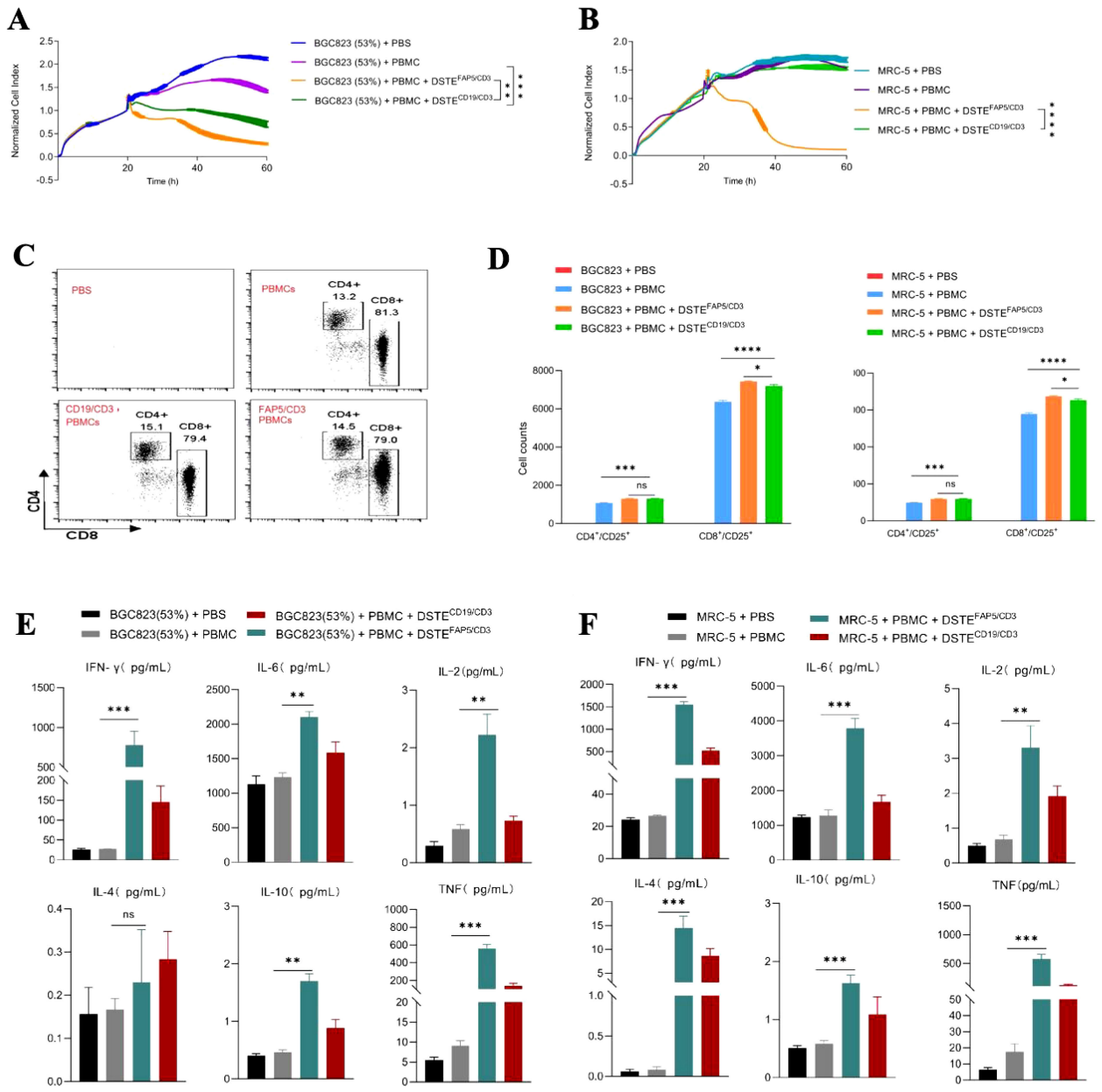

FIGURE 1
DSTE$^{FAP5/CD3}$ can significantly inhibit the proliferation of fibroblasts or BGC823 cells overexpressing FAP5 with PBMC. **(A)** Tumor cell-killing activity of DSTE$^{FAP5/CD3}$ monotherapy on BGC823-FAP+ cells (53% FAP expression). BGC823 cells were pre-seeded, followed by treatment with oncolytic virus (MOI = 0.1) and PBMCs (cancer cells: PBMC = 1:2). Cell index reflecting cell-killing activity was monitored through xCELLigence Real-Time Cell Analyzer over 60 h (*p < 0.05;** p < 0.01; ***p < 0.001; ****p < 0.0001, unpaired two-tailed Student's t-test.) **(B)** Tumor cell-killing activity of DSTE$^{FAP5/CD3}$ monotherapy on MRC-5 cells. **(C)** Flow cytometric analysis of CD4+ and CD8+ T-cell activation after 60 h co-culture. **(D)** Cell counts of positive CD4 and CD8 T cells following DSTE$^{FAP5/CD3}$ treatment. **(E, F)** Cytokine secretion profiles (IFN-γ, IL-2, IL-4, IL-6, IL-10, and TNF) in supernatants from **(E)** BGC823 and **(F)** MRC-5 co-cultures with DSTE$^{FAP5/CD3}$, measured by BD^{TM} Cytometric Bead Array (CBA) Human Th1/Th2 Cytokine Kit II. Data are represented as mean ± SD (n = 3 biological replicates; unpaired two-tailed Student's t-test).

respectively (Figures 4A, B). Conversely, FAP5 expression was nearly undetectable in other malignant tumor cells such as A375 and A549, consistent with its established role as a marker for tumor stroma. Following 48-h co-incubation, OHSV2-DSTE$^{FAP5/CD3}$ can perform greater cancer cell lysis in a FAP5 level-dependent manner, through comparing three cell lines of BGC823 with 90%, 53%, and 17% of FAP5 expression levels to parental BGC823 (Figures 4C, D) and HuH-7 (p < 0.05), suggesting that the additive antitumor activity of OHSV2-DSTE$^{FAP5/CD3}$ is dependent on the direct on-target effect of DSTE$^{FAP5/CD3}$. Moreover, T cells were significantly activated by OHSV2-DSTE$^{FAP5/CD3}$, supported by the upregulation of T-cell activation-related genes, including GZMB, IL-2RA, and

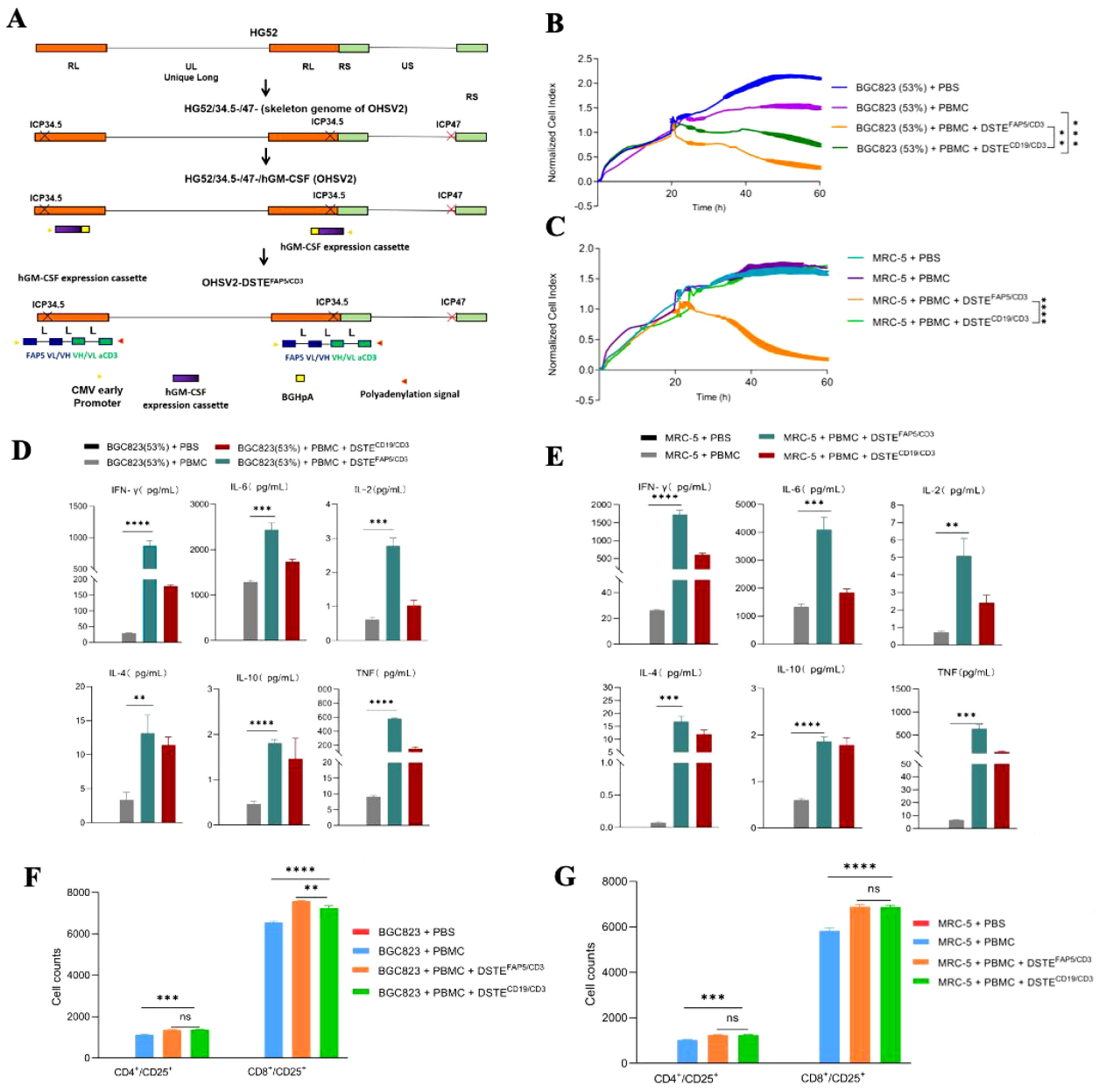

FIGURE 2
Construction and functional analysis of OHSV2-DSTE$^{FAP5/CD3}$. **(A)** Schematic representation of OHSV2-DSTE$^{FAP5/CD3}$ construction. HG52, herpes simplex virus type 2 virus strain; ICP34.5/ICP47, infected cell protein 34.5/47; RL, repeat long region; RS, repeat short region; UL/US, unique long/short; GFP, enhanced green fluorescent protein; CMV, cytomegalovirus. **(B, C)** DSTE$^{FAP5/CD3}$ secreted from OHSV2 inhibited the proliferation of BGC 823 cells overexpressing FAP5 (53%) and MRC-5 cells co-cultured with PBMC through activating T cells *in vitro* (unpaired two-tailed Student's t-test, $^{**}p < 0.01$; $^{***}p < 0.001$; $^{****}p < 0.0001$). **(D, E)** DSTE$^{FAP5/CD3}$ secreted from OHSV2 induced cytokines production, including IL-2, IL-4, IL-6, IL-10, TNF, and IFN-γin BGC 823 cells overexpressing FAP5 and MRC-5 cells *in vitro* by BD^{TM} Cytometric Bead Array (CBA) Human Th1/Th2 Cytokine Kit II. Data are presented as means ± SD (n=3 biological replicates; unpaired and two-tailed Student's t-test.). **(F, G)** Cell counts of CD4+ and CD8+ T cells on BGC 823 cells overexpressing FAP5 and MRC-5 cells after incubation with PBMC, assessed by flow cytometry. ns, non-significant.

PRF1, and increased secretion of cytokines (IL2, IL4, IL6, IL10, TNF, and IFN-γ) (Figures 4E, F).

These results collectively demonstrated that OHSV2 is an outstanding platform to express DSTE$^{FAP5/CD3}$, and HCC is a preferred prey for OHSV2-DSTE$^{FAP5/CD3}$ because of at least triple effects of promoting proliferation and activation of T cells, along with a direct oncolytic effect observed *in vitro*.

Screening for appropriate combination regimens based on OHSV2-DSTE$^{FAP5/CD3}$ *in vitro*

Based on the aforementioned findings, OHSV2-DSTE$^{FAP5/CD3}$ has been characterized as possessing robust oncolytic activity, moderate stromal elimination capability, significant immune activation potential,

10.3389/fimmu.2025.1509087

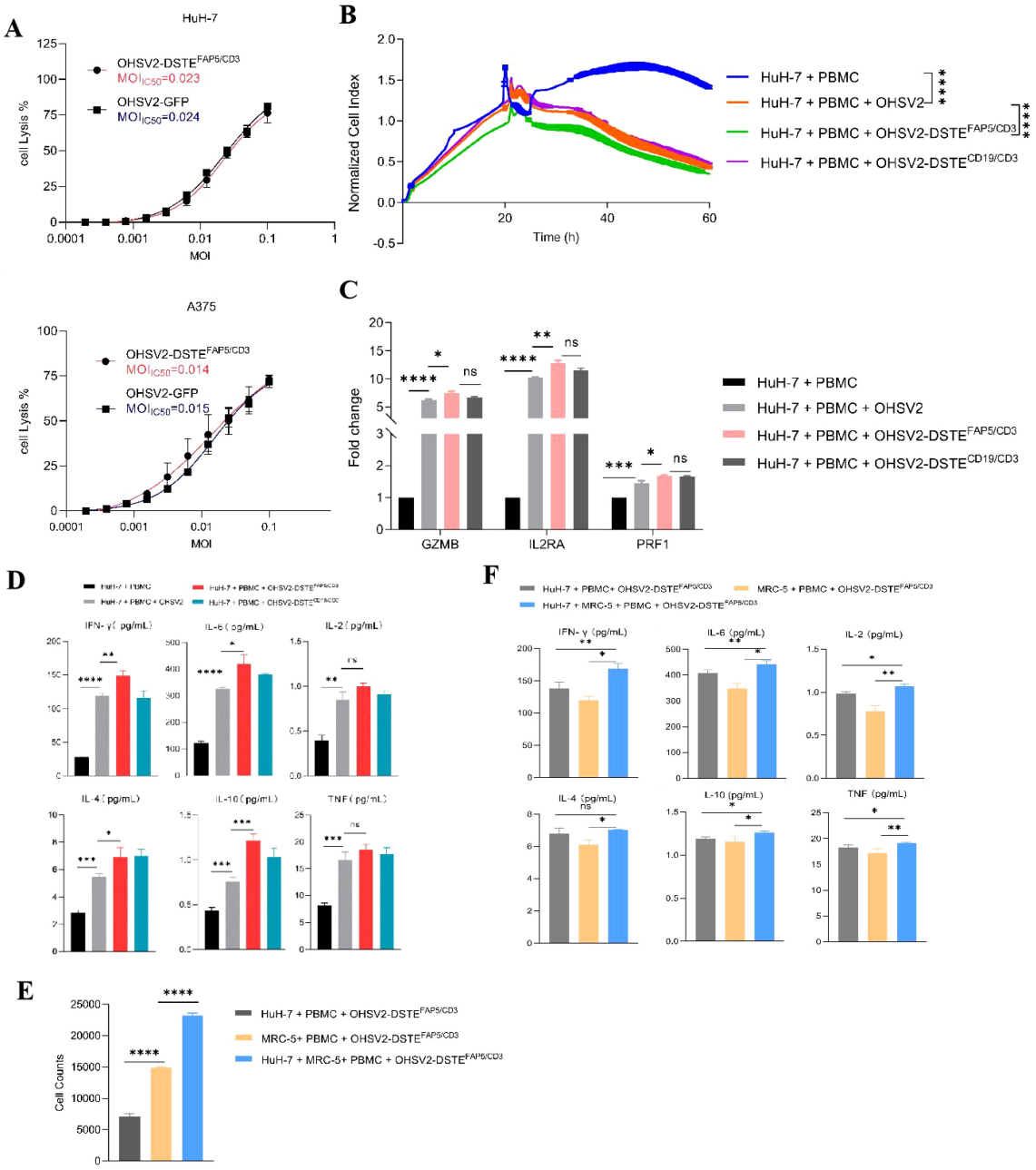

FIGURE 3
Anti-tumor efficacies of OHSV2-DSTE$^{FAP5/CD3}$ *in vitro*. **(A)** Oncolytic activities of OHSV2-DSTE$^{FAP5/CD3}$ in HuH-7 and A375 cell lines. HuH-7 and A375 cell lines were incubated with serial dilutions of OHSV2-GFP or OHSV2-DSTE$^{FAP5/CD3}$ by MTT assay. On day 3 post-infection, cell viability was detected, and the IC50 was calculated for each virus (n=4 biological replicates per experiment). MOI, multiplicity of infection; IC50, half-maximal inhibitory concentration. **(B)** Tumor cell-killing activity of OHSV2-DSTE$^{FAP5/CD3}$ monotherapy in Huh-7 cells. HuH-7 cells were seeded for 24 h before the experiment. Afterwards, oncolytic virus (MOI=0.1) and PBMCs (cancel cells: PBMCs =1: 2) were added and incubated. The cell index reflecting cell-killing activity was monitored through xCELLigence Real-Time Cell Analyzer over 60 h Unpaired two-tailed Student's t-test. ****p<0.0001. **(F)** Cytokine levels, including IL-2, IL-4, IL-6, IL-10, TNF, and IFN-γ, significantly increased in the co-culture group containing both cancer cells and fibroblasts compared to groups with either cancer cells or fibroblasts alone. **(C)** Expressions of T-cell activation-related genes, including granzyme B (GZMB), interleukin-2 receptor A (IL2RA), and Perforin 1 (PRF1) through RT qPCR. RNA was extracted from PBMCs, reverse-transcribed into cDNA, and analyzed. Data are presented as mean ± SD (n = 3 biological replicates; unpaired Student's two-tailed t-test; ns, not significant; *p<0.05; **p<0.01; ***p<0.001; ****p<0.0001). **(D)** Levels of cytokines IL2, IL4, IL6, IL10, TNF, and IFN-γ induced by OHSV2-DSTE$^{FAP5/CD3}$- *in vitro*, measured using BD^{TM} Cytometric Bead Array (CBA) Human Th1/Th2 Cytokine Kit II. **(E)** Cell counts significantly increased when Huh-7 cells were co-cultured with MRC-5 in OHSV2-DSTE$^{FAP5/CD3}$ treatment, compared to Huh-7 and MRC-5 cell alone groups. **(F)** The levels of cytokines, including IL-2, IL-4, IL-6, IL-10, TNF, and IFN-γ, significantly increased in the group co-cultured with both cancer cells and fibroblasts compared to groups with either cancer cells or fibroblasts alone.

TABLE 2 The functional parameters of OHSV2-DSTE$^{FAP5/CD3}$ *in vitro* at 48 h (MOI = 0.2).

Cell lines	Cytopathic effects (%)	hGM-CSF (ng/ml)	DSTE$^{FAP5/CD3}$ (ng/ml)
HT-29	81.5	105.2	81.1
HuH-7	89.6	113.3	86.4
BGC823	82.2	108.9	78.7
A375	99.9	152.1	102.2
A549	83.5	101.5	77.8

and a favorable safety profile. In addition, our previous research demonstrated that the CAR-T cells (CAR-T^{HN3}) and immunotoxins (J80A-PE24) targeting GPC3 developed in our laboratory exhibited significantly greater cytotoxicity than single-agent treatments, although further optimization is warranted. Therefore, we propose a high-order combination regimen comprising OHSV2-DSTE$^{FAP5/CD3}$, CAR-T^{HN3}, and J80A-PE24. This combination is anticipated to exhibit synergistic anti-tumor effects and is theoretically feasible while circumventing challenges associated with integrating therapeutics from different teams in future clinical studies.

First, we found that the combination of OHSV2-DSTE$^{FAP5/CD3}$ with GPC3-targeting immunotoxins exhibited significantly enhanced cytotoxicity against HuH-7 cells ($p<0.05$) compared to monotherapies (Figure 5A). It is worth mentioning that OHSV2-DSTE$^{FAP5/CD3}$ plus CAR-T^{HN3} induced higher cytokine levels than single-agent treatment (Figure 5B), which is a major contributor to severe toxicity in CAR-T cell therapy, although showing significant synergistic anti-tumor effects. Thus, we reduced the CAR-T cells dosage by 50% and found that cytokine levels were similar to those in the other treatments but with a 30% decrease in efficacy. Therefore, this adjusted dosing strategy was employed in subsequent *in vivo* experiments to balance safety and efficacy. Lastly, what exceeded our expectations is that adding GPC3-targeting immunotoxins into OHSV2-DSTE$^{FAP5/CD3}$ and GPC3-targeting CAR T cells group resulted in a significant increase in the killing effect on tumor cells (Figure 5C). We speculated that this may be due to a saturation of cytotoxic potential for the latter combination *in vitro*, where no major barriers hinder effector cell infiltration and activation. However, this scenario is difficult to replicate *in vivo*, especially in solid tumors. Therefore, this strategy remains valuable to be explored in HuH-7 mice models.

In addition, our results showed that T-cell activation markers, including GZMB, IL2RA, and PRF1, were more significantly upregulated in the OHSV2-DSTE$^{FAP5/CD3}$ plus CAR-T cell group compared to the OHSV2-DSTE$^{FAP5/CD3}$ or CAR-T cell group, suggesting an enhancement in T-cell effector function, consistent with the findings from plenty of preclinical studies (Figures 5D, E).

OHSV2-DSTE$^{FAP5/CD3}$ mediates tumor lysis *in vivo*

Given that GPC3-targeting immunotoxins and GPC3-targeting CAR T cells have already been explored *in vivo* in our previous research, we conducted a dose-finding research of OHSV2-DSTE$^{FAP5/CD3}$ in HuH-7 subcutaneous mouse model, intratumorally injected with three different doses of OHSV2-DSTE$^{FAP5/CD3}$ ($CCID_{50}$ = 1×10^6, 1×10^7, and 1×10^8) or control OHSV2-GFP. A relatively low dose of 1×10^7 was selected for subsequent experiments, as it exhibited more significant tumor regression than the 1×10^6 group or OHSV2-GFP group (Supplementary Figure 1) while showing comparable efficacy to the 1×10^8 group. However, a tendency of gradual acceleration in tumor growth was observed at a later stage, even though OHSV2-DSTE$^{FAP5/CD3}$ treatment effectively inhibited the tumor growth initially. These observations suggested that resistance to oncolytic viruses necessitates overcoming through the development of combination therapies.

Subsequently, we found that the innovative three-order combination by incorporating OHSV2-DSTE$^{FAP5/CD3}$, GPC3-targeting CAR-T cells (CAR-T^{HN3}), and immunotoxins (J80A-PE24) exerted the most potent anti-tumor effect in the mouse HCC model, as evidenced by the smallest tumor volumes at day 42 (Figures 6A, B). Unexpectedly, complete tumor eradication was observed in 40% of the mice (two out of five). Poor tumor growth could be ruled out, as the tumor volume increased to approximately 400 mm^3 during the initial stage of treatment. Moreover, all other mice exhibited normal tumor growth kinetics before receiving this triple-agent combination therapy. In addition, hallmark of T-cell activation and PBMC counts were more pronounced in OHSV2-DSTE$^{FAP5/CD3}$-based combined therapy group (Figures 6C, D). Therefore, our conceptual design of a high-order combination therapy integrating OHSV2-DSTE$^{FAP5/CD3}$, CAR-T cells, and immunotoxins—three agents with distinct, non-overlapping mechanisms—was successfully transformed into reality. Our results also demonstrated that OHSV2-DSTE$^{FAP5/CD3}$-based treatment was superior to anti-PD-1 antibody-based treatment, although this was not a head-to-head comparison between single agents. Furthermore, the OHSV2-DSTE$^{FAP5/CD3}$-based combinations were more effective than single- or dual-agent regimens, including lenvatinib plus anti-PD-1 treatment, which has shown high tumor response rates in clinical trials but has not been approved by the FDA recently.

OHSV2-DSTE$^{FAP5/CD3}$ exhibits a good safety profile *in vivo*

To evaluate the safety of OHSV2-DSTE$^{FAP5/CD3}$ in combination with GPC3-targeting CAR-T cells (CAR-T^{HN3}) and immunotoxins (J80A-PE24), a series of tests were conducted. Given the potential for increased toxicity due to the combined effects of these agents and the known risks of severe adverse events associated with CAR-T cell therapy (e.g., cytokine release syndrome or neurotoxicity), we selected a moderate dose of OVs and a half-dose of CAR-T cells.

First, mouse body weights showed no significant descending or differences across different groups through regular monitoring (Figure 7A). At the same time, the parameters reflecting organ function, including the glutathione transaminases, phosphocreatine kinases, myocardial enzymes, albumin, bilirubin, creatinine, hemocyte numbers, and glucose levels in peripheral blood,

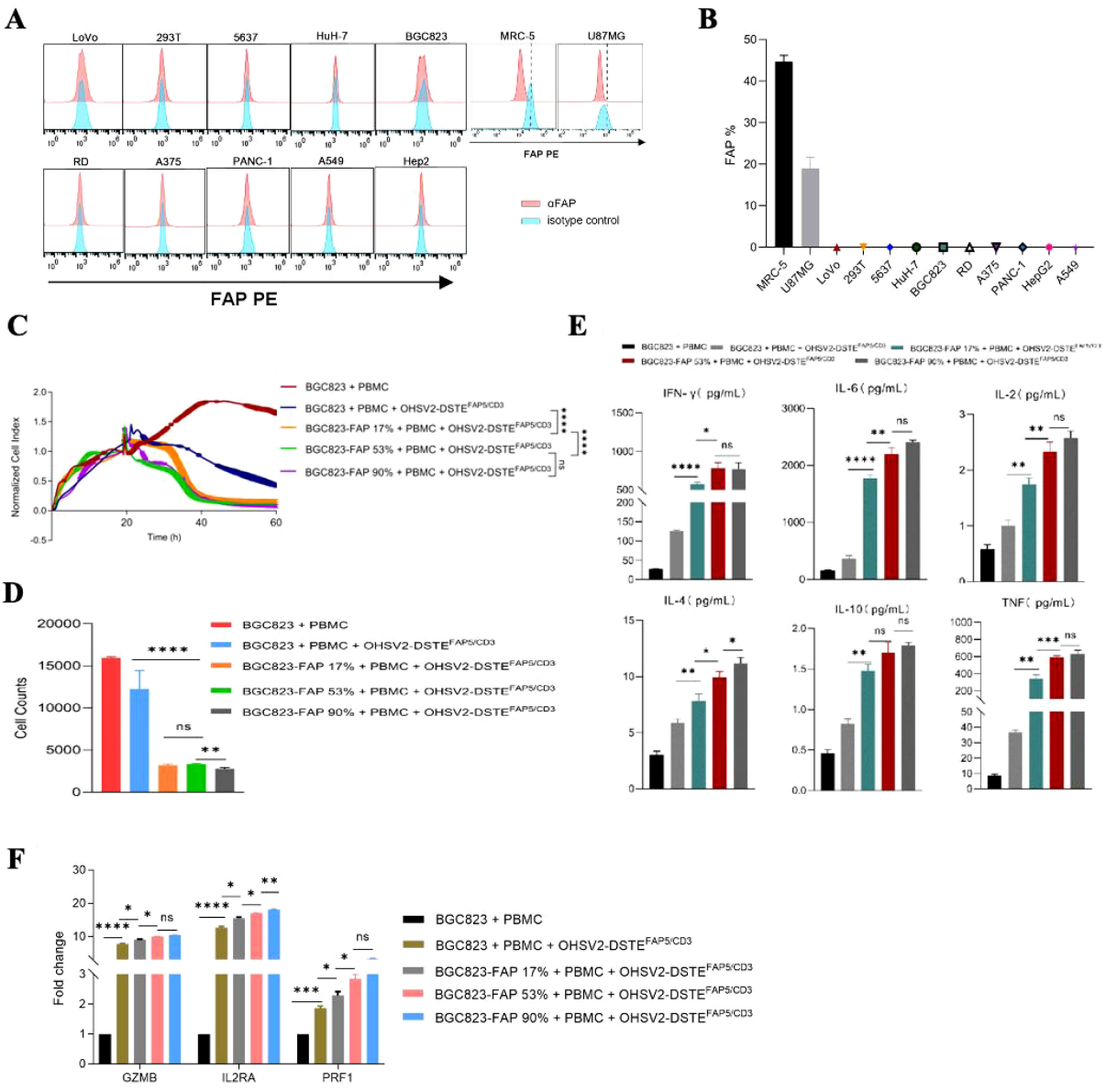

FIGURE 4
Anti-tumor efficacy of OHSV2-DSTE$^{FAP5/CD3}$ and its effects on T cells in high-FAP5 setting *in vitro*. **(A)** Expression of FAP in different cancer cell lines. Cancer cells were collected, stained with anti-FAP antibody, and analyzed by flow cytometry. **(B)** FAP positivity rate in different tumor cell lines based on the FAP expression analysis in part **(A)**. **(C)** Tumor cell-killing activity of OHSV2-DSTE$^{FAP5/CD3}$ in BGC823-FAP+ cells with different FAP expression levels. Tumor cells were seeded before the experiment. Afterwards, oncolytic virus (MOI=0.1) and PBMCs (cancer cells: PBMCs =1: 2) were added and incubated. Cell index reflecting cell-killing activity was monitored through xCELLigence Real-Time Cell Analyzer over 60 h Unpaired two-tailed Student's t-test. ns, not significant; *p<0.05; **p<0.01; ***p<0.001; ****p<0.0001. **(D)** Cell counts of tumor cells in OV treatment groups following OHSV2-DSTE$^{FAP5/CD3}$ infection. Data are presented as mean ± SD. (n = 3 biological replicates; unpaired Student's two-tailed t-test). **(E)** Levels of cytokines including IFN-γ, IL-6, IL-2, IL-4, IL-10, and TNF induced by OHSV2-DSTE$^{FAP5/CD3}$ in BGC823-FAP+ cells with different FAP expression levels. **(F)** Expressions of T-cell activation-related genes, including GZMB, IL2RA, and PRF1, as determined by RT-qPCR. RNA was extracted from PBMCs, reverse transcribed into cDNA, and analyzed.

occasionally displayed, at most, grade 1 deterioration (Supplementary Table S1), suggesting that all treatment schemes, especially our novel triple-agent combination, did not induce overlying toxic effects in major organs or tissues, such as the liver, kidney, myocardium, or bone marrow. Furthermore, these findings revealed a decoupling between therapeutic efficacy and toxicity, although the underlying mechanisms remain to be elucidated at present. Moreover, serum cytokine levels were not significantly increased in the triple-combination group at the end of the experiment on day 42 compared to controls (Figure 7B), suggesting that although the treatments activated immune responses within the tumor microenvironment, they did not lead to excessive systemic cytokine release. Additionally, histopathological analysis revealed no significant tissue damage in the monotherapy group (OHSV2-DSTE$^{FAP5/CD3}$) (Figure 7C) or in combination therapy groups compared to the blank control.

10.3389/fimmu.2025.1509087

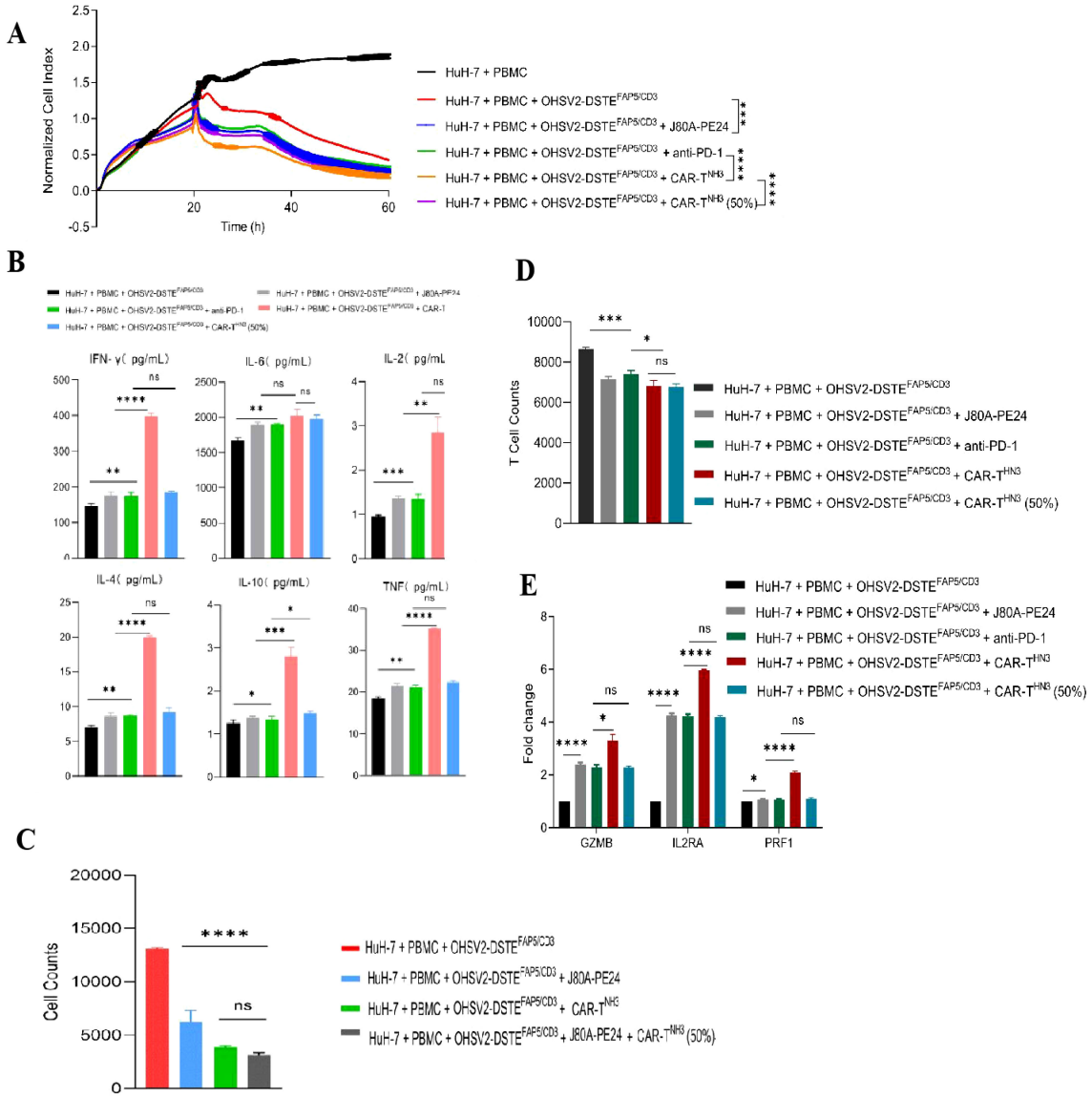

FIGURE 5
Screening for appropriate combination regimens based on OHSV2-DSTE$^{FAP5/CD3}$ *in vitro*. **(A)** Tumor cell-killing activity of combination therapy of OHSV2-DSTE$^{FAP5/CD3}$ ± immunotoxins ± PD-1 monoclonal antibody in HuH-7 cells through xCELLigence Real-Time Cell Analyzer. Unpaired two-tailed Student's t-test. ***p<0.001; ****p<0.0001. **(B)** Levels of the combination cytokines including IFN-γ, IL-6, IL-2, IL-4, IL-10, and TNF induced OHSV2-DSTE$^{FAP5/CD3}$ in HuH-7 cells. Data are presented as mean ± SD (n = 3 biological replicates; unpaired Student's two-tailed t-test; ns, not significant; *p<0.05; **p<0.01; ***p<0.001; ****p<0.0001). **(C)** Tumor cell counts in OHSV2-DSTE$^{FAP5/CD3}$ combination treatment groups. **(D)** T-cell numbers in OHSV2-DSTE$^{FAP5/CD3}$ combination treatment groups. **(E)** Expressions of T-cell activation-related genes, including GZMB, IL2RA, and PRF1 through RT qPCR.

Taken together, these findings have largely dispelled our initial concerns regarding the potential for severe on-tumor and off-target side effects, such as cytokine storms, interstitial pneumonia, and hepatic impairment, resulting from combination therapy containing OHSV2-DSTE$^{FAP5/CD3}$, because of the relatively low specificity of FAP and GPC3 target antigens, of course, suggesting that this novel strategy integrating different immune therapeutic drugs is worth further clinical development.

A preliminary exploration of the mechanisms underlying the novel strategy integrating OHSV2-DSTE$^{FAP5/CD3}$ with other immune therapeutic agents

Further exploration of the mechanism underlying the novel strategy combining OHSV2-DSTE$^{FAP5/CD3}$ with other immune therapeutic drugs is still necessary. Although not tremendously

10.3389/fimmu.2025.1509087

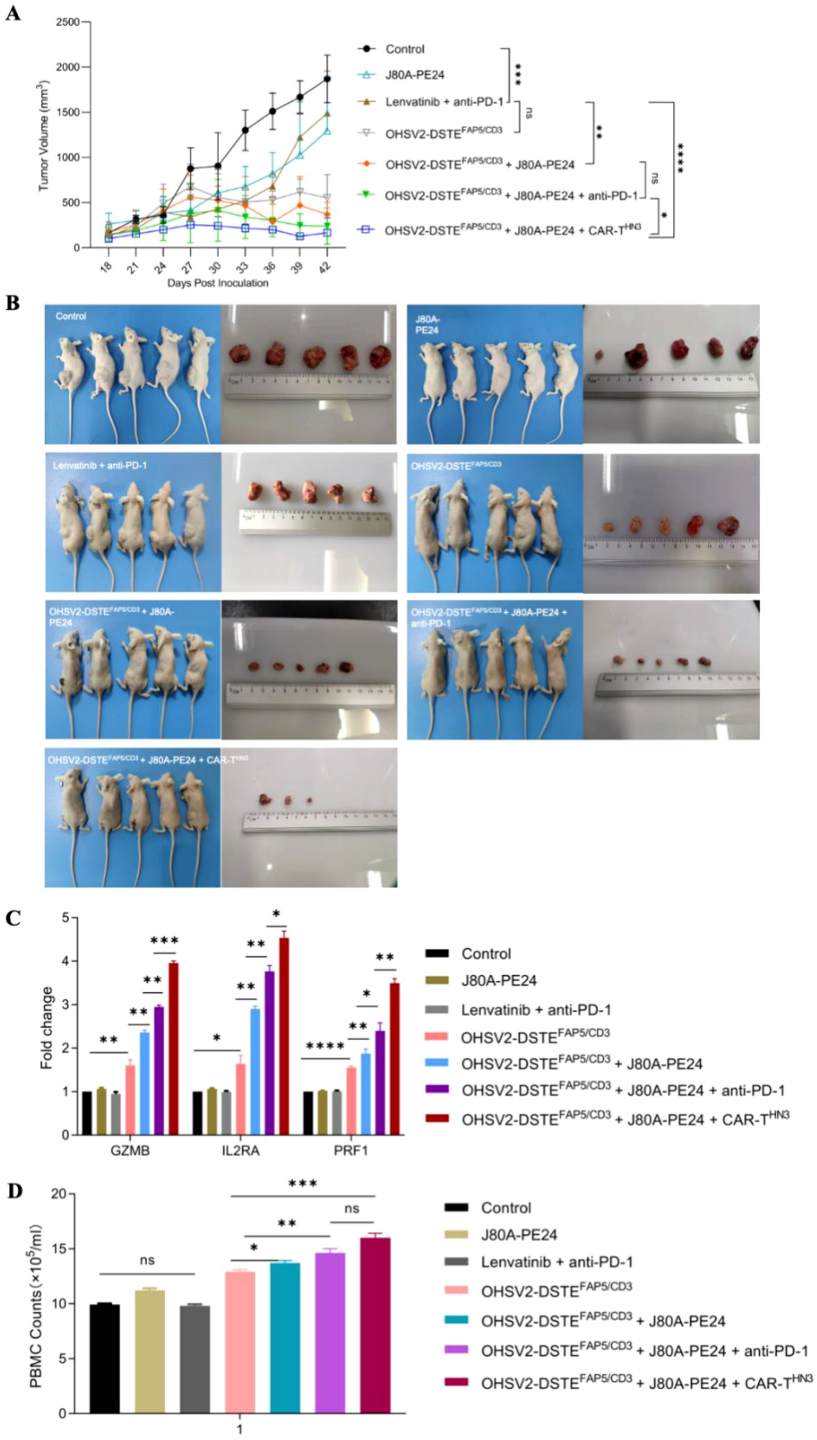

FIGURE 6
OHSV2-DSTE$^{FAP5/CD3}$-based combined therapy inhibits the tumor growth of HuH-7 *in vivo*. **(A)** Tumor growth curves of six different treatment groups and one control group. The control group consisted of untreated mice, while the treatment groups included immunotoxins J80A-PE24 + PBMCs, Lenvatinib + pembrolizumab (anti-PD-1) + PBMCs, OHSV2-DSTE$^{FAP5/CD3}$ + PBMCs, OHSV2-DSTE$^{FAP5/CD3}$ + J80A-PE24 + PBMCs, and OHSV2-DSTE$^{FAP5/CD3}$ + J80A-PE24 + pembrolizumab + PBMCs, OHSV2-DSTE$^{FAP5/CD3}$ + J80A-PE24 + CAR-T^{HN3} + PBMCs. The tumor volumes of mice were measured every 3 days. All mice were euthanized by cervical dislocation on day 42. Data were presented as mean ± SD and analyzed using an unpaired two-tailed Student's t-test. ns, not significant; *p < 0.05; **p<0.01; ***p<0.001; ****p<0.0001. **(B)** Images of mice in the control group and the six treatment groups and the corresponding tumor from each mouse (n=5 mice per group). **(C)** Expressions of T-cell activation-related genes, including GZMB, IL2RA, and PRF1. Data are presented as mean ± SD from three biological replicates and analyzed using an unpaired two-tailed Student's *t*-test. **(D)** PBMCs counts isolated from mice with OHSV2-DSTE$^{FAP5/CD3}$-based combined therapy.

10.3389/fimmu.2025.1509087

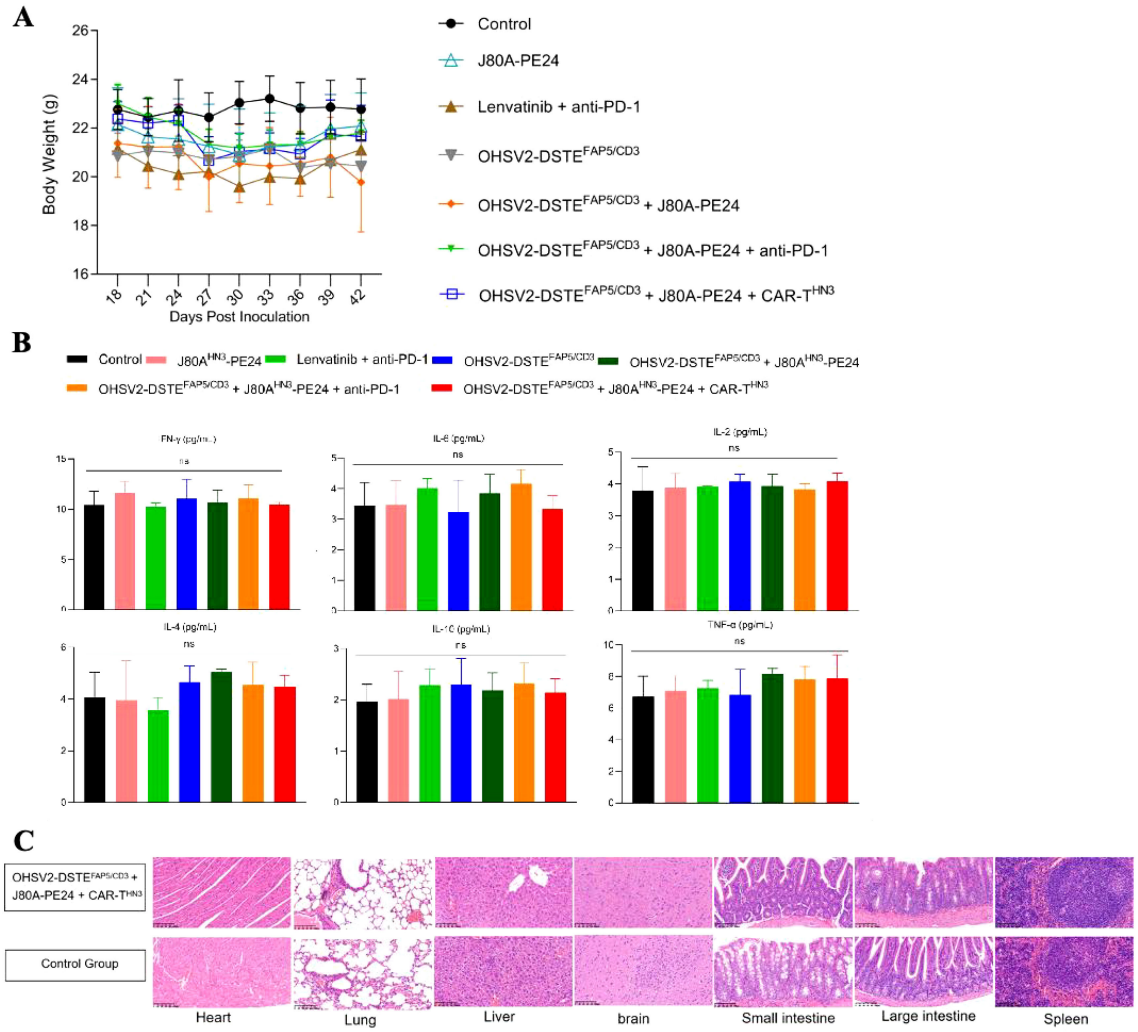

FIGURE 7
Safety evaluation of OHSV2-DSTE$^{FAP5/CD3}$. **(A)** Body weights of HuH-7 tumor-bearing mice in all groups from day 18 to day 42 post-inoculation. **(B)** Levels of cytokines IFN-γ, IL-6, IL-2, IL-4, IL-10, and TNF *in vivo*, measured using BD^{TM} Cytometric Bead Array (CBA) Human Th1/Th2 Cytokine Kit II. Blood samples were collected from the retro-orbital sinus of mice in all the groups. Data are presented as mean ± SD (n=5 mice per group, two-way ANOVA with Tukey's multiple comparisons test). **(C)** Histopathological assays of the heart, lung, liver, brain, small intestine, large intestine, and spleen of HuH-7 tumor-bearing mice from OHSV2-DSTE$^{FAP5/CD3}$-based triple regimen groups (OHSV2-DSTE$^{FAP5/CD3}$ + J80A-PE24 + CAR-T^{HN3}), evaluated by hematoxylin and eosin (H&E) (200×).

critical for clinical translation efforts, such insights can guide the iterative development of next-generation therapeutics. To this end, various cell populations, probably including CD3+ T cells, CAFs, and other immune cells T cells, were isolated from tumor tissues across different treatment groups and identified seven distinct cell clusters (types) based on gene marker expression profiles by single-cell sequencing (Supplementary Figure S2).

Notably, the proportions of CD4+ and CD8+ T cells were significantly increased in the OHSV2-DSTE$^{FAP5/CD3}$-based triple-agent regimen groups (including OHSV2-DSTE$^{FAP5/CD3}$ + J80A-PE24 + CAR-T^{HN3} group and OHSV2-DSTE$^{FAP5/CD3}$ + J80A-PE24 + anti-PD-1 group), compared to other treatment groups (Supplementary Table S2), however, there is no significant difference between two triple-agent regimen groups or among other dual-agent regimen groups, besides blank control (Figures 8A, B). The gene amplification related to CD8+ T cell exhaustion was also observed, suggesting that our constructed OHSV2-DSTE$^{FAP5/CD3}$ effectively activates T cells *in vivo*.

Lastly, following the expression profiling of CAFs, we categorized them into myofibroblast CAFs (myCAFs) and inflammatory CAFs (iCAFs). Remarkably, the OHSV2-DSTE$^{FAP5/CD3}$ + J80A-PE24 + CAR-T^{HN3} group demonstrated the most pronounced CAF depletion among all treatment groups (Figure 8A). Interestingly, the gene expression patterns of the OHSV2-DSTE$^{FAP5/CD3}$ +J80A-PE24 +CAR-T^{HN3} group did not significantly differ from those of other treatment groups (Supplementary Figure S2), suggesting that distinct treatment modalities did not impact the overall gene expression profiles of CAFs. To further corroborate the depletion of CAFs in the tumor microenvironment, we conducted immunohistochemistry to evaluate the expression of FAPs in the OHSV2-DSTE$^{FAP5/CD3}$ + CAR-T cells + immunotoxin combination group and revealed a significant reduction in CAFs, contrasting with the effect observed in

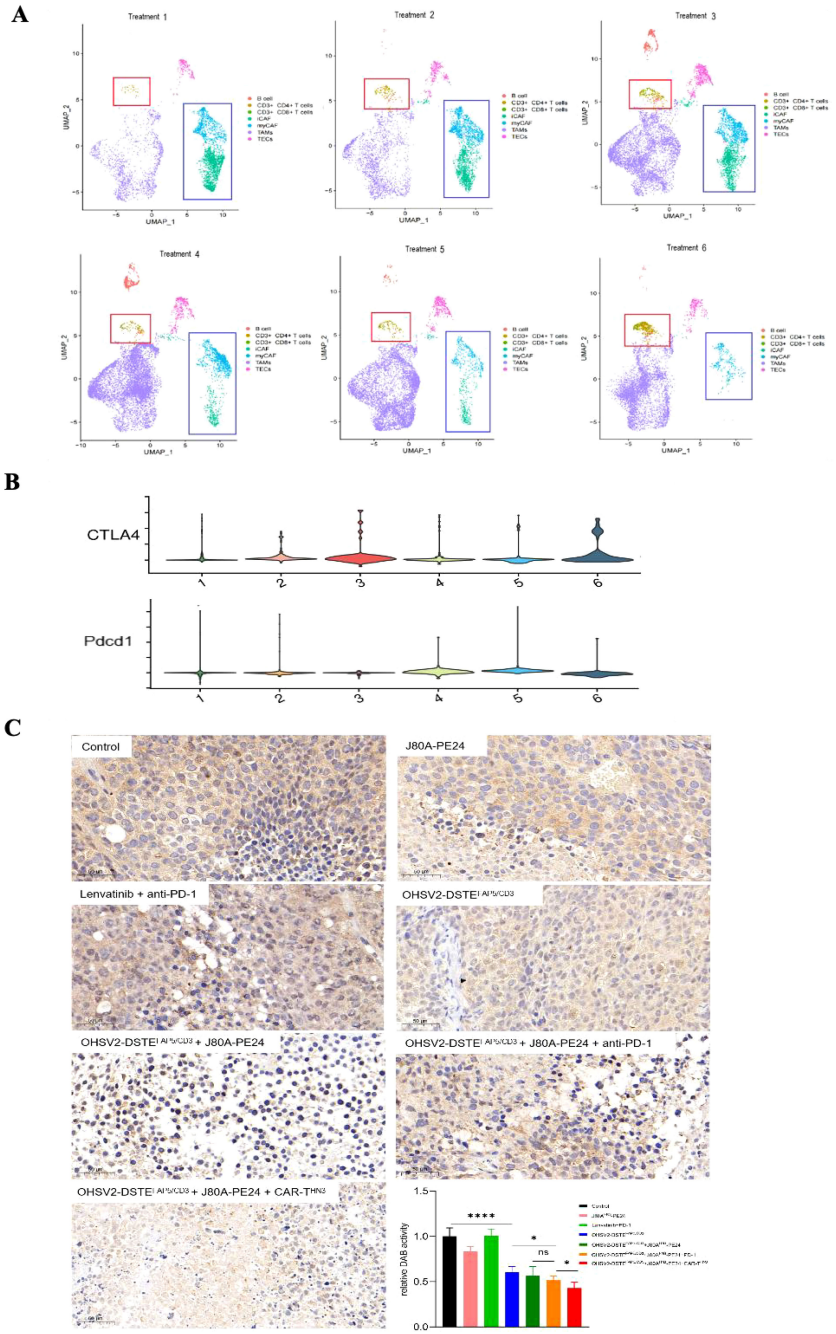

FIGURE 8
Narrow-scoped mechanism analysis on OHSV2-DSTE$^{FAP5/CD3}$-based triple-agent therapy. **(A)** UMPA plot of different lymphocyte subsets and CAFs derived from tumor tissues of each treatment group. The expressions of activation genes in CD3+ T cells was analyzed in the following OHSV2-DSTE$^{FAP5/CD3}$-based therapy groups: treatment 1, immunotoxins J80A-PE24; treatment 2, Lenvatinib + pembrolizumab (anti-PD-1); treatment 3, OHSV2-DSTE$^{FAP5/CD3}$; treatment 4, OHSV2-DSTE$^{FAP5/CD3}$ + J80A-PE24; treatment 5, OHSV2-DSTE$^{FAP5/CD3}$ + J80A-PE24 + pembrolizumab; and treatment 6, OHSV2-DSTE$^{FAP5/CD3}$ + J80A-PE24 + CAR-T^{HN3}). **(B)** Violin plot of expressions of inflammatory CAFs (iCAF) and myofibroblastic *CAFs* (myCAF) on their respective marker genes. **(C)** Immunohistochemical analysis of FAP expression in CAFs from tumor tissues of all seven groups (200×). FAP expression was detected across all the OHSV2-DSTE$^{FAP5/CD3}$-based therapy groups. Scale bar = 5 μm. Blue, nuclear; brown, FAP. *p< 0.05 and ****p < 0.0001.

the OHSV2-DSTE$^{FAP5/CD3}$ monotherapy group (Figure 8C), where the impact on CAF elimination was different *in vitro*. This finding suggests that CAFs and cancer cells are interdependent, sharing a common fate for survival. We propose that this interdependence may stem from the requirement of direct or indirect support from cancer cells for the survival of CAFs or could be facilitated by bidirectional communication between CAFs and tumor cells. In addition, we cannot discount the possibility that non-specific bystander T-cell activation may be triggered by various factors, rather than the activation of CD3+ T cells through CAF-dependent pathways.

Nonetheless, further insights into these mechanisms can be gained through T-cell receptor (TCR) sequencing.

Taken together, despite being derived from a limited set of assays, our findings provide evidence that, mechanistically, the synergistic anti-tumor effects of the high-order combination of OHSV2-DSTE$^{FAP5/CD3}$, CAR-T cells, and immunotoxins, are likely involved in the functions of OHSV2-DSTE$^{FAP5/CD3}$ to prime CD3+ T-cell activation and enhance proliferation of CD4+ and CD8+ T cells and even disrupt the entangled relationship between cancer cells and fibroblasts.

Discussion

In HCC, cancer cells are embedded within a complex TME composed of diverse non-malignant cell populations, including immune cells, stromal cells, endothelial cells, smooth muscle cells, adipocytes, and neurons. These cells, along with the various growth factors, cytokines, chemokines, kinases, and proteases secreted from them, all together form a highly structured and vascularized TME (29, 30). Given the intricate interactions within this ecosystem, the TME inevitably influences the efficacy of immunotherapies and contributes to the development of therapeutic resistance, which is characterized by interwoven and overlapped profiles in multiple aspects (31).

One of the predominant challenges of resistance lies in the quality and quantity of antigens, which determines the immunogenicity of HCC cells. In addition, numerous obstacles hinder the recruitment of effector T cells into tumors and the formation of tertiary lymphoid structures (TLS)—organized lymphoid aggregates containing CD4+ T cells, CD8+ T cells, and CD20+ B cells—which have been observed in HCC and other malignancies. Preclinical and clinical studies have provided substantial evidence supporting these immunological hurdles (31, 32). On the contrary, without doubt, immune-suppressive cells, such as Tregs, tumor-associated macrophages (TAMs), and MDSCs, which maintain immune balance in the host's homeostasis under normal physiological conditions, can naturally counter effector T cells or are hijacked by cancer cells in the TME to suppress T-cell trafficking, proliferation, and effector function. Alternatively, several stromal cells, especially CAFs, can undergo reprogramming to promote immune evasion and enhance cancer cell survival, leading to resistance to immunotherapies (33). Lastly, metabolic crosstalk between immune cells and cancer cells within the TME can also drive immunotherapeutic resistance by altering nutrient availability and immune cell functionality.

Therefore, expanding the arsenal of HCC treatments to overcome drug resistance represents a theoretically sound approach. Similarly, exploring finely tuned combination strategies is realistic due to emerging insights from clinical trials that combination therapy for HCC yields a better prognosis (3, 34).

OVs have emerged as promising therapeutic agents (35); however, their clinical efficacy as single-agent therapy is far from satisfactory in poorly immunogenic cancers, like HCC (6, 36). One of the putative challenges is the tumor stroma, like CAFs, which can prevent effective dissemination from OVs even following intratumoral injection. Hence, targeting CAFs presents an ideal strategy to enhance antitumor efficacy, as they are among the most abundant stromal components in the tumor microenvironment (TME) and exhibit minimal mutational evolution, reducing the likelihood of acquired drug resistance (20, 37–41). Indeed, our constructed OHSV2-DSTE$^{FAP/CD3}$ expressing DSTEs and an adenovirus ICO15K-FBiTE targeting FAP on CAFs both can exert superimposed effects through simultaneously inducing cancer cell lysis by OVs and fostering immune synapse-mediated depletion of FAP+ CAFs by CD3+ T cells (40, 42), thus outperforming their parental virus alone. Another aim of combining OVs with DSTEs is to balance antiviral and antitumor immunity by redirecting T cells to kill CAFs rather than clearing OVs because the total number of T cells is limited, especially in the TME. However, our OHSV2-DSTE$^{FAP/CD3}$ alone cannot eliminate CAFs to reduce the density of the extracellular matrix *in vivo* experiments, compared to that *in vitro*, where both various stakeholders and our DSTEs have great opportunities to closely contact, or intertwine with each other. Thus, while CAF targeting is conceptually appealing, our data suggest that monotherapeutic blocking CAFs may not be a perfect strategy, at least for HCC treatment *in vivo*, despite attractiveness. For this reason, we considered exploring new strategies, although whether a path ahead is hidden by towering mountains remains uncertain.

CAR-T cells have yet to achieve comparable success against solid tumors up to the present, although representing a revolutionary immunotherapy in B-cell-related hematological cancers. Potentially challenging issues have been highlighted, including low specificity and high heterogeneity of target antigens (increasing the risk of on-target/off-tumor toxicity), inadequate trafficking and persistence, and suboptimal effector function (17). While nearly 100 innovative therapeutic strategies are currently emerging in CAR-T cell development pipelines, combinatorial approaches remain the most promising avenue to improve CAR-T cell infiltration, proliferation, and functional persistence (43). Ovs represent a leading candidate for combination therapy, since they cannot only induce immunogenic cell death by releasing soluble tumor-derived antigens and danger-associated molecular patterns (DAMPs) but also exhibit favorable safety profiles when combined with other cancer treatment approaches with alternative mechanisms (44). Antibody–drug conjugates (ADCs) are promising cancer treatment modalities through selective delivery of highly cytotoxic payloads to tumors; however, the challenges remain evident, such as the lack of highly specific and internalizable antigens and payloads with low off-target toxicity. Alternatively, immunotoxins, like our J80A-PE24, which is derived from anti-GPC3 antibody fragments conjugated to PE24, possess high specificity and low toxicity, yet are accompanied by their insufficient standalone anti-tumor effect (27).

Indeed, our data demonstrated that the high-order combination of OHSV2-DSTE$^{FAP/CD3}$, J80A-PE24, and CAR-T^{HN3} can induce an utmost significant tumor regression and prolonged survival compared to the others, such as angiogenesis inhibition and PD-1 blockade. Meantime, we found that OHSV2-DSTE$^{FAP/CD3}$-based therapy exhibits the absence of off-tumor toxicity, including cytokine storm, inconsistent with previous studies on FAP

targeting therapy and CAR-T therapy, despite GPC3 and FAP are suboptimal targets owing to their low specificity (45, 46). Such findings could be explained by the intratumoral injection and selective replication of Ovs in cancer cells and the short half-life of DSTEs in serum and an appropriately optimized dosage, as supported by circulating cytokine levels and tissue histopathology analyses. Additionally, our expectation of selecting CAR-T^{HN3} and J80A-PE24 specifically targeting GPC3 (15, 27) was to avoid coordination challenges in later-stage development, considering the scarcity of successful immunotherapy combinations involving agents from different pharmaceutical sponsors. However, it should be noted that our data could not definitively establish the superiority of OHSV2-$DSTE^{FAP/CD3}$ over PD-1 inhibitors, since we did not directly compare them as monotherapies. Finally, OHSV2-$DSTE^{FAP/CD3}$-based combination therapy could potentially augment the vulnerability of tumors by fostering a hot TME, as evidenced by the heightened infiltration of CD4+ and CD8 + T cells and amplification of exhaustion-related genes. Thus, these findings lay the groundwork for future combination strategies involving ICIs, aligning with our previous research outcomes (10, 47). T-cell exhaustion is crucial for immunotherapy, as overall, antitumor immunity would not manifest in its absence. Our previous research found that oncolytic virus OHSV2 treatment significantly reduces T-cell exhaustion markers on the cell surface, such as CTLA-4, TIM3, LAG3, and TIGIT (48). Similarly, immunotoxin treatment has been shown to activate the antitumor activity of immune cells (49). Bispecific antibodies directly activate T cells, and previous studies have also shown that T-cell exhaustion correlates with drug resistance (50, 51). Regarding CAR-T cell therapy, the situation may be more complex because exhaustion of the CAR-T cells themselves may reduce immune effector function, and it remains unclear whether they affect the activation and subsequent exhaustion of circulating or tissue-resident T cells within the host per se. Thus, further in-depth investigation of key T-cell exhaustion-related markers in this high-order combination therapy is warranted, especially after clinical application, to confirm their predictive efficiency for therapeutic outcomes.

The effectiveness of OHSV2-$DSTE^{FAP/CD3}$ in eradicating CAFs is limited when used alone but becomes significantly powerful when combined with other treatments, implying a robust correlation between CAF reduction and tumor regression. Therefore, we speculated that this might be due to the survival of CAFs being supported by redundant signaling pathways and cytokines (such as TGF-β, POSTN, ACTA2, MMP11, TAGLN, and FN1). More importantly, mutual reshaping and interdependence between CAFs or other cells (like Treg cells) and cancer cells were successfully interrupted by our high-order combination therapy. The reason for the inconsistency in *in vitro* results could be that it is challenging to co-culture multiple cell types to accurately mimic the tumor microenvironment *in vitro*. Conversely, *in vivo*, fibroblasts receive additional external signaling inputs from other cell types such as tumor cells, Treg cells, or TAMs. Once a substantial number of tumor cells are eliminated, the suppression of fibroblasts may be further amplified. Logically, this discrepancy primarily reflects that conclusions drawn from *in vitro* studies cannot be simply extrapolated to *in vivo* conditions, much like how animal experiments cannot fully substitute for clinical trials, particularly in the development of immunotherapeutic agents. However, unraveling the underlying mechanism remains complex, as CAFs are considered to not only possess immunosuppressive or tumor-promoting functions but also potentially fuel anti-tumor immune functions in a specific context (52, 53).

Additionally, it is important to acknowledge the significant limitations of our study. First, it is still unclear whether the antitumor effects are predominantly mediated by CAR-T cells or whether all three drugs contribute equivalently. Second, our mechanistic analysis does not fully address the specific roles of CD3+ T cells, CD4+ T cells, and CD8+ T cells in antitumor immunity. Finally, we acknowledge that the subcutaneous model does not fully replicate the complex tumor microenvironment of HCC, particularly with respect to liver-specific stromal interactions and immune cell infiltration. However, in the context of immunotherapy drug development, designing antibodies based on mouse tumor antigens is not suitable for future human studies. Since immunocompetent mouse models possess their own intact immune systems, they are better suited for investigating the impact of the host immune system on immunomodulatory agents, although in our study, we transplanted human PBMCs to fall short of fully mimicking a complete immune system. For instance, they lack other lymphocyte components and are unable to adequately represent the immune responses occurring within the tumor microenvironment, lymph nodes, or other lymphoid structures, and the communication between them. Indeed, in our earlier studies on oncolytic viruses, we employed immunocompetent mouse models for mechanistic analysis. However, to develop drugs intended for future clinical application in humans, our study utilized human bispecific antibodies, immunotoxins, and CAR-T cells. Consequently, if normal immunocompetent mice were used as the model, the treatment would fail to exert inhibitory effects on the engrafted murine tumors. On the contrary, the immune system of mice would mount a robust response against the exogenous antibodies and T cells, leading to severe autoimmune reactions, which would not only undermine the ability to effectively kill tumor cells but could also result in life-threatening toxicities. This explains why many immunotherapeutic agents, despite demonstrating clear antitumor activity and gaining clinical approval, still have unclear mechanisms of efficacy and toxicity. Undoubtedly, our study also falls short in presenting a clear and comprehensive grand spectacle of the interactions between drug efficacy, toxicity, and mechanism, primarily due to the absence of in-depth, model-driven mechanistic investigations.

Moreover, while the absence of one or two additional groups may lead to incomplete mechanistic explanations, we are confident that this limitation does not significantly impact the robustness of our evidence regarding efficacy and safety.

While promising, the path to clinical translation remains fraught with challenges. Specifically, we suggest that this multi-drug combination strategy holds potential for future extension but will require further exploration through additional animal experiments and confirmation in clinical studies. Relative to OVs and

immunotoxins, the high cost of CAR-T cell therapy is a significant challenge, primarily due to the expenses associated with personalized manufacturing. In the future, if widely applied in solid tumors, cost-sharing mechanisms among individuals may help mitigate this burden. Additionally, advancements in preparation methods and technologies, such as *in vivo* gene editing and delivery techniques, accessible cell culture technologies in medical centers, or off-the-shelf stem cell preparation technologies, present potential solutions to reduce costs. Finally, the market regulation of CAR-T cell therapy remains challenging to standardize due to its unique personalized features, including factors such as preparation time, cell dosage, cell viability, bridging treatment strategies, and the logistical capabilities of medical centers. Addressing these challenges requires collaborative efforts among researchers, industry stakeholders, and regulatory agencies to develop scalable, affordable, and regulatory-compliant treatment strategies.

In summary, our findings highlight the utility of OHSV2-DSTE$^{FAP5/CD3}$ as a potent biological agent for enhancing local immune responses and suppressing CAFs, albeit their limited impact *in vivo* and reliance on cancer cells. Moreover, compelling evidence from our study underscores the efficacy of a high-order combination therapy with non-overlapping resistance profiles at sub-maximal tolerated doses, leading to substantial tumor regression, including a 40% complete response rate, as a Chinese proverb says: suddenly, another village with green trees and bright flowers comes in sight.

Conclusions

This study demonstrates that OHSV2-DSTE$^{FAP5/CD3}$ is capable of eradicating CAFs *in vitro* and remodeling the local tumor microenvironment *in vivo*. A proof-of-concept combination therapy involving OHSV2-DSTE$^{FAP5/CD3}$, J80A-PE24, and CAR-T^{HN3} shows promise, with synergistic anti-cancer effects and acceptable safety profiles. Thereby, without a doubt, this innovative approach paves the way for further investigation for translation into clinical applications for the treatment of HCC and potentially other types of cancer.

Data availability statement

The original contributions presented in the study are included in the article/Supplementary Material, further inquiries can be directed to the corresponding author/s.

Ethics statement

The studies involving humans were approved by the Ethics Committee of Huazhong University of Science and Technology, Tongji Medical College. The studies were conducted in accordance with the local legislation and institutional requirements. The participants provided their written informed consent to participate in this study. The animal study was approved by the Ethics Committee of Huazhong University of Science and Technology, Tongji Medical College. The study was conducted in accordance with the local legislation and institutional requirements.

Author contributions

SD: Conceptualization, Data curation, Funding acquisition, Project administration, Writing – original draft. XC: Data curation, Formal Analysis, Funding acquisition, Project administration, Writing – original draft. XL: Data curation, Investigation, Methodology, Writing – review & editing. YW: Resources, Software, Writing – original draft. QH: Conceptualization, Methodology, Writing – original draft. YL: Methodology, Validation, Writing – original draft, Writing – review & editing. JJ: Software, Writing – review & editing. XZ: Investigation, Writing – original draft. YZ: Investigation, Writing – original draft. QC: Methodology, Writing – review & editing. CX: Writing – review & editing. FG: Visualization, Writing – review & editing. LH: Investigation, Writing – review & editing. MF: Conceptualization, Validation, Writing – review & editing. BL: Methodology, Resources, Writing – review & editing. SH: Funding acquisition, Writing – original draft, Writing – review & editing.

Funding

The author(s) declare that financial support was received for the research and/or publication of this article. This work was supported by the Natural Science Foundation of China (81972308), Key Frontier Project of Application Foundation of Wuhan Science and Technology Bureau (2019020701011438), China Postdoctoral Science Foundation (2021M701338), Foundation of Health Commission of Hubei Province (WJ2021M190), and Wuhan Knowledge Innovation Foundation (2022020801020513 and 2023020201010175), and Natural Science Foundation of Hubei Province (2023AFB463).

Acknowledgments

The authors would like to thank Dr. Heng Yao for Flow Cytometry technical support a and Dr. Keji Yan for scRNA sequencing technical support.

Conflict of interest

Authors JJ and BL were employed by the company Wuhan Binhui Biopharmaceutical Co., Ltd.

The remaining authors declare that the research was conducted in the absence of any commercial or financial relationships that could be construed as a potential conflict of interest.

Generative AI statement

The author(s) declare that no Generative AI was used in the creation of this manuscript.

Publisher's note

Supplementary material

The Supplementary Material for this article can be found online at: https://www.frontiersin.org/articles/10.3389/fimmu.2025.1509087/full#supplementary-material

SUPPLEMENTARY FIGURE 1
OHSV2-DSTE$^{FAP5/CD3}$ dose-finding study *in vivo*. **(A)** Tumor growth curves in four OV treatment groups. The 4 groups were treated respectively with OHSV2-DSTE$^{FAP5/CD3}$-E6 (black), OHSV2-DSTE$^{FAP5/CD3}$-E7 (blue), OHSV2-DSTE$^{FAP5/CD3}$-E8 (orange), and OHSV2-GFP (green). HuH-7 tumor cells (3×10^6) were subcutaneously inoculated into BALB/c nude mouse. Treatment was initiated once tumors reached approximately 100 mm^3 (n=5 mice per group). Data were presented as mean ± SD, and two-way ANOVA with Tukey's multiple comparisons test was performed. ns, not significant; ***, $p<0.001$. **(B)** Levels of cytokines *in vivo*, including IFN-γ, IL-6, IL-2, IL-4, IL-10, and TNF.

SUPPLEMENTARY FIGURE 2
Single-cell RNA sequencing analysis of tumor tissues. **(A)** Seven cell clusters identified from tumor tissues by single-cell RNA sequencing, including B cells, CD3+CD4+T cells, CD3+CD8+T cells, iCAF, myCAF, TAMs, and TECs. CAFs, cancer-associated fibroblasts; myCAF, myofibroblastic CAFs; and iCAF, inflammatory CAFs. **(B)** UMPA plot of different lymphocytes and CAFs derived from tumor tissues of all groups. **(C)** Violin plot illustrating the expressions of iCAF and myCAF in their respective marker genes.

SUPPLEMENTARY TABLE 1
Partial parameters reflecting momentous organ system function. Seven groups are as follows: Group 1, control group; Group 2, J80A-P24; Group 3, Lenvatinab + anti-PD-1; Group 4, OHSV2-DSTE$^{FAP5/CD3}$; Group 5, OHSV2-DSTE$^{FAP5/CD3}$ + J80A-PE24; Group 6, OHSV2-DSTE$^{FAP5/CD3}$ + J80A-P24 + anti-PD-1; and Group 7, OHSV2-DSTE$^{FAP5/CD3}$ + J80A-PE24 + CAR-T^{HN3}. WBC, white blood cells; RBC, red blood cells; TBIL, total bilirubin; ALT, glutamate transaminase; CK-MB, phosphocreatine kinase; and Cr, creatinine.

SUPPLEMENTARY TABLE 2
Distribution of cell numbers of CD3+CD4 + T and CD3+CD8+ T cells in different treatment groups.

References

1. Siegel RL, Miller KD, Wagle NS, Jemal A. Cancer statistics, 2023. *CA Cancer J Clin*. (2023) 73:17–48. doi: 10.3322/caac.21763

2. Ntellas P, Chau I. Updates on systemic therapy for hepatocellular carcinoma. *Am Soc Clin Oncol Educ Book*. (2024) 44:e430028. doi: 10.1200/EDBK_430028

3. Roy A. Updated efficacy and safety data from IMbrave150: atezolizumab plus bevacizumab vs. Sorafenib for unresectable hepatocellular carcinoma. *J Clin Exp hepatology*. (2022) 12:1575–6. doi: 10.1016/j.jceh.2022.07.003

4. Fares CM, Van Allen EM, Drake CG, Allison JP, Hu-Lieskovan S. Mechanisms of resistance to immune checkpoint blockade: why does checkpoint inhibitor immunotherapy not work for all patients? *Am Soc Clin Oncol Educ Book*. (2019) 39:147–64. doi: 10.1200/EDBK_240837

5. Foerster F, Gairing SJ, Ilyas SI, Galle PR. Emerging immunotherapy for HCC: A guide for hepatologists. *Hepatology (Baltimore Md.)*. (2022) 75(6):1604–26. doi: 10.1002/hep.32447

6. Macedo N, Miller DM, Haq R, Kaufman HL. Clinical landscape of oncolytic virus research in 2020. *J immunotherapy Cancer*. (2020) 8:e001486. doi: 10.1136/jitc-2020-001486

7. Andtbacka RH, Kaufman HL, Collichio F, Amatruda T, Senzer N, Chesney J, et al. Talimogene laherparepvec improves durable response rate in patients with advanced melanoma. *J Clin oncology: Off J Am Soc Clin Oncol*. (2015) 33:2780–8. doi: 10.1200/JCO.2014.58.3377

8. Wang Y, Jin J, Wu Z, Hu S, Hu H, Ning Z, et al. Stability and anti-tumor effect of oncolytic herpes simplex virus type 2. *Oncotarget*. (2018) 9:24672–83. doi: 10.18632/oncotarget.25122

9. Wang Y, Zhou X, Wu Z, Hu H, Jin J, Hu Y, et al. Preclinical safety evaluation of oncolytic herpes simplex virus type 2. *Hum Gene Ther*. (2019) 30:651–60. doi: 10.1089/hum.2018.170

10. Dong S, Liu B, Hu S, Guo F, Zhong Y, Cai Q, et al. A novel oncolytic virus induces a regional cytokine storm and safely eliminates Malignant ascites of colon cancer. *Cancer Med*. (2022) 11:4297–309. doi: 10.1002/cam4.v11.22

11. Zhang B, Huang J, Tang J, Hu S, Luo S, Luo Z, et al. Intratumoral OH2, an oncolytic herpes simplex virus 2, in patients with advanced solid tumors: a multicenter, phase I/II clinical trial. *J immunotherapy Cancer*. (2021) 9:e002224. doi: 10.1136/jitc-2020-002224

12. Vesely MD, Zhang T, Chen L. Resistance mechanisms to anti-PD cancer immunotherapy. *Annu Rev Immunol*. (2022) 40:45–74. doi: 10.1146/annurev-immunol-070621-030155

13. El-Khazragy N, Ghozy S, Emad P, Mourad M, Razza D, Farouk YK, et al. Chimeric antigen receptor T cells immunotherapy: challenges and opportunities in hematological Malignancies. *Immunotherapy*. (2020) 12:1341–57. doi: 10.2217/imt-2020-0181

14. Ahmed HM, Moselhy SS, Mohamad MI, Soliman AF, Hassan MNM, El-Khazragy N. Targeting refractory diffuse large B cell lymphoma by CAR-WEE1 T-cells: *In vitro* evaluation. *Ann Hematol*. (2025) 104(3):1833–44. doi: 10.1007/s00277-024-06134-8

15. Li D, Li N, Zhang YF, Fu H, Feng M, Schneider D, et al. Persistent polyfunctional chimeric antigen receptor T cells that target glypican 3 eliminate orthotopic hepatocellular carcinomas in mice. *Gastroenterology*. (2020) 158:2250–2265.e20. doi: 10.1053/j.gastro.2020.02.011

16. Dal Bo M, De Mattia E, Baboci L, Mezzalira S, Cecchin E, Assaraf YG, et al. New insights into the pharmacological, immunological, and CAR-T-cell approaches in the treatment of hepatocellular carcinoma. *Drug resistance updates: Rev commentaries antimicrobial Anticancer chemotherapy*. (2020) 51:100702. doi: 10.1016/j.drup.2020.100702

17. Maalej KM, Merhi M, Inchakalody VP, Mestiri S, Alam M, Maccalli C, et al. CAR-cell therapy in the era of solid tumor treatment: current challenges and emerging therapeutic advances. *Mol Cancer*. (2023) 22:20. doi: 10.1186/s12943-023-01723-z

18. Mouw JK, Ou G, Weaver VM. Extracellular matrix assembly: a multiscale deconstruction. *Nat Rev Mol Cell Biol*. (2014) 15:771–85. doi: 10.1038/nrm3902

19. Sahai E, Astsaturov I, Cukierman E, DeNardo DG, Egeblad M, Evans RM, et al. A framework for advancing our understanding of cancer-associated fibroblasts. *Nat Rev Cancer*. (2020) 20:174–86. doi: 10.1038/s41568-019-0238-1

20. Chen Y, McAndrews KM, Kalluri R. Clinical and therapeutic relevance of cancer-associated fibroblasts. *Nat Rev Clin Oncol*. (2021) 18:792–804. doi: 10.1038/s41571-021-00546-5

21. Kraman M, Bambrough PJ, Arnold JN, Roberts EW, Magiera L, Jones JO, et al. Suppression of antitumor immunity by stromal cells expressing fibroblast activation protein-alpha. *Science*. (2010) 330:827–30. doi: 10.1126/science.1195300

22. Labanieh L, Mackall CL. CAR immune cells: design principles, resistance and the next generation. *Nature*. (2023) 614:635–48. doi: 10.1038/s41586-023-05707-3

23. Bughda R, Dimou P, D'Souza RR, Klampatsa A. Fibroblast activation protein (FAP)-targeted CAR-T cells: launching an attack on tumor stroma. *Immunotargets Ther*. (2021) 10:313–23. doi: 10.2147/ITT.S291767

24. Zamarin D, Holmgaard RB, Subudhi SK, Park JS, Mansour M, Palese P, et al. Localized oncolytic virotherapy overcomes systemic tumor resistance to immune checkpoint blockade immunotherapy. *Sci Trans Med*. (2014) 6:226ra32. doi: 10.1126/scitranslmed.3008095

25. Yap TA, Parkes EE, Peng W, Moyers JT, Curran MA, Tawbi HA. Development of immunotherapy combination strategies in cancer. *Cancer Discov*. (2021) 11:1368–97. doi: 10.1158/2159-8290.CD-20-1209

26. Swain SM, Miles D, Kim SB, Im YH, Im SA, Semiglazov V, et al. Pertuzumab, trastuzumab, and docetaxel for HER2-positive metastatic breast cancer (CLEOPATRA): end-of-study results from a double-blind, randomised, placebo-controlled, phase 3 study. *Lancet Oncol*. (2020) 21:519–30. doi: 10.1016/S1470-2045(19)30863-0

27. Li J, Xiang L, Wang Q, Ma X, Chen X, Zhu Y, et al. Highly potent immunotoxins targeting the membrane-distal N-lobe of GPC3 for immunotherapy of hepatocellular carcinoma. *J Cancer*. (2022) 13:1370–84. doi: 10.7150/jca.66978

28. Chen X, Chen Y, Liang R, Xiang L, Li J, Zhu Y, et al. Combination therapy of hepatocellular carcinoma by GPC3-targeted bispecific antibody and irinotecan is potent in suppressing tumor growth in mice. *Mol Cancer Ther*. (2022) 21:149–58. doi: 10.1158/1535-7163.MCT-20-1025

29. Liu Y, Xun Z, Ma K, Liang S, Li X, Zhou S, et al. Identification of a tumour immune barrier in the HCC microenvironment that determines the efficacy of immunotherapy. *J hepatology*. (2023) 78:770–82. doi: 10.1016/j.jhep.2023.01.011

30. Roy AM, Iyer R, Chakraborty S. The extracellular matrix in hepatocellular carcinoma: Mechanisms and therapeutic vulnerability. *Cell Rep. Med*. (2023) 4(9):101170. doi: 10.1016/j.xcrm.2023.101170

31. Dong S, Li X, Huang Q, Li Y, Li J, Zhu X, et al. Resistance to immunotherapy in non-small cell lung cancer: Unraveling causes, developing effective strategies, and exploring potential breakthroughs. *Drug resistance updates: Rev commentaries antimicrobial Anticancer chemotherapy*. (2025) 81:101215. doi: 10.1016/j.drup.2025.101215

32. Schumacher TN, Thommen DS. Tertiary lymphoid structures in cancer. *Science*. (2022) 375:eabf9419. doi: 10.1126/science.abf9419

33. Barry ST, Gabrilovich DI, Sansom OJ, Campbell AD, Morton JP. Therapeutic targeting of tumour myeloid cells. *Nat Rev Cancer*. (2023) 23:216–37. doi: 10.1038/s41568-022-00546-2

34. Kelley RK, Sangro B, Harris W, Ikeda M, Okusaka T, Kang YK, et al. Safety, efficacy, and pharmacodynamics of tremelimumab plus durvalumab for patients with unresectable hepatocellular carcinoma: randomized expansion of a phase I/II study. *J Clin oncology: Off J Am Soc Clin Oncol*. (2021) 39:2991–3001. doi: 10.1200/JCO.20.03555

35. Martin NT, Bell JC. Oncolytic virus combination therapy: killing one bird with two stones. *Mol Ther*. (2018) 26:1414–22. doi: 10.1016/j.ymthe.2018.04.001

36. Hecht JR, Raman SS, Chan A, Kalinsky K, Baurain JF, Jimenez MM, et al. Phase Ib study of talimogene laherparepvec in combination with atezolizumab in patients with triple negative breast cancer and colorectal cancer with liver metastases. *ESMO Open*. (2023) 8:100884. doi: 10.1016/j.esmoop.2023.100884

37. Chen X, Song E. Turning foes to friends: targeting cancer-associated fibroblasts. *Nat Rev Drug Discov*. (2019) 18:99–115. doi: 10.1038/s41573-018-0004-1

38. Biffi G, Tuveson DA. Diversity and biology of cancer-associated fibroblasts. *Physiol Rev*. (2021) 101:147–76. doi: 10.1152/physrev.00048.2019

39. Twumasi-Boateng K, Pettigrew JL, Kwok YYE, Bell JC, Nelson BH. Oncolytic viruses as engineering platforms for combination immunotherapy. *Nat Rev Cancer*. (2018) 18:419–32. doi: 10.1038/s41568-018-0009-4

40. Freedman JD, Duffy MR, Lei-Rossmann J, Muntzer A, Scott EM, Hagel J, et al. An oncolytic virus expressing a T-cell engager simultaneously targets cancer and immunosuppressive stromal cells. *Cancer Res*. (2018) 78:6852–65. doi: 10.1158/0008-5472.CAN-18-1750

41. Purcell JW, Tanlimco SG, Hickson J, Fox M, Sho M, Durkin L, et al. LRRC15 is a novel mesenchymal protein and stromal target for antibody-drug conjugates. *Cancer Res*. (2018) 78:4059–72. doi: 10.1158/0008-5472.CAN-18-0327

42. Goebeler ME, Bargou RC. T cell-engaging therapies - BiTEs and beyond. *Nat Rev Clin Oncol*. (2020) 17:418–34. doi: 10.1038/s41571-020-0347-5

43. Zhu Y, Wang K, Yue L, Zuo D, Sheng J, Lan S, et al. Mesothelin CAR-T cells expressing tumor-targeted immunocytokine IL-12 yield durable efficacy and fewer side effects. *Pharmacol Res*. (2024) 203:107186. doi: 10.1016/j.phrs.2024.107186

44. Bommareddy PK, Shettigar M, Kaufman HL. Integrating oncolytic viruses in combination cancer immunotherapy. *Nat Rev Immunol*. (2018) 18:498–513. doi: 10.1038/s41577-018-0014-6

45. Wang LC, Lo A, Scholler J, Sun J, Majumdar RS, Kapoor V, et al. Targeting fibroblast activation protein in tumor stroma with chimeric antigen receptor T cells can inhibit tumor growth and augment host immunity without severe toxicity. *Cancer Immunol Res*. (2014) 2:154–66. doi: 10.1158/2326-6066.CIR-13-0027

46. Roberts EW, Deonarine A, Jones JO, Denton AE, Feig C, Lyons SK, et al. Depletion of stromal cells expressing fibroblast activation protein-α from skeletal muscle and bone marrow results in cachexia and anemia. *J Exp Med*. (2013) 210:1137–51. doi: 10.1084/jem.20122344

47. Lu Y, He W, Huang X, He Y, Gou X, Liu X, et al. Strategies to package recombinant Adeno-Associated Virus expressing the N-terminal gasdermin domain for tumor treatment. *Nat Commun*. (2021) 12:7155. doi: 10.1038/s41467-021-27407-0

48. Zhu Y, Hu X, Feng L, Yang Z, Zhou L, Duan X, et al. Enhanced therapeutic efficacy of a novel oncolytic herpes simplex virus type 2 encoding an antibody against programmed cell death 1. *Mol Ther oncolytics*. (2019) 15:201–13. doi: 10.1016/j.omto.2019.10.003

49. Jiang Q, Ghafoor A, Mian I, Rathkey D, Thomas A, Alewine C, et al. Enhanced efficacy of mesothelin-targeted immunotoxin LMB-100 and anti-PD-1 antibody in patients with mesothelioma and mouse tumor models. *Sci Trans Med*. (2020) 12:eaaz7252. doi: 10.1126/scitranslmed.aaz7252

50. Labrijn AF, Janmaat ML, Reichert JM, Parren P. Bispecific antibodies: a mechanistic review of the pipeline. *Nat Rev Drug Discov*. (2019) 18:585–608. doi: 10.1038/s41573-019-0028-1

51. Wherry EJ, Kurachi M. Molecular and cellular insights into T cell exhaustion. *Nat Rev Immunol*. (2015) 15:486–99. doi: 10.1038/nri3862

52. McAndrews KM, Chen Y, Darpolor JK, Zheng X, Yang S, Carstens JL, et al. Identification of functional heterogeneity of carcinoma-associated fibroblasts with distinct IL6-mediated therapy resistance in pancreatic cancer. *Cancer Discov*. (2022) 12:1580–97. doi: 10.1158/2159-8290.CD-20-1484

53. Mao X, Xu J, Wang W, Liang C, Hua J, Liu J, et al. Crosstalk between cancer-associated fibroblasts and immune cells in the tumor microenvironment: new findings and future perspectives. *Mol Cancer*. (2021) 20:131. doi: 10.1186/s12943-021-01428-1

frontiers | Frontiers in Immunology

TYPE Original Research
PUBLISHED 05 June 2025
DOI 10.3389/fimmu.2025.1567969

OPEN ACCESS

EDITED BY
Sherif El-Kafrawy,
King Abdulaziz University, Saudi Arabia

REVIEWED BY
Zhi-Ping Liu,
Shandong University, China
Ahmed Abdelsadik,
Aswan University, Egypt

*CORRESPONDENCE
Lili Xiong
lxiong@swjtu.edu.cn

RECEIVED 28 January 2025
ACCEPTED 21 May 2025
PUBLISHED 05 June 2025

CITATION
Huai R, Mao C and Xiong L (2025) Dissecting the multi-omics landscape of TEAD1 in hepatocellular carcinoma: cycle regulation and metastatic potential.
Front. Immunol. 16:1567969.
doi: 10.3389/fimmu.2025.1567969

Dissecting the multi-omics landscape of TEAD1 in hepatocellular carcinoma: cycle regulation and metastatic potential

Ruiping Huai[1,2,3], Canquan Mao[2] and Lili Xiong[1*]

[1]Southwest Jiaotong University, School of Chemistry, Chengdu, China, [2]Southwest Jiaotong University, School of Life Science and Engineering, Chengdu, China, [3]Southwest Jiaotong University, School of Materials Science and Engineering, Chengdu, China

Background: The effects exerted by the TEA domain transcription factor family genes on tumorigenesis in various cancers have been extensively investigated. Nevertheless, the potential role of TEAD1 in cancer-related epigenetic alterations, immunological characteristics, and prognosis remains ambiguous. This study aims to clarify the function and potential mechanisms of action of TEAD1 in cancer.

Methods: We assessed pan-cancer expression, methylation, and mutation profiles of TEAD1 to determine its prognostic significance in clinical settings. Furthermore, we analyzed the pan-cancer immunological landscape of TEAD1, with a particular focus on liver hepatocellular carcinoma (LIHC), using correlation analysis. We also performed a subtype-specific analysis of TEAD1 in LIHC to identify its expression patterns, immunological traits, and constructed a prognostic model based on disulfidptosis-related genes. Lastly, we assessed the impact of TEAD1 knockdown on LIHC cell lines HepG2 and Huh-7 by using *in vitro* experiments.

Results: Our findings suggest that TEAD1 is differentially expressed across various cancer types and can act as an independent prognostic factor for multiple cancers. Moreover, we observed that epigenetic changes involving TEAD1 are highly heterogeneous among several cancers; abnormal methylation and copy number variations were associated with a poor prognosis in multiple malignancies, especially in LIHC. Immunoassays demonstrated a significant association between TEAD1 and numerous immune checkpoints in LIHC. Additionally, cellular experiments revealed that knocking down TEAD1 reduced the proliferation, migration, and invasion capabilities of LIHC cells.

Conclusions: The results of this study imply that TEAD1 may serve as a promising prognostic biomarker for tumors and an immunotherapy target, while playing a crucial role in the proliferation, migration, and invasion processes within LIHC.

KEYWORDS

TEAD1, biomarker, LIHC, single-cell, cell cycle, EMT

1 Introduction

Cancer continues to exert a substantial global burden, with increasing prevalence and impact across diverse populations. The disease's escalating incidence and the profound effects on various communities underscore the urgency of intensified research and intervention efforts. Liver hepatocellular carcinoma (LIHC) is the third leading cause of cancer-related mortality and the sixth most frequently diagnosed cancer worldwide, with approximately 906,000 new cases and 830,000 deaths reported in 2020 (1). As the most prevalent primary liver malignancy, LIHC accounts for approximately 90% of all liver cancer cases. Despite advancements in treatment strategies, the majority of LIHC patients are diagnosed at advanced stages, resulting in a five-year survival rate of less than 20% (2). There is an urgent need for a deeper understanding of LIHC pathogenesis and the identification of novel biomarkers.

The TEA domain family of transcription factors is highly conserved and ubiquitously expressed across mammalian tissues, with the four TEA domain genes exhibiting distinct tissue-specific expression patterns (3–6). TEA domain transcription factor 1 (TEAD1), the first member identified within this family, has been implicated in various cancers due to its deregulation (7). knockdown of TEAD1 has been shown to suppress cell proliferation in gastric cancer (8), conversely its overexpression enhances cell proliferation, migration and invasion in pancreatic cancer (9). Similarly, activation of the TEAD1 signaling pathway promotes malignant phenotypes in gastric cancer cells (10). Understanding the complex mechanisms by which TEAD1 contributes to cancer pathogenesis is crucial and holds significant promise for the developing of targeted and personalized therapeutic strategies.

In this study, we conducted a comprehensive analysis of TEAD1's pan-cancer expression levels, prognostic significance, epigenetic alterations, and immune landscape. We specifically investigated the immunological characteristics and associated with TEAD1 and established a prognostic model for LIHC based on disulfidptosis-related genes. Our findings were validated through *in vitro* experimentation and may provide valuable insights for future research on TEAD1.

2 Materials and methods

2.1 Datasets acquisition

mRNA expression profiles of normal tissues were obtained from the Genotype-Tissue Expression (GTEx) database (https://www.gtexportal.org/home/) and the Human Protein Atlas (HPA) database (https://www.proteinatlas.org/). Gene expression data for cancer cell lines were retrieved from the HPA database. Copy number variations (CNV), DNA methylation (Methylation450K) data, and TPM format RNAseq data from The Cancer Genome Atlas (TCGA) and GTEx, uniformly processed by the Toil pipeline (11), along with clinical features for 33 cancer types, were sourced from the UCSC XENA platform (https://xenabrowser.net/datapages/). TEAD1 protein expression profiles were extracted from the Clinical Proteomic Tumor Analysis Consortium (CPTAC) database to assess protein expression levels in cancer. To validate the differential expression of TEAD1 across cancers, six datasets (GSE93601, GSE16011, GSE6344, GSE36376, GSE19804, and GSE39791) were sourced from the Gene Expression Omnibus (GEO, https://www.ncbi.nlm.nih.gov/geo/) database, and the validation dataset E-MEXP-1327 for prostate adenocarcinoma (PRAD) was derived from the Affymetrix GeneChip Human Genome HG-U133A platform. Pan-cancer immune cell infiltration data were procured from Tumor Immune Estimation Resource 2.0 (TIMER2.0, http://timer.cistrome.org/). The liver cancer dataset, LIRI-JP, was accessed from the International Cancer Genome Consortium (ICGC, https://dcc.icgc.org/). Single-cell data were obtained from the Tumor Immune Single-cell Hub 2 database(https://tisch.comp-genomics.org/). Finally, information about the spatial transcriptome datasets is provided in Supplementary Table 1.

2.2 Pan-cancer differential expression, clinical prognostic, and epigenetic analysis of TEAD1

Using HPA and GTEx data, we analyzed the expression level of TEAD1 in normal human tissues and cancer cell lines. Based on TCGA pan-cancer expression profile data, we evaluated the expression of TEAD1 in 33 different cancer types. In addition, the differential expression of TEAD1 was validated based on additional datasets. Using the Clinical module of the TISIDB database, we explored the correlation between TEAD1 and pan-cancer clinical stage. Pan-cancer clinical survival information includes overall survival (OS), progression-free interval (PFI), disease-free interval (DFI), and disease-specific survival (DSS). We grouped all patients into 33 cancer types according to the median expression level of TEAD1 mRNA, and all patients were divided into the TEAD1 high expression group and the TEAD1 low expression group. R packages "survival" and "survminer" were used to perform COX analysis. In addition, we evaluated the CNV and methylation level of TEAD1 in pan-cancer, as well as the association with mRNA expression and clinical prognosis.

2.3 Immune-related analysis

The R package ESTIMATE (12) was used to calculate the StromalScore, ImmuneScore, ESTIMATEScore, and TumorPurity of tumor tissues, and the correlation between TEAD1 and different scores was evaluated. The correlation between TEAD1 and immune cell infiltration was evaluated using xCell, ssGSEA, and CIBERSORT algorithms (13–15). In addition, we obtained the information of 122 immune regulators collected by Charoentong et al., including MHC, receptors, chemokines, and immunostimulants (16), and calculated the Pearson correlation between TEAD1 and pan-cancer immune regulators. In addition,

we used the TIP (tracking tumor immunophenotype) database (17) to evaluate the anti-cancer immune status at seven different stages of the tumor-immunity cycle: release of cancer cell antigens (step 1), cancer antigen presentation (step 2), priming and activation (step 3), trafficking of immune cells to tumors (step 4), infiltration of immune cells into tumors (step 5), T cell recognition of cancer cells (step 6), and killing of cancer cells (step 7). The Cancer Immunome Database (TCIA) (16) was used to evaluate the relationship between TEAD1 and immunotherapy.

2.4 Single-cell and spatial transcriptomic analysis

We downloaded the LIHC single-cell dataset GSE146115 from the TISCH2 (18) database and used the uniform manifold approximation and projection (UMAP) technique to visualize the high-dimensional data into a two-dimensional heatmap, and visualized the expression data of the TEAD1 gene. The Kruskal-Wallis rank sum test was used to evaluate the expression difference of the TEAD1 gene in different cell types. All cells were divided into positive/negative expression groups according to whether the TEAD1 gene was expressed, and the proportion of each cell type in the positive/negative expression group was calculated respectively. The AUCell package was used to evaluate the scores of immune, metabolic, signaling pathways, proliferation, cell death, and mitochondrial-related biological pathways. The limma package was used to compare the differences in scores between the TEAD1 expression positive and negative groups. Based on previous research methods, we processed the LIHC spatial transcriptome data. The Cottrazm package was used to deconvolute different cell components (19). The cell type with the highest content in each microregion was calculated, and the SpatialDimPlot function in the Seurat package was used to visualize the maximum value of the cell component in each microregion and the expression landscape of the TEAD1 gene in each microregion. Spearman correlation analysis was used to calculate the correlation between cell content and cell content in all spots, as well as the correlation between cell content and gene expression, and the linkET package was used for visualization.

2.5 Functional enrichment analysis

According to the median expression value of TEAD1, LIHC patients were divided into two groups, namely, the TEAD1 high expression group and the TEAD1 low expression group. The limma package was used to perform differential analysis. Genes with Fold change (FC) greater than 2 and p-value less than 0.05 were considered to have significant differences. Volcano plots were drawn for visualization. The clusterProfiler package completed Gene Ontology (GO) and Kyoto Encyclopedia of Genes and Genomes (KEGG) enrichment analysis. In addition, all genes were sorted according to log2FC, and the clusterProfiler package performed gene set enrichment analysis based on GO-Biological Process (BP) gene set, GO-Molecular Function (MF) gene set, GO-Cellular Component (CC) gene set, reactome gene set, and wikipathways gene set, calculated the gene set enrichment score ES, and performed significance tests and multiple hypothesis tests on the ES values of the gene sets. The top 5 pathways that were significantly enriched in the high/low expression groups were selected for visualization. The z-score parameter in the R package GSVA was used to calculate the gene set and obtain the combined z-score score. We used the scale function to define the gene set score and calculated the Pearson correlation between TEAD1 and each gene set score.

2.6 Construction of a prognostic model based on disulfidptosis-related genes

Based on the study of Xu et al. (20), we collected 24 disulfidptosis-related genes. We also performed correlation analysis with TEAD1 to obtain hub genes related to disulfidptosis. Then, we used the lasso-cox regression method to reduce the dimension and build a prognostic model. The specific steps were as follows: the TPM format expression spectrum of TCGA-LIHC was normalized by log2(TPM+1), and samples with RNAseq data and clinical information were retained. The lasso algorithm in the R package "glmnet" was used for feature selection, and 10-fold cross-validation was used. The R package "survival" was combined with multivariate Cox regression analysis to build a prognostic model. Iterative analysis was performed through the step function to select the optimal model. Log-rank was used to test the KM survival analysis to compare the survival differences between the above two or more groups, and timeROC analysis was performed to discriminate the accuracy of the prediction model. Univariate and multivariate Cox analysis was used to determine the potential of risk factors as independent prognostic factors.

2.7 Cell culture and transfection

HepG2 and Huh-7 cells were purchased from Shanghai Cell Bank Library of the Chinese Academy of Sciences (Shanghai, China) and incubated with Dulbecco's Modified Eagle Medium (DMEM) (HyClone) with 10% fetal bovine serum (Biological Industries, ISRAEL), 100 U/ml penicillin, and 100 μg/ml streptomycin solution (HyClone) at 37 °C in 5% CO2. Two siRNAs specific targeting TEAD1 and a scramble negative control siRNA were designed and synthesized by GenePharma Company (Shanghai, China). These siRNAs were transfected into HepG2 or Huh-7 cells using the Lipofectamine 3000 Reagent (Invitrogen, California, USA) in accordance with the manufacturer's instructions. The experiment was conducted in triplicate. The sequences of siRNA1 sense(5'-3'): CCACUGCCAUUCAUAACAATT, antisense(5'-3'): UUGUUAUGAAUGGCAGUGGTT. The sequences of siRNA2 sense(5'-3'): CAUGGCCUGUGUGUUUGAATT, antisense(5'-3'): UUCAAACACACAGGCCAUGTT.

2.8 RNA extraction and quantitative real-time PCR

Total RNA was extracted with TRIzol reagent (Invitrogen, USA) and reverse transcribed with random primers using the Hiscipt III 1st strand cDNA synthesis kit (Vazyme, Nanjing, China) according to the manufacturer's instructions. Then, we used SYBR Green Real-Time qPCR analysis (Vazyme, Nanjing, China) to analyze the transcriptional cDNA. The relative expression level of transcripts was normalized to that of the internal control GAPDH and analyzed using the 2^-ΔΔCt method. The forward and reverse primers for GAPDH were GGAGCGAGATCCC TCCAAAAT and GGCTGTTGTCATACTTCTCATGG, respectively. The forward and reverse primers for TEAD1 were ACGTCAAGCCTTTTGTGCAG and CTGAAAATTCCAC CAGGCGAAG, respectively.

2.9 Western blotting

Cells were harvested after treatment with siRNAs or miRNA and collected by centrifugation after washing with phosphate-buffered saline (PBS) three times. Total protein extracts were prepared in RIPA buffer supplemented with proteinase inhibitors (Solarbio Life Sciences, China). TEAD1 antibody (Abcam, USA), GAPDH, CCND1, CDK4, CDKN1A, CDH1, CDH2, and Vimentin antibody (Proteintech, China) were used for western blot analysis according to the manufacturer's instructions. Goat Anti-Mouse IgG-HRP (Proteintech, China) and Goat Anti-Rabbit IgG-HRP (Proteintech, China) were used as the secondary antibody. GAPDH was used as a protein loading control. The signals were visualized using the enhanced chemiluminescence (ECL) reagent (4A Biotech, China).

2.10 Cell viability assay

Cell viability was evaluated using the Cell Counting Kit-8 (AbMol, USA). HepG2 and Huh-7 cells transfected with siRNAs-TEAD1 were harvested upon reaching 60% confluency. They were then seeded onto 96-well culture plates, with five multiple wells allocated to each group, and 5,000 cells per well. The CCK-8 kit was used to examine the cells at 0 h, 24 h, 48 h, and 72 h after they were incubated at 37°C and 5% CO2.

2.11 Flow cytometric analysis of cell cycle

The cell cycle of HepG2 and Huh-7 cells was detected by the Cell Cycle Detection Kit (KeyGen Biotech, China). In brief, cells were collected and fixed in 70% cold ethanol overnight at 4°C. After washing with PBS twice, cells were incubated with PI/RNase A staining buffer for 30 min and subsequently analyzed by Beckman flow cytometry and CytExpert Software.

2.12 Transwell assay to detect cell migration and invasion

The migration and invasion of cells were assessed using a Transwell assay. A total of 2 × 10^4 transfected HepG2 and Huh-7 cells were seeded in the upper chamber with or without matrigel and incubated in a serum-free medium, while the lower chamber was incubated in 10% serum medium. After 48 h, the transwell chamber was taken out, fixed with 4% paraformaldehyde for 15 min, and stained with crystal violet for 5 min. Finally, the images were observed and obtained under an optical microscope.

2.13 Statistical analysis

Pearson or Spearman correlation coefficients were calculated to evaluate relationships between variables. Real-time fluorescence quantitative PCR and Western blotting were repeated three times. Data analysis was completed using GraphPad Prism 9 software. The student's t-test was used for the comparison between the two groups, and Two-way ANOVA was used for the comparison between multiple groups to determine the significance; statistical significance was determined at $p < 0.05$, with *$p < 0.05$, **$p < 0.01$, ***$p < 0.001$, and ns indicating not significant. The data are expressed as Mean ± SD.

3 Results

3.1 Pan-cancer expression pattern and clinical prognostic significance of TEAD1

TEAD1 expression in normal tissues is ubiquitous, expressed to varying degrees in almost all tissues, rather than being organ-specific. As shown in Figure 1A, its presence is relatively high in skeletal muscle and adipose tissue. Expression profiling analysis of cancer cell lines showed that TEAD1 was highly expressed in adrenocortical carcinoma, non-cancerous cancers, and testicular cancer cell lines (Figure 1B). Differential expression analysis based on TCGA paired samples showed that TEAD1 was mainly highly expressed in cholangiocarcinoma (CHOL), LIHC, and lung squamous cell carcinoma (LUSC), while significantly lowly expressed in cancers such as bladder urothelial carcinoma (BLCA), breast invasive carcinoma (BRCA), and kidney chromophobe (KICH) (Figure 1C). Differential expression analysis based on all cancer and normal samples from TCGA also confirmed the high expression of TEAD1 in cancers including CHOL, glioma (GBM), and LIHC (Figure 1D). To expand the sample size and obtain more reliable results, we integrated normal samples from the GTEx database and observed widespread dysregulation of TEAD1 in more than four-fifths of cancer types (Figure 1E). These results were validated by multiple GEO datasets (Figures 1F–K). In addition, we evaluated the correlation between TEAD1 and the clinical stage of cancer using the TISIDB database. We found that TEAD1 expression was

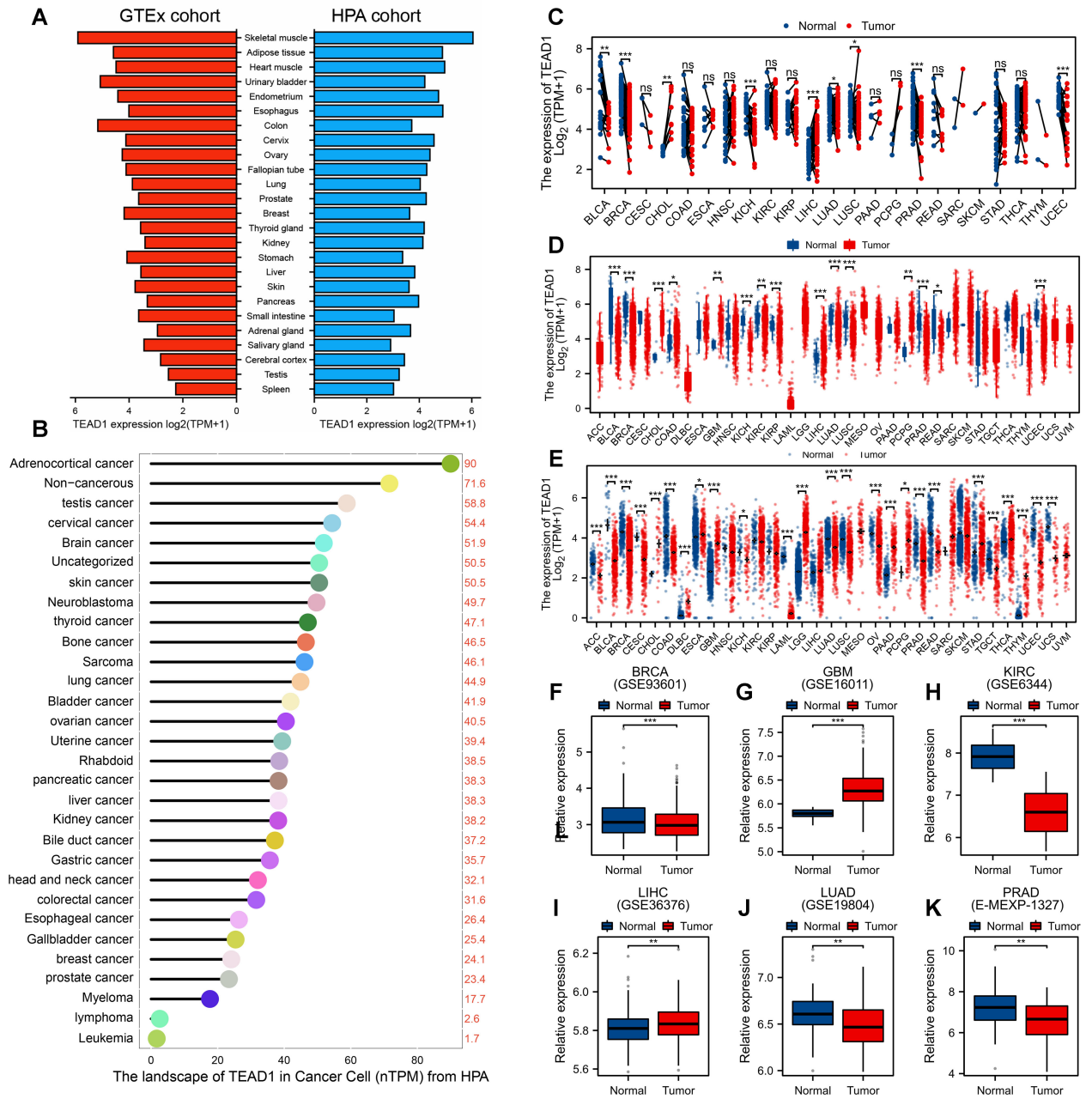

FIGURE 1
Expression of TEAD1 in human normal tissues and cancers. **(A)** Expression level of TEAD1 in human normal tissues (HPA+GTEx datasets). **(B)** TEAD1 expression in human cancer cell lines. **(C)** Evaluation of differential expression of TEAD1 based on TCGA paired samples. **(D)** Differential expression analysis based on all cancer and normal samples from TCGA. **(E)** Evaluation of TEAD1 mRNA expression levels by combining TCGA and GTEx datasets. **(F-K)** The differential expression of TEAD1 was verified based on multiple cancer datasets in GEO. *p < 0.05; **p < 0.01; ***p < 0.001; ns, no significance.

significantly associated with higher clinical stages of multiple cancers, including adrenocortical carcinoma (ACC), BLCA, head and neck squamous cell carcinoma (HNSC), and kidney renal clear cell carcinoma (KIRC) (Supplementary Figures 1A–L). Prognostic analysis showed a significant correlation between TEAD1 and the prognosis of ACC, BLCA, KICH, and KIRC. In particular, high TEAD1 expression in ACC and BLCA patients was significantly associated with shorter OS, DSS, and PFI. In addition, it was also associated with shorter OS in BRCA patients, shorter DSS in KICH patients, and shorter DSS and PFI in LUSC patients. In addition, low TEAD1 expression in KIRC patients was significantly associated with shorter OS, DSS, and PFI (Supplementary Figure 1M).

In addition, we evaluated the expression of TEAD1 in pan-cancer at spatial transcriptome resolution. We observed that TEAD1 expression in tumor cells was dominant in multiple cancer types, including BRCA, CRC, and LIHC (Figure 2A). Further localization analysis also showed that TEAD1 was significantly highly expressed in tumor cells in BRCA, KIRC, and

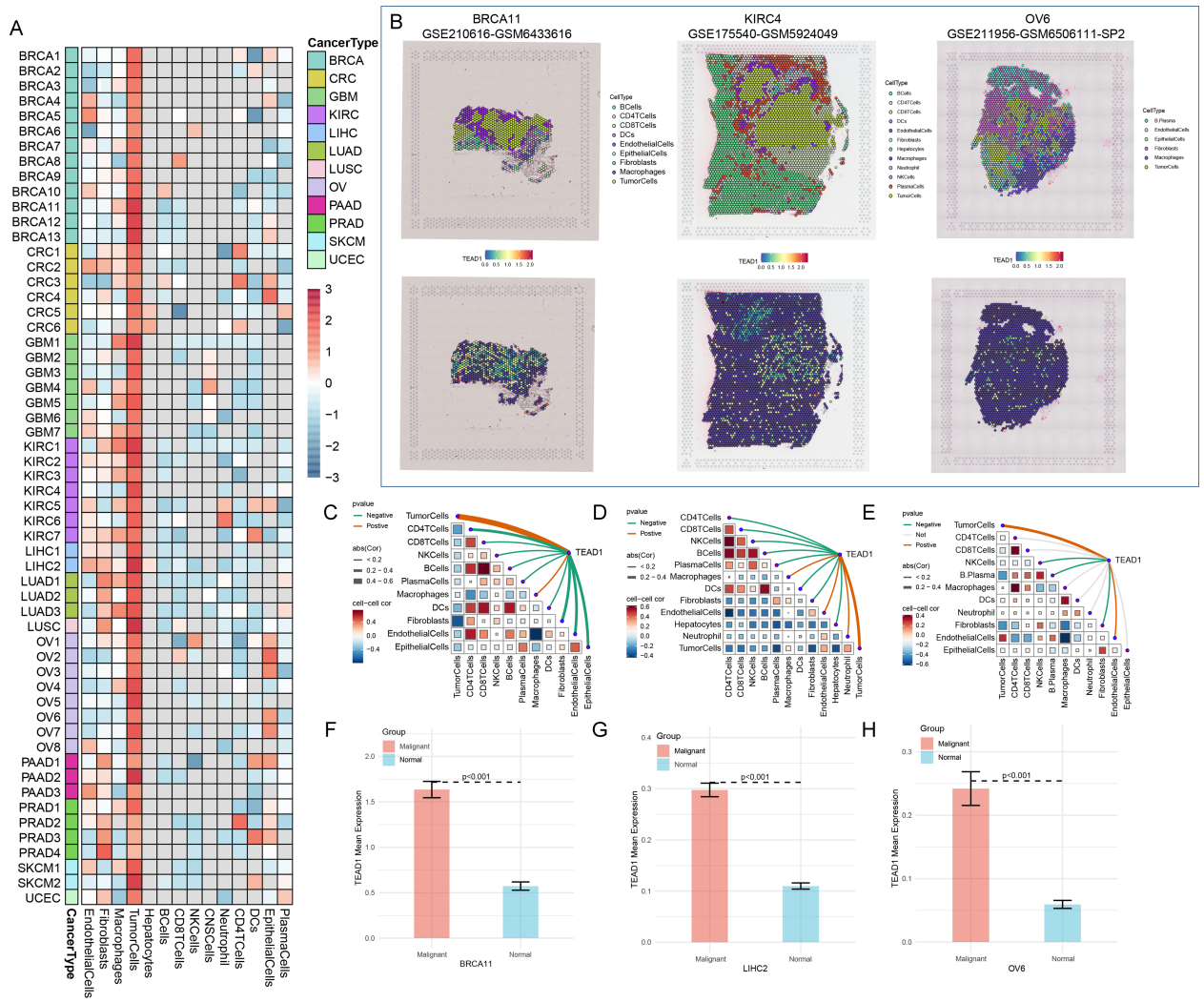

FIGURE 2
TEAD1 was significantly associated with tumor cells. **(A)** Single cell expression of TEAD1 in pan-cancer (TISCH2 database). **(B)** UMAP localization map of TEAD1 in BRCA, LIHC, and OV. **(C–E)** Evaluation of the correlation of each cell type in the TEAD1 gene expression. **(F–H)** Evaluation of TEAD1 gene expression differences between malignant and normal cells.

ovarian serous cystadenocarcinoma (OV) (Figure 2B). Highly consistent with the localization results, the expression level of TEAD1 was significantly positively correlated with the content of tumor cells in the spot (Figures 2C–E). In addition, TEAD1 was more highly expressed in malignant areas compared to non-malignant areas (Figures 2F–H). These results highlight the important role of TEAD1 in various tumors.

3.2 The epigenetic variations of TEAD1 in pan-cancer

To reveal the mechanisms leading to dysregulated TEAD1 expression, we evaluated the CNV and methylation levels of TEAD1 in pan-cancer. We observed more copy number amplifications in multiple tumor types, including ACC, BLCA, GBM, and rectum adenocarcinoma (READ), while more copy number losses were observed in OV (Figure 3A). Methylation analysis showed that compared with normal tissues, lower methylation levels were observed in multiple tumor samples, including CHOL, KIRC, kidney renal papillary cell carcinoma (KIRP), LIHC, and lung adenocarcinoma (LUAD), while higher methylation levels were observed in BRCA and PRAD (Figure 3B). Survival analysis showed that patients with high methylation levels of TEAD1 had better prognoses in GBM, LUSC, and skin cutaneous melanoma (SKCM), while the opposite was true in KIRC, lower grade glioma (LGG), and uveal melanoma (UVM) (Figures 3C–H). We also analyzed the correlation between TEAD1 CNV, methylation levels, and mRNA expression. The results showed that in various cancers, TEAD1 mRNA expression was significantly positively correlated with its CNV (Figure 3I) and negatively correlated with its methylation level (Figure 3J). In addition, TEAD1 was also significantly associated with genes associated with RNA methylation modification in pan-cancer (Figure 3K). These results emphasize that epigenetic variations in TEAD1 may mediate its mRNA expression and participate in cancer progression.

10.3389/fimmu.2025.1567969

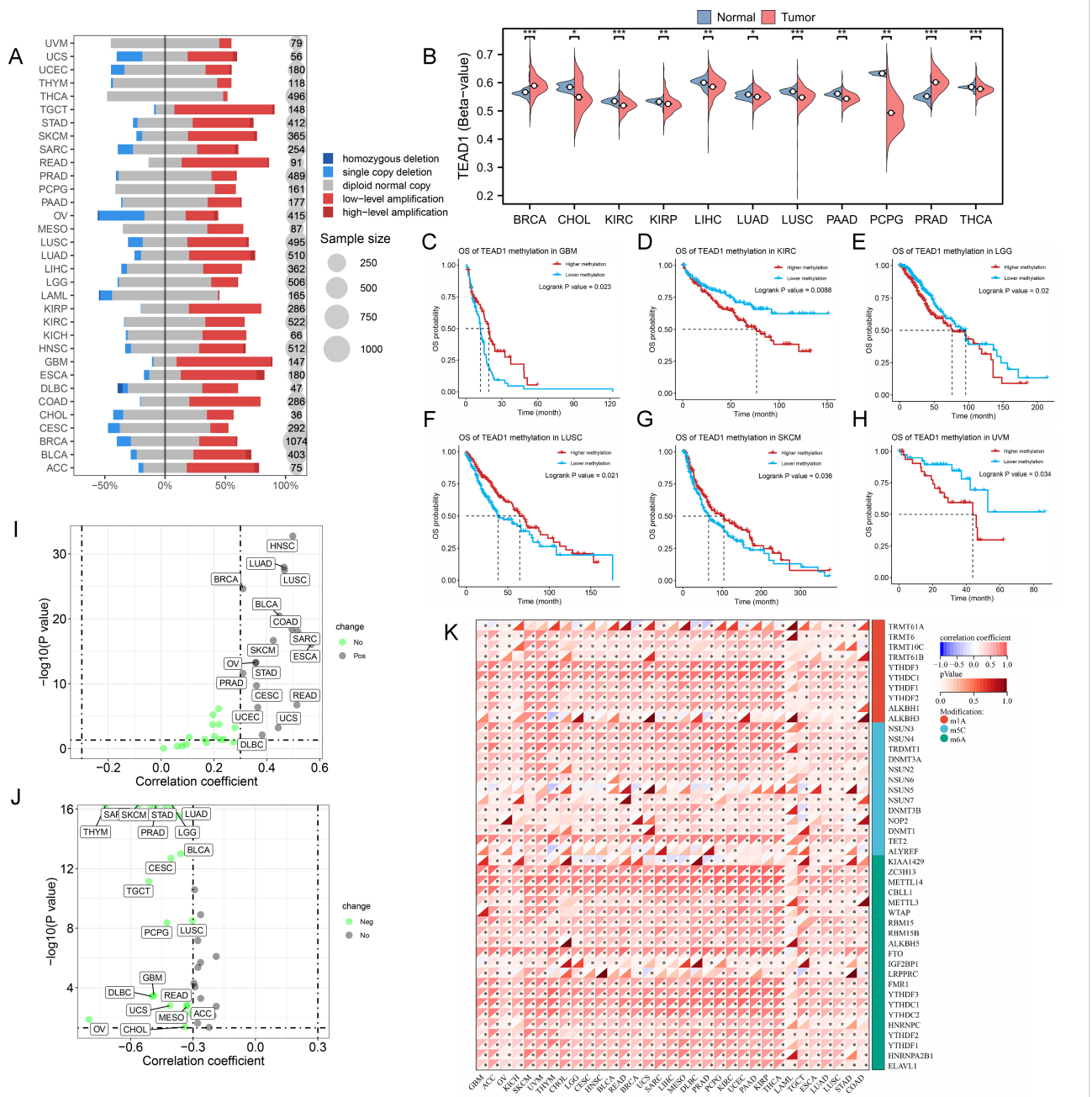

FIGURE 3
The epigenetic variations of TEAD1 in pan-cancer. **(A)** Copy number variation levels of TEAD1 in pan-cancer. **(B)** Differential methylation levels of TEAD1 in normal and tumor tissues in multiple cancer types. **(C-H)** The relationship between methylation of TEAD1 and prognosis in GBM, KIRC, LGG, LUSC, SKCM and UVM. **(I)** The relationship between copy number variation of TEAD1 and mRNA expression of TEAD1 in pan-cancer. **(J)** The relationship between methylation of TEAD1 and mRNA expression of TEAD1 in pan-cancer. **(K)** Correlation between TEAD1 and RNA-modifying genes in pan-cancer. *p < 0.05; **p < 0.01; ***p < 0.001; ns, no significance.

3.3 Single-cell analysis reveals a link between TEAD1 and LIHC malignant cells

Based on the Open Targets platform (https://platform.opentargets.org/), we analyzed the connection between TEAD1 and disease. We observed a significant correlation between TEAD1 and LIHC in cancer types (Figure 4A). Therefore, we focused on the association between TEAD1 and LIHC. We first verified the significantly high expression of TEAD1 in hepatocellular carcinoma in additional GEO datasets (Figure 4B). In addition, at the protein level, we also observed significantly high expression of TEAD1 in LIHC tumor samples (Figure 4C). Single-cell analysis results showed that

10.3389/fimmu.2025.1567969

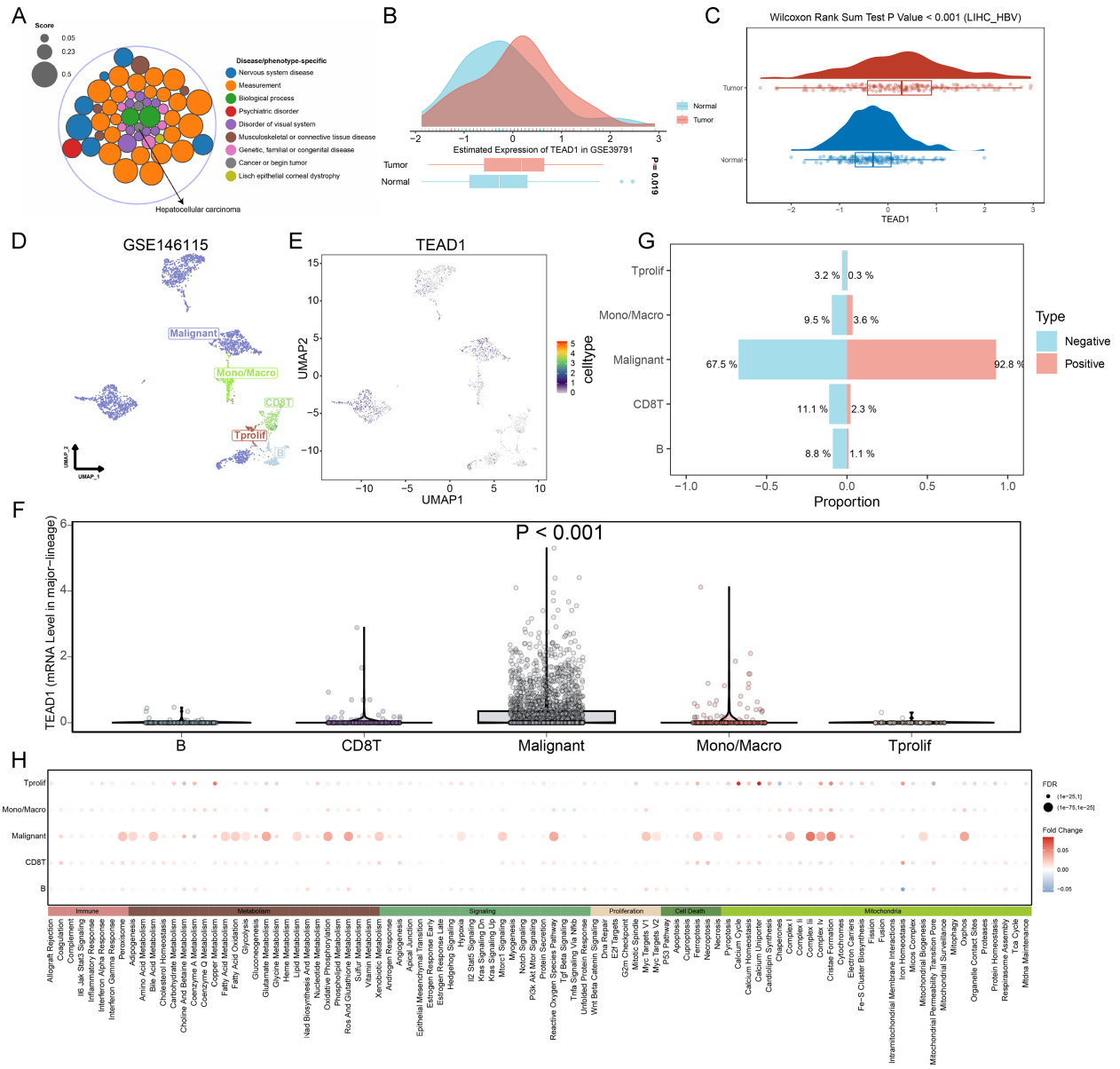

FIGURE 4
Single-cell analysis reveals a link between TEAD1 and LIHC malignant cells. **(A)** Based on the Open the Targets of Platform (https://platform.opentargets.org/) link between TEAD1 and disease were analyzed. **(B)** Evaluation of TEAD1 expression in hepatocellular carcinoma based on GEO datasets. **(C)** TEAD1 protein expression in LIHC based on the Clinical Proteomic Tumor Analysis Consortium database. **(D)** UMAP of major cell lineages in the single-cell dataset LIHC_GSE146115. **(E)** UMAP localization map of TEAD1 in the single-cell dataset LIHC_GSE146115. **(F)** Evaluation of TEAD1 gene expression differences between different cells based on single cell dataset LIHC_GSE146115. **(G)** Evaluation of the proportion of each cell type in the TEAD1 gene expression positive group and negative group based on the single cell dataset LIHC_GSE146115. **(H)** Evaluation of pathway differences in each cell type between the TEAD1 gene expression positive group and the negative group based on the single cell dataset LIHC_GSE146115.

TEAD1 was significantly highly expressed in malignant cells of LIHC (Figures 4D–F). In addition, we also observed that in the LIHC_GSE146115 dataset, the proportion of malignant cells in the TEAD1-positive expression group was much higher than that in the TEAD1-negative expression group (Figure 4G). Pathway analysis showed that in malignant cells, Metabolism and Mitochondria-related biological pathways scored higher in the TEAD1-positive group (Figure 4H).

3.4 Immunological characteristics of TEAD1 in LIHC

TEAD1 was significantly negatively correlated with the immune score in LIHC (Figure 5A). Immune cell infiltration analysis based on the CIBERSORT algorithm showed that TEAD1 was significantly positively correlated with Tcm cells ($R = 0.492$, $P < 0.001$) and T helper cells ($R = 0.320$, $P < 0.001$), but significantly

10.3389/fimmu.2025.1567969

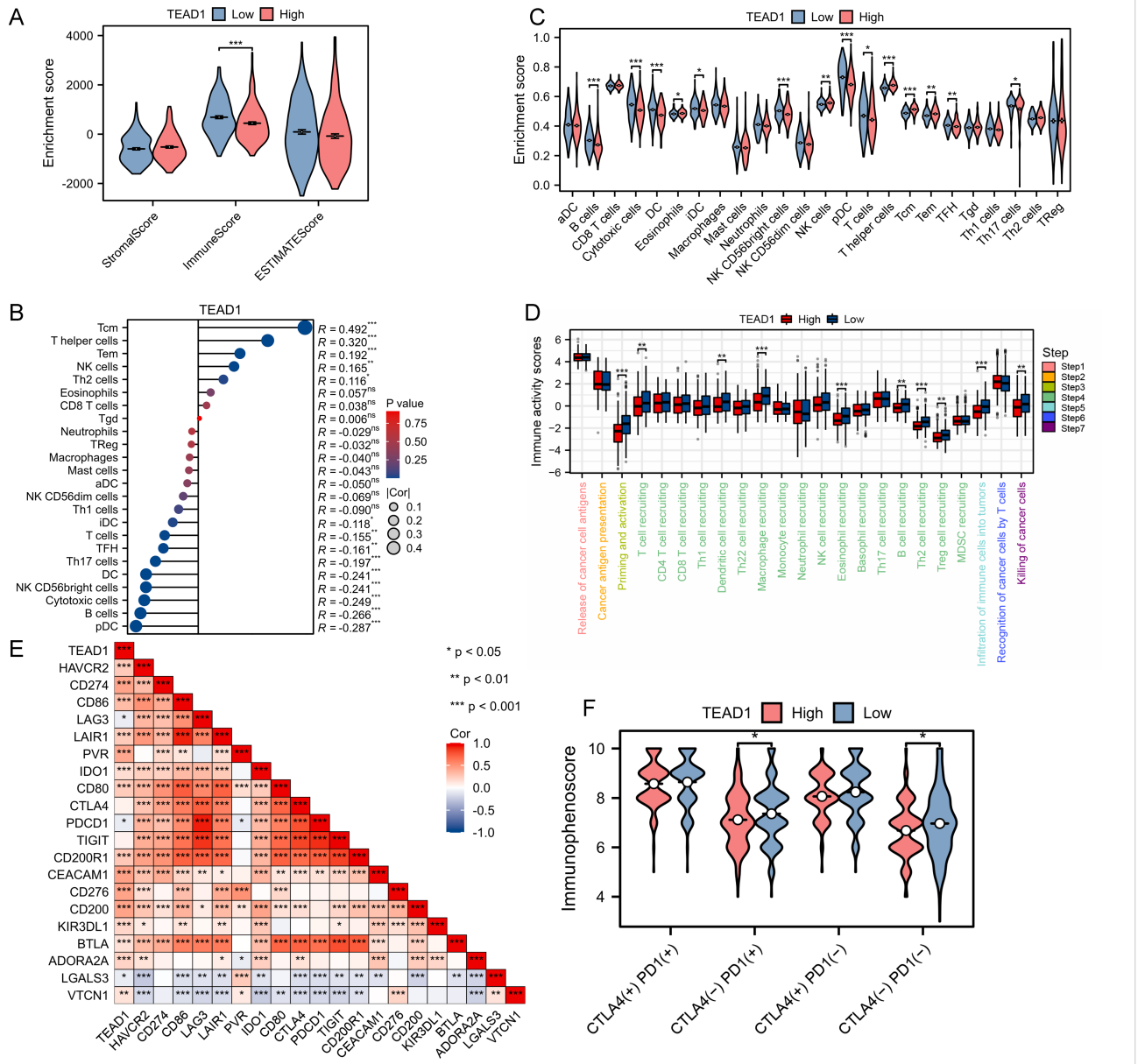

FIGURE 5
Immunological characteristic of TEAD1 in LIHC. **(A)** Differences in the immune scores between high- and low-TEAD1 groups. **(B)** Correlation between TEAD1 and 24 immune cell in LIHC. **(C)** Differences in Enrichment scores among the 24 immune cells between high- and low-TEAD1 groups. **(D)** Differences in the various steps of the cancer immunity cycle between high- and low-TEAD1 groups. **(E)** Correlation between immune checkpoints and TEAD1 in LIHC. **(F)** Differences in immune checkpoint therapy between high- and low-TEAD1 groups. *p < 0.05; **p < 0.01; ***p < 0.001; ns, no significance.

negatively correlated with pDC cells (R = -0.287, P < 0.001) and B cells (-0.266, P < 0.001) (Figure 5B). In addition, immune cell infiltration analysis based on the ssGSEA algorithm also showed that the TEAD1 low expression group had higher B cell enrichment scores, DC cell enrichment scores, and T cell enrichment scores, while higher T helper cell enrichment scores and Tcm enrichment scores were observed in the TEAD1 high expression group (Figure 5C). In addition, we analyzed the anti-cancer immune status of the TEAD1 high and low expression groups at seven different stages of the tumor immune cycle (Figure 5D). We observed that the activity of most steps in the TEAD1 high expression group was downregulated, including priming and activation (step 3), immune cell infiltration into tumors (step 5), and immune cell trafficking to tumors (step 4) (T cell recruitment, dendritic cell recruitment, macrophage recruitment, eosinophil recruitment, B cell recruitment, Th2 cell recruitment, Treg cell recruitment). The downregulation of the activity of these steps may reduce the infiltration level of effector immune cells. It is worth noting that the TEAD1 low expression group has higher infiltration of immune cells into tumors and killing of cancer cells activity. Correlation analysis showed that TEAD1 was significantly positively correlated with multiple immune checkpoints in LIHC,

including CD274, D86, and CD276 (Figure 5E). Immunotherapy analysis showed that patients with lower TEAD1 expression in LIHC benefited more from PD1 therapy (Figure 5F).

3.5 Functional enrichment analysis of TEAD1 and construction of a prognostic model based on disulfidptosis in LIHC

To explore the potential molecular mechanism of TEAD1 in LIHC, we first grouped LIHC samples according to the median expression value of TEAD1 and performed differential analysis. A total of 270 upregulated genes and 12 downregulated genes were identified (Figure 6A). We selected 270 upregulated genes for GO and KEGG enrichment analysis. The results showed that GO-BP functional enrichment analysis showed that differentially expressed genes were mainly significantly enriched in pathways such as histone modification, cell-matrix adhesion, positive regulation of the cell cycle, and regulation of the Wnt signaling pathway. For GO-CC, differentially expressed genes were mainly enriched in spindles, cell-cell junctions, and cell leading edges. For GO-MF, differentially expressed genes were mainly enriched in transcriptional co-regulatory activity, small GTPase binding, and Ras GTPase binding (Figure 6B). KEGG enrichment analysis (Figure 6C) showed that differentially expressed genes were mainly enriched in multiple cancer-related sets in human diseases. In addition, significant enrichment of multiple cancer-related pathways such as the PI3K-Akt signaling pathway, ECM-receptor interaction, and TGF-β signaling pathway was observed. Gene set enrichment analysis (GSEA) based on multiple datasets showed that TEAD1 was mainly associated with cell adhesion, organization of the extracellular matrix, signal transduction, neural development and function, and assembly and maintenance of cell junctions and synapses (Figure 6D).

Disulfidptosis is a newly discovered cell death mechanism caused by cytoskeletal collapse caused by disulfide stress. Using the correlation analysis module in GEPIA2 (http://gepia2.cancer-pku.cn/), we observed a significant positive correlation between TEAD1 and disulfidptosis in LIHC (R=0.63, P<0.001) (Figure 6E). In addition, using the ssGSEA algorithm, we calculated the disulfidptosis score of TCGA-LIHC patients, and we observed higher disulfidptosis scores in the TEAD1 high expression group (Figure 6F). In addition, there was a significant positive correlation between TEAD1 and 24 disulfidptosis-related genes in LIHC (Figure 6G). We further constructed a prognostic model for hepatocellular carcinoma using 22 disulfide apoptosis genes that were significantly positively correlated with TEAD1 (Figures 7A, B). The lambda.min of LASSOS cox was 0.0404, and the model formula was Riskscore=(0.1088)*CAPZB+(0.1654)*INF2+(0.1927)*RPN1+(0.1584)*LRPPRC+(0.1401)*OXSM. Survival analysis showed that patients in the high riskScore group had a shorter survival time, and the AUCs of the model predicting 1-, 2-, and 3-year survival rates were 0.723, 0.643, and 0.660, respectively (Figures 7C–E), indicating that the model has good predictive performance. In addition, we used the liver cancer dataset of ICGC to validate our model, and the results showed that the high riskScore group had a poor prognosis. The AUCs of this model for predicting the 1-year, 2-year, and 3-year survival rates of ICGC liver cancer patients were 0.688, 0.639, and 0.639, respectively (Figures 7F–H), which showed good predictive performance. In addition, the results of univariate and multivariate Cox regression analysis showed that this prediction model was an independent prognostic factor for LIHC (Figure 7I).

3.6 TEAD1 regulates LIHC cell proliferation and cell cycle

Functional enrichment analysis based on GSVA and GSEA showed that TEAD1 was significantly positively correlated with cell cycle and cell proliferation in LIHC (Figures 8A, B). To further verify this result, we selected HepG2 and Huh-7 cell lines for cell function experiments. As shown in Figure 8C, the mRNA expression and protein expression of TEAD1 were significantly knocked down in both cells after siRNA transfection. Correlation analysis based on TCGA-LIHC showed that TEAD1 was positively correlated with cell cycle-related genes, including CDK2 (r = 0.57), CDK4 (r = 0.30), CDK6 (r = 0.33), and CCNE2 (r = 0.41) (Figure 8D). Western blot analysis showed that after knocking down TEAD1, the expression of CCND1 and CDK4 was significantly reduced, while the expression of CDKN1A was significantly increased (Figure 8E). Furthermore, we examined the effect of TEAD1 knockdown on the cell cycle and observed G0/G1 phase arrest in both cell lines (Figures 8F, G). In addition, CCK-8 assay showed that after TEAD1 knockdown, cell proliferation ability was significantly reduced (Figure 8H).

3.7 TEAD1 affects the migration and invasion in LIHC

GSVA and GSEA analysis showed that TEAD1 was significantly correlated with the epithelial-mesenchymal transition (EMT) and invasion pathways of LIHC (Figures 9A, B). It is well known that the programmed activation of EMT is involved in the metastasis of epithelial malignant tumor cells (21). The relationship between TEAD1 expression and tumor metastasis was further verified. The results of Transwell migration assay and matrigel invasion assay (Figures 9C–F) confirmed that reducing TEAD1 expression could inhibit the migration and invasion of LIHC cells. Correlation analysis based on TCGA-LIHC showed that TEAD1 was positively correlated with EMT proteins, including CDH2 (r=0.57), VIM (r=0.28), CLDN1 (r=0.51), and TJP1 (r=0.69) (Figure 9G). Interestingly, western blot results showed that low expression of TEAD1 was accompanied by an increase in CDH1 and a decrease in the expression levels of VIM and CDH2 (Figure 9H).

4 Discussion

LIHC is a highly aggressive malignancy characterized by metabolic heterogeneity (22). Despite the implementation of

10.3389/fimmu.2025.1567969

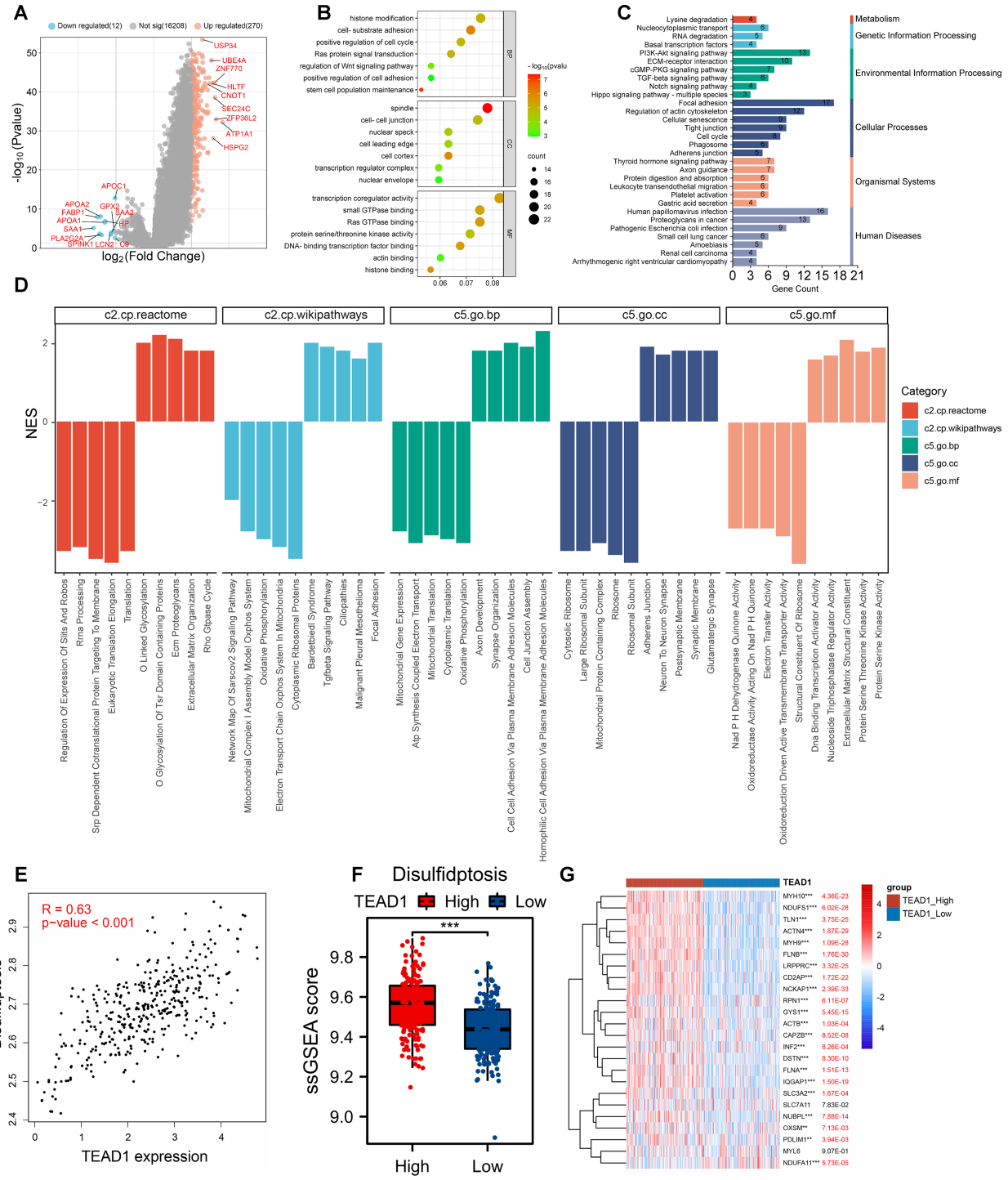

FIGURE 6
Functional enrichment analysis of TEAD1 in hepatocellular carcinoma. **(A)** Volcano map of differential genes in TEAD1 high and low expression groups. **(B, C)** GO and KEGG functional enrichment analysis. **(D)** GSEA enrichment analysis. **(E)** Correlation between TEAD1 and disulfidptosis in LIHC. **(F)** The disulfidptosis score of LIHC patients were evaluated based on ssGESA in high- and low-TEAD1 groups. **(G)** Correlation between TEAD1 and disulfidptosis -related genes in LIHC. **p < 0.01; ***p < 0.001.

multidisciplinary diagnostic and therapeutic strategies, including surgical resection, radical hepatectomy, targeted therapies, and immunotherapies, the overall survival (OS) rates for patients with advanced LIHC remain disappointingly low (23, 24). Consequently, there is an urgent need for innovative biomarkers that can predict prognosis, facilitate risk stratification, and identify therapeutic targets for individuals diagnosed with LIHC. TEAD1/Tef-1, encoded by TEAD1 gene, has garnered extensive attention due to its critical role in multiple cancers (25–27). Previous studies have demonstrated that TEAD1 can function as either a promoter or a

10.3389/fimmu.2025.1567969

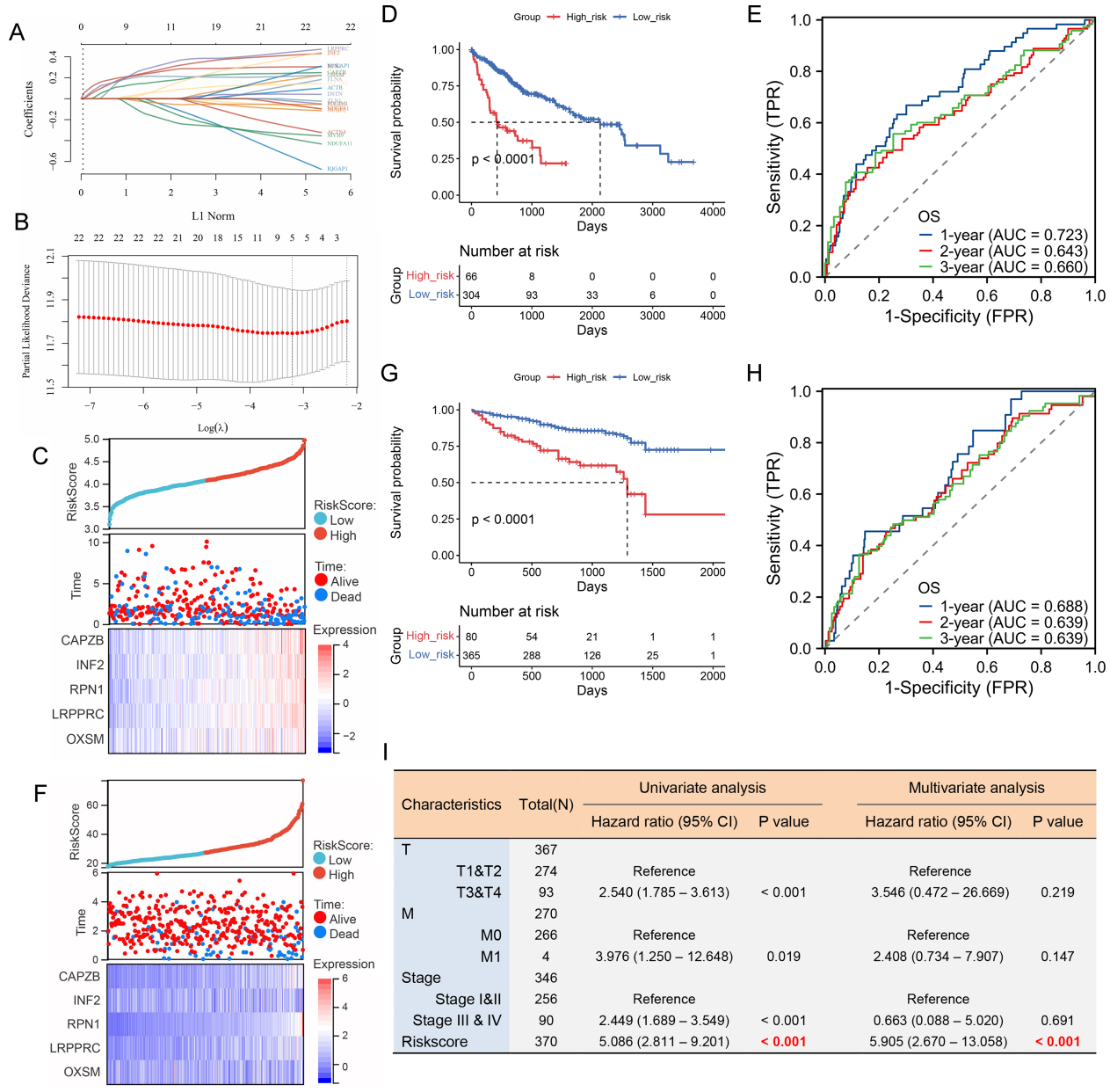

I

Characteristics	Total(N)	Univariate analysis		Multivariate analysis	
		Hazard ratio (95% CI)	P value	Hazard ratio (95% CI)	P value
T	367				
T1&T2	274	Reference		Reference	
T3&T4	93	2.540 (1.785 – 3.613)	< 0.001	3.546 (0.472 – 26.669)	0.219
M	270				
M0	266	Reference		Reference	
M1	4	3.976 (1.250 – 12.648)	0.019	2.408 (0.734 – 7.907)	0.147
Stage	346				
Stage I&II	256	Reference		Reference	
Stage III & IV	90	2.449 (1.689 – 3.549)	< 0.001	0.663 (0.088 – 5.020)	0.691
Riskscore	370	5.086 (2.811 – 9.201)	**< 0.001**	5.905 (2.670 – 13.058)	**< 0.001**

FIGURE 7
A LIHC prognostic model was constructed using 22 disulfidptosis-related genes that were significantly correlated with TEAD1. **(A)** LASSO coefficient profiles for 22 disulfidptosis -related genes in the TCGA cohort. **(B)** Partial likelihood deviations were plotted versus log(λ) using a LASSO Cox regression model. **(C–E)** Risk factor heat map, survival analysis and ROC analysis of prognostic model in TCGA dataset. **(F–H)** Risk factor heat map, survival analysis and ROC analysis of prognostic model in ICGC dataset. **(I)** The univariate and multivariate Cox regression analysis showed that this prediction model was an independent prognostic factor for LIHC.

suppressor of tumorigenesis, depending on the specific cancer context (28–30). Therefore, a deeper comprehension of the mechanisms through which TEAD1 participates in oncogenesis is highly desirable. This study thoroughly investigates the multifaceted roles of the TEAD1 gene in cancer biology, particularly in LIHC. Our results indicate that TEAD1expression levels vary significantly across different cancer types. Furthermore, we found that TEAD1 expression was closely associated with clinical outcomes across multiple cancers; these findings are consistent with existing literature. In addition, our study also found that the epigenetic changes of TEAD1 are highly heterogeneous in multiple cancers, and its abnormal methylation and CNV are associated with poor prognosis in multiple cancers. This finding emphasizes the importance of epigenetics in TEAD1 regulation and may provide new targets for personalized treatment of cancer.

In LIHC, the significant correlation between TEAD1and malignant cells highlights the multifaceted roles that TEAD1 may play in hepatocellular carcinoma, including its potential as both a biomarker and therapeutic target. The tumor immune microenvironment is intricately linked to the initiation and

10.3389/fimmu.2025.1567969

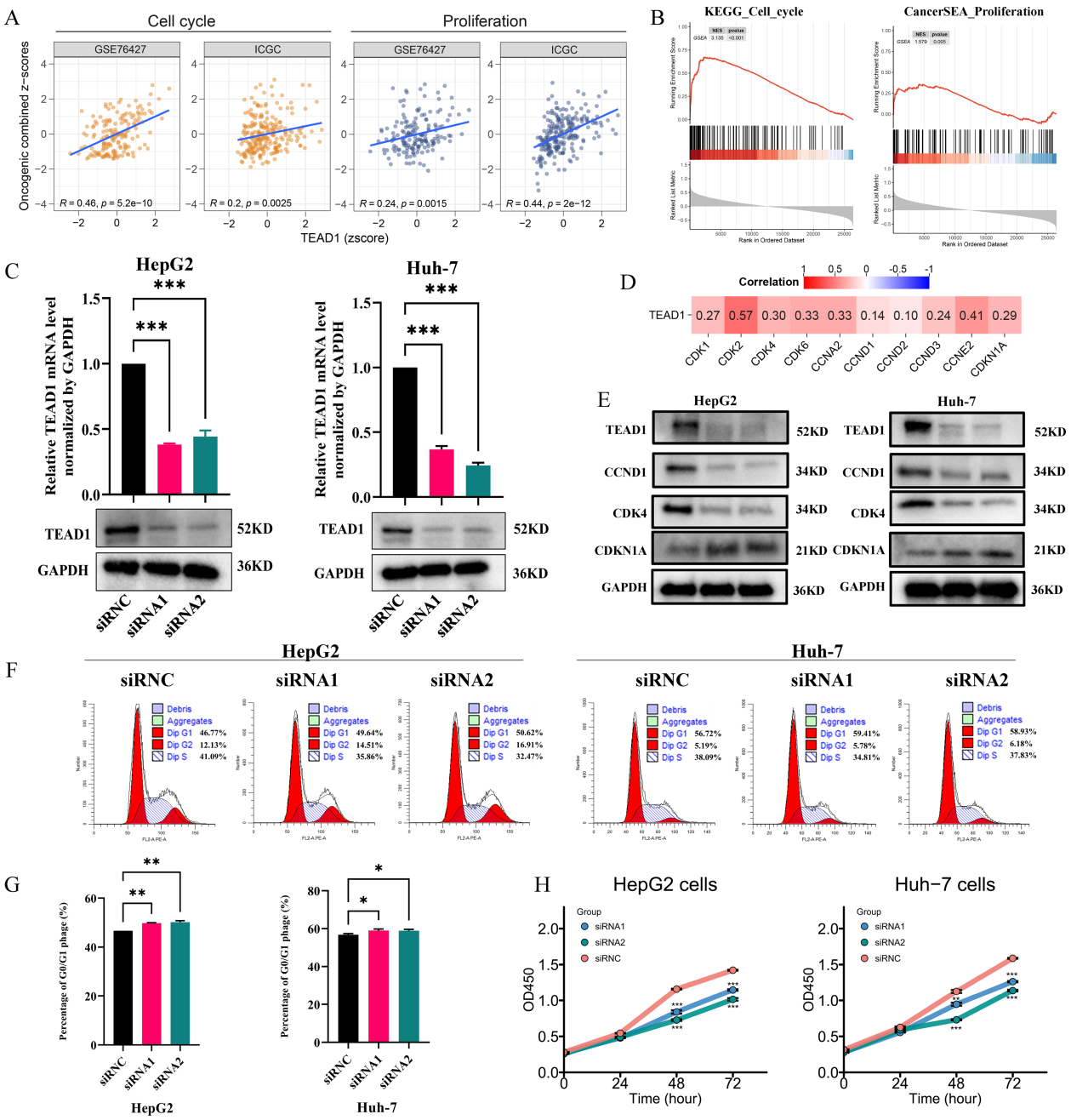

FIGURE 8
TEAD1 regulates LIHC cell proliferation and cell cycle. **(A, B)** Functional enrichment analysis based on GSVA and GSEA. **(C)** After HepG2 and Huh-7 cells were transfected with siRNA1/2 or scrambled control (siRNC), mRNA and protein of TEAD1 was detected. **(D)** Heatmap of the correlation between TEAD1 expression and cell cycle related genes. **(E)** The protein level of cell cycle related genes with/without TEAD1 knockdown in HepG2 and Huh-7 cells. **(F, G)** Flow cytometry detected the cell cycle distribution in HepG2 and Huh-7 cells. **(H)** CCK-8 assay with/without TEAD1 depletion in HepG2 and Huh-7 cells. The data are presented as the mean ± SD. from three independent experiments. ***P < 0.001, **P < 0.01, *P < 0.05.

progression of tumors (31, 32). We found that the expression of TEAD1 in LIHC was significantly negatively correlated with the immune score, suggesting its critical role in suppressing tumor immune responses. In addition, TEAD1 was associated with the infiltration level of specific subsets of immune cell, thereby influencing the composition of the tumor microenvironment. We observed that the high TEAD1 expression group exhibited active downregulation at multiple stages of the tumor immune cycle, which may lead to reduce the infiltration levels of effector immune cells. Notably, there was a positively correlation between TEAD1 and multiple immune checkpoints, patients with low expressions of TEAD1 appeared to benefit more from PD1 treatment. This indicates that the level of TEAD1 expression could serve as a predictive biomarker for immunotherapy response. These findings elucidate the potential role of TEAD1 in modulating both the LIHC immune microenvironment and responses to

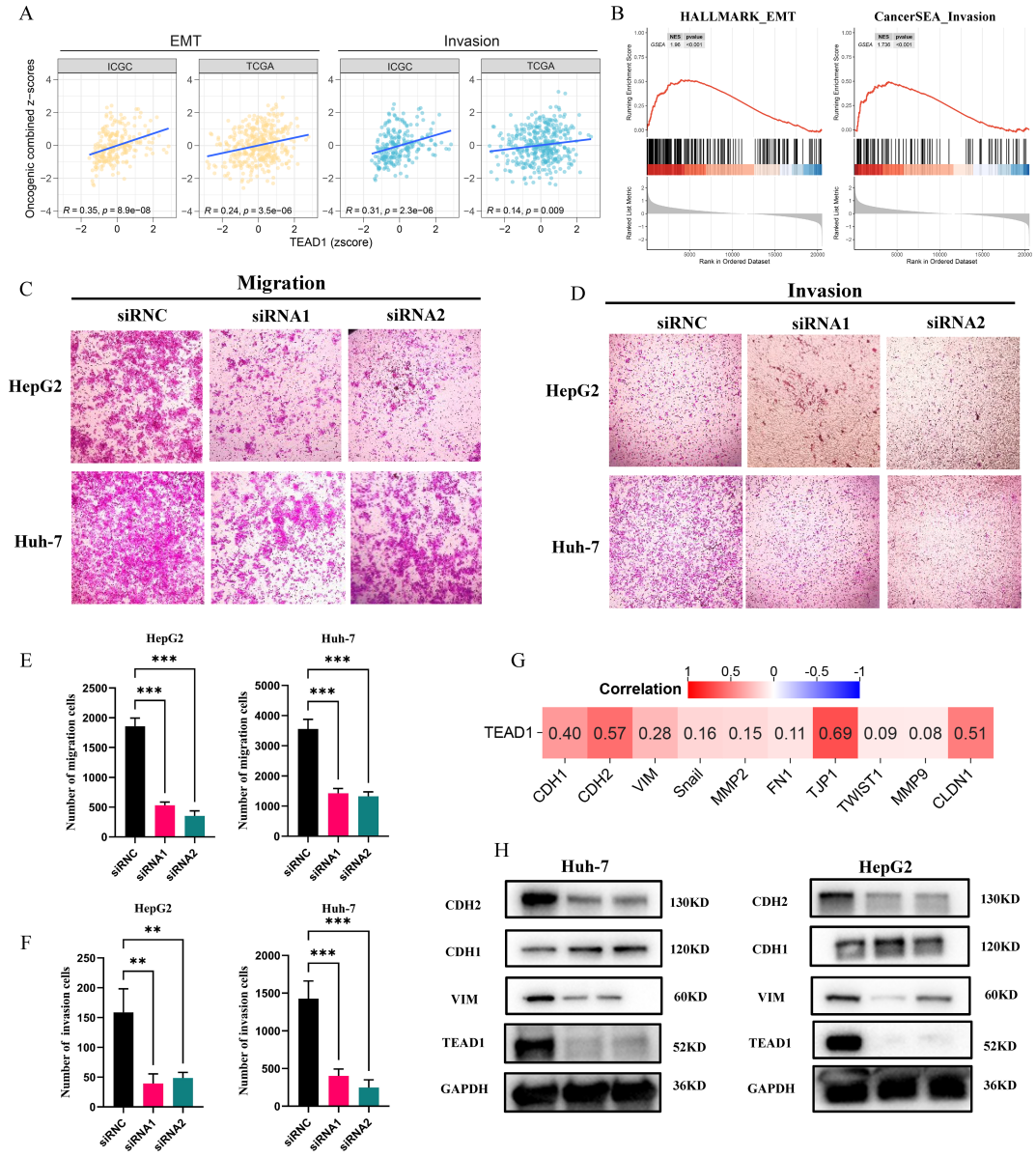

FIGURE 9
TEAD1 affects the migration and invasion in LIHC. **(A, B)** Functional enrichment analysis based on GSVA and GSEA. **(C–F)** Transwell assay was conducted used for HepG2 and Huh-7cell migration and invasion. **(G)** Heatmap of the correlation between TEAD1 expression and EMT and invasion related genes. **(H)** The protein level of EMT related genes with/without TEAD1 knockdown in HepG2 and Huh-7 cells. The data are presented as the mean ± SD. from three independent experiments. ***P < 0.001, **P < 0.01, *P < 0.05.

immunotherapy. They also provide new avenues for future research aimed at gaining deeper insights into the mechanisms by which TEAD1 operates in LIHC and developing novel therapeutic strategies.

The TEAD family of transcription factors, which are evolutionarily conserved across species, exhibit minimal intrinsic transcriptional activity and require the presence of coactivators to effectively induce target genes (33–35). YAP/TAZ, as core downstream components of the Hippo pathway, have emerged as the most well-established activators of TEAD (36, 37). The YAP/TAZ-TEAD complex has been identified as a significant driver in cancer progression, influencing tumorigenesis, growth, EM, metastasis, and drug resistance (38–42). In this study, we found that TEAD1 was significantly correlated with the expression of genes involved in the cell regulation, cell proliferation, EMT processes, and invasion pathways through functional enrichment analysis. Furthermore, our experimental results demonstrated that knockdown of TEAD1 led to a reduction in the proliferation, migration, and invasion capabilities of LIHC cells. Interestingly, In contrast to correlation analysis based on TCGA-LIHC, western blot results showed that low expression of TEAD1 was accompanied by an increase in CDH1. This discrepancy may reflect post-translational modifications influenced by TEAD1, warranting further investigation into its role in protein regulation.

We further developed a prognostic model incorporating disulfidptosis-related genes, which demonstrated robust predictive performance in LIHC patients. Unlike network-based approaches such as mRank that identify biomarker modules within gene regulatory networks (43), our lasso-Cox-based model (44, 45) uniquely integrates the novel cell death mechanism of disulfidptosis with TEAD1 activity, providing mechanistic insights into HCC prognosis. This model not only offers a clinically relevant prognostic tool but also suggests new avenues for understanding TEAD1's functional mechanisms in LIHC.

Several limitations of our study should be noted. First, while our *in vitro* findings are compelling, they require validation in animal models and clinical samples to establish translational relevance. Second, the precise mechanisms underlying TEAD1's apparent regulation of CDH1 and its potential role in post-translational modifications remain to be elucidated. Third, although we observed associations between TEAD1 and the tumor immune microenvironment, the specific immunomodulatory mechanisms merit further investigation. Finally, while our prognostic model shows promise, its generalizability across diverse patient populations and disease stages requires additional validation through multicenter studies and multi-omics integration (e.g., incorporating methylation and proteomic data).

5 Conclusions

In summary, our study not only elucidates the multifaceted roles of TEAD1 in LIHC but also offers new avenues for future research. Subsequent investigations should concentrate on the molecular mechanisms underlying TEAD1`s function, its potential in the tumor immune microenvironment, and its potential as a therapeutic target. Through these endeavors, we aspire to develop more effective treatment strategies for patients with LIHC.

Data availability statement

The datasets presented in this study are openly available in online repositories. Detailed information, including repository names and accession numbers, is provided within the article and/or Supplementary Material.

Author contributions

LX: Conceptualization, Formal Analysis, Funding acquisition, Methodology, Project administration, Supervision, Writing – review & editing. RH: Data curation, Formal Analysis, Investigation, Software, Visualization, Writing – original draft. CM: Conceptualization, Resources, Supervision, Writing – review & editing.

Funding

The author(s) declare that financial support was received for the research and/or publication of this article. This work was supported by Department of Science and Technology of Sichuan Province (Grant No.18YYJC0551) and Fundamental Research Funds for the Central Universities of China (Grant No. 2682020ZT112).

Conflict of interest

The authors declare that the research was conducted in the absence of any commercial or financial relationships that could be construed as a potential conflict of interest.

Generative AI statement

The author(s) declare that no Generative AI was used in the creation of this manuscript.

Publisher's note

Supplementary material

The Supplementary Material for this article can be found online at: https://www.frontiersin.org/articles/10.3389/fimmu.2025.1567969/full#supplementary-material

SUPPLEMENTARY FIGURE 1
(A–L) Correlation between TEAD1 expression and clinical stages. **(M)** Forest plots show univariable Cox regression analysis for OS, DSS, DFI and PFI of TEAD1 expression in 33 TCGA cancer types.

References

1. Sung H, Ferlay J, Siegel RL, Laversanne M, Soerjomataram I, Jemal A, et al. Global cancer statistics 2020: GLOBOCAN estimates of incidence and mortality worldwide for 36 cancers in 185 countries. *CA Cancer J Clin*. (2021) 71:209–49. doi: 10.3322/caac.21660

2. Farvardin S, Patel J, Khambaty M, Yerokun OA, Mok H, Tiro JA, et al. Patient-reported barriers are associated with lower hepatocellular carcinoma surveillance rates in patients with cirrhosis. *Hepatology*. (2017) 65:875–84. doi: 10.1002/hep.28770

3. Azakie A, Larkin SB, Farrance IK, Grenningloh G, Ordahl CP. DTEF-1, a novel member of the transcription enhancer factor-1 (TEF-1) multigene family. *J Biol Chem*. (1996) 271:8260–5. doi: 10.1074/jbc.271.14.8260

4. Anbanandam A, Albarado DC, Nguyen CT, Halder G, Gao XL, Veeraraghavan S. Insights into transcription enhancer factor 1 (TEF-1) activity from the solution structure of the TEA domain. *Proc Natl Acad Sci USA*. (2006) 103:17225–30. doi: 10.1073/pnas.0607171103

5. Jacquemin P, Martial JA, Davidson I. Human TEF-5 is preferentially expressed in placenta and binds to multiple functional elements of the human chorionic somatomammotropin-B gene enhancer. *J Biol Chem*. (1997) 272:12928–37. doi: 10.1074/jbc.272.20.12928

6. Jacquemin P, Hwang JJ, Martial JA, Dolle P, Davidson I. A novel family of developmentally regulated mammalian transcription factors containing the TEA/ATTS DNA binding domain. *J Biol Chem*. (1996) 271:21775–85. doi: 10.1074/jbc.271.36.21775

7. Xiao JH, Davidson I, Ferrandon D, Rosales R, Vigneron M, Macchi M, et al. One cell-specific and three ubiquitous nuclear proteins bind *in vitro* to overlapping motifs in the domain B1 of the SV40 enhancer. *EMBO J*. (1987) 6:3005–13. doi: 10.1002/j.1460-2075.1987.tb02606.x

8. Zhou Y, Huang T, Zhang J, Wong CC, Zhang B, Dong Y, et al. TEAD1/4 exerts oncogenic role and is negatively regulated by miR-4269 in gastric tumorigenesis. *Oncogene*. (2017) 36:6518–30. doi: 10.1038/onc.2017.257

9. Chen J, Li L, Feng Y, Zhao Y, Sun F, Zhou X, et al. MKLN1-AS promotes pancreatic cancer progression as a crucial downstream mediator of HIF-1α through miR-185-5p/TEAD1 pathway. *Cell Biol Toxicol*. (2024) 40:30. doi: 10.1007/s10565-024-09863-8

10. Zhang M, Cai F, Guo J, Liu S, Ma G, Cai M, et al. ACAT2 suppresses the ubiquitination of YAP1 to enhance the proliferation and metastasis ability of gastric cancer via the upregulation of SETD7. *Cell Death Dis*. (2024) 15:297. doi: 10.1038/s41419-024-06666-x

11. Vivian J, Rao AA, Nothaft FA, Ketchum C, Armstrong J, Novak A, et al. Toil enables reproducible, open source, big biomedical data analyses. *Nat Biotechnol*. (2017) 35:314–6. doi: 10.1038/nbt.3772

12. Yoshihara K, Shahmoradgoli M, Martínez E, Vegesna R, Kim H, Torres-Garcia W, et al. Inferring tumour purity and stromal and immune cell admixture from expression data. *Nat Commun*. (2013) 4:2612. doi: 10.1038/ncomms3612

13. Aran D, Hu Z, Butte AJ. xCell: digitally portraying the tissue cellular heterogeneity landscape. *Genome Biol*. (2017) 18:220. doi: 10.1186/s13059-017-1349-1

14. Barbie DA, Tamayo P, Boehm JS, Kim SY, Moody SE, Dunn IF, et al. Systematic RNA interference reveals that oncogenic KRAS-driven cancers require TBK1. *Nature*. (2009) 462:108–12. doi: 10.1038/nature08460

15. Becht E, Giraldo NA, Lacroix L, Buttard B, Elarouci N, Petitprez F, et al. Estimating the population abundance of tissue-infiltrating immune and stromal cell populations using gene expression. *Genome Biol*. (2016) 17:218. doi: 10.1186/s13059-016-1070-5

16. Charoentong P, Finotello F, Angelova M, Mayer C, Efremova M, Rieder D, et al. Pan-cancer immunogenomic analyses reveal genotype-immunophenotype relationships and predictors of response to checkpoint blockade. *Cell Rep*. (2017) 18:248–62. doi: 10.1016/j.celrep.2016.12.019

17. Xu L, Deng C, Pang B, Zhang X, Liu W, Liao G, et al. TIP: A web server for resolving tumor immunophenotype profiling. *Cancer Res*. (2018) 78:6575–80. doi: 10.1158/0008-5472.CAN-18-0689

18. Han Y, Wang Y, Dong X, Sun D, Liu Z, Yue J, et al. TISCH2: expanded datasets and new tools for single-cell transcriptome analyses of the tumor microenvironment. *Nucleic Acids Res*. (2023) 51:D1425–31. doi: 10.1093/nar/gkac959

19. Xun Z, Ding X, Zhang Y, Zhang B, Lai S, Zou D, et al. Reconstruction of the tumor spatial microenvironment along the Malignant-boundary-nonmalignant axis. *Nat Commun*. (2023) 14:933. doi: 10.1038/s41467-023-36560-7

20. Xu K, Zhang Y, Yan Z, Wang Y, Li Y, Qiu Q, et al. Identification of disulfidptosis related subtypes, characterization of tumor microenvironment infiltration, and development of DRG prognostic prediction model in RCC, in which MSH3 is a key gene during disulfidptosis. *Front Immunol*. (2023) 14:1205250. doi: 10.3389/fimmu.2023.1205250

21. Bakir B, Chiarella AM, Pitarresi JR, Rustgi AK. EMT, MET, plasticity, and tumor metastasis. *Trends Cell Biol*. (2020) 30:764–76. doi: 10.1016/j.tcb.2020.07.003

22. Llovet JM, Kelley RK, Villanueva A, Singal AG, Pikarsky E, Roayaie S, et al. Hepatocellular carcinoma. *Nat Rev Dis Primers*. (2021) 7:6. doi: 10.1038/s41572-021-00245-6

23. Reig M, Forner A, Rimola J, Ferrer-Fabrega J, Burrel M, Garcia-Criado Á, et al. BCLC strategy for prognosis prediction and treatment recommendation: The 2022 update. *J Hepatol*. (2022) 76:681–93. doi: 10.1016/j.jhep.2021.11.018

24. Vogel A, Meyer T, Sapisochin G, Salem R, Saborowski A. Hepatocellular carcinoma. *Lancet*. (2022) 400:1345–62. doi: 10.1016/S0140-6736(22)01200-4

25. Lou J, Lu Y, Cheng J, Zhou F, Yan Z, Zhang D, et al. A chemical perspective on the modulation of TEAD transcriptional activities: Recent progress, challenges, and opportunities. *Eur J Med Chem*. (2022) 243:114684. doi: 10.1016/j.ejmech.2022.114684

26. Huh HD, Kim DH, Jeong HS, Park HW. Regulation of TEAD transcription factors in cancer biology. *Cells*. (2019) 8:600. doi: 10.3390/cells8060600

27. Heng BC, Zhang X, Aubel D, Bai Y, Li X, Wei Y, et al. An overview of signaling pathways regulating YAP/TAZ activity. *Cell Mol Life Sci*. (2021) 78:497–512. doi: 10.1007/s00018-020-03579-8

28. Li N, Yang G, Luo L, Ling L, Wang X, Shi L, et al. lncRNA THAP9-AS1 Promotes Pancreatic Ductal Adenocarcinoma Growth and Leads to a Poor Clinical Outcome via Sponging miR-484 and Interacting with YAP. *Clin Cancer Res*. (2020) 26:1736–48. doi: 10.1158/1078-0432.CCR-19-0674

29. Li F, Negi V, Yang P, Lee J, Ma K, Moulik M, et al. TEAD1 regulates cell proliferation through a pocket-independent transcription repression mechanism. *Nucleic Acids Res*. (2022) 50:12723–38. doi: 10.1093/nar/gkac1063

30. Cruz SP, Zhang Q, Devarajan R, Paia C, Luo B, Zhang K, et al. Dampened regulatory circuitry of TEAD1/ITGA1/ITGA2 promotes TGFβ1 signaling to orchestrate prostate cancer progression. *Adv Sci*. (2024) 11:e2305547. doi: 10.1002/advs.202305547

31. Lu C, Liu Y, Ali NM, Zhang B, Cui X. The role of innate immune cells in the tumor microenvironment and research progress in anti-tumor therapy. *Front Immunol*. (2023) 13:1039260. doi: 10.3389/fimmu.2022.1039260

32. Du Q, An Q, Zhang J, Liu C, Hu Q. Unravelling immune microenvironment features underlying tumor progression in the single-cell era. *Cancer Cell Int*. (2024) 24:143. doi: 10.1186/s12935-024-03335-z

33. Currey L, Thor S, Piper M. TEAD family transcription factors in development and disease. *Development*. (2021) 148:dev196675. doi: 10.1242/dev.196675

34. Lin KC, Park HW, Guan KL. Regulation of the hippo pathway transcription factor TEAD. *Trends Biochem Sci*. (2017) 42:862–72. doi: 10.1016/j.tibs.2017.09.003

35. Xiao JH, Davidson I, Matthes H, Garnier JM, Chambon P. Cloning, expression, and transcriptional properties of the human enhancer factor TEF-1. *Cell*. (1991) 65:551–68. doi: 10.1016/0092-8674(91)90088-g

36. Mahoney WM Jr, Hong JH, Yaffe MB, Farrance IK. The transcriptional co-activator TAZ interacts differentially with transcriptional enhancer factor-1 (TEF-1) family members. *Biochem J*. (2005) 388:217–25. doi: 10.1042/BJ20041434

37. Seo E, Basu-Roy U, Gunaratne PH, Coarfa C, Lim DS, Basilico C, et al. SOX2 regulates YAP1 to maintain stemness and determine cell fate in the osteo-adipo lineage. *Cell Rep*. (2013) 3:2075–87. doi: 10.1016/j.celrep.2013.05.029

38. Zhang H, Liu CY, Zha ZY, Zhao B, Yao J, Zhao SM, et al. TEAD transcription factors mediate the function of TAZ in cell growth and epithelial-mesenchymal transition. *J Biol Chem*. (2009) 284:13355–62. doi: 10.1074/jbc.M900843200

39. Zhao B, Ye X, Yu J, Li L, Li W, Li S, et al. TEAD mediates YAP-dependent gene induction and growth control. *Gene Dev*. (2008) 22:1962–71. doi: 10.1101/gad.1664408

40. Overholtzer M, Zhang J, Smolen GA, Muir B, Li W, Sgroi DC, et al. Transforming properties of YAP, a candidate oncogene on the chromosome 11q22 amplicon. *Proc Natl Acad Sci USA*. (2006) 103:12405–10. doi: 10.1073/pnas.0605579103

41. Lei QY, Zhang H, Zhao B, Zha ZY, Bai F, Pei XH, et al. TAZ promotes cell proliferation and epithelial-mesenchymal transition and is inhibited by the hippo pathway. *Mol Cell Biol*. (2008) 28:2426–36. doi: 10.1128/MCB.01874-07

42. Lamar JM, Stern P, Liu H, Schindler JW, Jiang ZG, Hynes RO. The Hippo pathway target, YAP, promotes metastasis through its TEAD-interaction domain. *Proc Natl Acad Sci USA*. (2012) 109:E2441–50. doi: 10.1073/pnas.1212021109

43. Shang H, Liu ZP. Network-based prioritization of cancer biomarkers by phenotype-driven module detection and ranking. *Comput Struct Biotechnol J*. (2021) 20:206–17. doi: 10.1016/j.csbj.2021.12.005

44. Zhengdong A, Xiaoying X, Shuhui F, Rui L, Zehui T, Guanbin S, et al. Identification of fatty acids synthesis and metabolism-related gene signature and prediction of prognostic model in hepatocellular carcinoma. *Cancer Cell Int*. (2024) 24:130. doi: 10.1186/s12935-024-03306-4

45. Zhuo W, Xia H, Lan B, Chen Y, Wang X, Liu J. Signature of immune-related metabolic genes predicts the prognosis of hepatocellular carcinoma. *Front Immunol*. (2024) 15:1481331. doi: 10.3389/fimmu.2024.1481331

frontiers | Frontiers in Immunology

TYPE Review
PUBLISHED 20 June 2025
DOI 10.3389/fimmu.2025.1533874

OPEN ACCESS

EDITED BY
Hongwei Cheng,
University of Macau, China

REVIEWED BY
Mohammad Imran K. Khan,
Columbia University, United States
Dmitry Aleksandrovich Zinovkin,
Gomel State Medical University, Belarus

*CORRESPONDENCE
Sherif A. El-Kafrawy
saelkfrawy@kau.edu.sa
Ashraf A. Tabll
aa.tabll@nrc.sci.eg

RECEIVED 25 November 2024
ACCEPTED 04 June 2025
PUBLISHED 20 June 2025

CITATION
El-Kafrawy SA, Elkafrawy MS, Azhar EI, Saeed A and Tabll AA (2025) Antibody treatment of hepatocellular carcinoma: a review of current and emerging approaches. *Front. Immunol.* 16:1533874. doi: 10.3389/fimmu.2025.1533874

Antibody treatment of hepatocellular carcinoma: a review of current and emerging approaches

Sherif A. El-Kafrawy[1,2*], Mostafa S. Elkafrawy[3], Esam I. Azhar[1,2], Anwaar Saeed[4] and Ashraf A. Tabll[5,6*]

[1]Special Infectious Agents Unit- BioSafety Level 3 (BSL3), King Fahd Medical Research Center, King Abdulaziz University, Jeddah, Saudi Arabia, [2]Department of Medical Laboratory Sciences, Faculty of Applied Medical Sciences, King Abdulaziz University, Jeddah, Saudi Arabia, [3]Faculty of Medicine, Menoufia University, Shebin El-Koam, Egypt, [4]Department of Medicine, Division of Hematology & Oncology, University of Pittsburgh Medical Center, Pittsburgh, PA, United States, [5]Immunology Department, Egypt Center for Research and Regenerative Medicine (ECRRM), Cairo, Egypt, [6]Microbial Biotechnology Department, Biotechnology Research Institute, National Research Centre, Giza, Egypt

Hepatocellular carcinoma (HCC) remains a leading cause of cancer-related deaths worldwide, underscoring the urgent need for innovative therapeutic strategies. Antibody-based therapies have emerged as a transformative approach, offering specificity and the potential to overcome the limitations of traditional treatments. This comprehensive review evaluates the current and emerging applications of antibody therapies in HCC, including monoclonal antibodies (mAbs), bispecific antibodies, and antibody-drug conjugates (ADCs). It explores their mechanisms of action, such as immune modulation, angiogenesis inhibition, and targeted cytotoxicity. Key advancements include the integration of immune checkpoint inhibitors (ICIs) like PD-1/PD-L1 and CTLA-4 inhibitors into clinical practice and the development of bispecific antibodies and ADCs targeting tumor-specific antigens like glypican-3. While these therapies have shown promise in improving patient outcomes, challenges such as tumor heterogeneity, resistance mechanisms, and immune-related adverse events persist. This review highlights recent clinical trial data, identifies areas for future research, and emphasizes the potential of combining antibody therapies with other modalities to enhance efficacy and overcome therapeutic barriers. By addressing these challenges and leveraging advancements in antibody engineering and biomarker discovery, antibody-based therapies hold significant promise for revolutionizing the treatment paradigm for HCC.

KEYWORDS

HCC, antibody therapy, monoclonal antibodies, bispecific antibodies, antibody-drug conjugates, immune checkpoints inhibitors

1 Overview of hepatocellular carcinoma

1.1 Epidemiology of HCC

HCC is the most common primary liver cancer, accounting for approximately 75-85% of all liver cancer cases. It is a major global health problem, with significant geographical variation in incidence rates due to differences in underlying risk factors and healthcare practices. HCC is the sixth most common cancer worldwide and the third leading cause of cancer-related deaths. In 2020, it was estimated that there were over 900,000 new cases and more than 830,000 deaths attributable to liver cancer globally (1). The highest incidence rates are found in East Asia and sub-Saharan Africa, with intermediate rates in Southern Europe and low rates in North America and Northern Europe (2).

East Asia Countries like China, Japan, and Korea have the highest incidence rates of HCC. In China alone, over 50% of the world's HCC cases occur, largely due to the high prevalence of chronic hepatitis B virus (HBV) infection (3). Similar to East Asia, the high incidence in Sub-Saharan Africa is also linked to chronic HBV infection, which is often acquired perinatally or in early childhood (4). On the other hand, the incidence of HCC has been rising in Europe and North America, partly due to the increasing prevalence of hepatitis C virus (HCV) infection and metabolic dysfunction-associated steatotic liver disease (MASLD) (2).

Chronic HBV and HCV infections are the primary risk factors for HCC, responsible for about 80% of all cases globally (5). Regardless of the underlying cause, cirrhosis significantly increases the risk of developing HCC. Cirrhosis is most commonly caused by chronic viral hepatitis, alcoholic liver disease, and MASLD. Heavy alcohol consumption is a major risk factor, contributing to the development of cirrhosis and subsequently HCC (6). In some regions, such as sub-Saharan Africa and Southeast Asia, exposure to aflatoxin B1, a toxin produced by certain fungi in improperly stored grains and nuts, is a significant risk factor (7). Metabolic Disorders like obesity, diabetes, and MASLD are increasingly recognized as important risk factors, particularly in Western countries (8).

The global burden of HCC is expected to increase in the coming decades due to the aging population, the ongoing epidemic of metabolic risk factors, and variations in the success of HBV vaccination and HCV antiviral treatments. Efforts to control HCC must focus on prevention, early detection, and effective treatment of underlying liver diseases (9).

2 Drawbacks of traditional therapies

Traditional therapies for HCC have shown limited efficacy and considerable side effects, necessitating the development of innovative treatment strategies. While surgical resection and liver transplantation are considered potentially curative treatments for HCC, these options are viable only for a small subset of patients with early-stage disease and preserved liver function. Many patients are diagnosed at advanced stages, making them ineligible for surgery. Moreover, the availability of donor organs for transplantation is limited, and there is a risk of tumor recurrence even after surgery (10).

Treatments such as transarterial chemoembolization (TACE), radiofrequency ablation (RFA), and percutaneous ethanol injection (PEI) are commonly used for patients who are not candidates for surgery. While these therapies can control tumor growth and prolong survival, they are rarely curative and often associated with local recurrence (11). Additionally, their effectiveness can be limited in patients with large or multifocal tumors.

Systemic chemotherapy has historically shown limited efficacy in HCC, with low response rates and significant toxicity. The advent of targeted therapies, such as sorafenib and lenvatinib, has improved outcomes to some extent, but their benefits are modest, and they are often associated with adverse effects that can limit their use. Resistance to these therapies also develops over time, reducing their long-term effectiveness (12).

3 Antibody therapy: mechanisms of action in the HCC tumor microenvironment

Antibody-based therapies have transformed cancer treatment, including HCC, by targeting tumor-specific pathways, modulating the immune microenvironment, and delivering cytotoxic agents directly to cancer cells. The efficacy of these therapies is deeply influenced by the HCC TME, which is characterized by immune evasion, angiogenesis, and stromal interactions. Understanding these mechanisms provides insight into the rationale behind combination therapies, particularly those involving Immune-checkpoint Inhibitors (ICIs) and anti-angiogenic agents. The TME-centered approach to antibody therapy in HCC highlights the rationale for combination regimens. By disrupting angiogenesis, restoring immune surveillance, and selectively delivering cytotoxic agents, antibody-based therapies offer multi-faceted strategies to overcome resistance mechanisms in HCC. Future biomarker-driven approaches will further refine patient selection and enhance efficacy.

3.1 Targeting specific antigens in the TME

Monoclonal antibodies (mAbs) exert anti-tumor effects by selectively binding tumor-associated antigens, disrupting key oncogenic pathways, and engaging immune effector cells.

3.1.1 Anti-VEGF therapy and its role in HCC

Vascular endothelial growth factor (VEGF) is a key driver of angiogenesis in the HCC TME, promoting neovascularization, immune suppression, and tumor progression. Bevacizumab, an anti-VEGF monoclonal antibody, inhibits VEGF-A, leading to vascular normalization, improved immune infiltration, and reduced tumor hypoxia (13). Anti-VEGF therapy complements

ICIs such as atezolizumab, nivolumab, and pembrolizumab. By enhancing T-cell infiltration, VEGF-induced abnormal vasculature limits immune cell access to the tumor. Bevacizumab normalizes blood vessels, allowing better T-cell penetration (14).

Anti-VEGF antibodies like bevacizumab enhance the effectiveness of PD-1/PD-L1 inhibitors in hepatocellular carcinoma (HCC) through multiple mechanisms. By inhibiting angiogenesis, bevacizumab limits the formation of tumor-associated blood vessels, thereby increasing T-cell infiltration while reducing the presence of immunosuppressive cells within the TME (15, 16). This shift fosters conditions that promote immune activation and improve the response to PD-1/PD-L1 blockade (17). Additionally, bevacizumab contributes to vascular normalization, which optimizes oxygenation and facilitates the efficient delivery of therapeutic agents, further enhancing immune responses (18). Moreover, by alleviating tumor hypoxia, it influences PD-L1 expression, creating a more pro-inflammatory environment that makes tumor cells more vulnerable to immune-mediated destruction (19). These combined effects support the rationale for using anti-VEGF antibodies alongside PD-1/PD-L1 inhibitors to improve treatment outcomes in HCC.

3.1.2 Antibody-dependent cellular cytotoxicity

Monoclonal antibodies can engage innate immune responses through Fcγ receptor (FcγR)-mediated ADCC, in which antibody-coated tumor cells are recognized and destroyed by natural killer (NK) cells and macrophages (20). For example, anti-GPC3 antibodies, which target glypican-3 (GPC3), a cell surface glycoprotein overexpressed in HCC, can induce ADCC, leading to tumor cell lysis (21).

3.2 Immune modulation and checkpoint blockade in HCC

HCC tumors create an immunosuppressive microenvironment dominated by exhausted T cells, myeloid-derived suppressor cells (MDSCs), and Tregs, which collectively inhibit anti-tumor immunity (22).

3.2.1 PD-1/PD-L1 axis: reversing t-cell exhaustion

PD-1 (on T cells) binds PD-L1 (on tumor or immune cells), suppressing T-cell activation and proliferation. Nivolumab and pembrolizumab restore T-cell function by blocking PD-1/PD-L1 interaction, reinvigorating exhausted CD8+ T cells (17). CTLA-4 blockade (e.g., Ipilimumab, Tremelimumab) acts earlier in the immune response by expanding effector T cells and reducing regulatory T cells (Tregs) (23). PD-1 blockade acts later, preventing T-cell exhaustion within the TME. CTLA-4 blockade enhances priming and expansion of tumor-reactive T cells. PD-1 blockade sustains the activity of these expanded T cells in the TME. This synergistic mechanism is demonstrated in STRIDE (Tremelimumab + Durvalumab) from the HIMALAYA trial, which showed OS benefit in HCC (24).

Emerging treatment modalities include TIGIT inhibitors (e.g., Tiragolumab) targeting TIGIT which is an alternative checkpoint that suppresses NK and CD8+ T cells; blocking TIGIT can synergize with PD-1 blockade (25). LAG-3 inhibitors (e.g., Relatlimab): LAG-3 restrains exhausted T cells; LAG-3 blockade enhances anti-PD-1 efficacy (26).

3.3 Antibody-drug conjugates for targeted cytotoxicity

In this approach, ADCs deliver potent chemotherapy directly to tumor cells, minimizing off-target toxicity where ADC binds to the tumor antigen leading to internalization of the cytotoxic compound by the tumor cell. Cytotoxic payload (e.g., microtubule inhibitor) is released intracellularly hence inducing apoptosis (27).

3.4 Bispecific antibodies: dual-targeting strategy

BsAbs bridges T cells and tumor cells, enhancing immune cell cytotoxicity (28). For example, Blinatumomab (CD19 x CD3) in leukemia; GPC3 x CD3 BsAbs are being explored for HCC (29). Mechanistically BsAbs improve specificity while reducing systemic toxicity compared to ICIs (30).

4 Monoclonal antibodies in HCC treatment

Monoclonal antibodies represent a significant advancement in cancer treatment. These therapies are designed to specifically target antigens expressed on cancer cells, thereby reducing off-target effects and enhancing therapeutic efficacy. In HCC, mAbs such as bevacizumab, which targets VEGF, have shown promising results, particularly when used in combination with other treatments like atezolizumab, an anti-programmed cell death protein 1 (PD-1) antibody (anti-PD-L1) (31) (32).

Below is an in-depth exploration of key monoclonal antibodies used in HCC treatment.

4.1 Overview of monoclonal antibodies

mAbs are laboratory-generated molecules engineered to serve as substitute tools that can restore, enhance, or mimic the attack of the human immune system on cancer cells. They are highly specific, targeting particular antigens associated with cancer cells, and can work through various mechanisms, including blocking growth signals, inducing apoptosis, and recruiting immune cells to attack tumors (33).

Key mAbs in HCC treatment include:

4.2 mAbs targeting angiogenesis

4.2.1 Bevacizumab (Avastin)

It is a monoclonal antibody that targets and inhibits VEGF, a key molecule involved in angiogenesis (the formation of new blood vessels). By inhibiting VEGF, bevacizumab reduces the blood supply to tumors, which is essential for their growth and metastasis (34). The combination of bevacizumab with atezolizumab (an anti-PD-L1 antibody) has shown promising results in the treatment of unresectable HCC. The IMbrave150 trial was a global, randomized, open-label, phase III study evaluating the efficacy and safety of atezolizumab combined with bevacizumab versus sorafenib as first-line treatment for patients with unresectable hepatocellular carcinoma (HCC). Patients were randomized in a 2:1 ratio to receive either the combination therapy or sorafenib (35).

At the primary analysis, with a median follow-up of 8.6 months, the combination therapy demonstrated a statistically significant improvement in (OS) compared to sorafenib. The hazard ratio (HR) for death was 0.58 (95% CI: 0.42, 0.79; $p < 0.001$), indicating a 42% reduction in the risk of death. The median progression-free survival (PFS) was 6.8 months for the combination therapy versus 4.3 months for sorafenib, with an HR of 0.59 (95% CI: 0.47, 0.76; $p < 0.001$). The objective response rate (ORR) was 27% for the combination therapy compared to 12% for sorafenib (36).

An updated analysis with an additional 12 months of follow-up (median follow-up of 15.6 months) confirmed the sustained benefit of the combination therapy. The median OS was 19.2 months for the combination therapy versus 13.4 months for sorafenib, with an HR of 0.66 (95% CI: 0.52, 0.85; $p = 0.0009$). The median PFS was 6.9 months for the combination therapy versus 4.3 months for sorafenib, with an HR of 0.65 (95% CI: 0.53, 0.81; $p = 0.0001$). The ORR was 30% for the combination therapy compared to 11% for sorafenib (37). These results established atezolizumab plus bevacizumab as a new standard of care for patients with unresectable HCC, offering significant improvements in survival outcomes over sorafenib.

4.2.2 Ramucirumab (Cyramza)

It is a monoclonal antibody that targets VEGF receptor-2 (VEGFR-2), thereby inhibiting the VEGF signaling pathway involved in tumor angiogenesis. By blocking VEGFR-2, ramucirumab helps to reduce the growth of blood vessels that supply the tumor (38). Ramucirumab has shown efficacy in patients with advanced HCC, particularly in those with elevated alpha-fetoprotein (AFP) levels. The REACH-2 trial was a randomized, double-blind, placebo-controlled, phase III study evaluating the efficacy and safety of ramucirumab as a second-line treatment for patients with advanced hepatocellular carcinoma (HCC) and elevated alpha-fetoprotein (AFP) levels (≥400 ng/mL) who had previously been treated with sorafenib (39). In this study, 292 patients were randomized in a 2:1 ratio to receive either ramucirumab (8 mg/kg intravenously every two weeks) or placebo. The primary endpoint was OS, with secondary endpoints including PFS and ORR.

The results demonstrated a statistically significant improvement in OS for patients receiving ramucirumab compared to placebo. The median OS was 8.5 months for the ramucirumab group versus 7.3 months for the placebo group, with a hazard ratio (HR) of 0.71 (95% CI: 0.531–0.949; $p = 0.0199$). The median PFS was 2.8 months for the ramucirumab group compared to 1.6 months for the placebo group, with an HR of 0.452 (95% CI: 0.339–0.603; $p < 0.0001$). The ORR was 4.6% for the ramucirumab group versus 1.1% for the placebo group (40).

4.3 mAbs targeting immune checkpoints

Programmed cell death protein 1 (PD-1) is an inhibitory receptor expressed on T cells, and its ligand, PD-L1, can be expressed on tumor cells and other cells within the TME. The interaction between PD-1 and PD-L1 inhibits T-cell activity, reducing the immune response against the tumor (41). Cytotoxic T-lymphocyte-associated protein 4 (CTLA-4) is another inhibitory receptor found on T cells. It competes with the costimulatory receptor CD28 for binding to B7 molecules (CD80/CD86) on antigen-presenting cells, thereby attenuating T-cell activation early in the immune response (23).

ICIs are monoclonal antibodies designed to block these inhibitory pathways, enhancing the immune system's ability to recognize and destroy cancer cells (42). ICIs, such as PD-1/Programmed death ligand 1 (PD-L1) and Cytotoxic T-lymphocyte-associated protein 4 (CTLA-4), are often exploited by cancer cells to evade immune detection. ICIs, like nivolumab and pembrolizumab, have demonstrated efficacy in a subset of HCC patients, leading to durable responses and improved survival in some cases (43). Figure 1 describes a schematic representation of the types and modes of action of antibody-based therapy of HCC.

Pembrolizumab is a humanized IgG4 monoclonal antibody that also targets PD-1, preventing it from binding to PD-L1 and PD-L2, thus enhancing T-cell activity against tumor cells (44). The KEYNOTE-240 trial evaluated pembrolizumab in patients with advanced HCC who had previously been treated with sorafenib (45). While the trial did not meet its primary endpoints of OS and PFS, pembrolizumab demonstrated a clinically meaningful improvement in both measures. The ORR was 18.3%, and some patients experienced prolonged responses (46). Pembrolizumab is approved for the treatment of HCC following sorafenib based on the results from the KEYNOTE-224 (47) and KEYNOTE-240 trials (46).

The combination of anti-VEGF therapy (e.g., bevacizumab) with immune ICIs such as atezolizumab or pembrolizumab is not merely additive but mechanistically synergistic, as it targets distinct but interconnected pathways within the TME. The efficacy of PD-1/PD-L1 inhibitors depends on adequate T-cell priming, activation, infiltration, and persistence—all of which are negatively impacted by VEGF signaling. Bevacizumab enhances ICI efficacy by overcoming VEGF-mediated immunosuppression at multiple levels:

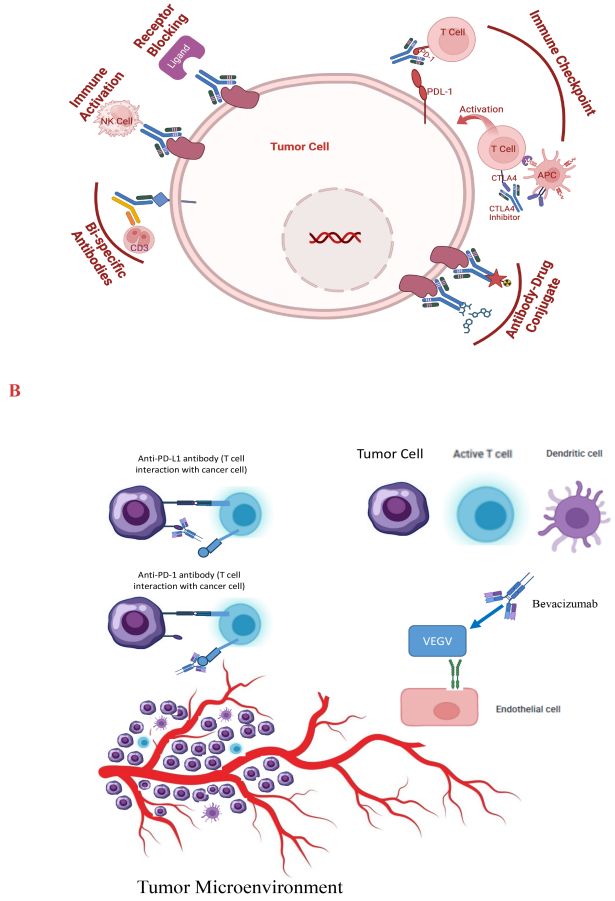

FIGURE 1
(A) Schematic presentation of the modes of action of antibody therapy of HCC. **(B)** VEGF signaling inhibition pathway and the impact on the tumor microenvironment.

4.3.1 Reversing VEGF-induced immune suppression

VEGF inhibits dendritic cell (DC) maturation, leading to poor antigen presentation and impaired T-cell priming (48). Bevacizumab restores DC function, thereby enhancing tumor antigen presentation and T-cell activation (14).

4.3.2 Enhancing T-cell infiltration by normalizing tumor vasculature

Pathological angiogenesis induced by VEGF results in chaotic, leaky blood vessels, limiting effective immune cell infiltration (49). Anti-VEGF therapy promotes vascular normalization, stabilizing endothelial junctions and pericyte coverage, allowing efficient CD8 + T-cell entry into tumors (50). This effect reduces hypoxia, which in turn lowers immunosuppressive regulatory T cells (Tregs) and myeloid-derived suppressor cells (MDSCs) (51).

4.3.3 Upregulating PD-L1 expression to enhance ICI sensitivity

VEGF-induced hypoxia upregulates PD-L1 expression on tumor cells, promoting immune evasion (52). Bevacizumab reduces hypoxia, downregulating PD-L1 expression and making tumor cells more susceptible to PD-1/PD-L1 blockade (53).

4.3.4 Increasing CD8+ T-cell cytotoxicity and IFN-γ release

VEGF suppresses effector T-cell function via multiple mechanisms, including induction of exhaustion markers (54). Bevacizumab reverses this suppression, enhancing interferon-gamma (IFN-γ) production and cytotoxic activity of CD8+ T cells (55).

The clinical evidence supporting this synergy was evident by the IMbrave150 trial (Atezolizumab + Bevacizumab) which demonstrated that this combination achieved superior OS and PFS compared to sorafenib, confirming the mechanistic synergy in HCC (36). Unlike single-agent ICIs, which are often ineffective in highly immunosuppressive tumors, combining anti-VEGF therapy with PD-1/PD-L1 blockade overcomes multiple resistance mechanisms in the TME. This approach enhances antigen presentation, T-cell infiltration, immune activation, and cytotoxicity, making it a cornerstone of modern HCC therapy.

Identifying biomarkers that predict response to ICIs is crucial for optimizing patient selection and improving outcomes. Potential biomarkers include PD-L1 expression, tumor mutational burden (TMB), and specific gene signatures associated with immune response (56).

Ongoing research focuses on combining ICIs with other treatments, such as targeted therapies, locoregional treatments, and other immunotherapies, to enhance their efficacy and overcome resistance. Understanding the optimal sequencing and combination of these therapies is critical for maximizing their benefits (57) (Figure 2).

The dual-targeting capability of bispecific antibodies allows them to bring two different cells or molecules into proximity, thereby enhancing their therapeutic efficacy (58). One of the primary mechanisms by which bispecific antibodies function is by bringing T cells, which express CD3, into proximity with cancer cells expressing a specific tumor antigen. This engagement can lead to T cell activation, proliferation, and subsequent killing of the cancer cells. For example, blinatumomab, a bispecific T cell engager (BiTE), targets CD19 on B cells and CD3 on T cells, facilitating T cell-mediated lysis of B cell malignancies (59).

While bispecific antibodies are well established in the treatment of hematologic malignancies, their application in solid tumors, including HCC, is still in the early stages of research. Preclinical and early clinical trials are investigating the efficacy and safety of various bispecific constructs in HCC (60). Researchers are developing bispecific antibodies targeting specific antigens expressed on HCC cells, such as glypican-3 (GPC3). For instance,

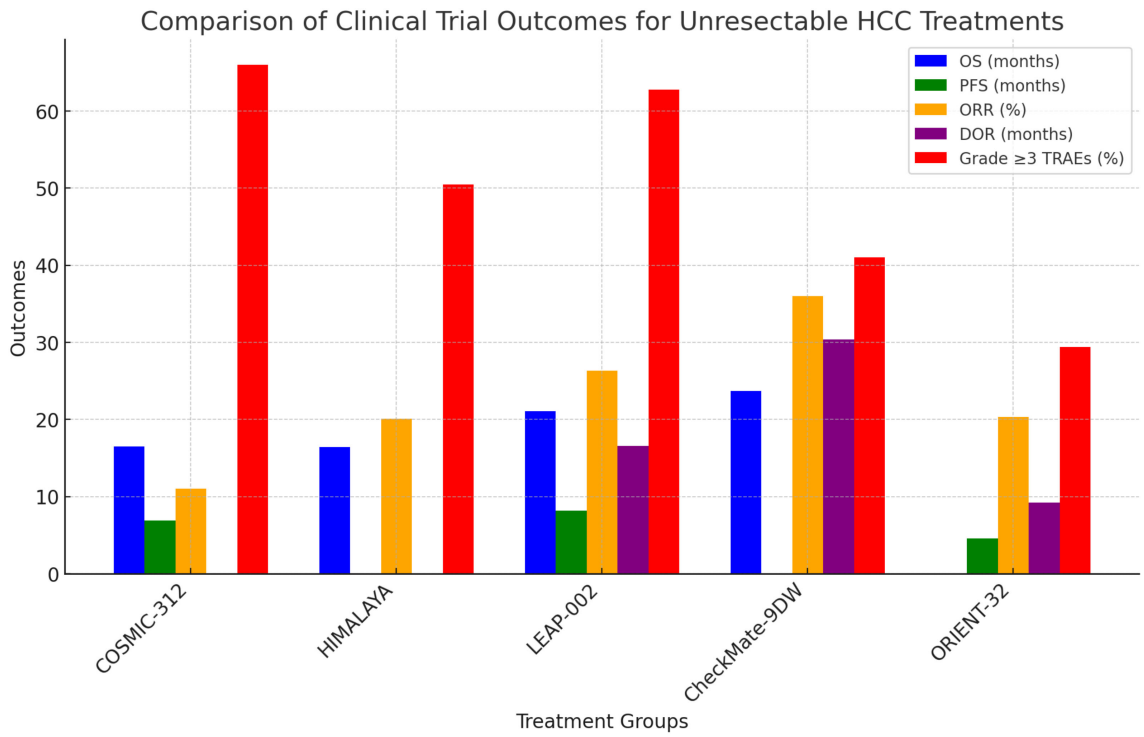

FIGURE 2
Comparison of clinical trial outcomes for unresectable HCC treatments. Confidence Progression-Free Survival (PFS), Objective Response Rate (ORR), Overall Survival (OS).

a bispecific antibody targeting GPC3 and CD3 is designed to redirect T cells to GPC3-expressing HCC cells, thereby promoting targeted immune responses against the tumor (29).

Some bispecific antibodies are designed to combine the mechanisms of immune checkpoint inhibition and T-cell engagement. These constructs can block inhibitory signals while simultaneously directing T cells to the tumor, enhancing the overall immune response (61). One of the significant challenges in treating solid tumors like HCC with bispecific antibodies is the complex TME. Factors such as immunosuppressive cells, physical barriers, and cytokines within the tumor milieu can hinder the efficacy of bispecific antibodies. The engagement of immune cells, especially T cells, must be tightly regulated to avoid excessive immune activation and potential off-target effects, which could lead to adverse events such as cytokine release syndrome (CRS) (62). Ongoing research aims to improve the specificity and potency of bispecific antibodies. Strategies include optimizing the binding affinities to the target antigens and engineering the antibody structures to enhance their stability and efficacy.

Several early-phase clinical trials are exploring the safety and efficacy of bispecific antibodies in patients with advanced HCC. These trials are essential for understanding the pharmacokinetics, optimal dosing, and potential therapeutic benefits of these novel agents. A phase II clinical trial was performed to investigate the efficacy of AK104 plus lenvatinib in patients with unresectable HCC, BCLC stage B or C, Child-Pugh class A, who had not previously received systemic treatment (63). AK104 is a humanized IgG1 bispecific antibody that simultaneously binds to PD-1 and CTLA-4. This single-arm, multicenter trial involved 30 patients who received AK104 intravenously every two or three weeks alongside daily oral lenvatinib. The primary endpoint was the objective response rate (ORR) per RECIST v1.1 criteria. Secondary endpoints included disease control rate (DCR), duration of response (DOR), PFS, and OS. As of February 1, 2021, among 18 evaluable patients, the study reported an ORR of 44.4% and a DCR of 77.8%. The median PFS had not been reached at the time of reporting. Treatment-related adverse events (TRAEs) occurred in 83.3% of patients, with Grade 3 TRAEs in 26.7%. No Grade 4 TRAEs or treatment-related deaths were observed. Common TRAEs included increased AST and ALT levels, decreased platelet and neutrophil counts, and increased blood bilirubin, predominantly of Grade 1 or 2 severity. Further studies with longer follow-up are needed to assess the durability of the response.

The success of bispecific antibodies in other cancers provides a strong rationale for their development in HCC. Future research will likely focus on combining bispecific antibodies with other therapeutic modalities, such as ICIs, tyrosine kinase inhibitors, and locoregional therapies, to enhance their efficacy and overcome resistance mechanisms.

4.4 Emerging monoclonal antibodies

Atezolizumab and durvalumab are mAb designed to target and inhibit the activity of the programmed death-ligand 1 (PD-L1) protein, a critical component in immune regulation and cancer immune evasion (64). They specifically bind to PD-L1 on tumor cells and antigen-presenting cells. Under normal conditions, PD-L1 binds to PD-1 receptors on T cells, inhibiting T cell activity and allowing cancer cells to evade immune detection. By blocking the interaction between PD-L1 and PD-1, both atezolizumab and durvalumab prevent the "off" signal from being sent to T cells. This blockade helps restore T cell activity, enabling the immune system to recognize and attack cancer cells more effectively. Both mAbs have been extensively investigated for HCC treatment either alone or in combination with each other or with other mAbs, as discussed earlier.

Research continues to identify and develop new monoclonal antibodies for treating HCC. Several novel targets are under investigation, including:

Glypican-3 (GPC3): GPC3 is a cell surface protein that is overexpressed in HCC. Monoclonal antibodies targeting GPC3 are being developed to exploit this specificity (21).

C-MET: The hepatocyte growth factor receptor (c-MET) is implicated in HCC progression. Antibodies targeting c-MET are being studied for their potential to inhibit tumor growth and metastasis (65).

Additionally, ongoing studies are exploring combinations of monoclonal antibodies with other treatment modalities, such as tyrosine kinase inhibitors, chemotherapy, and locoregional therapies, to enhance efficacy and overcome resistance mechanisms.

T-cell immunoreceptor with Ig and ITIM domains (TIGIT) has emerged as a promising target in hepatocellular carcinoma (HCC) immunotherapy. TIGIT is an immune checkpoint receptor that, when inhibited, can enhance T-cell and natural killer (NK) cell responses against tumors (66). Recent clinical trials have explored the efficacy of combining anti-TIGIT antibodies with existing therapies in HCC. A notable study is the MORPHEUS-liver trial, a phase Ib/II randomized trial evaluating the addition of tiragolumab, an anti-TIGIT monoclonal antibody, to the standard regimen of atezolizumab (an anti-PD-L1 antibody) and bevacizumab (an anti-VEGF antibody) in patients with unresectable or metastatic HCC. The trial reported a confirmed objective response rate of 43% in the tiragolumab combination group, compared to 11% in the control group receiving only atezolizumab and bevacizumab. Median progression-free survival was also extended to 12.3 months in the tiragolumab group versus 4.2 months in the control group. Importantly, the addition of tiragolumab did not result in a substantial increase in treatment-related adverse events, suggesting a favorable safety profile (67).

The phase III IMbrave152/SKYSCRAPER-14 trial aimed to assess the efficacy and safety of combining tiragolumab with atezolizumab and bevacizumab as a first-line treatment for patients with advanced HCC. This randomized, double-blind, placebo-controlled study aims to determine whether the addition of tiragolumab can improve OS and PFS compared to the standard therapy alone (68). These studies underscore the potential of targeting TIGIT in combination with established immunotherapies to enhance anti-tumor responses in HCC. Ongoing and future trials will provide more definitive insights into the clinical benefits of this approach.

5 Antibody-drug conjugates

ADCs consist of three main components: a monoclonal antibody specific to a tumor-associated antigen, a potent cytotoxic drug, and a linker that connects the drug to the antibody. Upon binding to its target antigen on the cancer cell surface, the ADC-antigen complex is internalized into the cell via endocytosis (69). Once inside the cancer cell, the ADC is trafficked to lysosomes where the linker is cleaved, releasing the cytotoxic drug. The released drug then exerts its cytotoxic effects, typically by disrupting critical cellular processes such as DNA replication or microtubule function, leading to cell death. The primary advantage of ADCs is their ability to deliver high concentrations of cytotoxic drugs directly to cancer cells, enhancing anti-tumor efficacy while reducing systemic exposure and associated toxicities. This targeted approach is particularly beneficial for cancers with specific and well-characterized surface antigens.

Glypican-3 (GPC3) is a cell surface protein overexpressed in HCC but not in normal adult tissues, making it an attractive target for ADC development. Several GPC3-targeting ADCs are under investigation, including codrituzumab (also known as GC33), which is linked to a cytotoxic drug and designed to target GPC3-expressing HCC cells (70). Preclinical studies have demonstrated that GPC3-targeting ADCs can effectively bind to HCC cells, induce internalization, and deliver cytotoxic payloads, resulting in significant anti-tumor activity *in vitro* and *in vivo* (71). In an imaging study, each patient received an intravenous injection of approximately 185 MBq (10 mg) of I-124 codrituzumab. Serial positron emission tomography/computed tomography (PET/CT) scans were conducted over seven days to assess the biodistribution and tumor uptake of the radiolabeled antibody. Pharmacokinetic analyses were performed using blood samples collected at specified intervals. Seven patients, undergoing treatment with sorafenib and cold codrituzumab (2.5 or 5 mg/kg), had repeat imaging with co-infusion of I-124 codrituzumab. Three patients who progressed on sorafenib/immunotherapy were re-imaged after a four-week washout period to assess antigen presence. Thirteen out of fourteen patients exhibited tumor localization of I-124 codrituzumab, with noted heterogeneity in tumor uptake. The pharmacokinetic profile of I-124 codrituzumab was comparable to that of other intact iodinated humanized IgG antibodies. No significant adverse events related to I-124 codrituzumab were observed during the study period. The study concluded that I-124 codrituzumab effectively localized to tumors in most HCC patients, demonstrating a favorable pharmacokinetic profile and safety. These findings suggest the potential utility of I-124 codrituzumab in imaging applications for HCC, warranting further investigation.

Despite their potential, ADCs face several challenges. The development of resistance through antigen downregulation or

modifications in intracellular trafficking pathways can reduce efficacy. Additionally, the heterogeneity of antigen expression within tumors can limit the effectiveness of ADCs. The stability of the linker and the choice of the cytotoxic drug also play critical roles in the overall success of ADCs.

Multiple clinical trials are evaluating the safety and efficacy of ADCs in patients with HCC. These trials aim to determine optimal dosing, assess therapeutic outcomes, and identify potential biomarkers for response. Early-phase clinical trials have shown promising results for ADCs targeting GPC3 in HCC. For instance, in a Phase Ib, open-label, dose-escalation study (72), 41 patients with advanced HCC, aged ≥18 years, ECOG performance status 0–1, Child-Pugh class A or B7, adequate organ function, and no prior systemic therapy were enrolled. Patients received intravenous codrituzumab at varying doses (2.5 mg/kg weekly, 5 mg/kg weekly, 10 mg/kg weekly, 1600 mg every two weeks, or 1600 mg weekly) in combination with oral sorafenib 400 mg twice daily. No patients achieved a complete or partial ORR and 9 patients (25.7%) experienced stable disease as their best response. The majority of patients exhibited disease progression. Two cases encountered Dose-Limiting Toxicities (DLTs): one case of grade 3 hyponatremia at the 5 mg/kg dose and one case of grade 3 hyponatremia and hyperglycemia at the 1600 mg every two weeks dose. 80% of patients experienced treatment-related adverse events (AEs), with the most common being increased AST in 10 patients (25%), increased ALT in 3 patients (7.5%), and increased lipase in 10 patients (25%). Most AEs were grade 1 or 2; however, some patients experienced grade 3 elevations in liver enzymes and lipase. The maximum concentration (C_max) and area under the curve (AUC) of codrituzumab and sorafenib were comparable to those observed in single-agent studies, indicating no significant drug-drug interactions. The study concluded that the combination of codrituzumab and sorafenib was generally well-tolerated at the tested doses, with manageable safety profiles. However, the lack of objective responses indicates limited efficacy in this patient population. The study suggests that while codrituzumab effectively targets GPC3-expressing tumors, its combination with sorafenib does not provide significant clinical benefit in advanced HCC.

Combining ADCs with other treatment modalities, such as immune ICIs, tyrosine kinase inhibitors, or locoregional therapies, may enhance therapeutic efficacy and overcome resistance mechanisms.

6 Challenges in antibody therapy for HCC

While antibody therapies, including mAbs, bispecific antibodies, and antibody-drug conjugates (ADCs), have shown significant promise in the treatment of hepatocellular carcinoma (HCC), several challenges hinder their optimal effectiveness. Understanding and addressing these challenges is crucial for improving patient outcomes.

One of the significant challenges in antibody therapy is the development of resistance, both primary (innate) and acquired. Primary resistance occurs when patients do not respond to therapy from the outset, while acquired resistance develops after an initial period of responsiveness. Mechanisms of resistance include antigen loss or modification, changes in intracellular signaling pathways, and adaptive immune resistance (73).

Tumor cells can downregulate or lose the expression of target antigens, rendering antibody therapies ineffective. For example, in the context of immune checkpoint inhibitors, tumors may downregulate PD-L1 or mutate the PD-1/PD-L1 pathway components to escape immune detection (74). Tumor cells can also activate alternative signaling pathways to bypass the inhibited pathway. For instance, resistance to anti-VEGF therapy like bevacizumab can arise through the activation of alternative angiogenic pathways (75).

Another mechanism by which tumors can evade antibody therapy is by creating an immunosuppressive microenvironment by recruiting regulatory T cells (Tregs), myeloid-derived suppressor cells (MDSCs), and secreting immunosuppressive cytokines, which can inhibit the effectiveness of immune-modulating antibody therapies (76, 77).

One of the challenges encountered in antibody therapy is the Immune-Related Adverse Events (irAEs). Antibody therapies, particularly immune checkpoint inhibitors, can cause irAEs due to heightened immune activity. These adverse effects can affect various organs and systems, leading to conditions such as colitis, hepatitis, pneumonitis, dermatitis, and endocrinopathies (78). Managing irAEs often requires immunosuppressive treatment, which can complicate therapy and impact patient quality of life.

ADCs and bispecific antibodies, while designed to be highly specific, can sometimes bind to antigens expressed at low levels on normal tissues, leading to On-Target, Off-Tumor Toxicity. This can result in adverse effects such as myelosuppression, hepatotoxicity, and nephrotoxicity (79).

While ICIs have shown significant promise in the treatment of HCC, several challenges remain. Some patients do not respond to ICIs (primary resistance), and others who initially respond may eventually develop resistance (acquired resistance). Mechanisms of resistance include upregulation of alternative immune checkpoints, loss of antigen presentation, and immunosuppressive TME (80). ICIs can cause a range of Immune-Related Adverse Events (irAEs) due to increased immune activity. Common irAEs include colitis, hepatitis, dermatitis, and endocrinopathies. Managing these side effects requires careful monitoring and prompt intervention with immunosuppressive therapies when necessary (81).

Nivolumab is a human IgG4 monoclonal antibody that targets PD-1, blocking its interaction with PD-L1 and PD-L2. This blockade enhances T-cell responses against tumor cells (82). The CheckMate 459 trial was a phase III study comparing nivolumab to sorafenib as first-line treatments for advanced hepatocellular carcinoma (HCC). The primary endpoint was OS. Results failed to show a statistically significant difference between the outcomes of the two treatments (a median OS of 16.4 months for nivolumab and

14.7 months for sorafenib). This was followed by the setup of the phase 3 CheckMate-9DW trial to evaluate the efficacy and safety of the combination of nivolumab plus ipilimumab as a first-line treatment for patients with advanced, unresectable hepatocellular carcinoma (HCC) (83). The trial compares this immunotherapy regimen against the current standard-of-care treatments, such as sorafenib or lenvatinib. Key endpoints include OS, PFS, and ORR, with a particular focus on whether the combination can deliver a significant survival benefit while maintaining a manageable safety profile. Preliminary findings have been promising enough to support further regulatory submissions, including a supplemental Biologics License Application (sBLA) for first-line treatment in advanced HCC. This underscores the importance of combination therapy in cases where monotherapy fails to provide an efficient therapeutic option.

The development, production, and administration of antibody therapies are expensive, making them costly for healthcare systems and patients. This high cost can limit accessibility, particularly in low- and middle-income countries. The economic burden of these therapies is a significant barrier to their widespread use (84). Another challenge is that administering antibody therapies often requires specialized infrastructure and expertise. This includes facilities for intravenous infusions, monitoring for adverse effects, and managing complications. Ensuring a reliable supply chain for biological medications can be challenging because of logistical obstacles, such as storage and transportation needs. Another challenge for the widespread use of antibody therapies is the lack of early screening programs for tumor detection which allows for optimal selection of therapy and better response (85). Approval and regulation of novel therapies can be intricate and differ greatly among countries, resulting in delays in accessing new treatments (86). In regions with limited healthcare infrastructure, the delivery of these advanced therapies can be challenging. Insufficient local clinical trials and research on HCC in LMICs may lead to a lack of information regarding the efficacy of these therapies in different populations (87).

The TME in HCC is highly immunosuppressive, characterized by the presence of Tregs, MDSCs, and immunosuppressive cytokines like TGF-β and IL-10. This environment can inhibit the activity of therapeutic antibodies, particularly those designed to stimulate an anti-tumor immune response (88). The TME and tumor cells themselves can be highly heterogeneous, meaning that different areas of the tumor may respond differently to therapy. This heterogeneity can lead to incomplete responses and relapse (89).

Large molecules like antibodies often have difficulty penetrating solid tumors effectively due to their size and the dense extracellular matrix of tumors. This can result in suboptimal drug delivery to all areas of the tumor (90). The stability and half-life of antibodies in the bloodstream can affect their efficacy. Some antibodies may be rapidly cleared from the body or degraded, reducing their therapeutic potential (91).

6.1 Biomarker-based patient selection

HCC is a highly heterogeneous disease with various etiologies, including hepatitis B or C infection, alcohol-related liver disease, and non-alcoholic steatohepatitis. This biological complexity makes identifying universal biomarkers predicting response to antibody-based therapies challenging (92). Given the variability in TMEs, genetic mutations, and immune profiles, stratifying patients using predictive biomarkers is essential for optimizing therapeutic efficacy and minimizing unnecessary exposure to ineffective treatments (93). Key Biomarkers for Antibody Therapy Response in HCC include:

1. PD-L1 Combined Positive Score (CPS) for Immune Checkpoint Inhibitors: Programmed death-ligand 1 (PD-L1) expression has been widely investigated as a potential biomarker for response to ICIs like nivolumab and pembrolizumab. Studies have suggested that a higher PD-L1 combined positive score (CPS), which accounts for PD-L1 expression in tumor and immune cells, correlates with better responses to anti-PD-1/PD-L1 therapy (94). However, PD-L1 expression alone has not been a definitive predictor in HCC, as responses to ICIs have also been observed in patients with low or undetectable PD-L1 levels. This highlights the need for additional biomarkers or combination approaches to refine patient selection.
2. Tumor Mutational Burden (TMB) is a measure of the number of somatic mutations within a tumor and has been explored as a potential predictor of response to immunotherapy (95). While higher TMB has been associated with improved responses to ICIs in various cancers (e.g., melanoma, lung cancer), its role in HCC remains less well-defined. Emerging evidence suggests that a subset of HCC patients with high TMB may derive greater benefit from checkpoint blockade, but further studies are needed to validate this as a robust biomarker in liver cancer.
3. Glypican-3 (GPC3) Expression for Targeted Antibody Therapies: GPC3 has been targeted for antibody-based therapies, including antibody-drug conjugates (ADCs) and bispecific T-cell engagers (BiTEs) (96). Biomarker-driven patient selection based on GPC3 expression could enhance the efficacy of these novel therapies, making it a promising avenue for future personalized treatment strategies (97).
4. Alpha-fetoprotein (AFP) is a well-established serum biomarker in HCC and has been explored as a predictive marker for treatment response. The REACH-2 trial demonstrated that patients with AFP levels ≥400 ng/mL derived significant survival benefits from ramucirumab, a VEGFR-2 monoclonal antibody (98). This finding led to

FDA approval of ramucirumab for HCC patients with high AFP levels, establishing AFP as the first biomarker-driven selection criterion for an HCC therapy.

Despite these advancements, significant challenges remain in identifying and validating reliable biomarkers for antibody therapy in HCC. The different etiologies (HBV, HCV, alcohol, NAFLD) influence tumor biology and immune responses, complicating the development of a one-size-fits-all biomarker. Here arises the need for dynamic biomarkers such as PD-L1 whose expression may change over time due to treatment-induced immune modulation, requiring longitudinal monitoring. Multimodal biomarker approaches combining genomic (TMB, GPC3), proteomic (AFP, PD-L1), and immunological markers may enhance the predictive power for treatment response.

6.2 Immune-related adverse events in HCC treatment

Although rare, immune myocarditis is a serious and potentially fatal immune-related adverse event (irAE) associated with ICIs, particularly in combination regimens. Immune myocarditis is thought to result from T-cell infiltration and immune-mediated destruction of cardiac myocytes, leading to impaired cardiac function. The incidence of immune myocarditis in ICI-treated patients is estimated to be 0.1–0.3%, but it carries a high mortality rate of 40–50%, making early detection and aggressive management essential (99).

Timely identification of immune myocarditis can significantly improve outcomes. Key strategies include routine measurement of cardiac troponins (e.g., hs-TnI or hs-TnT), which can detect subclinical myocarditis before overt cardiac dysfunction develops. Another approach is the Electrocardiogram (ECG) and Echocardiography, where abnormalities (ST-segment changes, conduction delays) and echocardiographic findings (reduced ejection fraction, regional wall motion abnormalities) may indicate myocarditis. Cardiac Magnetic Resonance Imaging (MRI) with late gadolinium enhancement on MRI can help confirm myocarditis in ambiguous cases (100).

These irAEs can be managed by immediate administration of High-dose corticosteroids (methylprednisolone), which should be initiated upon suspicion of immune myocarditis, with a slow taper over weeks to prevent relapse. Immunosuppressive Therapy using Abatacept, a CTLA-4 agonist, due to its ability to dampen T-cell activation while preserving anti-tumor immunity. Infliximab is generally avoided due to its potential to exacerbate cardiac inflammation. A Multidisciplinary Approach with Cardio-oncology collaboration is critical for optimizing treatment decisions and monitoring for long-term sequelae (101).

7 Future directions and innovations

The future of antibody therapies for HCC involves the development of next-generation antibodies designed to improve efficacy, reduce resistance, and minimize side effects. These innovations aim to address the current limitations of existing therapies and offer new hope for patients with advanced HCC.

Smaller antibody fragments and nanobodies (single-domain antibodies) are being developed to improve tissue penetration and reduce immunogenicity. These smaller molecules can access tumor sites more effectively than full-sized antibodies, potentially enhancing therapeutic outcomes (102). Advances in antibody engineering have led to the development of bispecific and multispecific antibodies that can simultaneously target multiple antigens or pathways. This approach can enhance the specificity and potency of the immune response against cancer cells, reducing the likelihood of resistance and improving overall efficacy (103).

Ongoing research is focused on discovering new tumor-specific antigens that antibody therapies can target. Glypican-3 (GPC3) is an example of a promising target in HCC, and further identification of such targets can lead to the development of more effective treatments (104). Table 1 summarizes the outcome of the current guideline studies vs the exploratory studies for the immunotherapeutic regimens for HCC.

In addition to targeting tumor cells directly, new strategies aim to modulate the TME to enhance anti-tumor immunity. This includes targeting immunosuppressive cells (e.g., regulatory T cells, myeloid-derived suppressor cells) and cytokines (e.g., TGF-β, IL-10) that inhibit the immune response (105).

Personalized medicine involves tailoring treatments to the specific genetic, molecular, and cellular characteristics of an individual's cancer. This approach has the potential to improve the effectiveness of antibody therapies for HCC by ensuring that patients receive treatments most likely to benefit them. Identifying biomarkers that predict response to antibody therapies is critical for selecting the right patients for each treatment. For example, PD-L1 expression, TMB, and specific gene signatures can help identify patients who are likely to respond to ICIs (106). Comprehensive genomic profiling of tumors can reveal actionable mutations and alterations that can be targeted by specific antibody therapies. This

TABLE 1 Guideline vs. Exploratory Regimens in HCC.

Regimen	Category	Key trials	Primary outcomes
Atezolizumab + Bevacizumab (IMbrave150)	Guideline-Recommended	IMbrave150	OS: 19.2m vs 13.4m (HR: 0.66, P<0.001)
Durvalumab + Tremelimumab (STRIDE)	Guideline-Recommended	HIMALAYA	OS: 16.4m vs 13.8m (HR: 0.78, P=0.0035)
Lenvatinib + Pembrolizumab	Exploratory	LEAP-002	OS: 21.1m vs 19.0m (HR: 0.836)
AK104 + Lenvatinib	Exploratory	NCT05020236	ORR: 34.8% | DCR: 78.3%
TIGIT Inhibitors + Checkpoint Blockade	Exploratory	NCT04354246	Ongoing - Early Phase

OS, Overall Survival (in months); HR, Hazard Ratio; ORR, Objective Response Rate; DCR, Disease Control Rate; m, months.

approach allows for the customization of treatment plans based on the unique molecular characteristics of each patient's cancer (107).

Adaptive trial designs, such as basket and umbrella trials, allow for the simultaneous evaluation of multiple treatments in different patient subgroups based on their molecular profiles. These innovative trial designs can accelerate the identification of effective therapies and improve patient outcomes (108).

Recent phase III clinical trials for unresectable HCC have continued to use sorafenib as the primary comparator, despite the establishment of atezolizumab plus bevacizumab as the SOC in the IMbrave150 trial. This approach is evident in trials such as HIMALAYA, which evaluated tremelimumab plus durvalumab versus sorafenib (109), and COSMIC-312, which assessed cabozantinib plus atezolizumab versus sorafenib (110). While these trials were designed before the results of IMbrave150 were available, their continued use of sorafenib as the control arm at the time of readout limits their generalizability and clinical impact.

The IMbrave150 trial demonstrated that atezolizumab plus bevacizumab significantly outperformed sorafenib in OS and PFS, with improved tolerability. Despite this, trials like HIMALAYA and COSMIC-312 continued to use sorafenib as the control arm, making their findings less applicable to current clinical practice. The HIMALAYA trial showed non-inferiority of the STRIDE regimen (tremelimumab plus durvalumab) versus sorafenib but did not evaluate its efficacy against atezolizumab plus bevacizumab. The COSMIC-312 trial failed to demonstrate OS superiority of cabozantinib plus atezolizumab versus sorafenib, raising doubts about its potential clinical role when the actual benchmark should have been atezolizumab plus bevacizumab. Without head-to-head comparisons to the true gold standard, clinicians are left uncertain about whether these therapies offer a real improvement or simply outperform an outdated regimen. Using an outdated comparator delays innovation because it does not challenge novel agents against the best available treatments. Trials with suboptimal control arms can misallocate resources and delay approval for more effective therapies that should be tested in a more competitive landscape. The persistent use of sorafenib as a comparator in recent HCC trials undermines clinical relevance, delays innovation, and hinders progress. Moving forward, trial designs must evolve to reflect the most current SOC, ensuring that new therapies are tested in the most competitive, clinically meaningful settings.

Combining antibody therapies with other treatment modalities can enhance their efficacy and overcome resistance mechanisms. Synergistic combinations can target different aspects of the tumor and its microenvironment, leading to improved therapeutic outcomes. Combining antibody therapies with locoregional treatments like TACE and RFA can enhance the overall anti-tumor effect. Locoregional therapies can reduce tumor burden, making the residual disease more susceptible to systemic treatments (111).

Radiotherapy has historically played a limited role in HCC treatment due to concerns about radiation-induced liver disease (RILD). However, advancements in stereotactic body radiotherapy (SBRT) have significantly improved precision, enabling its use in select patient populations, particularly those with portal vein tumor thrombosis (PVTT) (112). SBRT delivers high-dose radiation to tumor sites while minimizing liver toxicity, achieving local control rates of 70–90% in PVTT cases.

Radiotherapy is increasingly being explored in combination with ICIs and monoclonal antibodies, leveraging its ability to modulate the TME. Radiation induces tumor antigen release, promoting dendritic cell activation and antigen presentation. It upregulates PD-L1 expression, which may enhance response rates to anti-PD-1/PD-L1 checkpoint inhibitors (e.g., nivolumab, pembrolizumab, atezolizumab). The abscopal effect, where localized radiotherapy induces systemic anti-tumor immunity, has been observed in patients receiving ICIs (113, 114).

Several trials (e.g., RTOG-1112, NCT03316872) are evaluating SBRT in combination with PD-1/PD-L1 inhibitors to improve survival outcomes in advanced HCC (115). Early-phase results suggest increased response rates and prolonged progression-free survival compared to ICIs alone. Radiation therapy also induces hypoxia-driven VEGF upregulation, promoting angiogenesis and tumor progression. Combining SBRT with VEGF-targeting antibodies (e.g., bevacizumab, ramucirumab) may counteract this effect, improving local tumor control and reducing recurrence. IMbrave150 findings support the rationale for atezolizumab + bevacizumab + SBRT, which is currently under investigation (116). Combined antibody therapy and SBRT is challenged by the optimal dose and fractionation selection, the optimal treatment sequencing of antibody therapy relative to radiotherapy, and the selection of proper biomarkers to guide the treatment and select eligible patients.

While the potential for triple antibody therapy in HCC exists, current research is primarily focused on dual antibody combinations and integrating antibodies with other treatment modalities. Further studies are necessary to explore the safety, efficacy, and feasibility of triple antibody regimens in HCC treatment. A recent study has investigated the combination of transarterial chemoembolization (TACE), lenvatinib (a tyrosine kinase inhibitor), and anti-PD-1 antibodies, which has shown promising results in converting unresectable HCC to resectable status (117). Combining multiple antibodies increases the risk of immune-related adverse events, which necessitates a careful assessment of safety profiles through clinical trials to determine their effectiveness over existing therapies.

Nanotechnology offers innovative solutions for the targeted delivery of antibody therapies. Nanoparticles can be engineered to carry antibodies and release them in a controlled manner at the tumor site, enhancing the precision and effectiveness of the treatment (118).

8 Conclusion

Antibody-based therapies have revolutionized the treatment paradigm for hepatocellular carcinoma, offering new hope for patients with advanced disease. While significant progress has been made, continued research and innovation are essential to overcome current challenges and fully realize the potential of these

therapies. By integrating cutting-edge technologies and personalized medicine approaches, the future holds promise for more effective, targeted, and accessible treatments for HCC, ultimately improving patient outcomes and survival rates.

Author contributions

SE-K: Conceptualization, Data curation, Formal Analysis, Funding acquisition, Investigation, Methodology, Project administration, Resources, Software, Supervision, Validation, Visualization, Writing – original draft, Writing – review & editing. ME: Data curation, Investigation, Software, Writing – original draft, Writing – review & editing. EA: Funding acquisition, Investigation, Resources, Supervision, Writing – review & editing. AS: Formal Analysis, Investigation, Methodology, Validation, Writing – review & editing. AT: Conceptualization, Data curation, Formal Analysis, Investigation, Methodology, Supervision, Validation, Writing – original draft, Writing – review & editing.

Funding

The author(s) declare that financial support was received for the research and/or publication of this article. This research work was funded by the Institutional Fund Projects under grant No. (IFPRC-021-140-2020). The authors gratefully acknowledge the technical and financial support provided by the Ministry of Education and King Abdulaziz University, DSR, Jeddah, Saudi Arabia.

Conflict of interest

AS reports consulting or advisory board role with AstraZeneca, Bristol-Myers Squibb, Merck, Exelixis, Pfizer, Xilio therapeutics, Taiho, Amgen, Autem therapeutics, Arcus therapeutics, KAHR medical, and Daiichi Sankyo; and institutional research funding from AstraZeneca, Bristol-Myers Squibb, Merck, Clovis, Exelixis, Actuate therapeutics, Incyte Corporation, Daiichi Sankyo, Five prime therapeutics, Amgen, Innovent biologics, Dragonfly therapeutics, Oxford Biotherapeutics, Arcus therapeutics, and KAHR medical.

The authors declare that the research was conducted in the absence of any commercial or financial relationships that could be construed as a potential conflict of interest.

Generative AI statement

The author(s) declare that no Generative AI was used in the creation of this manuscript.

Publisher's note

References

1. Ferlay J, Colombet M, Soerjomataram I, Parkin DM, Piñeros M, Znaor A, et al. Cancer statistics for the year 2020: an overview. *Int J Cancer J Int du Cancer*. (2021). 778–89. doi: 10.1002/ijc.33588

2. Kim DY. Changing etiology and epidemiology of hepatocellular carcinoma: asia and worldwide. *J Liver Cancer*. (2024) 24:62–70. doi: 10.17998/jlc.2024.03.13

3. Bai S, Dang W, Hong W, Liao W, Smith RD. The prevalence of hepatitis B in chinese general population from 2018 to 2022: A systematic review and meta-analysis. *BMC Infect Dis*. (2024) 24:211. doi: 10.1186/s12879-024-09103-8

4. Kedar Mukthinuthalapati VVP, Sewram V, Ndlovu N, Kimani S, Abdelaziz AO, Chiao EY, et al. Hepatocellular carcinoma in sub-saharan africa. *JCO Glob Oncol*. (2021) 7:756–66. doi: 10.1200/go.20.00425

5. Zamor PJ, deLemos AS, Russo MW. Viral hepatitis and hepatocellular carcinoma: etiology and management. *J Gastrointest Oncol*. (2017) 8:229–42. doi: 10.21037/jgo.2017.03.14

6. Bengtsson B, Widman L, Wahlin S, Stål P, Björkström NK, Hagström H. The risk of hepatocellular carcinoma in cirrhosis differs by etiology, age and sex: A swedish nationwide population-based cohort study. *United Eur Gastroenterol J*. (2022) 10:465–76. doi: 10.1002/ueg2.12238

7. Zhou R, Liu M, Liang X, Su M, Li R. Clinical features of aflatoxin B1-exposed patients with liver cancer and the molecular mechanism of aflatoxin B1 on liver cancer cells. *Environ Toxicol Pharmacol*. (2019) 71:103225. doi: 10.1016/j.etap.2019.103225

8. Chavez-Tapia NC, Murúa-Beltrán Gall S, Ordoñez-Vázquez AL, Nuño-Lambarri N, Vidal-Cevallos P, Uribe M. Understanding the role of metabolic syndrome as a risk factor for hepatocellular carcinoma. *J Hepatocell Carcinoma*. (2022) 9:583–93. doi: 10.2147/jhc.S283840

9. Yang JD, Hainaut P, Gores GJ, Amadou A, Plymoth A, Roberts LR. A global view of hepatocellular carcinoma: trends, risk, prevention and management. *Nat Rev Gastroenterol Hepatol*. (2019) 16:589–604. doi: 10.1038/s41575-019-0186-y

10. Suresh D, Srinivas AN, Prashant A, Harikumar KB, Kumar DP. Therapeutic options in hepatocellular carcinoma: A comprehensive review. *Clin Exp Med*. (2023) 23:1901–16. doi: 10.1007/s10238-023-01014-3

11. Vogl TJ, Adwan H, Wolff L, Lahrsow M, Gruber-Rouh T, Nour-Eldin N-EA, et al. Retrospective long-term evaluation of conventional transarterial chemoembolization for hepatocellular carcinoma over 20 years. *Cancers*. (2024) 16. doi: 10.3390/cancers16081498

12. Leowattana W, Leowattana T, Leowattana P. Systemic treatment for unresectable hepatocellular carcinoma. *World J Gastroenterol*. (2023) 29:1551–68. doi: 10.3748/wjg.v29.i10.1551

13. Fallah A, Sadeghinia A, Kahroba H, Samadi A, Heidari HR, Bradaran B, et al. Therapeutic targeting of angiogenesis molecular pathways in angiogenesis-dependent diseases. *Biomedicine Pharmacotherapy*. (2019) 110:775–85. doi: 10.1016/j.biopha.2018.12.022

14. Fukumura D, Kloepper J, Amoozgar Z, Duda DG, Jain RK. Enhancing cancer immunotherapy using antiangiogenics: opportunities and challenges. *Nat Rev Clin Oncol*. (2018) 15:325–40. doi: 10.1038/nrclinonc.2018.29

15. Lin YY, Tan CT, Chen CW, Ou DL, Cheng AL, Hsu C. Immunomodulatory effects of current targeted therapies on hepatocellular carcinoma: implication for the future of immunotherapy. *Semin Liver Dis*. (2018) 38:379–88. doi: 10.1055/s-0038-1673621

16. Oura K, Morishita A, Tadokoro T, Fujita K, Tani J, Kobara H. Immune microenvironment and the effect of vascular endothelial growth factor inhibition in hepatocellular carcinoma. *Int J Mol Sci*. (2024) 25. doi: 10.3390/ijms252413590

17. Li Q, Han J, Yang Y, Chen Y. Pd-1/pd-L1 checkpoint inhibitors in advanced hepatocellular carcinoma immunotherapy. *Front Immunol*. (2022) 13:1070961. doi: 10.3389/fimmu.2022.1070961

18. Ganss R. Tumour vessel normalization and immune checkpoint blockade: A new synergism. *Immunol Cell Biol*. (2017) 95:497–8. doi: 10.1038/icb.2017.30

19. Hao L, Li S, Deng J, Li N, Yu F, Jiang Z, et al. The current status and future of pd-L1 in liver cancer. *Front Immunol*. (2023) 14:1323581. doi: 10.3389/fimmu.2023.1323581

20. Shimasaki N, Jain A, Campana D. Nk cells for cancer immunotherapy. *Nat Rev Drug Discov*. (2020) 19:200–18. doi: 10.1038/s41573-019-0052-1

21. Xie CM, Monge CM, Mabry-Hrones D, Coffman KL, Hicks S, Redd B, Highfill S, Ho M, Greten TF, et al. A phase I study of gpc3 targeted car-T cell therapy in advanced gpc3-expressing hepatocellular carcinoma (Hcc). *J Clin Oncol*. (2023) 41:TPS624–TPS. doi: 10.1200/JCO.2023.41.4_suppl.TPS624

22. Yin Y, Feng W, Chen J, Chen X, Wang G, Wang S, et al. Immunosuppressive tumor microenvironment in the progression, metastasis, and therapy of hepatocellular carcinoma: from bench to bedside. *Exp Hematol Oncol*. (2024) 13:72. doi: 10.1186/s40164-024-00539-x

23. Sobhani N, Tardiel-Cyril DR, Davtyan A, Generali D, Roudi R, Li Y. Ctla-4 in regulatory T cells for cancer immunotherapy. *Cancers*. (2021) 13. doi: 10.3390/cancers13061440

24. Rimassa L, Finn RS, Sangro B. Combination immunotherapy for hepatocellular carcinoma. *J Hepatol*. (2023) 79:506–15. doi: 10.1016/j.jhep.2023.03.003

25. Zhang P, Liu X, Gu Z, Jiang Z, Zhao S, Song Y, et al. Targeting tigit for cancer immunotherapy: recent advances and future directions. *biomark Res*. (2024) 12:7. doi: 10.1186/s40364-023-00543-z

26. Ren Z, Guo Y, Bai Y, Ying J, Meng Z, Chen Z, et al. Tebotelimab, a pd-1/lag-3 bispecific antibody, in patients with advanced hepatocellular carcinoma who had failed prior targeted therapy and/or immunotherapy: an open-label, single-arm, phase 1/2 dose-escalation and expansion study. *J Clin Oncol*. (2023) 41:578. doi: 10.1200/JCO.2023.41.4_suppl.578

27. Riccardi F, Dal Bo M, Macor P, Toffoli G. A comprehensive overview on antibody-drug conjugates: from the conceptualization to cancer therapy. *Front Pharmacol*. (2023) 14:1274088. doi: 10.3389/fphar.2023.1274088

28. Liguori L, Polcaro G, Nigro A, Conti V, Sellitto C, Perri F, et al. Bispecific antibodies: A novel approach for the treatment of solid tumors. *Pharmaceutics*. (2022) 14. doi: 10.3390/pharmaceutics14112442

29. Yu L, Yang X, Huang N, Lang QL, He QL, Jian-Hua W, et al. A novel targeted gpc3/cd3 bispecific antibody for the treatment hepatocellular carcinoma. *Cancer Biol Ther*. (2020) 21:597–603. doi: 10.1080/15384047.2020.1743158

30. Gu Y, Zhao Q. Clinical progresses and challenges of bispecific antibodies for the treatment of solid tumors. *Mol Diagnosis Ther*. (2024) 28:669–702. doi: 10.1007/s40291-024-00734-w

31. Psilopatis I, Damaskos C, Garmpi A, Sarantis P, Koustas E, Antoniou EA, et al. Fda-approved monoclonal antibodies for unresectable hepatocellular carcinoma: what do we know so far? *Int J Mol Sci*. (2023) 24. doi: 10.3390/ijms24032685

32. Aghanejad A, Bonab SF, Sepehri M, Haghighi FS, Tarighatnia A, Kreiter C, et al. A review on targeting tumor microenvironment: the main paradigm shift in the mab-based immunotherapy of solid tumors. *Int J Biol macromolecules*. (2022) 207:592–610. doi: 10.1016/j.ijbiomac.2022.03.057

33. Zahavi D, Weiner L. Monoclonal antibodies in cancer therapy. *Antibodies (Basel)*. (2020) 9. doi: 10.3390/antib9030034

34. Frenette CT. Current status of bevacizumab for advanced hepatocellular carcinoma. *Chin Clin Oncol*. (2012) 1:13. doi: 10.3978/j.issn.2304-3865.2012.09.01

35. Al-Sharif H A, El-Kafrawy SA, Yousef JM, Kumosani TA, Kamal MA, Khathlan NA, et al. Dominance of the on1 genotype of rsv-a and ba9 genotype of rsv-B in respiratory cases from jeddah, Saudi Arabia. *Genes*. (2020) 11:1323. doi: 10.3390/genes11111323

36. Finn RS, Qin S, Ikeda M, Galle PR, Ducreux M, Kim TY, et al. Atezolizumab plus bevacizumab in unresectable hepatocellular carcinoma. *New Engl J Med*. (2020) 382:1894–905. doi: 10.1056/NEJMoa1915745

37. Liu X, Lu Y, Qin S. Atezolizumab and bevacizumab for hepatocellular carcinoma: mechanism, pharmacokinetics and future treatment strategies. *Future Oncol*. (2021) 17:2243–56. doi: 10.2217/fon-2020-1290

38. Singh AD, Parmar S. Ramucirumab (Cyramza): A breakthrough treatment for gastric cancer. *P t*. (2015) 40:430–68.

39. Zhu AX, Kang Y-K, Yen C-J, Finn RS, Galle PR, Llovet JM, et al. Ramucirumab after sorafenib in patients with advanced hepatocellular carcinoma and increased &X3b1;-fetoprotein concentrations (Reach-2): A randomised, double-blind, placebo-controlled, phase 3 trial. *Lancet Oncol*. (2019) 20:282–96. doi: 10.1016/S1470-2045(18)30937-9

40. Kudo M, Okusaka T, Motomura K, Ohno I, Morimoto M, Seo S, et al. Ramucirumab after prior sorafenib in patients with advanced hepatocellular carcinoma and elevated alpha-fetoprotein: Japanese subgroup analysis of the reach-2 trial. *J Gastroenterol*. (2020) 55:627–39. doi: 10.1007/s00535-020-01668-w

41. Han Y, Liu D, Li L. Pd-1/pd-L1 pathway: current researches in cancer. *Am J Cancer Res*. (2020) 10:727–42.

42. Shiravand Y, Khodadadi F, Kashani SMA, Hosseini-Fard SR, Hosseini S, Sadeghirad H, et al. Immune checkpoint inhibitors in cancer therapy. *Curr Oncol*. (2022) 29:3044–60. doi: 10.3390/curroncol29050247

43. Ruli TM, Pollack ED, Lodh A, Evers CD, Price CA, Shoreibah M. Immune checkpoint inhibitors in hepatocellular carcinoma and their hepatic-related side effects: A review. *Cancers*. (2024) 16. doi: 10.3390/cancers16112042

44. Kwok G, Yau TC, Chiu JW, Tse E, Kwong YL. Pembrolizumab (Keytruda). *Hum Vaccin Immunother*. (2016) 12:2777–89. doi: 10.1080/21645515.2016.1199310

45. Finn RS, Chan SL, Zhu AX, Knox J, Cheng AL, Siegel AB, et al. Keynote-240: phase 3, randomized study of pembrolizumab (Pembro) vs best supportive care (Bsc) for second-line advanced hepatocellular carcinoma (Hcc). *Ann Oncol*. (2017) 28:v266. doi: 10.1093/annonc/mdx369.157

46. Merle P, Kudo M, Edeline J, Bouattour M, Cheng AL, Chan SL, et al. Pembrolizumab as second-line therapy for advanced hepatocellular carcinoma: longer term follow-up from the phase 3 keynote-240 trial. *Liver Cancer*. (2023) 12:309–20. doi: 10.1159/000529636

47. Finn RS, Ryoo B-Y, Merle P, Kudo M, Bouattour M, Lim HY, et al. Pembrolizumab as second-line therapy in patients with advanced hepatocellular carcinoma in keynote-240: A randomized, double-blind, phase iii trial. *J Clin Oncol*. (2019) 38:193–202. doi: 10.1200/JCO.19.01307

48. Gabrilovich DI, Nagaraj S. Myeloid-derived suppressor cells as regulators of the immune system. *Nat Rev Immunol*. (2009) 9:162–74. doi: 10.1038/nri2506

49. Jain RK. Normalizing tumor vasculature with anti-angiogenic therapy: A new paradigm for combination therapy. *Nat Med*. (2001) 7:987–9. doi: 10.1038/nm0901-987

50. Hodi FS, Lawrence D, Lezcano C, Wu X, Zhou J, Sasada T, et al. Bevacizumab plus ipilimumab in patients with metastatic melanoma. *Cancer Immunol Res*. (2014) 2:632–42. doi: 10.1158/2326-6066.Cir-14-0053

51. Zhang Y, Brekken RA. Direct and indirect regulation of the tumor immune microenvironment by vegf. *J Leukoc Biol*. (2022) 111:1269–86. doi: 10.1002/jlb.5ru0222-082r

52. Shrimali RK, Yu Z, Theoret MR, Chinnasamy D, Restifo NP, Rosenberg SA. Antiangiogenic agents can increase lymphocyte infiltration into tumor and enhance the effectiveness of adoptive immunotherapy of cancer. *Cancer Res*. (2010) 70:6171–80. doi: 10.1158/0008-5472.Can-10-0153

53. Wallin JJ, Bendell JC, Funke R, Sznol M, Korski K, Jones S, et al. Atezolizumab in combination with bevacizumab enhances antigen-specific T-cell migration in metastatic renal cell carcinoma. *Nat Commun*. (2016) 7:12624. doi: 10.1038/ncomms12624

54. Joyce JA, Fearon DT. T cell exclusion, immune privilege, and the tumor microenvironment. *Science*. (2015) 348:74–80. doi: 10.1126/science.aaa6204

55. Socinski MA, Jotte RM, Cappuzzo F, Orlandi F, Stroyakovskiy D, Nogami N, et al. Atezolizumab for first-line treatment of metastatic nonsquamous nsclc. *New Engl J Med*. (2018) 378:2288–301. doi: 10.1056/NEJMoa1716948

56. Catalano M, Iannone LF, Nesi G, Nobili S, Mini E, Roviello G. Immunotherapy-related biomarkers: confirmations and uncertainties. *Crit Rev Oncology/Hematology*. (2023) 192:104135. doi: 10.1016/j.critrevonc.2023.104135

57. Wei H, Dong C, Li X. Treatment options for hepatocellular carcinoma using immunotherapy: present and future. *J Clin Trans Hepatol*. (2024) 12:389–405. doi: 10.14218/JCTH.2023.00462

58. Klein C, Brinkmann U, Reichert JM, Kontermann RE. The present and future of bispecific antibodies for cancer therapy. *Nat Rev Drug Discov*. (2024) 23:301–19. doi: 10.1038/s41573-024-00896-6

59. Tian Z, Liu M, Zhang Y, Wang X. Bispecific T cell engagers: an emerging therapy for management of hematologic Malignancies. *J Hematol Oncol*. (2021) 14:75. doi: 10.1186/s13045-021-01084-4

60. Huang S-L, Wang Y-M, Wang Q-Y, Feng G-G, Wu F-Q, Yang L-M, et al. Mechanisms and clinical trials of hepatocellular carcinoma immunotherapy. *Front Genet*. (2021) 12:691391. doi: 10.3389/fgene.2021.691391

61. Cheng A-L, Hsu C, Chan SL, Choo S-P, Kudo M. Challenges of combination therapy with immune checkpoint inhibitors for hepatocellular carcinoma. *J Hepatol*. (2020) 72:307–19. doi: 10.1016/j.jhep.2019.09.025

62. Cheng L, Chen L, Shi Y, Gu W, Ding W, Zheng X, et al. Efficacy and safety of bispecific antibodies vs. Immune checkpoint blockade combination therapy in cancer: A real-world comparison. *Mol Cancer*. (2024) 23:77. doi: 10.1186/s12943-024-01956-6

63. Bai L, Sun M, Xu A, Bai Y, Wu J, Shao G, et al. Phase 2 study of ak104 (Pd-1/ctla-4 bispecific antibody) plus lenvatinib as first-line treatment of unresectable hepatocellular carcinoma. *J Clin Oncol*. (2021) 39:4101. doi: 10.1200/JCO.2021.39.15_suppl.4101

64. Childs A, Aidoo-Micah G, Maini MK, Meyer T. Immunotherapy for hepatocellular carcinoma. *JHEP Rep*. (2024) 6:101130. doi: 10.1016/j.jhepr.2024.101130

65. Woo HY, Heo J. The role of C-met inhibitors in advanced hepatocellular carcinoma: now and future. *Ann Transl Med*. (2020) 8:1617. doi: 10.21037/atm-20-3387

66. Dumbrava E, Rasco D, Patnaik A, Vaena D, Papadopoulos K, ElNaggar A, et al. 477 com902 (Anti-tigit antibody) monotherapy – preliminary evaluation of safety, tolerability, pharmacokinetics and receptor occupancy in patients with advanced solid tumors (Nct04354246). *J ImmunoTherapy Cancer*. (2021) 9:A507. doi: 10.1136/jitc-2021-SITC2021.477

67. Finn RS, Ryoo BY, Hsu CH, Li D, Burgoyne AM, Cotter C, et al. Tiragolumab in combination with atezolizumab and bevacizumab in patients with unresectable, locally advanced or metastatic hepatocellular carcinoma (Morpheus-liver): A randomised, open-label, phase 1b-2, study. *Lancet Oncol*. (2025) 26:214–26. doi: 10.1016/s1470-2045(24)00679-x

68. Badhrinarayanan S, Cotter C, Zhu H, Lin YC, Kudo M, Li D. Imbrave152/skyscraper-14: A phase iii study of atezolizumab, bevacizumab and tiragolumab in advanced hepatocellular carcinoma. *Future Oncol*. (2024) 20:2049–57. doi: 10.1080/14796694.2024.2355863

69. Dahlgren D, Lennernäs H. Antibody-drug conjugates and targeted treatment strategies for hepatocellular carcinoma: A drug-delivery perspective. *Molecules (Basel Switzerland)*. (2020) 25. doi: 10.3390/molecules25122861

70. Li J, Xiang L, Wang Q, Ma X, Chen X, Zhu Y, et al. Highly potent immunotoxins targeting the membrane-distal N-lobe of gpc3 for immunotherapy of hepatocellular carcinoma. *J Cancer*. (2022) 13:1370–84. doi: 10.7150/jca.66978

71. Carrasquillo JA, O'Donoghue JA, Beylergil V, Ruan S, Pandit-Taskar N, Larson SM, et al. I-124 codrituzumab imaging and biodistribution in patients with hepatocellular carcinoma. *EJNMMI Res*. (2018) 8:20. doi: 10.1186/s13550-018-0374-8

72. Abou-Alfa GK, Yen CJ, Hsu CH, O'Donoghue J, Beylergil V, Ruan S, et al. Phase ib study of codrituzumab in combination with sorafenib in patients with non-curable advanced hepatocellular carcinoma (Hcc). *Cancer Chemother Pharmacol*. (2017) 79:421–9. doi: 10.1007/s00280-017-3241-9

73. Manfredi GF, Celsa C, John C, Jones C, Acuti N, Scheiner B, et al. Mechanisms of resistance to immunotherapy in hepatocellular carcinoma. *J Hepatocell Carcinoma*. (2023) 10:1955–71. doi: 10.2147/jhc.S291553

74. Sukowati C, Cabral LKD, Anfuso B, Dituri F, Negro R, Giannelli G, et al. Pd-L1 downregulation and DNA methylation inhibition for molecular therapy against cancer stem cells in hepatocellular carcinoma. *Int J Mol Sci*. (2023) 24. doi: 10.3390/ijms241713357

75. Shiragannavar VD, Karunakara SH, Puttahanumantharayappa LD, Sannappa Gowda NG, Santhekadur PK. Unraveling key signaling pathways altered in hepatocellular carcinoma. *Gene Expression*. (2023) 22:28–40. doi: 10.14218/GE.2022.00009S

76. Lindau D, Gielen P, Kroesen M, Wesseling P, Adema GJ. The immunosuppressive tumour network: myeloid-derived suppressor cells, regulatory T cells and natural killer T cells. *Immunology*. (2013) 138:105–15. doi: 10.1111/imm.12036

77. Saeed A, Park R, Pathak H, Al-Bzour AN, Dai J, Phadnis M, et al. Clinical and biomarker results from a phase ii trial of combined cabozantinib and durvalumab in patients with chemotherapy-refractory colorectal cancer (Crc): camilla crc cohort. *Nat Commun*. (2024) 15:1533. doi: 10.1038/s41467-024-45960-2

78. Fukushima T, Morimoto M, Kobayashi S, Ueno M, Uojima H, Hidaka H, et al. Association between immune-related adverse events and survival in patients with hepatocellular carcinoma treated with atezolizumab plus bevacizumab. *Oncologist*. (2023) 28:e526–e33. doi: 10.1093/oncolo/oyad090

79. Nguyen TD, Bordeau BM, Balthasar JP. Mechanisms of adc toxicity and strategies to increase adc tolerability. *Cancers*. (2023) 15. doi: 10.3390/cancers15030713

80. Hu-Lieskovan S, Malouf GG, Jacobs I, Chou J, Liu L, Johnson ML. Addressing resistance to immune checkpoint inhibitor therapy: an urgent unmet need. *Future Oncol*. (2021) 17:1401–39. doi: 10.2217/fon-2020-0967

81. Darnell EP, Mooradian MJ, Baruch EN, Yilmaz M, Reynolds KL. Immune-related adverse events (Iraes): diagnosis, management, and clinical pearls. *Curr Oncol Rep*. (2020) 22:39. doi: 10.1007/s11912-020-0897-9

82. Yau T, Park J-W, Finn RS, Cheng A-L, Mathurin P, Edeline J, et al. Nivolumab versus sorafenib in advanced hepatocellular carcinoma (Checkmate 459): A randomised, multicentre, open-label, phase 3 trial. *Lancet Oncol*. (2022) 23:77–90. doi: 10.1016/S1470-2045(21)00604-5

83. Galle PR, Decaens T, Kudo M, Qin S, Fonseca L, Sangro B, et al. Nivolumab (Nivo) plus ipilimumab (Ipi) vs lenvatinib (Len) or sorafenib (Sor) as first-line treatment for unresectable hepatocellular carcinoma (Uhcc): first results from checkmate 9dw. *J Clin Oncol*. (2024) 42:LBA4008–LBA. doi: 10.1200/JCO.2024.42.17_suppl.LBA4008

84. Gong H, Ong SC, Li F, Shen Y, Weng Z, Zhao K, et al. Cost-effectiveness of immune checkpoint inhibitors as a first-line therapy for advanced hepatocellular carcinoma: A systematic review. *Health Economics Rev*. (2024) 14:48. doi: 10.1186/s13561-024-00526-2

85. Shah SC, Kayamba V, Peek RM Jr., Heimburger D. Cancer control in low- and middle-income countries: is it time to consider screening? *J Glob Oncol*. (2019) 5:1–8. doi: 10.1200/jgo.18.00200

86. André N, Banavali S, Snihur Y, Pasquier E. Has the time come for metronomics in low-income and middle-income countries? *Lancet Oncol*. (2013) 14:e239–48. doi: 10.1016/s1470-2045(13)70056-1

87. Jaquet A, Muula G, Ekouevi DK, Wandeler G. Elimination of viral hepatitis in low and middle-income countries: epidemiological research gaps. *Curr Epidemiol Rep*. (2021) 8:89–96. doi: 10.1007/s40471-021-00273-6

88. Guizhen Z, Guanchang J, Liwen L, Huifen W, Zhigang R, Ranran S, et al. The tumor microenvironment of hepatocellular carcinoma and its targeting strategy by car-T cell immunotherapy. *Front Endocrinol (Lausanne)*. (2022) 13:918869. doi: 10.3389/fendo.2022.918869

89. Safri F, Nguyen R, Zerehpooshnesfchi S, George J, Qiao L. Heterogeneity of hepatocellular carcinoma: from mechanisms to clinical implications. *Cancer Gene Ther*. (2024) 31:1105–12. doi: 10.1038/s41417-024-00764-w

90. Chung C, Kudchodkar SB, Chung CN, Park YK, Xu Z, Pardi N, et al. Expanding the reach of monoclonal antibodies: A review of synthetic nucleic acid delivery in immunotherapy. *Antibodies*. (2023) 12. doi: 10.3390/antib12030046

91. Dai J-M, Zhang X-Q, Dai J-Y, Yang X-M, Chen Z-N. Modified therapeutic antibodies: improving efficacy. *Engineering*. (2021) 7:1529–40. doi: 10.1016/j.eng.2020.06.030

92. Sung PS, Lee IK, Roh PR, Kang MW, Ahn J, Yoon SK. Blood-based biomarkers for immune-based therapy in advanced hcc: promising but a long way to go. *Front Oncol*. (2022) 12:1028728. doi: 10.3389/fonc.2022.1028728

93. Tai D, Choo SP, Chew V. Rationale of immunotherapy in hepatocellular carcinoma and its potential biomarkers. *Cancers*. (2019) 11. doi: 10.3390/cancers11121926

94. Onuma AE, Zhang H, Huang H, Williams TM, Noonan A, Tsung A. Immune checkpoint inhibitors in hepatocellular cancer: current understanding on mechanisms of resistance and biomarkers of response to treatment. *Gene Expression*. (2020) 20:53–65. doi: 10.3727/105221620x15880179864121

95. Sha D, Jin Z, Budczies J, Kluck K, Stenzinger A, Sinicrope FA. Tumor mutational burden as a predictive biomarker in solid tumors. *Cancer Discov*. (2020) 10:1808–25. doi: 10.1158/2159-8290.Cd-20-0522

96. Tehrani HA, Zangi M, Fathi M, Vakili K, Hassan M, Rismani E, et al. Gpc-3 in hepatocellular carcinoma; a novel biomarker and molecular target. *Exp Cell Res*. (2025) 444:114391. doi: 10.1016/j.yexcr.2024.114391

97. Liu J, Park K, Shen Z, Lee H, Geetha P, Pakyari M, et al. Immunotherapy, targeted therapy, and their cross talks in hepatocellular carcinoma. *Front Immunol*. (2023) 14:1285370. doi: 10.3389/fimmu.2023.1285370

98. Choucair K, Kamran S, Saeed A. Clinical evaluation of ramucirumab for the treatment of hepatocellular carcinoma (Hcc): place in therapy. *Onco Targets Ther*. (2021) 14:5521–32. doi: 10.2147/ott.S268309

99. Palaskas N, Lopez-Mattei J, Durand JB, Iliescu C, Deswal A. Immune checkpoint inhibitor myocarditis: pathophysiological characteristics, diagnosis, and treatment. *J Am Heart Assoc*. (2020) 9:e013757. doi: 10.1161/jaha.119.013757

100. Schneider BJ, Naidoo J, Santomasso BD, Lacchetti C, Adkins S, Anadkat M, et al. Management of immune-related adverse events in patients treated with immune checkpoint inhibitor therapy: asco guideline update. *J Clin Oncol*. (2021) 39:4073–126. doi: 10.1200/JCO.21.01440

101. Chitnis SD, Mortazavi A. Clinical guideline highlights for the hospitalist: management of immune-related adverse events in patients treated with immune checkpoint inhibitor therapy. *J Hosp Med*. (2023) 18:1013–6. doi: 10.1002/jhm.13097

102. Fayn S, King AP, Gutsche NT, Duan Z, Buffington J, Olkowski CP, et al. Site-specifically conjugated single-domain antibody successfully identifies glypican-3-expressing liver cancer by immuno-pet. *J Nucl Med*. (2023) 64:1017–23. doi: 10.2967/jnumed.122.265171

103. Keri D, Walker M, Singh I, Nishikawa K, Garces F. Next generation of multispecific antibody engineering. *Antibody Ther*. (2024) 7:37–52. doi: 10.1093/abt/tbad027

104. Liu H-Q, Sun L-X, Yu L, Liu J, Sun L-C, Yang Z-H, et al. Hsp90, as a functional target antigen of a mab 11c9, promotes stemness and tumor progression in hepatocellular carcinoma. *Stem Cell Res Ther*. (2023) 14:273. doi: 10.1186/s13287-023-03453-x

105. Argentiero A, Delvecchio A, Fasano R, Andriano A, Caradonna IC, Memeo R, et al. The complexity of the tumor microenvironment in hepatocellular carcinoma and emerging therapeutic developments. *J Clin Med*. (2023) 12. doi: 10.3390/jcm12237469

106. Gabbia D, De Martin S. Tumor mutational burden for predicting prognosis and therapy outcome of hepatocellular carcinoma. *Int J Mol Sci*. (2023) 24. doi: 10.3390/ijms24043441

107. Ishido S, Tsuchiya K, Kano Y, Yasui Y, Takaura K, Uchihara N, et al. Clinical utility of comprehensive genomic profiling in patients with unresectable hepatocellular carcinoma. *Cancers*. (2023) 15. doi: 10.3390/cancers15030719

108. Lu CC, Li XN, Broglio K, Bycott P, Jiang Q, Li X, et al. Practical considerations and recommendations for master protocol framework: basket, umbrella and platform trials. *Ther Innov Regul Sci*. (2021) 55:1145–54. doi: 10.1007/s43441-021-00315-7

109. Sangro B, Chan SL, Kelley RK, Lau G, Kudo M, Sukeepaisarnjaroen W, et al. Four-year overall survival update from the phase iii himalaya study of tremelimumab plus durvalumab in unresectable hepatocellular carcinoma. *Ann Oncol*. (2024) 35:448–57. doi: 10.1016/j.annonc.2024.02.005

110. Cheng AL, Qin S, Ikeda M, Galle PR, Ducreux M, Kim TY, et al. Updated efficacy and safety data from imbrave150: atezolizumab plus bevacizumab vs. Sorafenib for unresectable hepatocellular carcinoma. *J Hepatol*. (2022) 76:862–73. doi: 10.1016/j.jhep.2021.11.030

111. Bajestani N, Wu G, Hussein A, Makary MS. Examining the efficacy and safety of combined locoregional therapy and immunotherapy in treating hepatocellular carcinoma. *Biomedicines*. (2024) 12. doi: 10.3390/biomedicines12071432

112. Tsilimigras DI, Aziz H, Pawlik TM. Critical analysis of the updated barcelona clinic liver cancer (Bclc) group guidelines. *Ann Surg Oncol*. (2022) 29:7231–4. doi: 10.1245/s10434-022-12242-4

113. Voronova V, Vislobokova A, Mutig K, Samsonov M, Peskov K, Sekacheva M, et al. Combination of immune checkpoint inhibitors with radiation therapy in cancer: A hammer breaking the wall of resistance. *Front Oncol*. (2022) 12:1035884. doi: 10.3389/fonc.2022.1035884

114. Chami P, Diab Y, Khalil DN, Azhari H, Jarnagin WR, Abou-Alfa GK, et al. Radiation and immune checkpoint inhibitors: combination therapy for treatment of hepatocellular carcinoma. *Int J Mol Sci*. (2023) 24. doi: 10.3390/ijms242316773

115. Dawson LA, Winter KA, Knox JJ, Zhu AX, Krishnan S, Guha C, et al. Stereotactic body radiotherapy vs sorafenib alone in hepatocellular carcinoma: the nrg oncology/rtog 1112 phase 3 randomized clinical trial. *JAMA Oncol*. (2025) 11:136–44. doi: 10.1001/jamaoncol.2024.5403

116. Su C-W, Teng W, Shen EY-L, Huang B-S, Lin P-T, Hou M-M, et al. Concurrent atezolizumab plus bevacizumab and high-dose external beam radiotherapy for highly advanced hepatocellular carcinoma. *Oncologist*. (2024) 29:e922–e31. doi: 10.1093/oncolo/oyae048

117. Wu J-Y, Wu J-Y, Fu Y-K, Ou X-Y, Li S-Q, Zhang Z-B, et al. Outcomes of salvage surgery versus non-salvage surgery for initially unresectable hepatocellular carcinoma after conversion therapy with transcatheter arterial chemoembolization combined with lenvatinib plus anti-pd-1 antibody: A multicenter retrospective study. *Ann Surg Oncol*. (2024) 31:3073–83. doi: 10.1245/s10434-024-14944-3

118. Metkar SP, Fernandes G, Navti PD, Nikam AN, Kudarha R, Dhas N, et al. Nanoparticle drug delivery systems in hepatocellular carcinoma: A focus on targeting strategies and therapeutic applications. *OpenNano*. (2023) 12:100159. doi: 10.1016/j.onano.2023.100159

frontiers | Frontiers in Cellular and Infection Microbiology

TYPE Original Research
PUBLISHED 17 July 2025
DOI 10.3389/fcimb.2025.1598193

OPEN ACCESS

EDITED BY
Ashraf A. Tabll,
National Research Centre, Egypt

REVIEWED BY
Jian Chen,
Fudan University, China
Sherif El-Kafrawy,
King Abdulaziz University, Saudi Arabia

*CORRESPONDENCE
Feixiang Wu
wufeixiang@gxmu.edu.cn
Zhihong Tang
tangzhihong@gxmu.edu.cn

†These authors share first authorship

RECEIVED 22 March 2025
ACCEPTED 24 June 2025
PUBLISHED 17 July 2025

CITATION
Xu S, Pang Q, Wei M, Liu D, Yuan D, Bai T, Wang X, Tang Z and Wu F (2025) Postoperative hepatitis B virus reactivation and its impact on survival in HBV-related hepatocellular carcinoma patients undergoing conversion therapy with interventional therapy combined with tyrosine kinase inhibitors and immune checkpoint inhibitors. *Front. Cell. Infect. Microbiol.* 15:1598193. doi: 10.3389/fcimb.2025.1598193

Postoperative hepatitis B virus reactivation and its impact on survival in HBV-related hepatocellular carcinoma patients undergoing conversion therapy with interventional therapy combined with tyrosine kinase inhibitors and immune checkpoint inhibitors

Shaowei Xu[1†], Qingqing Pang[2†], Meng Wei[1], Danxi Liu[1], Du Yuan[1], Tao Bai[1], Xiaobo Wang[1], Zhihong Tang[1*] and Feixiang Wu[1*]

[1]Department of Hepatobiliary Surgery, Guangxi Medical University Cancer Hospital, Nanning, Guangxi, China, [2]Department of Oncology, Liuzhou Workers' Hospital, Liuzhou, Guangxi, China

Objective: This study aimed to investigate hepatitis B virus (HBV) reactivation and its impact on postoperative survival in patients with HBV-related hepatocellular carcinoma (HCC) who underwent conversion therapy. The therapeutic regimen consisted of interventional procedures (hepatic artery infusion chemotherapy [HAIC] and/or transarterial chemoembolization [TACE]) combined with tyrosine kinase inhibitors (TKIs) and immune checkpoint inhibitors (ICIs).

Methods: A retrospective analysis was performed at a single institution involving 91 patients *who had* initially unresectable HCC linked to the hepatitis B virus. These patients achieved resectability following conversion therapy and subsequently underwent surgical tumor removal. Logistic regression identified risk factors for HBV reactivation (HBVr). Kaplan-Meier survival analysis and log-rank tests assessed survival differences. Cox proportional hazards regression was used to identify independent predictors of progression-free survival (PFS) and overall survival (OS).

Results: In our cohort, HBVr occurred in 17 patients (18.7%), all of whom received antiviral therapy. The incidence of HBVr was 16.7% (14/84) in patients with detectable baseline HBV DNA and 42.9% (3/7) in those with undetectable levels. Baseline HBV DNA ≥2000 IU/ml was identified as an independent protective factor against HBVr (OR 0.090, 95% CI 0.015–0.532; P = 0.008). The median PFS was significantly shorter in the reactivation group than in the non-reactivation group (12.1 months [95% CI 5.5–18.7] *vs.* 29.2 months [95% CI 23.6–34.7]; P < 0.001). However, no significant difference was observed in

median OS between the two groups (not reached *vs*. 45.6 months [95% CI 41.7–49.5]; P = 0.117).

Conclusion: HBVr represents a potential complication in subjects receiving hepatectomy for hepatitis B virus associated HCC following conversion therapy involving interventional therapies combined with TKIs and ICIs. Patients experiencing HBVr exhibited significantly shorter progression-free survival compared to those without reactivation. Therefore, prophylactic antiviral therapy and meticulous HBV DNA monitoring are warranted during both conversion therapy and the perioperative period.

KEYWORDS

hepatocellular carcinoma, conversion therapy, surgery, HBV reactivation, survival

1 Introduction

Hepatocellular carcinoma (HCC) is a prevalent malignancy worldwide, with approximately 70% of new cases occurring in Asia (Sung et al., 2021). Projections estimate that there will be over one million new HCC cases and related deaths annually by 2040 (Rumgay et al., 2022). In regions with high HCC incidence, hepatitis B virus (HBV) infection is the primary etiological factor (Mysore and Leung, 2018). In recent years, systemic therapy has emerged as the mainstream treatment for advanced HCC. Specifically, the combination of tyrosine kinase inhibitors (TKIs) and immune checkpoint inhibitors (ICIs) has achieved objective response rates (ORRs) of 20–30% in advanced or unresectable HCC, as demonstrated in landmark trials such as IMbrave150, ORIENT-32, HIMALAYA, and CARES-310. Furthermore, combining these systemic agents with locoregional therapies, such as transarterial chemoembolization (TACE) or hepatic arterial infusion chemotherapy (HAIC), has yielded even better outcomes (Ju et al., 2021; Cai et al., 2022; Fu et al., 2023; Zhu et al., 2023). Multiple studies have shown that surgical resection following successful conversion therapy offers superior long-term survival benefits compared to palliative treatments alone (Kulik et al., 2006; Lewandowski et al., 2009; Shindoh et al., 2021). Therefore, for patients with initially unresectable HCC, the selection of optimal treatment strategies and timing, alongside the effective management of complications, is of paramount importance for improving prognosis.

Among these complications, hepatitis B virus reactivation (HBVr) is a well-recognized challenge during HCC treatment (Voican et al., 2016). While HBVr is more frequent in patients positive for hepatitis B surface antigen (HBsAg) and antibody to hepatitis B core antigen (anti-HBc), it can also manifest in individuals with resolved HBV infection (Hoofnagle, 2009). Existing antiviral agents are unable to completely eradicate covalently closed circular DNA (cccDNA), the viral reservoir in patients with chronic hepatitis B. Consequently, when cccDNA persists in the context of immunosuppression, control over HBV replication is compromised, leading to reactivation (Shi and Zheng, 2020). HBVr can trigger a spectrum of clinical events, ranging from mild hepatitis to fulminant liver failure and even death (Papatheodoridis et al., 2022). Moreover, HBVr can necessitate the interruption of anti-tumor therapy and adversely affect overall survival (Yang et al., 2024).

Previous research has reported an elevated risk of HBVr following surgical resection for HCC, which detrimentally affects patient prognosis (Huang et al., 2012; Dan et al., 2013; Xie et al., 2015). HBVr has also been observed during and after various anti-tumor regimens for intermediate-to-advanced HCC, including interventional therapies, TKIs, and ICIs, often leading to severe complications and negatively impacting long-term survival (Shen et al., 2023; Yang et al., 2024). Conversion therapy, the process of transforming an initially unresectable HCC into a resectable state, aims to enhance surgical eligibility and prognosis. Presently, a growing number of patients with unresectable HCC are undergoing triple therapy (interventional therapy plus TKIs and ICIs), which subsequently allows them to receive surgical treatment. However, for this specific population, the incidence of HBVr and its impact on prognosis remain unclear. This retrospective study, therefore, aims to investigate the occurrence of HBVr in HBV-related HCC patients who underwent surgical resection after conversion therapy with interventional treatment plus TKIs and ICIs, and to evaluate its influence on their prognosis.

2 Materials and methods

2.1 Patient recruitment and study design

This retrospective study enrolled patients with HCC who underwent tumor resection following conversion therapy with HAIC or TACE combined with TKIs and ICIs at the Guangxi Medical University Cancer Hospital from January 2021 to April 2024.The inclusion criteria were as follows: (1) age between 18 and

85 years; (2) histologically confirmed HCC; (3) Barcelona Clinic Liver Cancer (BCLC) stage A–C; (4) chronic or resolved HBV infection (defined as HBsAg-positive, or HBsAg-negative and anti-HBc-positive); (5) initiation of TACE/HAIC and TKIs within two weeks before or after the first dose of ICI; (6) receipt of at least one cycle of TACE/HAIC combined with at least one dose of a TKI and an ICI preoperatively; (7) concurrent receipt of prophylactic anti-HBV therapy during anti-tumor treatment; (8) Child-Pugh class A or B liver function; and (9) an Eastern Cooperative Oncology Group (ECOG) performance status score of 0–2.The exclusion criteria included: (1) presence of any other primary malignancy or extrahepatic metastases; (2) any prior anti-HCC treatment; (3) co-infection with other hepatotropic viruses or human immunodeficiency virus (HIV); (4) survival time of less than 3 months; (5) lack of HBV serological markers, HBV DNA monitoring, or imaging data during treatment; (6) history of organ or allogeneic bone marrow transplantation; (7) pregnancy or lactation; and (8) severe heart failure, uncontrolled diabetes, active infection, or other severe comorbidities. This study was approved by the Ethics Committee of Guangxi Medical University Cancer Hospital. The requirement for informed consent was waived due to the retrospective nature of the study. A total of 91 patients were ultimately included in the final analysis.

2.2 Conversion therapy

The conversion therapy regimen was tailored for each patient by a multidisciplinary team (MDT) based on their tumor status and liver function. The regimen consisted of transarterial interventional therapy (including TACE and HAIC) combined with a tyrosine kinase inhibitor (TKI) and a programmed cell death protein 1 (PD-1) inhibitor. Vascular interventional procedures (TACE and HAIC) were performed by interventional radiologists at our institution. Treatment with TKIs and PD-1 inhibitors was initiated within one week following the TACE or HAIC procedure, contingent upon the patient's liver function recovery. The TKIs used in this study, consistent with the first-line treatment recommendations for advanced HCC in Chinese guidelines, included lenvatinib (8 mg daily for body weight <60 kg or 12 mg daily for body weight ≥60 kg), donafenib (0.2 g twice daily), sorafenib (400 mg twice daily), and apatinib (250 mg once daily). Bevacizumab was administered at 15 mg/kg every three weeks. The PD-1 inhibitors used were camrelizumab (200 mg intravenously IV every 2 weeks), tislelizumab (200 mg IV every 3 weeks), and sintilimab (200 mg IV every 3 weeks). The choice of specific agents was determined by the attending physician's clinical judgment, the patient's economic status, and personal preference. The dosage and frequency of all TKIs and PD-1 inhibitors were administered according to their respective package inserts.

2.3 Antiviral therapy

All patients were routinely screened for HBsAg, anti-HBs, HBeAg, anti-HBe, anti-HBc, and serum HBV DNA levels upon their initial admission. HBV DNA was quantified using a real-time quantitative polymerase chain reaction (qPCR) assay with a lower limit of detection of 20 IU/ml. Antiviral therapy was immediately initiated for patients with HBsAg-positive status or those who were HBsAg-negative but had detectable HBV DNA. The antiviral agents included entecavir (ETV, 0.5 mg/day), tenofovir disoproxil fumarate (TDF, 300 mg/day), and tenofovir alafenamide (TAF, 25 mg/day). Patients were allowed to make an informed choice regarding the specific drug based on their socioeconomic status and personal preference. For patients already receiving antiviral treatment prior to admission, their existing regimen was continued. Lifelong antiviral therapy was recommended for all patients with HBV-related HCC. To monitor for HBVr and ensure medication adherence, HBV DNA levels were measured every 6 weeks during conversion therapy, and medication intake was documented. Antiviral therapy was continued throughout the perioperative period, with HBV DNA levels checked on postoperative day 7. For patients who developed HBVr during treatment, their antiviral regimen was switched, although drug resistance testing was not performed.

2.4 Postoperative management and follow-up

Following surgery, patients were followed up every 2–3 months for the first two years and every 6 months thereafter. Monitoring included serum tumor markers (e.g., alpha-fetoprotein [AFP], protein induced by vitamin K absence-II [PIVKA-II]), HBV DNA, HBV serological markers, abdominal ultrasound, and contrast-enhanced computed tomography (CT) or magnetic resonance imaging (MRI).

2.5 Clinical and laboratory variables

Patient demographic characteristics and treatment histories were extracted from the electronic medical record system. Data on complete blood counts, blood biochemistry, AFP, HBV DNA, HBV serological markers, imaging studies, and tumor pathology were collected before and during anti-tumor treatment.

2.6 Outcome assessments

The primary endpoint was the incidence of HBVr, defined according to the Asian-Pacific Association for the Study of the Liver (APASL) clinical practice guidelines as one of the following: for patients with chronic HBV infection (HBsAg-positive), either (1) a ≥2 $\log_{10}$ IU/mL increase in HBV DNA level from baseline, or (2) an HBV DNA level >100 IU/mL in patients with previously undetectable baseline HBV DNA; for patients with resolved HBV infection (HBsAg-negative and anti-HBc-positive), either (1) HBsAg seroreversion (a change from HBsAg-negative to HBsAg-positive), or (2) a change from undetectable to detectable HBV

DNA (Lau et al., 2021). Meeting any of these criteria signified an HBVr event. Secondary outcomes were overall survival (OS), progression-free survival (PFS), and loss to follow-up. OS was defined as the time from the initiation of the first treatment to cancer-related death or the last follow-up. PFS was defined as the time from surgical resection to disease progression, death from any cause, or the last follow-up. Tumor response was evaluated using the Response Evaluation Criteria in Solid Tumors (RECIST, version 1.1) and the HCC-specific modified RECIST (mRECIST) (Eisenhauer et al., 2009; Llovet and Lencioni, 2020). Tumor response was independently assessed by two radiologists who were blinded to the patients' HBVr status.

2.7 Statistical analysis

Continuous variables were presented as mean ± standard deviation (SD) for normally distributed data and as median with interquartile range (IQR) for non-normally distributed data. Differences between groups were compared using the Student's t-test or the Mann-Whitney U test, as appropriate. Categorical variables were described as numbers (n) and percentages (%) and were compared using the Chi-square (χ^2) test or Fisher's exact test. Univariate and multivariate logistic regression analyses were performed to identify risk factors for HBVr. Survival curves for PFS and OS were generated using the Kaplan-Meier method and compared with the log-rank test. The proportional hazards assumption for the Cox model was verified using the Schoenfeld residuals test. To identify independent prognostic factors for PFS and OS, univariate and multivariate analyses were conducted using the Cox proportional hazards model. A two-sided P-value of less than 0.05 was considered statistically significant. All statistical analyses were performed using SPSS software (version 25.0), and figures were generated with R software (version 4.4.2).

3 Results

3.1 Patient characteristics

From January 2021 to April 2024, a total of 123 patients with HCC who underwent tumor resection following conversion therapy with TACE and/or HAIC plus TKIs and ICIs were initially screened. Of these, 32 patients were excluded: 3 were anti-HBc negative, and 29 had missing baseline or follow-up data. Ultimately, 91 patients were eligible and included in the final analysis (Figure 1). The detailed baseline characteristics of the enrolled patients are summarized in Table 1. The ICIs administered included sintilimab, camrelizumab, or tislelizumab. The TKIs included sorafenib, lenvatinib, bevacizumab, donafenib, or apatinib. The patient age ranged from 27 to 72 years (median, 47 years), with a predominance of male patients (n=81, 89.0%). At baseline, 90 patients (98.9%) were HBsAg-positive, while one patient had occult HBV infection (HBsAg-negative, anti-HBc-positive, and HBV DNA-positive). A detectable baseline HBV DNA level (median, 221 IU/mL; range, 20–1,270,000 IU/mL) was present in 84 patients (92.3%), and 11 of these patients had a serum HBV DNA level >2000 IU/mL. All patients received antiviral therapy during conversion treatment, with agents including entecavir, tenofovir disoproxil fumarate, or tenofovir alafenamide. The cohort comprised 84 patients (92.3%) with Child-Pugh class A liver function and 7 (7.7%) with class B. According to the BCLC

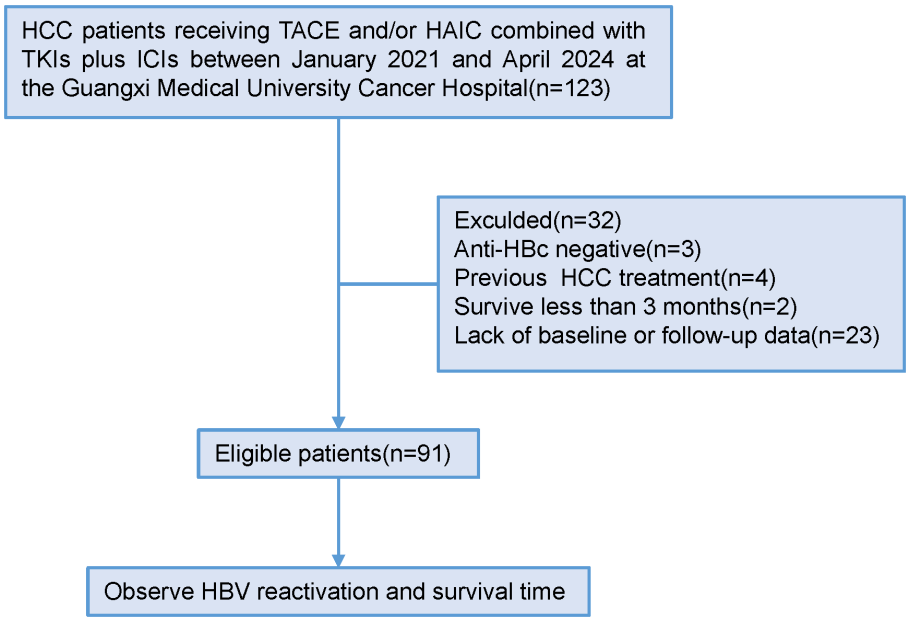

FIGURE 1
Patient enrollment and study flow. (Anti-HBc, antibody to hepatitis B core antigen; HAIC, hepatic artery infusion chemotherapy; HBV, hepatitis B virus; HCC, hepatocellular carcinoma; ICIs, immune checkpoint inhibitors; TACE, transarterial chemoembolization; TKIs, tyrosine kinase inhibitors).

10.3389/fcimb.2025.1598193

TABLE 1 Baseline characteristics of patients with hepatocellular carcinoma.

Characteristics	Total (n=91)	HBV reactivation (n=17)	Non-reactivation (n=74)	P value
Age, years	47.00 (42.00,58.00)	45.00 (43.00,50.50)	48.00 (41.75,59.00)	0.280
Sex				0.778
Male	81 (89.0%)	15 (88.2%)	66 (89.2%)	
Female	10 (11.0%)	3 (11,8%)	8 (10.8%)	
Antiviral prophylaxis type				0.752
Entecavir	81 (89.0%)	16 (94.1%)	65 (87.8%)	
Tenofovir	10 (11.0%)	1 (5.9%)	9 (12.2%)	
HBsAg				0.340
Seropositive	89 (97.8%)	16 (94.1%)	73 (98.6%)	
Seronegative	2 (2.2%)	1 (5.9%)	1 (1.4%)	
HBeAg				0.690
Seropositive	36 (39.6%)	6 (35.3%)	30 (40.5%)	
Seronegative	55 (60.4%)	11 (64.7%)	44 (59.5%)	
ECOG PS				0.934
0	42 (46.2%)	8 (47.1%)	34 (45.9%)	
1-2	49 (53.8)	9 (52.9%)	40 (54.1%)	
Child Pugh grade				0.229
A	84 (92.3%)	14 (82.4%)	70 (94.6%)	
B	7 (7.7%)	3 (17.6%)	4 (5.4%)	
BCLC				0.478
A	24 (26.4%)	5 (29.4%)	19 (25.7%)	
B	27 (29.7%)	3 (17.6%)	24 (32.4%)	
C	40 (44.0%)	9 (52.9%)	31 (41.9%)	
HBV DNA, IU/ml				
Undetectable	7 (7.7%)	3 (17.6%)	4 (5.4%)	0.229
Detectable	84 (92.3)	14 (82.4%)	70 (94.6%)	
>2000	11 (12.1%)	3 (17.6%)	8 (10.8%)	0.713
≤2000	80 (87.9%)	14 (82.4%)	66 (89.2%)	
Median baseline HBV DNA (range), IU/mL	221.0 (0-3110000)	455.0 (0-3110000)	180.5 (0-30300)	
ALT, U/L				0.067
>40	46 (50.5%)	12 (70.6%)	34 (45.9%)	
≤ 40	45 (49.5%)	5 (29.4%)	40 (54.1%)	
TBil, mmol/L	16.61 (10.30,20.30)	17.28 (11.30,23.45)	16.46 (10.30,19.88)	0.521
ALB, g/L	38.05 (± 4.36)	37.44 (± 4.33)	38.19 (± 4.39)	0.524
ALBI grade				0.582
I	32 (35.2%)	5 (29.4%)	27 (36.5%)	
II	59 (64.8%)	12 (70.6%)	47 (63.5%)	

(Continued)

TABLE 1 Continued

Characteristics	Total (n=91)	HBV reactivation (n=17)	Non-reactivation (n=74)	P value
AFP, ng/mL				0.675
AFP≥1000	44 (48.4%)	9 (52.9%)	35 (47.3%)	
AFP<1000	47 (51.6%)	8 (47.1%)	39 (52.7%)	
WBC, ×109/L	6.45 (5.01,7.50)	6.95 (5.33,7.93)	6.19 (4.97,7.36)	0.261
Hemoglobin, g/L	136.03 (± 21.19)	127.94 (± 24.43)	137.89 (± 20.10)	0.081
Platelet, ×109/L	214 (170,278)	201 (153,293)	216 (170,271)	0.867
Cirrhosis				0.641
Yes	74 (81.3%)	15 (88.2%)	59 (79.7%)	
No	17 (18.7%)	2 (11.8%)	15 (20.3%)	
Tumor diameter (cm)	10.07 (± 4.18)	10.94 (± 5.41)	9.88 (± 3.87)	0.349
≥10cm	43 (47.3%)	8 (47.1%)	35 (47.3%)	0.986
<10cm	48 (52.7%)	9 (52.9%)	39 (52.7%)	
Tumor number				0.578
Single	48 (52.7%)	10 (58.8%)	38 (51.4%)	
Multiple	43 (47.3%)	7 (41.2%)	36 (48.6%)	
PVTT				0.893
Yes	28 (30.8%)	5 (29.4%)	23 (31.1%)	
No	63 (69.2%)	12 (70.6%)	51 (68.9%)	
MVI				0.560
Yes	18	2 (11.8%)	16 (21.6%)	
No	73	15 (88.2%)	58 (78.4%)	
Vascular invasion				0.493
Yes	31 (34.1%)	7 (41.2%)	24 (32.4%)	
No	60 (65.9%)	10 (58.8%)	50 (67.6%)	
pCR				0.083
Yes	23 (25.3%)	1 (5.9%)	22 (29.7%)	
No	68 (74.7%)	16 (94.1%)	52 (70.3%)	
Types of TKIs				0.342
Lenvatinib	77 (84.6%)	16 (94.1%)	61 (82.4%)	
Donafenib	8 (8.8%)	1 (5.9%)	7 (9.5%)	
Apatinib	3 (3.3%)	0 (0%)	3 (4.1%)	
Sorafanib	1 (1.1%)	0 (0%)	1 (1.4%)	
Bevacizumab	1 (1.1%)	0 (0%)	1 (1.4%)	
Donafenib+ Lenvatinib	1 (1.1%)	0 (0%)	1 (1.4%)	
Types of ICIs				0.743
Camrelizumab	51 (56.0%)	10 (58.8%)	41 (55.4%)	
Tislelizumab	32 (35.2%)	6 (35.3%)	26 (35.1%)	
Sintilimab	4 (4.4%)	0 (0%)	4 (5.4%)	

(Continued)

TABLE 1 Continued

Characteristics	Total (n=91)	HBV reactivation (n=17)	Non-reactivation (n=74)	P value
Types of ICIs				0.743
Tislelizumab+ Sintilimab	2 (2.2%)	1 (5.9%)	1 (1.4%)	
Tislelizumab+ Camrelizumab	1 (1.1%)	0 (0%)	1 (1.4%)	
Sintilimab+ Camrelizumab	1 (1.1%)	0 (0%)	1 (1.4%)	
Types of interventional therapy				0.938
HAIC	19 (20.9%)	4 (23.5%)	15 (20.3%)	
TACE	65 (71.4%)	11 (64.7%)	54 (73.0%)	
HAIC+TACE	7 (7.7%)	2 (11.8%)	5 (6.8%)	

HBV, hepatitis B virus; HBsAg, hepatitis B surface antigen; HBeAg, hepatitis B e antigen; AFP, alpha-fetoprotein; ALT, alanine aminotransferase; AST, aspartate aminotransferase; TBil, total bilirubin; WBC, white blood cell; BCLC, Barcelona Clinic Liver Cancer; ECOG PS, Eastern Cooperative Oncology Group performance status; ALBI grade, Albumin-Bilirubin grade; MVI, microvascular invasion; PVTT, portal vein tumor thrombosis; DNA, deoxyribonucleic acid; HAIC, hepatic arterial infusion chemotherapy; PD-1 inhibitors, programmed death receptor-1 inhibitors; TACE, transarterial chemoembolization; TKIs, tyrosine kinase inhibitors; pCR, pathological complete response.

staging system, 24 patients (26.4%) were stage A, 27 (29.7%) were stage B, and 40 (44.0%) were stage C. Postoperative pathology revealed that 48 patients had a solitary tumor, and 43 had multiple tumors. The mean tumor size was 10.07 ± 4.18 cm. Portal vein tumor thrombus (PVTT) was present in 28 patients (30.8%), and microvascular invasion (MVI) was observed in 31 patients (34.1%). A pathological complete response (pCR) was achieved in 23 patients (25.3%).

3.2 HBV reactivation

Among the 91 enrolled patients, HBVr occurred in a total of 17 patients (18.7%), with a median time to reactivation of 3 months (range, 1–10 months). Additionally, 19 patients experienced a certain degree of increase in viral load that did not meet the criteria for reactivation. Detailed characteristics of the 17 patients with HBVr are presented in Table 2 and Figure 2. Of these 17 patients, 15 were male. Three patients had undetectable HBV DNA at baseline. Among those with detectable baseline DNA, 12 achieved virological suppression during preoperative antiviral therapy. One patient was HBsAg-negative at baseline. At the onset of HBVr, the median HBV DNA level was 495 IU/mL (range, 109–6,710,000 IU/mL). All 17 patients with reactivation had received antiviral therapy since their initial diagnosis of hepatitis B, with 16 of them taking entecavir. The incidence of HBVr was 16.7% (14/84) in patients with detectable baseline HBV DNA and 42.9% (3/7) in those with undetectable baseline HBV DNA.

3.3 Patterns of HBV reactivation

Among the 17 patients who experienced HBVr, a notable pattern was observed in 12 individuals who had initially achieved virological suppression (from detectable to undetectable) during preoperative antiviral therapy but subsequently showed detectable HBV DNA postoperatively. Furthermore, one HBsAg-negative patient experienced HBsAg seroreversion after surgery. All these patients were receiving ETV during the treatment period and remained HBsAg-positive post-reactivation, except for the single case of seroreversion.

3.4 Univariate and multivariable analyses for HBV reactivation

The results of the univariate and multivariable logistic regression analyses for HBVr are shown in Table 3. Both analyses consistently identified baseline HBV DNA ≥2000 IU/mL as the sole independent risk factor for HBVr (OR 3.939, 95% CI 1.169–13.272; P = 0.027).

3.5 Patient prognosis

The median OS and PFS for the entire cohort of 91 patients were 47.0 months and 23.6 months, respectively (Supplementary Figure S1). The median follow-up time was 28.8 months in the HBVr group and 20.6 months in the non-reactivation group. No deaths were observed in the HBVr group during the follow-up period. The median OS was not reached in the HBVr group, compared to 45.6 months (95% CI 41.7–49.5) in the non-reactivation group (P = 0.117) (Figure 3A). However, the median PFS was significantly shorter in the HBVr group than in the non-reactivation group (12.1 months [95% CI 5.5–18.7] *vs.* 29.2 months [95% CI 23.6–34.7]; P < 0.001) (Figure 3B). These findings suggest that patients in the HBVr group had a higher risk of disease recurrence.

3.6 Univariate and multivariable analyses for PFS and OS

The results of the univariate and multivariable Cox regression analyses for PFS and OS are presented in Table 4. For PFS, univariate analysis identified several significant risk factors:

TABLE 2 Characteristics of patients with hepatitis B virus reactivation.

Patient characteristics					Baseline			At reactivation			
NO	Age/Sex	Types of ICIs	Types of TKIs	Types of interventional therapy	HBsAg	HBV DNA IU/ml	Antiviral treatment	Intervals (months)	HBsAg	HBV DNA IU/ml	Antiviral treatment
1	39/M	Camrelizumab	Lenvatinib	TACE	+	1610	Entecavir	4	+	386	Entecavir
2	46/M	Tislelizumab	Lenvatinib	TACE	+	Undetectable	Entecavir	2	+	180	Entecavir
3	44/M	Tislelizumab	Lenvatinib	HAIC+TACE	+	389	Entecavir	3	+	150	Entecavir
4	47/M	Tislelizumab	Donafenib	HAIC	+	833	Tenofovir	3	+	145	Tenofovir
5	58/M	Camrelizumab	Lenvatinib	HAIC+TACE	+	3670	Entecavir	2	+	362	Entecavir
6	45/M	Tislelizumab	Lenvatinib	HAIC	+	566	Entecavir	8	+	109	Entecavir
7	60/M	Camrelizumab	Lenvatinib	TACE	+	Undetectable	Entecavir	14	+	6710000	Entecavir
8	44/F	Camrelizumab	Lenvatinib	TACE	+	137	Entecavir	10	+	6790	Entecavir
9	42/M	Camrelizumab	Lenvatinib	TACE	–	455	Entecavir	4	+	706	Entecavir
10	45/M	Camrelizumab	Lenvatinib	TACE	+	857	Entecavir	1	+	1500	Entecavir
11	35/M	Camrelizumab	Lenvatinib	TACE	+	47	Entecavir	2	+	526	Entecavir
12	61/M	Camrelizumab	Lenvatinib	TACE	+	Undetectable	Entecavir	2	+	135	Entecavir
13	34/M	Camrelizumab	Lenvatinib	TACE	+	722	Entecavir	2	+	151	Entecavir
14	50/M	Camrelizumab	Lenvatinib	TACE	+	2300	Entecavir	3	+	11500	Entecavir
15	51/M	Tislelizumab	Lenvatinib	HAIC	+	109	Entecavir	4	+	495	Entecavir
16	44/F	Tislelizumab	Lenvatinib	TACE	+	442	Entecavir	5	+	79300	Entecavir
17	45/M	Tislelizumab + Sintilimab	Lenvatinib	HAIC	+	3110000	Entecavir	4	+	737	Entecavir

DNA, deoxyribonucleic acid; F, female; HAIC, hepatic artery infusion chemotherapy; HBV, hepatitis B virus; HBsAg, hepatitis B surface antigen; M, male; TACE, transarterial chemoembolization.

10.3389/fcimb.2025.1598193

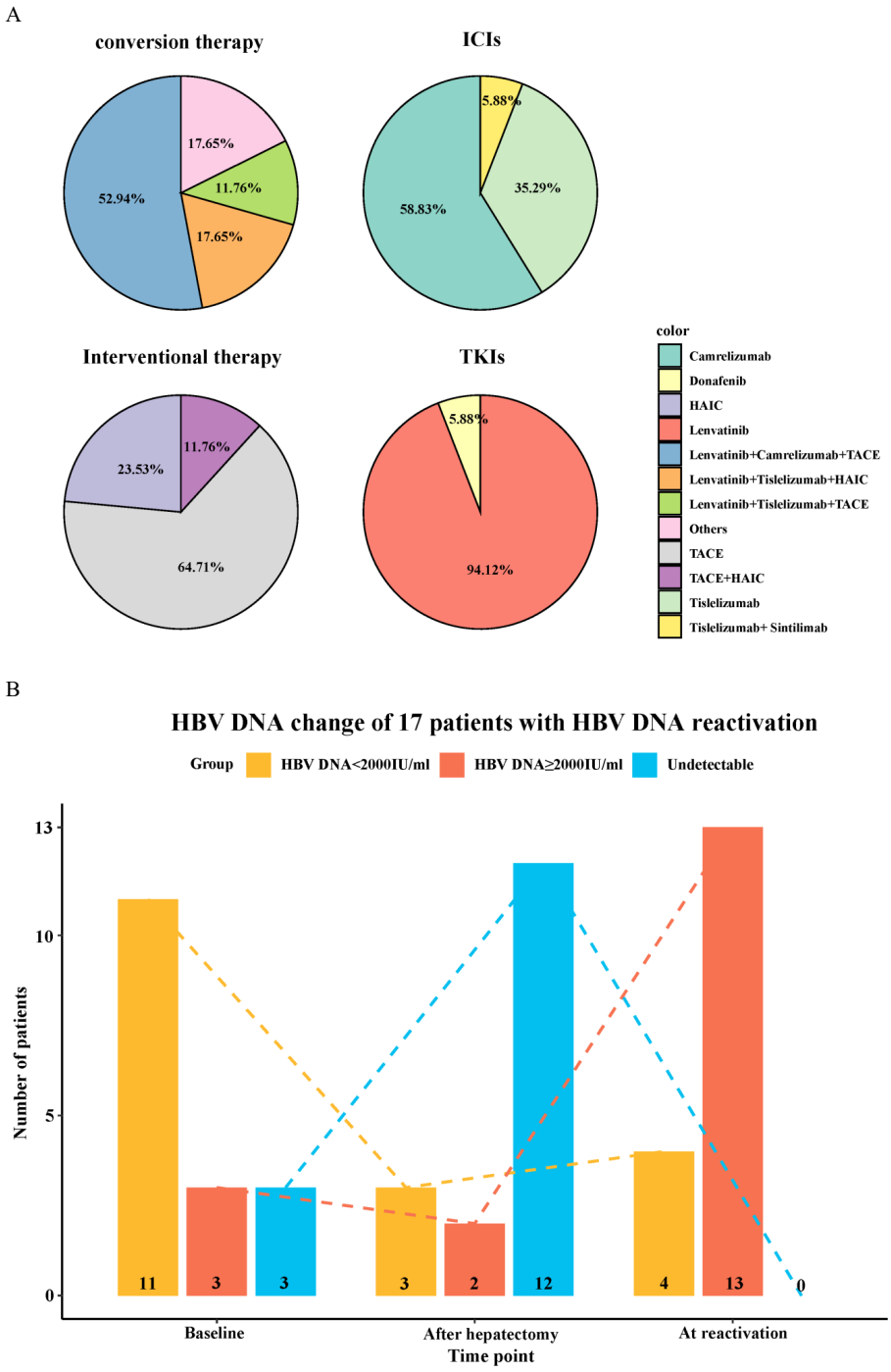

FIGURE 2
Characteristics of patients with hepatitis B virus reactivation. **(A)** Baseline demographics and clinical characteristics of the 17 patients who experienced HBVr. **(B)** Changes in HBV DNA levels over time in the 17 patients with HBVr.

multiple tumors (HR 2.418, 95% CI 1.283–4.557; P = 0.006), tumor diameter ≥10 cm (HR 2.433, 95% CI 1.256–4.714; P = 0.009), baseline HBV DNA ≥2000 IU/mL (HR 2.385, 95% CI 1.227–4.636; P = 0.010), HBVr (HR 3.085, 95% CI 1.623–5.863; P = 0.001), presence of satellite nodules (HR 2.117, 95% CI 1.058–4.236; P = 0.034), and MVI (HR 4.804, 95% CI 2.506–9.210; P < 0.001). pCR was a significant protective factor (HR 0.103, 95% CI 0.025–0.428; P = 0.002). In the multivariable analysis for PFS, multiple tumors (HR 2.584, 95% CI 1.244–5.371; P = 0.011), HBVr (HR 2.427, 95% CI 1.172–5.027; P = 0.017), and MVI (HR 2.303, 95% CI 1.099–4.823; P = 0.027) remained independent risk factors. pCR remained an independent protective factor (HR 0.153, 95% CI 0.035–0.681; P = 0.014) (Figure 4). For OS, both univariate and multivariable analyses identified baseline HBV DNA ≥2000 IU/mL as the sole

TABLE 3 Univariate and multivariate logistic regression analysis of risk factors for hepatitis B virus reactivation.

	Univariate		Multivariate	
	OR(95%CI)	P value	OR(95%CI)	P value
Age (≥50 years)	0.490(0.157-1.531)	0.220		
Sex(female)	0.909(0.175-4.723)	0.910		
BCLC (C)	1.560(0.541-4.497)	0.410		
ECOG (≥1)	0.956(0.332-2.750)	0.934		
HBV DNA (detectable)	0.267(0.054-1.325)	0.106		
HBV DNA (≥2000 IU/ml)	3.939(1.169-13.272)	0.027	3.939(1.169-13.272)	0.027
Child Pugh score (B)	3.750(0.755-18.633)	0.106		
Tumor diameter (≥10cm)	0.990(0.345-2.848)	0.986		
Tumor number (multiple)	0.739(0.254-2.150)	0.579		
PVTT (yes)	0.924(0.291-2.928)	0.893		
MVI (yes)	0.483(0.100-2.337)	0.366		
AFP (≥400ng/ml)	0.905(0.315-2.606)	0.854		
AFP (≥200 ng/ml)	0.870(0.297-2.545)	0.799		
ALT (≥50IU/L)	1.552(0.525-4.589)	0.427		
Albumin (≥35 g/L)	0.771(0.239-2.487)	0.664		
TBil (≥17.1mmol/L)	0.971(0.333-2.832)	0.957		
WBC (≥11*109/L)	0.999(0-0)	1		
Liver cirrhosis (yes)	1.907(0.393-9.262)	0.423		
Antiviral prophylaxis type	2.215(0.261-18.776)	0.466		
Types of TKIs (Lenvatinib)	3.410(0.415-28.045)	0.254		
Types of ICIs (Camrelizumab)	1.150(0.395-3.349)	0.798		
Types of interventional therapy (multiple)	1.840(0.325-10.402)	0.490		

AFP, alpha-fetoprotein; ALBI grade, Albumin-Bilirubin grade; ALT, alanine aminotransferase; AST, aspartate aminotransferase; BCLC, Barcelona Clinic Liver Cancer; DNA, deoxyribonucleic acid; ECOG PS, Eastern Cooperative Oncology Group performance status; HBeAg, hepatitis B e antigen; HBsAg, hepatitis B surface antigen; HBV, hepatitis B virus; MVI, microvascular invasion; PD-1 inhibitors, programmed death receptor-1 inhibitors; pCR, pathological complete response; PVTT, portal vein tumor thrombosis; TBil, total bilirubin; TKIs, tyrosine kinase inhibitors; WBC, white blood cell.

independent risk factor (HR 6.549, 95% CI 1.458–29.408; P = 0.014). The proportional hazards assumption was met for all Cox models, as verified by Schoenfeld residual tests (P > 0.05 for all variables).

4 Discussion

This retrospective study is the first to elucidate the incidence of HBVr and evaluate its prognostic impact in patients with HBV-related HCC who underwent surgical resection following conversion therapy with interventional treatment, TKIs, and ICIs. We found that 17 (18.7%) patients experienced HBVr. Compared to the non-reactivation group, the HBVr group had a significantly shorter PFS, although no significant difference in OS was observed. The lack of a statistically significant OS difference may be attributable to the relatively small sample size, rendering the analysis underpowered. Furthermore, we identified a baseline HBV DNA level ≥2000 IU/mL as an independent risk factor for HBVr. For prognosis, multiple tumors, MVI, and HBVr were independent risk factors for tumor recurrence, whereas pCR was an independent protective factor. A baseline HBV DNA level ≥2000 IU/mL was the sole independent predictor of mortality.

Anti-tumor therapies, including surgery, TACE, HAIC, TKIs, and ICIs, have all been associated with HBVr. In our cohort, HBVr was observed in 18.7% of patients. This incidence is notably higher than that reported in studies of patients receiving combination therapies without subsequent surgery. For instance, the reported HBVr rate in HCC patients undergoing surgical resection with prophylactic antiviral therapy is typically between 1% and 5% (Papatheodoridi et al., 2022). In patients treated with TACE plus targeted and immune therapies, the HBVr rate was 10.1% (Shen et al., 2023), while for those on HAIC plus targeted and immune therapies, it was 7.5% (Yang et al., 2024). The primary cause of HBVr is an imbalance between the host's immune response and viral replication. Surgical resection itself is a known risk factor for HBVr in HBsAg-positive patients, largely due to the surgical stress

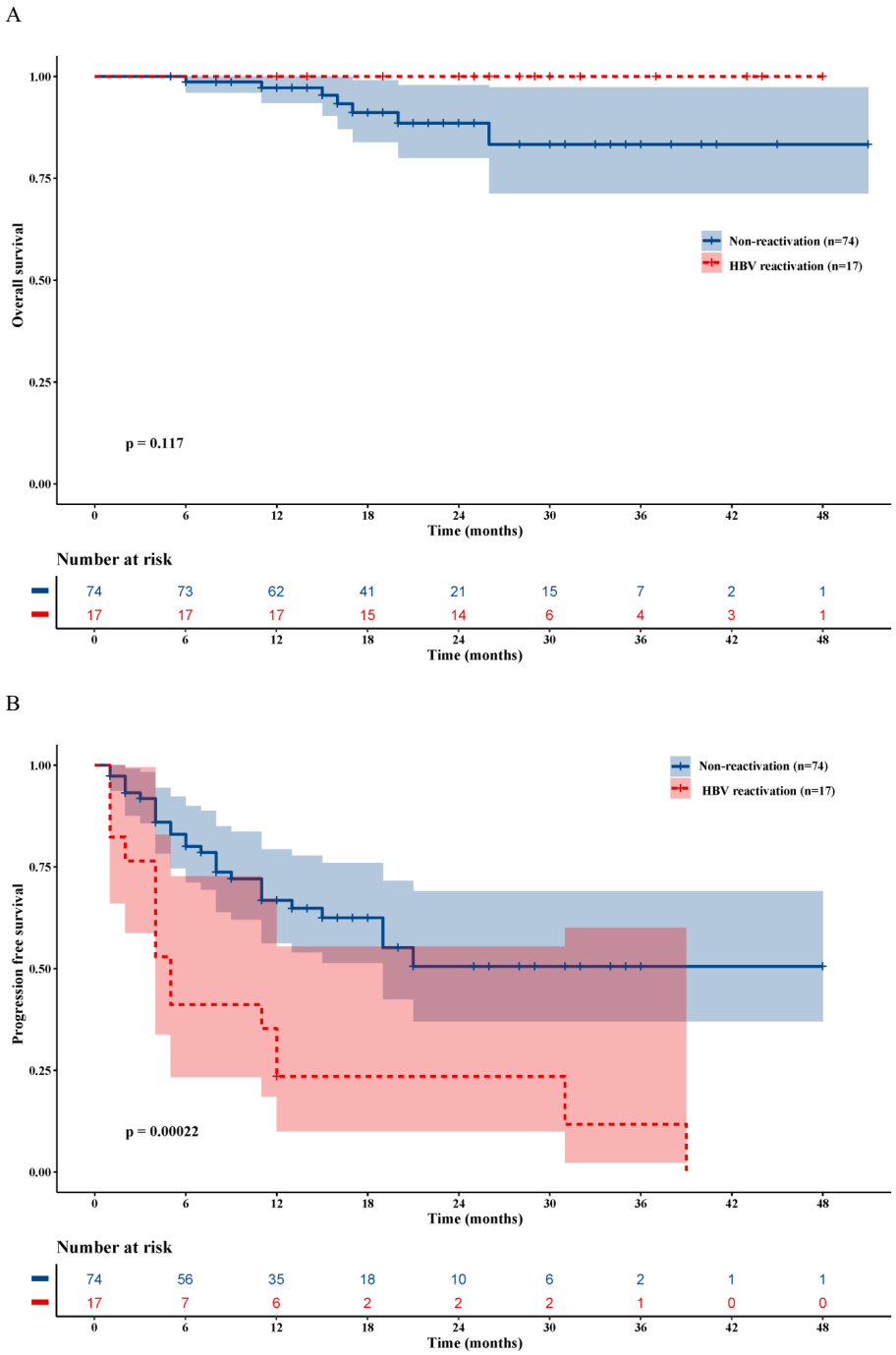

FIGURE 3
Kaplan-Meier survival analysis. **(A)** Overall survival curves for patients with and without HBVr. **(B)** Progression-free survival curves for patients with and without HBVr.

response, which can impair the host's immune status, particularly in cases of concurrent infection or decompensated liver function (Papatheodoridi et al., 2022). The metabolic and immunological stress induced by hepatectomy, along with the acute release of stress hormones and cytokines, creates a transient window of immunosuppression, rendering patients susceptible to HBVr Burpee (Burpee et al., 2002). Moreover, partial hepatectomy can enhance viral replication due to immunosuppression from blood transfusions and ischemia-reperfusion injury (Huang et al., 2012). It is plausible that the combination of immunosuppression from conversion therapy and the subsequent surgical stress synergistically exacerbates immune dysfunction, leading to a higher HBVr rate than either treatment modality alone (Liu et al., 2021). Combination therapy is associated with an increased risk of HBVr. Indeed, several recent studies have identified combination therapy as an independent risk factor for this event (Lei et al., 2023;

10.3389/fcimb.2025.1598193

TABLE 4 Univariate and multivariate Cox regression analysis of independent predictors for progression-free survival and overall survival.

Variables	Progression-free survival						Overall survival					
	Univariate			Multivariate			Univariate			Multivariate		
	HR	95% CI	P	HR	95% CI	P	HR	95% CI	P	HR	95% CI	P
Age, years≥50:<50	0.662	0.352-1.246	0.201				1.115	0.249-4.989	0.887			
Sex, male: female	1.927	0.585-6.347	0.281				23.528	0-1388629.090	0.573			
AFP, μg/L ≥ 400, yes: no	1.061	0.577-1.953	0.848				2.437	0.469-12.653	0.289			
Tumor number, multiple: single	2.418	1.283-4.557	0.006	2.584	1.244-5.371	0.011	2.822	0.546-14.587	0.216			
Liver cirrhosis, yes: no	1.069	0.492-2.323	0.867				0.476	0.092-2.470	0.377			
Diameter, cm, ≥10:< 10	0.411	0.212-0.797	0.009	0.534	0.258-1.102	0.090	0.703	0.157-3.151	0.646			
BCLC staging, C: AB	1.271	0.693-2.331	0.438				6.552	0.787-54.538	0.082			
ECOG, ≥1:0	0.758	0.284-2.022	0.580				0.699	0.258-1.889	0.480			
Total bilirubin, μmol/L	0.999	0.957-1.044	0.981				0.922	0.804-1.058	0.247			
Albumin, g/L	1.012	0.944-1.084	0.743				0.969	0.827-1.135	0.692			
Platelets, 10^9/L	0.999	0.996-1.003	0.702				0.999	0.990-1.007	0.778			
Prothrombin time, s	1.120	0.885-1.417	0.347				0.916	0.550-1.525	0.736			
ALT, U/L,>40:≤40	1.224	0.664-2.258	0.517				0.149	0.018-1.243	0.079			
HBV-DNA, IU/mL, ≥ 2000: < 2000	2.385	1.227-4.636	0.010	1.718	0.734-4.020	0.212	6.549	1.458-29.408	0.014	9.825	2.114-45.667	0.004
HBV reactivation, yes: no	3.085	1.623-5.863	0.001	2.427	1.172-5.027	0.017	0.030	0-42.929	0.344			
History of alcoholism, yes: no	1.035	0.557-1.924	0.913				0.524	0.102-2.706	0.441			
Interventional therapy, Entecavir: Tenofovir	1.687	0.520-5.477	0.384				0.191	0.036-1.002	0.050			
PVTT, yes: no	1.081	0.573-2.042	0.810				2.486	0.555-11.144	0.234			
Large vascular invasion, yes: no	1.177	0.634-2.187	0.606				1.166	0.260-5.236	0.841			
Tumor satellites, yes: no	2.117	1.058-4.236	0.034	0.720	0.320-1.620	0.427	1.544	0.295-8.077	0.607			
pCR, yes: no	0.103	0.025-0.428	0.002	0.153	0.035-0.681	0.014	0.029	0-28.133	0.312			
MVI, yes: no	4.804	2.506-9.210	0.000	2.303	1.099-4.823	0.027	2.450	0.470-12.759	0.287			

AFP, alpha-fetoprotein; ALBI grade, Albumin-Bilirubin grade; ALT, alanine aminotransferase; AST, aspartate aminotransferase; BCLC, Barcelona Clinic Liver Cancer; DNA, deoxyribonucleic acid; ECOG PS, Eastern Cooperative Oncology Group performance status; HBeAg, hepatitis B e antigen; HBsAg, hepatitis B surface antigen; HBV, hepatitis B virus; MVI, microvascular invasion; pCR, pathological complete response; PD-1 inhibitors, programmed death receptor-1 inhibitors; PVTT, portal vein tumor thrombosis; TBil, total bilirubin; TKIs, tyrosine kinase inhibitors; WBC, white blood cell.

Wang et al., 2024). However, the underlying mechanisms for the elevated risk of HBV reactivation in patients undergoing surgical resection after conversion therapy remain to be fully elucidated. We speculate that this may be attributed to the incomplete recovery of host immune function following conversion therapy. This pre-existing immune compromise, when compounded by surgical stress, could lead to further immunosuppression, thereby resulting in a higher incidence of HBV reactivation.

In our study, HBVr occurred in 27.3% (3/11) of patients with baseline HBV DNA ≥2000 IU/mL and 17.5% (14/80) of those with levels <2000 IU/mL. Furthermore, multivariate analysis identified a baseline HBV DNA level of ≥2000 IU/mL as an independent risk factor for HBV reactivation. These findings are consistent with those of several previous reports. For instance, a study on HBV reactivation after radiofrequency ablation in patients with HCC reported that an HBV DNA level ≥2000 IU/mL was a significant risk factor (Liu et al., 2023). The observation that patients with higher HBV DNA levels are more prone to reactivation than those with lower levels has been well-documented in multiple studies (Cholongitas et al., 2018; Wang et al., 2021; Shen et al., 2023). However, some studies have reported no significant association between baseline HBV DNA levels and HBV reactivation in the context of combination therapy (He et al., 2021; Yang et al., 2024). This discrepancy may be attributable to the subsequent surgical intervention following conversion therapy, which could further alter both local and systemic immune statuses. This suggests that different treatment modalities may confer varying

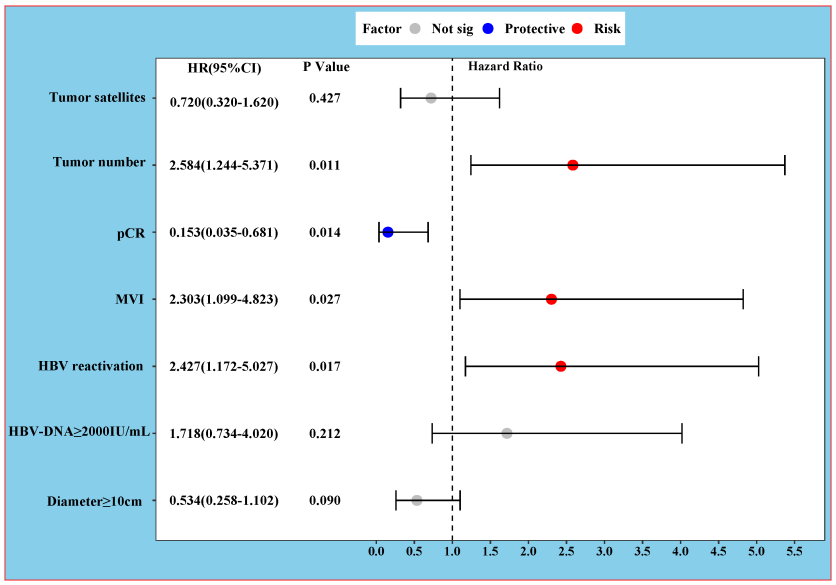

FIGURE 4
Forest Plot of Hazard Ratios for Progression-Free Survival.

risks of HBV reactivation. Despite all patients receiving antiviral prophylaxis, HBVr still occurred. One possible explanation is the development of antiviral resistance resulting from prior treatments (Tenney et al., 2009; Guo et al., 2018). Another potential reason could be the disruption of antiviral therapy due to poor patient adherence, where patients fail to take their medication regularly. This phenomenon is not uncommon and has been documented in numerous studies (Jang, 2014; Shen et al., 2023; Yang et al., 2024). Our results showed no definitive link between the choice of specific interventional, targeted, or immune agents and HBVr risk. This suggests that the profound immunological insult from surgery may overshadow the differential effects of various conversion regimens. Therefore, for patients with high baseline HBV DNA levels, adopting a more potent antiviral strategy perioperatively may be warranted.

Histopathological features of the tumor were strongly associated with PFS. Our analysis confirmed that multiple tumors and MVI are independent risk factors for postoperative recurrence, while pCR is a strong protective factor. These findings align with established literature, where tumor size, multifocality, satellite nodules, and MVI have been consistently identified as predictors of a higher recurrence risk (Imamura et al., 2003; Sala et al., 2004; Ishizawa et al., 2008; Schiffman et al., 2010; Fuks et al., 2012; Li et al., 2013). Interestingly, we did not find a significant association between tumor size or satellite nodules and recurrence, which might be due to the larger tumor burden in our cohort compared to previous studies, or perhaps the preoperative conversion therapy altered the biological characteristics of the tumors.

Crucially, our study identified HBVr as an independent risk factor for postoperative tumor recurrence, corroborating findings from other recent studies (Lei et al., 2023; Yang et al., 2024). This association likely reflects a vicious cycle between the virus and the tumor. On one hand, HBVr involves a surge in viral replication and antigen release, triggering a robust inflammatory response. This chronic inflammation, often involving the activation of NF-κB and MAPK signaling pathways, creates a microenvironment conducive to hepatocellular mutagenesis and epigenetic alterations, thereby promoting HCC progression (Feitelson et al., 2022; Sivasudhan et al., 2022). This inflammatory state can also foster an immunosuppressive milieu by recruiting regulatory T cells (Tregs) and promoting anti-inflammatory cytokines, which impair immune surveillance (Chekol Abebe et al., 2021). On the other hand, the immunosuppressive environment created by tumor progression can facilitate HBVr. Tumors can upregulate immunosuppressive molecules like TGF-β and PD-L1 and pro-angiogenic factors like VEGF, which collectively inhibit T cell and NK cell function and promote the accumulation of Tregs and myeloid-derived suppressor cells (MDSCs) (Wang et al., 2011; Kalluri, 2016; Yang et al., 2018). Given this interplay, we propose that a more aggressive antiviral strategy should be considered during the perioperative period to minimize the risk of HBVr and, consequently, reduce the likelihood of tumor recurrence. However, the optimal timing to de-escalate back to a standard antiviral regimen postoperatively requires further investigation.

A high HBV DNA load is known to correlate with poor prognosis in HCC patients. In our study, a baseline HBV DNA level ≥2000 IU/mL was the sole independent risk factor for OS, although the wide confidence interval (HR 6.549, 95% CI 1.458–29.408) suggests that this finding may be limited by the sample size. This association has been repeatedly documented in the literature (Yu and Kim, 2014; Sun et al., 2021; Yang et al., 2024). We also observed a high HBVr rate (42.9%) among patients with undetectable baseline HBV DNA. This underscores the persistence of cccDNA in hepatocytes, which serves as a template for reactivation even when serum DNA is suppressed by nucleos(t)ide analogues (NAs) (Xia and Guo, 2020). Theoretically, even a single copy of cccDNA can lead to viral rebound and trigger chronic

inflammation, perpetuating the malignant cycle of HBV and HCC (Shi and Zheng, 2020). Contrary to some previous reports, we did not find an association between tumor pathology or HBVr and OS. This could be due to the heterogeneity of post-recurrence treatments received by patients in our cohort, which would significantly influence survival outcomes. The impact of post-recurrence therapies in this specific patient population warrants further investigation.

This study has several limitations. First, as a single-center retrospective study with a relatively small sample size, selection bias cannot be ruled out. Second, we did not perform mechanistic studies to elucidate the biological links between HBVr and the combined treatment modality. Basic research is needed to explore these mechanisms. Finally, the screening intervals for HBV DNA and serological markers were not standardized, which may have led to delays in detecting some endpoint events. Therefore, large-scale, prospective, multicenter, randomized controlled trials are warranted to validate our conclusions.

5 Conclusion

This study indicates that in patients with HBV-related HCC undergoing surgery after conversion therapy, a high baseline HBV DNA level may lead to HBV reactivation and adversely affect long-term survival. Patients who experience HBV reactivation have a higher risk of recurrence than those who do not. Therefore, antiviral therapy and HBV DNA monitoring should be administered to patients with HBV-related HCC during conversion therapy and throughout the perioperative period.

Data availability statement

The datasets presented in this study can be found in online repositories. The names of the repository/repositories and accession number(s) can be found in the article/Supplementary Material.

Ethics statement

The studies involving humans were approved by Guangxi Medical University Cancer Hospital Science and Technology Ethical Review Committee. The studies were conducted in accordance with the local legislation and institutional requirements. Written informed consent for participation was not required for this study in accordance with the national legislation and the institutional requirements.

Author contributions

SX: Software, Conceptualization, Writing – original draft, Investigation, Formal analysis, Project administration, Data curation, Methodology. QP: Methodology, Investigation, Data curation, Writing – original draft, Software. MW: Methodology, Data curation, Writing – review & editing, Funding acquisition. DL: Project administration, Validation, Writing – review & editing. DY: Project administration, Data curation, Writing – original draft, Investigation. TB: Investigation, Conceptualization, Validation, Writing – review & editing. XW: Writing – review & editing, Validation, Supervision. ZT: Writing – review & editing, Project administration, Funding acquisition, Investigation, Validation, Conceptualization. FW: Conceptualization, Resources, Project administration, Writing – review & editing.

Funding

The author(s) declare that financial support was received for the research and/or publication of this article. This work was supported by National Natural Science Foundation of China (82360537), Guangxi Natural Science Foundation Project (2025GXNSFBA069386), Guangxi Key Laboratory of Early Prevention and Treatment for Regional High Frequency Tumor (GKE-ZZ202309), Youth Fund Project of Guangxi Medical University Cancer Hospital (2024-02) and Guangxi Science and Technology Program under Grant No.AD25069077.

Acknowledgments

The authors acknowledge and express their deepest gratitude to the participants of this research.

Conflict of interest

The authors declare that the research was conducted in the absence of any commercial or financial relationships that could be construed as a potential conflict of interest.

Generative AI statement

The author(s) declare that no Generative AI was used in the creation of this manuscript.

Publisher's note

Supplementary material

The Supplementary Material for this article can be found online at: https://www.frontiersin.org/articles/10.3389/fcimb.2025.1598193/full#supplementary-material

References

Burpee, S. E., Kurian, M., Murakame, Y., Benevides, S., and Gagner, M. (2002). The metabolic and immune response to laparoscopic versus open liver resection. *Surg. Endosc* 16, 899–904. doi: 10.1007/s00464-001-8122-x

Cai, M., Huang, W., Huang, J., Shi, W., Guo, Y., Liang, L., et al. (2022). Transarterial chemoembolization combined with lenvatinib plus PD-1 inhibitor for advanced hepatocellular carcinoma: A retrospective cohort study. *Front. Immunol.* 13. doi: 10.3389/fimmu.2022.848387

Chekol Abebe, E., Asmamaw Dejenie, T., Mengie Ayele, T., Dagnew Baye, N., Agegnehu Teshome, A., and Tilahun Muche, Z. (2021). The role of regulatory B cells in health and diseases: A systemic review. *J. Inflammation Res.* 14, 75–84. doi: 10.2147/jir.S286426

Cholongitas, E., Haidich, A. B., Apostolidou-Kiouti, F., Chalevas, P., and Papatheodoridis, G. V. (2018). Hepatitis B virus reactivation in HBsAg-negative, anti-HBc-positive patients receiving immunosuppressive therapy: a systematic review. *Ann. Gastroenterol.* 31, 480–490. doi: 10.20524/aog.2018.0266

Dan, J. Q., Zhang, Y. J., Huang, J. T., Chen, M. S., Gao, H. J., Peng, Z. W., et al. (2013). Hepatitis B virus reactivation after radiofrequency ablation or hepatic resection for HBV-related small hepatocellular carcinoma: a retrospective study. *Eur. J. Surg. Oncol.* 39, 865–872. doi: 10.1016/j.ejso.2013.03.020

Eisenhauer, E. A., Therasse, P., Bogaerts, J., Schwartz, L. H., Sargent, D., Ford, R., et al. (2009). New response evaluation criteria in solid tumours: revised RECIST guideline (version 1.1). *Eur. J. Cancer* 45, 228–247. doi: 10.1016/j.ejca.2008.10.026

Feitelson, M. A., Arzumanyan, A., Spector, I., and Medhat, A. (2022). Hepatitis B x (HBx) as a component of a functional cure for chronic hepatitis B. *Biomedicines* 10. doi: 10.3390/biomedicines10092210

Fu, Y., Peng, W., Zhang, W., Yang, Z., Hu, Z., Pang, Y., et al. (2023). Induction therapy with hepatic arterial infusion chemotherapy enhances the efficacy of lenvatinib and pd1 inhibitors in treating hepatocellular carcinoma patients with portal vein tumor thrombosis. *J. Gastroenterol.* 58, 413–424. doi: 10.1007/s00535-023-01976-x

Fuks, D., Dokmak, S., Paradis, V., Diouf, M., Durand, F., and Belghiti, J. (2012). Benefit of initial resection of hepatocellular carcinoma followed by transplantation in case of recurrence: an intention-to-treat analysis. *Hepatology* 55, 132–140. doi: 10.1002/hep.24680

Guo, X., Wu, J., Wei, F., Ouyang, Y., Li, Q., Liu, K., et al. (2018). Trends in hepatitis B virus resistance to nucleoside/nucleotide analogues in North China from 2009-2016: A retrospective study. *Int. J. Antimicrob. Agents* 52, 201–209. doi: 10.1016/j.ijantimicag.2018.04.002

He, M. K., Peng, C., Zhao, Y., Liang, R. B., Lai, Z. C., Kan, A., et al. (2021). Comparison of HBV reactivation between patients with high HBV-DNA and low HBV-DNA loads undergoing PD-1 inhibitor and concurrent antiviral prophylaxis. *Cancer Immunol. Immunother.* 70, 3207–3216. doi: 10.1007/s00262-021-02911-w

Hoofnagle, J. H. (2009). Reactivation of hepatitis B. *Hepatology* 49, S156–S165. doi: 10.1002/hep.22945

Huang, L., Li, J., Lau, W. Y., Yan, J., Zhou, F., Liu, C., et al. (2012). Perioperative reactivation of hepatitis B virus replication in patients undergoing partial hepatectomy for hepatocellular carcinoma. *J. Gastroenterol. Hepatol.* 27, 158–164. doi: 10.1111/j.1440-1746.2011.06888.x

Imamura, H., Matsuyama, Y., Tanaka, E., Ohkubo, T., Hasegawa, K., Miyagawa, S., et al. (2003). Risk factors contributing to early and late phase intrahepatic recurrence of hepatocellular carcinoma after hepatectomy. *J. Hepatol.* 38, 200–207. doi: 10.1016/s0168-8278(02)00360-4

Ishizawa, T., Hasegawa, K., Aoki, T., Takahashi, M., Inoue, Y., Sano, K., et al. (2008). Neither multiple tumors nor portal hypertension are surgical contraindications for hepatocellular carcinoma. *Gastroenterology* 134, 1908–1916. doi: 10.1053/j.gastro.2008.02.091

Jang, J. W. (2014). Hepatitis B virus reactivation in patients with hepatocellular carcinoma undergoing anti-cancer therapy. *World J. Gastroenterol.* 20, 7675–7685. doi: 10.3748/wjg.v20.i24.7675

Ju, S., Zhou, C., Yang, C., Wang, C., Liu, J., Wang, Y., et al. (2021). Apatinib plus camrelizumab with/without chemoembolization for hepatocellular carcinoma: A real-world experience of a single center. *Front. Oncol.* 11. doi: 10.3389/fonc.2021.835889

Kalluri, R. (2016). The biology and function of fibroblasts in cancer. *Nat. Rev. Cancer* 16, 582–598. doi: 10.1038/nrc.2016.73

Kulik, L. M., Atassi, B., van Holsbeeck, L., Souman, T., Lewandowski, R. J., Mulcahy, M. F., et al. (2006). Yttrium-90 microspheres (TheraSphere) treatment of unresectable hepatocellular carcinoma: downstaging to resection, RFA and bridge to transplantation. *J. Surg. Oncol.* 94, 572–586. doi: 10.1002/jso.20609

Lau, G., Yu, M. L., Wong, G., Thompson, A., Ghazinian, H., Hou, J. L., et al. (2021). APASL clinical practice guideline on hepatitis B reactivation related to the use of immunosuppressive therapy. *Hepatol. Int.* 15, 1031–1048. doi: 10.1007/s12072-021-10239-x

Lei, J., Yan, T., Zhang, L., Chen, B., Cheng, J., Gao, X., et al. (2023). Comparison of hepatitis B virus reactivation in hepatocellular carcinoma patients who received tyrosine kinase inhibitor alone or together with programmed cell death protein-1 inhibitors. *Hepatol. Int.* 17, 281–290. doi: 10.1007/s12072-022-10450-4

Lewandowski, R. J., Kulik, L. M., Riaz, A., Senthilnathan, S., Mulcahy, M. F., Ryu, R. K., et al. (2009). A comparative analysis of transarterial downstaging for hepatocellular carcinoma: chemoembolization versus radioembolization. *Am. J. Transplant.* 9, 1920–1928. doi: 10.1111/j.1600-6143.2009.02695.x

Li, S. H., Wei, W., Guo, R. P., Shi, M., Guo, Z. X., Chen, Z. Y., et al. (2013). Long-term outcomes after curative resection for patients with macroscopically solitary hepatocellular carcinoma without macrovascular invasion and an analysis of prognostic factors. *Med. Oncol.* 30, 696. doi: 10.1007/s12032-013-0696-3

Liu, K. X., Hong, J. G., Wu, R., Dong, Z. R., Yang, Y. F., Yan, Y. C., et al. (2021). Clinical benefit of antiviral agents for hepatocellular carcinoma patients with low preoperative HBV-DNA loads undergoing curative resection: A meta-analysis. *Front. Oncol.* 11. doi: 10.3389/fonc.2021.605648

Liu, J., Shen, H., Huang, S., Lin, J., Yan, Z., Qian, G., et al. (2023). Antiviral therapy inhibited HBV-reactivation and improved long-term outcomes in patients who underwent radiofrequency ablation for HBV-related hepatocellular carcinoma. *World J. Surg. Oncol.* 21, 42. doi: 10.1186/s12957-023-02921-1

Llovet, J. M., and Lencioni, R. (2020). mRECIST for HCC: Performance and novel refinements. *J. Hepatol.* 72, 288–306. doi: 10.1016/j.jhep.2019.09.026

Mysore, K. R., and Leung, D. H. (2018). Hepatitis B and C. *Clin. Liver Dis.* 22, 703–722. doi: 10.1016/j.cld.2018.06.002

Papatheodoridi, M., Tampaki, M., Lok, A. S., and Papatheodoridis, G. V. (2022). Risk of HBV reactivation during therapies for HCC: A systematic review. *Hepatology* 75, 1257–1274. doi: 10.1002/hep.32241

Papatheodoridis, G. V., Lekakis, V., Voulgaris, T., Lampertico, P., Berg, T., Chan, H. L. Y., et al. (2022). Hepatitis B virus reactivation associated with new classes of immunosuppressants and immunomodulators: A systematic review, meta-analysis, and expert opinion. *J. Hepatol.* 77, 1670–1689. doi: 10.1016/j.jhep.2022.07.003

Rumgay, H., Arnold, M., Ferlay, J., Lesi, O., Cabasag, C. J., Vignat, J., et al. (2022). Global burden of primary liver cancer in 2020 and predictions to 2040. *J. Hepatol.* 77, 1598–1606. doi: 10.1016/j.jhep.2022.08.021

Sala, M., Fuster, J., Llovet, J. M., Navasa, M., Solé, M., Varela, M., et al. (2004). High pathological risk of recurrence after surgical resection for hepatocellular carcinoma: an indication for salvage liver transplantation. *Liver Transpl* 10, 1294–1300. doi: 10.1002/lt.20202

Schiffman, S. C., Woodall, C. E., Kooby, D. A., Martin, R. C., Staley, C. A., Egnatashvili, V., et al. (2010). Factors associated with recurrence and survival following hepatectomy for large hepatocellular carcinoma: a multicenter analysis. *J. Surg. Oncol.* 101, 105–110. doi: 10.1002/jso.21461

Shen, J., Wang, X., Wang, N., Wen, S., Yang, G., Li, L., et al. (2023). HBV reactivation and its effect on survival in HBV-related hepatocarcinoma patients undergoing transarterial chemoembolization combined with tyrosine kinase inhibitors plus immune checkpoint inhibitors. *Front. Cell Infect. Microbiol.* 13. doi: 10.3389/fcimb.2023.1179689

Shi, Y., and Zheng, M. (2020). Hepatitis B virus persistence and reactivation. *Bmj* 370, m2200. doi: 10.1136/bmj.m2200

Shindoh, J., Kawamura, Y., Kobayashi, Y., Kobayashi, M., Akuta, N., Okubo, S., et al. (2021). Prognostic impact of surgical intervention after lenvatinib treatment for advanced hepatocellular carcinoma. *Ann. Surg. Oncol.* 28, 7663–7672. doi: 10.1245/s10434-021-09974-0

Sivasudhan, E., Blake, N., Lu, Z., Meng, J., and Rong, R. (2022). Hepatitis B viral protein HBx and the molecular mechanisms modulating the hallmarks of hepatocellular carcinoma: A comprehensive review. *Cells* 11. doi: 10.3390/cells11040741

Sun, F., Liu, Z., and Wang, B. (2021). Correlation between low-level viremia and hepatitis B-related hepatocellular carcinoma and recurrence: a retrospective study. *BMC Cancer* 21, 1103. doi: 10.1186/s12885-021-08483-3

Sung, H., Ferlay, J., Siegel, R. L., Laversanne, M., Soerjomataram, I., Jemal, A., et al. (2021). Global cancer statistics 2020: GLOBOCAN estimates of incidence and mortality worldwide for 36 cancers in 185 countries. *CA Cancer J. Clin.* 71, 209–249. doi: 10.3322/caac.21660

Tenney, D. J., Rose, R. E., Baldick, C. J., Pokornowski, K. A., Eggers, B. J., Fang, J., et al. (2009). Long-term monitoring shows hepatitis B virus resistance to entecavir in nucleoside-naïve patients is rare through 5 years of therapy. *Hepatology* 49, 1503–1514. doi: 10.1002/hep.22841

Voican, C. S., Mir, O., Loulergue, P., Dhooge, M., Brezault, C., Dréanic, J., et al. (2016). Hepatitis B virus reactivation in patients with solid tumors receiving systemic anticancer treatment. *Ann. Oncol.* 27, 2172–2184. doi: 10.1093/annonc/mdw414

Wang, B. J., Bao, J. J., Wang, J. Z., Wang, Y., Jiang, M., Xing, M. Y., et al. (2011). Immunostaining of PD-1/PD-Ls in liver tissues of patients with hepatitis and hepatocellular carcinoma. *World J. Gastroenterol.* 17, 3322–3329. doi: 10.3748/wjg.v17.i28.3322

Wang, R., Tan, G., Lei, D., Li, Y., Gong, J., Tang, Y., et al. (2024). Risk of HBV reactivation in HCC patients undergoing combination therapy of PD-1 inhibitors and angiogenesis inhibitors in the antiviral era. *J. Cancer Res. Clin. Oncol.* 150, 158. doi: 10.1007/s00432-024-05677-7

Wang, X., Yang, X., Chen, F., Wu, S., Song, Z., and Fei, J. (2021). Hepatitis B virus reactivation potential risk factors in hepatocellular carcinoma via transcatheter arterial chemoembolization: A retrospective research. *Can. J. Gastroenterol. Hepatol.* 2021, 8864655. doi: 10.1155/2021/8864655

Xia, Y., and Guo, H. (2020). Hepatitis B virus cccDNA: Formation, regulation and therapeutic potential. *Antiviral Res.* 180, 104824. doi: 10.1016/j.antiviral.2020.104824

Xie, Z. B., Zhu, S. L., Peng, Y. C., Chen, J., Wang, X. B., Ma, L., et al. (2015). Postoperative hepatitis B virus reactivation and surgery-induced immunosuppression in patients with hepatitis B-related hepatocellular carcinoma. *J. Surg. Oncol.* 112, 634–642. doi: 10.1002/jso.24044

Yang, Z., Guan, R., Fu, Y., Hu, D., Zhou, Z., Chen, M., et al. (2024). Risk of hepatitis B virus reactivation and its effect on survival in advanced hepatocellular carcinoma patients treated with hepatic arterial infusion chemotherapy and lenvatinib plus programmed death receptor-1 inhibitors. *Front. Cell Infect. Microbiol.* 14. doi: 10.3389/fcimb.2024.1336619

Yang, J., Yan, J., and Liu, B. (2018). Targeting VEGF/VEGFR to modulate antitumor immunity. *Front. Immunol.* 9. doi: 10.3389/fimmu.2018.00978

Yu, S. J., and Kim, Y. J. (2014). Hepatitis B viral load affects prognosis of hepatocellular carcinoma. *World J. Gastroenterol.* 20, 12039–12044. doi: 10.3748/wjg.v20.i34.12039

Zhu, H. D., Li, H. L., Huang, M. S., Yang, W. Z., Yin, G. W., Zhong, B. Y., et al. (2023). Transarterial chemoembolization with PD-(L)1 inhibitors plus molecular targeted therapies for hepatocellular carcinoma (CHANCE001). *Signal Transduct Target Ther.* 8, 58. doi: 10.1038/s41392-022-01235-0

frontiers | Frontiers in Oncology

TYPE Case Report
PUBLISHED 11 September 2025
DOI 10.3389/fonc.2025.1637847

OPEN ACCESS

EDITED BY
Sherif El-Kafrawy,
King Abdulaziz University, Saudi Arabia

REVIEWED BY
Andreas Recke,
University of Lübeck, Germany
Cheng Zeng,
Chinese Academy of Medical Sciences and Peking Union Medical College, China
Rajesh Kumar,
All India Institute of Medical Sciences Jodhpur, India

*CORRESPONDENCE
Antonio David Lázaro Sánchez
anlazaro@hotmail.com

RECEIVED 29 May 2025
ACCEPTED 29 August 2025
PUBLISHED 11 September 2025

CITATION
Noblejas Quiles CT, Macías Cerrolaza JA, Benitez Fuentes JD, López Gómez L, Sánchez Cánovas M, Nevado Rodríguez M, Martín Cascón M, Vigueras Campuzano I, Chaves Benito A and Lázaro Sánchez AD (2025) Atezolizumab-induced vanishing bile duct syndrome: a case report. *Front. Oncol.* 15:1637847. doi: 10.3389/fonc.2025.1637847

Atezolizumab-induced vanishing bile duct syndrome: a case report

Carlos Tomás Noblejas Quiles[1], José Antonio Macías Cerrolaza[2], Javier David Benitez Fuentes[3], Laura López Gómez[4], Manuel Sánchez Cánovas[2], María Nevado Rodríguez[2], Miguel Martín Cascón[1], Isabel Vigueras Campuzano[1], Asunción Chaves Benito[5] and Antonio David Lázaro Sánchez[2]*

[1]Department of Internal Medicine, Morales Meseguer General University Hospital, Murcia, Spain, [2]Department of Medical Oncology, Morales Meseguer General University Hospital, Murcia, Spain, [3]Department of Medical Oncology, Elche General University Hospital, Alicante, Spain, [4]Department of Intensive Care Unit, Morales Meseguer General University Hospital, Murcia, Spain, [5]Department of Pathological Anatomy, Morales Meseguer General University Hospital, Murcia, Spain

Vanishing bile duct syndrome (VBDS) is a rare but potentially fatal cause of intrahepatic cholestasis, usually associated with autoimmune, infectious or drug-induced etiologies. We present the first documented case of VBDS induced by Atezolizumab, an immune checkpoint inhibitor approved as adjuvant therapy in resected stage II-IIIA non-small cell lung cancer. A 63-year-old man developed cholestatic liver injury after three cycles of Atezolizumab, with progressive jaundice and elevated bilirubin despite immunosuppressive therapy. The diagnosis was confirmed by liver biopsy, which revealed intrahepatic bile duct leakage in more than 50% of the portal tracts. Despite initial stabilization, the patient's bilirubin levels continued to rise and liver transplantation was contraindicated. He was discharged with immunosuppressive and supportive treatment, under close follow-up. This case highlights the need for greater clinical awareness of rare immunotherapy-associated immune-mediated hepatotoxicities, and underlines the importance of histological confirmation in severe or atypical presentations.

KEYWORDS

Vanishing bile duct syndrome, Atezolizumab, immune-related adverse events, non-small cell lung cancer, case report

Introduction

Lung cancer is the leading cause of cancer deaths worldwide, with an estimated incidence of 234,580 new cases and mortality up to 125,070 in the United States in 2024 (1, 2).

According to histological classification, non-small cell lung cancer (NSCLC) is the most common type (85%) (3). Surgery followed by chemotherapy has classically been the standard treatment for NSCLC, both in early and locally advanced stages (II-IIIA).

However, based on the results of the phase III IMpower 010 study, adjuvant Atezolizumab has been approved for use for one year after chemotherapy in patients with resected stage II-IIIA lung cancer without EGFR or ALK alterations, and with PD-L1 expression ≥50%. This strategy offers an increase in disease-free survival and thus redefines the therapeutic paradigm in this subgroup of patients (4, 5).

Although immunotherapy has been a true revolution in cancer treatment, its growing and recent application in oncology has revealed adverse effects whose frequency and long-term impact have yet to be clearly determined. This represents a problem both at present and in the near future, as the emergence of immune-mediated toxicities could restrict the available therapeutic options and consequently jeopardize the continuity of cancer treatment.

In this context, immune checkpoint inhibitor-induced liver damage is the third most frequent immune-mediated adverse event (15%), after dermatological and gastrointestinal toxicity. Although its incidence with these drugs in monotherapy varies between 5-10%, cases of severe hepatotoxicity are less common, affecting less than 2% of the patients (6).

Clinically, liver damage usually presents as a hepatocellular pattern in 65-80%, with asymptomatic hepatitis being the most common form, followed by a cholestatic pattern in 10-25% of the cases (7). Within this latter pattern, an unusual but potentially serious entity stands out: vanishing bile duct syndrome, whose rarity and clinical relevance justify the publication of this case.

Case report

This is a 63-year-old male with a history of pharmacologically controlled arterial hypertension and type 2 diabetes mellitus, with a significant smoking history corresponding to a 40 pack-year cumulative exposure. The patient was evaluated by Internal Medicine in April 2023 for constitutional syndrome accompanied by diarrhea with hematic debris.

The initial study was based on a thoraco-abdomino-pelvic CT scan, which showed a solitary 7mm pulmonary nodule in the right upper lobe (RUL), and a colonoscopy showing signs of mild aphthous ileitis, suggesting the possibility of Crohn's disease.

In May 2024, lobectomy of the RUL was performed with mediastinal lymph node sampling by videothoracoscopy (VATS), with a definitive diagnosis of pulmonary adenocarcinoma (ADC) pT1bN2M0, PD-L1 49%, triple negative, for which he was referred to Medical Oncology in June 2024. Simultaneously, he was studied by the Digestive Department and the diagnosis of Crohn's disease could not be confirmed.

In July 2024, adjuvant chemotherapy was started with Cisplatin 80 mg/m^2 and Pemetrexed 500 mg/m^2 every three weeks for four cycles, during which time the diarrhea ceased and there was a tendency towards constipation. In October 2024, he was started on Atezolizumab 1875 mg subcutaneous injection every three weeks. However, after the third cycle the hematochezia reappeared, leading to a new re- evaluation colonoscopy in December 2024 and discontinuation of treatment.

Colonoscopy findings were compatible with distal ulcerative colitis, ruling out cytomegalovirus infection. Mesalazine, both oral and topical, was prescribed and, given the cases of Atezolizumab-induced ulcerative colitis reported in the literature (8), immune-mediated toxicity was suspected.

However, the clinical situation worsened, with an increase in the number of bowel movements, abdominal pain and the appearance of febrile peaks, leading to several visits to the emergency department. At the end of January, methylprednisolone 150 mg/day oral pulses were prescribed on an outpatient basis for three days, during which time the patient remained afebrile. In addition, Metronidazole 500mg/12h was added for seven days with transient improvement of the gastrointestinal symptoms.

Finally, at the beginning of February, he consulted the emergency department again due to recurrence of fever and stools with pathological products. Blood tests showed only an elevation of liver transaminases 10 times the upper limit of normal. Suspicion of acute hepatitis led to admission (Figure 1).

During his hospital stay, in addition to persistent fever, the patient developed mucocutaneous jaundice, choluria and acholia, with rapidly progressive cholestasis and mixed hyperbilirubinemia at the expense of direct bilirubin.

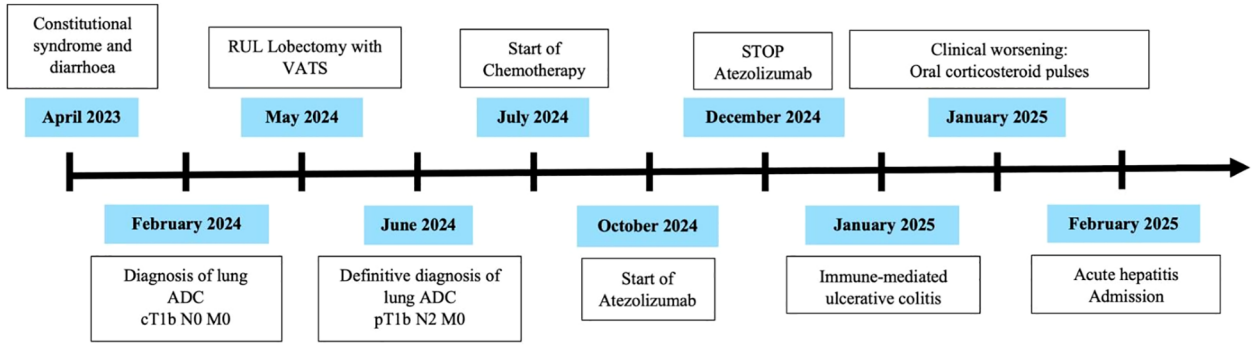

FIGURE 1
Timeline of clinical events.

Firstly, after two pairs of blood cultures, empirical antibiotherapy was administered with Piperacillin-tazobactam 4/0.5g/6h and all possible hepatotoxic drugs were suspended. A complete blood test was performed with autoimmunity, antinuclear antibodies (ANA), anti-neutrophil cytoplasmic antibodies (ANCA), liver and kidney microsomal type 1 antibodies (LKM-1), anti-mitochondrial antibodies (AMA) and anti- smooth muscle antibodies (SMA), as well as immunoglobulin levels. These tests proved to be normal and viral serology was carried out, resulting negative.

After the initial complementary tests, an abdomino-pelvic ultrasound and a magnetic resonance cholangiopancreatography, no evidence of choledocholithiasis or intra- or extrahepatic bile duct dilation was found. However, the distal portion of the intrapancreatic common bile duct could not be visualized in detail and minimal ectasia of the Wirsung immediately proximal to the papilla was observed, so the study needed to be completed with an echo-endoscopy. The latter revealed a lymphadenopathy located in the pancreatic head, for which fine-needle aspiration was performed and the cytological evaluation resulted negative for malignancy.

Nevertheless, given a liver profile that only worsened at the expense of a cholestatic pattern (Figure 2) with no dilatation of the biliary tree, along with the high suspicion of probable immune-mediated hepatitis, a liver biopsy was requested.

Afterwards, intravenous methylprednisolone 250 mg pulses were prescribed for 3 days and, after the first round, there was a decrease in bilirubin levels, which remained at a plateau (Figure 3). Considering this possible initial response, the administration of 250 mg intravenous methylprednisolone was repeated for another three days followed by Prednisone 30 mg/day. Immunosuppressive treatment was also administered with oral mycophenolate mofetil in increasing doses until reaching 1,000 mg every 12 hours. Clinically, the patient presented only mild pruritus, with no associated encephalopathy or coagulopathy.

The anatomopathological results of the liver biopsy confirmed the diagnosis of vanishing bile duct syndrome (Figure 4) induced by Atezolizumab, so ursodeoxycholic acid was started at a dose of 15mg/kg/12h with disappearance of pruritus, as well as intravenous vitamin K 10mg daily and oral calcium and vitamin D supplements.

Despite the initial improvement, bilirubin levels continued to rise rapidly and the case was discussed with the Liver Transplant Committee who, given the high risk of recurrence (70% at 5 years) and the need for a 5-year disease-free period (9), considered that the patient was not a candidate and therefore contraindicated this therapeutic alternative.

Finally, given his clinical stability, although with a guarded prognosis, the patient was discharged from the hospital with oral Prednisone 20 mg/24h, Mycophenolate Mofetil 1.000mg/12h, ursodeoxycholic acid 300mg/8h, prophylaxis with Trimethoprim/sulfamethoxazole 160/800mg/12h three times a week and oral calcium and vitamin D supplements, in addition to close follow-up in the Oncology Outpatient Clinic and support from the Autoimmune Unit of Internal Medicine (Figure 5).

Discussion

This case highlights the relevance of recognizing that, although immunotherapy has redefined the therapeutic approach in lung cancer, it is important to consider the occurrence of infrequent adverse effects, but with a potentially lethal clinical impact, such as vanishing bile duct syndrome.

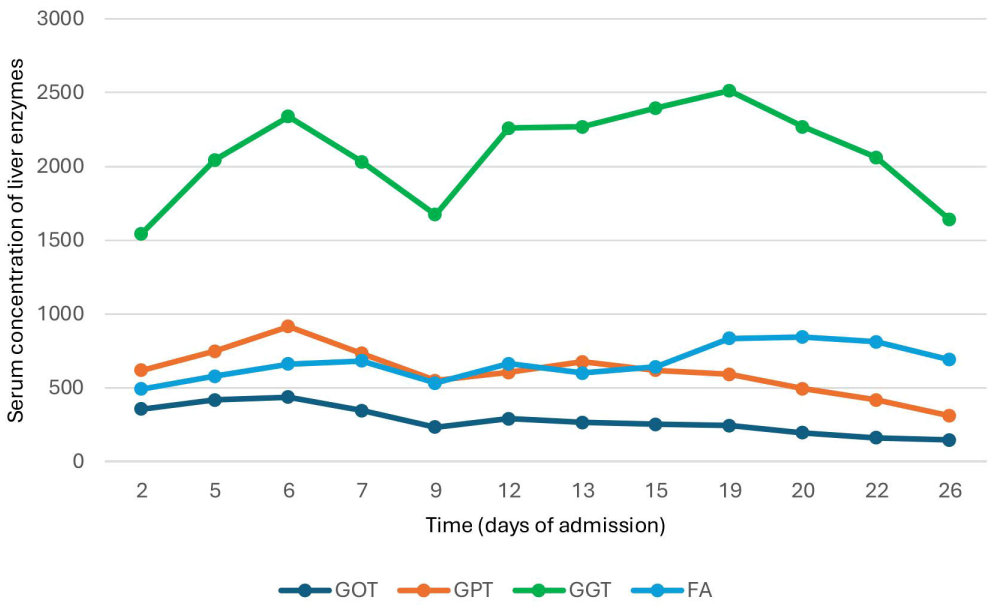

FIGURE 2
Variation in plasma liver enzyme concentration during hospitalization.

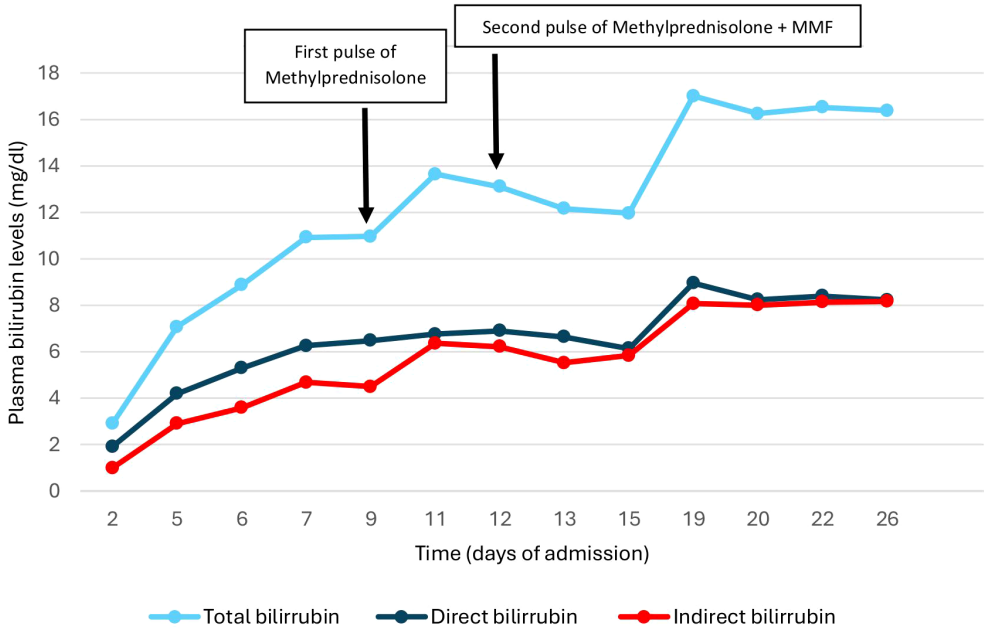

FIGURE 3
Changes in bilirubin levels during admission.

The initial approach in the differential diagnosis of cholestatic jaundice is based on establishing whether its origin lies in an intrahepatic or extrahepatic process.

Within the extrahepatic etiology, the presence of Charcot's triad (fever, mucocutaneous jaundice and abdominal pain), described in up to 50-75% of cases, means that acute cholangitis must be ruled out first (10).

For intrahepatic jaundice, pharmacological hepatotoxicity must be excluded. In this particular case, the patient has been receiving Paracetamol, administered at a dose of 1g every 8 hours. While it is true that this drug is a well-established cause of liver damage and, in fact, is the main cause of acute liver failure, liver damage is dose-dependent and typically manifests as centrolobular necrosis which, at the analytical level, is reflected by a predominance of cytolysis.

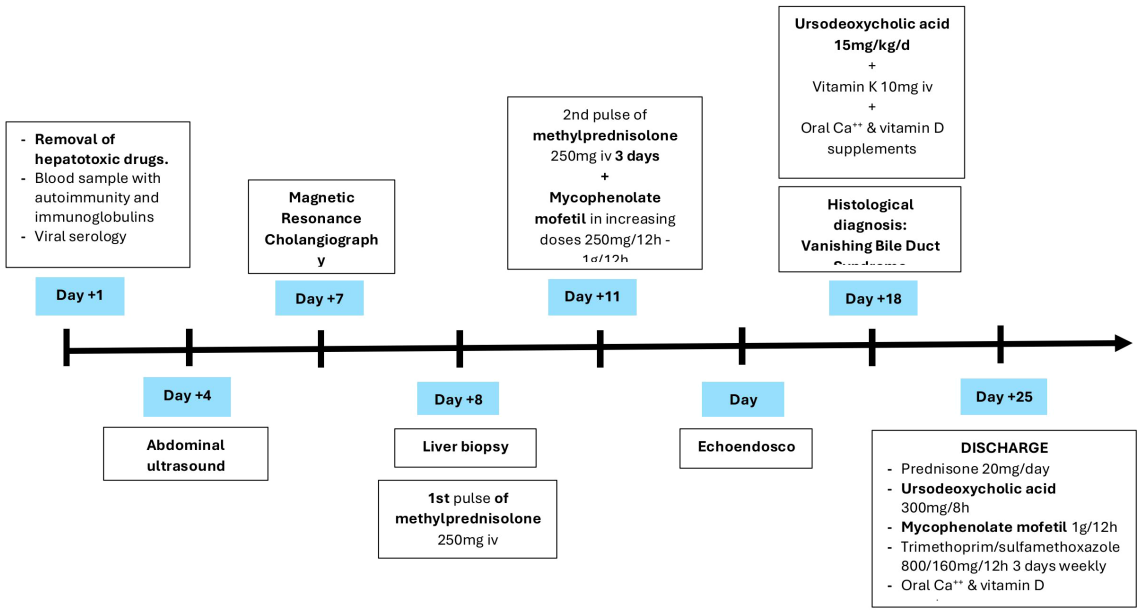

FIGURE 4
Timeline of events during hospital day.

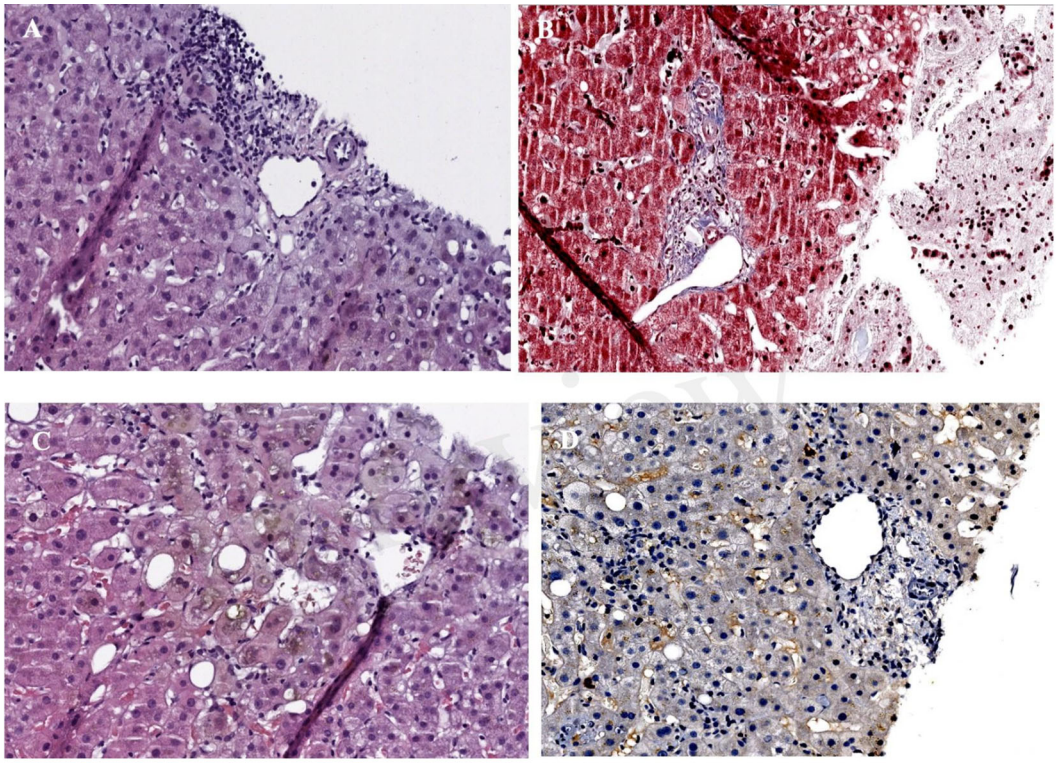

FIGURE 5
(A) Haematoxylin-eosin x40 (H-E): portal space with no bile ducts, only the branch of the hepatic artery and the branch of the portal vein are visible. **(B)** Masson x40: portal space with portal space with portal vein branch, several branches of the hepatic artery, as well as minimal fibrosis and inflammation, without distortion of the architecture. **(C)** H-E x40 centrolobulillar vein and bile pgment-laden hepatocytes reflecting intrahepatic cholestasis. **(D)** Immunohistochemistry with cytokeratin-19: absence of bile ducts in the portal space.

However, the dose received by the patient (3 g/day) is considered safe according to the Food and Drug Administration in the absence of underlying liver disease or chronic alcohol consumption (11).

On the other hand, although less frequent, both Metronidazole and Mesalazine have been implicated in isolated cases of liver damage, manifesting mixed or purely cholestatic hepatitis. Although the level of evidence supporting this probable association is weak, the possibility of liver injury induced by these drugs should be considered in the differential diagnosis (12, 13). In this particular case, there was no previous consumption of herbal products.

In the context of intrahepatic cholestatic jaundice, viral hepatitis should also be considered, with special emphasis on hepatitis A virus (14) and hepatitis E virus (15). Both can progress, in 5% and up to 60% respectively, to cholestatic hepatitis, characterized by persistent jaundice for more than three months. Despite its prolonged course, this form of presentation usually resolves spontaneously without significant sequelae. In this particular case, serology for hepatotropic viruses was negative.

Given the close relationship between inflammatory bowel disease, specifically Ulcerative Colitis present in almost 90% of cases, and Primary Sclerosing Cholangitis (16), it is imperative to include this entity in the differential diagnosis. In most cases (70%) there is an intrahepatic and extrahepatic involvement, being much more unusual, in less than 25% of cases, exclusively intrahepatic involvement (17). In this patient, imaging tests, especially magnetic resonance cholangiopancreatography, ruled out intra- and extrahepatic biliary tree dilatation, making it possible to rule out not only this disease, in addition to an incompatible liver biopsy, but also the other causes of extrahepatic cholestasis, including acute cholangitis.

Among the chronic autoimmune cholestatic diseases, primary biliary cholangitis, which affects only the intrahepatic bile duct and almost exclusively women, should be considered. However, the absence of antimitochondrial antibodies, detectable in more than 95% of cases, together with an atypical biliary histological lesion for this entity (18), allowed it to be excluded with a high degree of certainty.

Once all other entities have been excluded, immuno-mediated hepatitis should be considered, usually presenting 6–14 weeks after the start of immunotherapy with resolution within 4–6 weeks with appropriate treatment. Although the most common clinical picture is hepatocellular damage, usually early between the first and third immunotherapy cycle, in a quarter of cases it may present late, between the third and tenth treatment cycle, as a cholestatic pattern (7).

Staging of severity has direct implications for the management of immune- mediated hepatitis. For this purpose, the Common Terminology Criteria for Adverse Events (CTCAE) (6), traditionally used and accepted in oncology, classifies immune-

mediated hepatitis into four grades according to the level of increase of transaminases and total bilirubin. In this case, an elevated total bilirubin greater than ten times the upper limit of normal was categorized as grade 4. In this subgroup, therapeutic management is based on permanent withdrawal of immunotherapy and initiation of intravenous corticosteroids at doses ranging from 1 to 2 mg/kg/day, which are considered the cornerstone of treatment (19).

In addition, routine blood tests with liver biochemistry should be performed every 1–3 days. In case of refractoriness to systemic steroids, defined by the absence of clinical and biological response within 3–7 days after starting corticosteroid treatment, mycophenolate mofetil at a dose of 1g/12h should be used first as second-line therapy, since it is the most studied drug and, therefore, the one for which most evidence is available, with response rates >80%. Another pharmacological alternative, although with little evidence, is Tacrolimus. As a last therapeutic option, in those who are refractory even to immunosuppressive treatment and/or rapidly progressive, isolated case series have used antithymocyte globulin and 5 sessions of plasmapheresis interspersed every 48 hours. Nonetheless, the lack of solid data on its efficacy precludes its widespread use (7).

Although liver biopsy is not recommended as standard, it can be crucial in the differential diagnosis of severe hepatitis, as in the present case. In this context, histological analysis of liver tissue confirmed the definitive diagnosis of vanishing bile duct syndrome.

VBDS is a rare, acquired but potentially severe form of chronic cholestatic liver disease (20). Although the pathogenesis remains unknown, it has been proposed to be an immune-mediated injury of biliary epithelial cells mediated directly by T lymphocytes (21), leading to apoptosis and thus progressive destruction of intrahepatic bile ducts, ultimately resulting in intrahepatic cholestasis.

As for the origin of ductopenia, although its association has been described with immune disorders (e.g. primary biliary cholangitis, primary sclerosing cholangitis, sarcoidosis and graft-versus-host disease), with infectious processes (e.g. cytomegalovirus, Epstein-Barr virus and hepatitis B and C virus), as well as with lymphoproliferative neoplasms (e.g. Hodgkin's lymphoma) (22), it has classically been related to pharmacological etiology.

In fact, the first case, described in 1996, was secondary to the administration of Erythromycin (23), although others have also been reported such as Amoxicillin- Clavulanic acid, Trimethoprim-Sulfamethoxazole and Chlorpromazine (24). The medical literature has documented cases of this syndrome associated with the use of immunotherapy, particularly Pembrolizumab (25–28) in the context of metastatic NSCLC (25, 26), melanoma (27, 28) and mesothelioma (28). In most cases, liver toxicity manifested after the first treatment cycle, with the exception of one case in which the onset of liver toxicity occurred after the twelfth session (27). However, to date, no cases of VBDS directly induced by Atezolizumab have been reported, being this the first case.

The diagnosis is of exclusion and is established by histological examination. Therefore, in addition to clinical, analytical and serological evaluation to identify possible underlying causes and rule out extrahepatic bile duct obstruction, diagnostic confirmation requires histological identification of a loss of bile ducts in more than 50% of the portal spaces in a specimen with at least 10 portal tracts, obtained at least one month after the onset of liver damage (29). Another criterion in favor of this diagnosis is the temporal concordance between drug exposure and the onset of liver damage, usually between 1 and 6 months after the start of treatment.

From a biochemical point of view, the persistence of elevated alkaline phosphatase (>3 times the upper limit of normal) and hyperbilirubinemia for more than 6 months after drug exposure reinforces the diagnostic suspicion (24). Although moderate increases in transaminases may be observed, it is unusual for these to exceed 10 times the high threshold of normal.

Initial treatment, similar to that described in the literature for cases induced with Pembrolizumab, is based on ursodeoxycholic acid at a dose of 13–15 mg/kg per day for its cytoprotective, anti-apoptotic and immunomodulatory effects associated with methylprednisolone at 1 mg/kg or, less clearly, 2 mg/kg intravenously (28), although with limited scientific evidence on the impact on the natural course of the disease.

The prognosis is variable, although generally unfavorable, with the main determinant being the extent of ductopenia. In the available literature of cases with Pembrolizumab, four died, three of them despite an initial improvement of the liver profile; two from progression of the underlying oncological disease (28), one from non- neutropenic sepsis (25) and the remaining from acute liver failure (27). Only one patient survived with normalized liver biochemistry (26). Therefore, the natural history is unpredictable with two possible scenarios: gradual intrinsic recovery of the biliary epithelium may occur over months and/or years with progressive resolution of symptoms, or irreversible and progressive loss of bile ducts may occur, ultimately leading to cirrhosis (30).

In this case, both clinical and hepatic biochemical evolution is favorable, with normalization of serum bilirubin levels after 6 months of treatment with mycophenolate mofetil and ursodeoxycholic acid in combination with decreasing doses of corticosteroids, being currently 5 mg of oral prednisone in maintenance (Table 1).

Signaling mediated by programmed death receptor-1 (PD-1) and its ligand (PD-L1) plays a key role in tumor evasion of the immune system. Although both PD-1 inhibitors and PD-L1 inhibitors share the goal of blocking this immunosuppressive pathway to restore the immune effector activity of T lymphocytes against tumor cells, they differ in their mechanism of action, leading to pathophysiological differences with relevant clinical implications.

Anti-PD-1 monoclonal antibodies bind directly to the PD-1 receptor, expressed on activated T lymphocytes, B lymphocytes, macrophages, regulatory T cells, and natural killer cells, blocking its interaction with both PD-L1 and PD-L2.

This dual inhibition enhances broader immune activation, although at the expense of a higher risk of immune tolerance disruption and immune-mediated adverse events (31).

In contrast, PD-L1 inhibitors such as Atezolizumab selectively bind to their ligand, which is expressed in tumor cells, stromal cells and antigen-presenting cells in the tumor microenvironment,

TABLE 1 Comparison between Pembrolizumab and Atezolizumab-induced vanishing bile duct syndrome cases.

Study	Time to hepatotoxicity	Biopsy findings	Management	Outcomes
Gemelli et al.	11 days after the first administration of Pembrolizumab	Extensive intracanalicular and cellular cholestasis + severe ductal loss + mild lymphocytic inflammation	• Discontinuation of Pembrolizumab • High-dose steroid therapy (methylprednisolone 2 mg/kg IV) + MMF 1g/day + UDCA 600mg/day	Death from non- neutropenic sepsis
Masseti et al.	20 days after the first infusion of Pembrolizumab	Absence of interlobular bile ducts in >50% of portal tracts examined + prominent canalicular cholestasis + mild portal inflammatory infiltrate + no features of destructive cholangitis	Discontinuation of Pembrolizumab (no corticosteroids or other immunosuppressive therapies)	Progressive improvement of clinical and biochemical parameters over 16 weeks
Thorsteindottir et al.	After the twelfth infusion of pembrolizumab	Absence of bile ducts in the majority of the portal tracts + extensive intracellular and intracanalicular cholestasis + mild lymphocytic inflammation and mild microvesicular steatosis	• Discontinuation of Pembrolizumab • Methylprednisolone 125 mg IV daily + MMF 1g/12h + Plasmapheresis daily up to 8 cycles	Death from acute liver failure
Doherty et al.	8 days after the first infusion of Pembrolizumab	• H&E staining: only a single small bile duct • Cytokeratin 7 immunohistochemistry staining: absence of bile ducts and typical autoimmune hepatitis-like features + very minimal and focal intermediate hepatobiliary phenotype	• Discontinuation of Pembrolizumab • Oral methylprednisolone 1mg/kg/día + MMF 1g/12h + UDCA	Death from progression of the underlying oncological disease
Doherty et al.	24 days after a single infusion of Pembrolizumab	Absence of bile ducts + severe cholestasis and duct injury with evidence of parenchymal loss and regeneration	• Discontinuation of Pembrolizumab • Methylprednisolone 2 mg/kg/day + MMF 500mg/12h + UDCA	Initial improvement in liver biochemistry. Later death from progression of the underlying oncological disease
Noblejas, Lazaro et al.	After the third infusion of Atezolizumab	Absence of bile ducts + intrahepatic cholestasis in all portal spaces and hepatic lobules	• Discontinuation of Atezolizumab • Methylprednisolone 250mg/day IV for three days (x2) + MMF 1g/12h + UDCA 15mg/kg/day	Progressive improvement of clinical and biochemical parameters (normal bilirubin levels after 6 months of treatment)

MMF, mycophenolate mofetil; UDCA, ursodeoxycholic acid; H&E, hematoxylin and eosin.

allowing the interaction between PD-1 and PD-L2 to be preserved. Precisely, the degree of expression of PD-1 and PD-L2 in this microenvironment could influence the modulation of the immune response to these agents. Thus, this selectivity could contribute to the maintenance of immune tolerance and a tendency towards a potentially more favorable immune-mediated toxicity profile, without compromising antitumor therapeutic efficacy (32).

According to ESMO and NCCN guidelines (33, 34), atezolizumab is an adjuvant treatment for locally advanced non-small cell lung cancer. Although this therapy can cause unusual but serious adverse effects, as in this case, since it has been shown to induce complete and durable responses with a generally favorable safety profile, the therapeutic benefit clearly outweighs the associated risks. Therefore, in the event of a hypothetical tumor relapse, retreatment with Atezolizumab as an adjuvant could be considered, given the prolonged response and adequate clinical progression observed in this patient.

In conclusion, although immunotherapy has represented a significant advance in cancer treatment, its increasing use has revealed rare but potentially fatal adverse effects. In this context, we present the first documented case of Atezolizumab-induced vanishing bile duct syndrome, a finding of notable clinical relevance and with high impact on oncological pharmacovigilance, highlighting the need for a thorough evaluation of the hepatotoxic profile of this immunotherapeutic drug.

Patient perspective

The patient's experience, marked by intense anxiety stemming from uncertainty and diagnostic rarity, as well as prolonged clinical progression, highlights the importance of considering not only the clinical management of immune-mediated toxicity, but also its emotional impact throughout the therapeutic process, with a multidisciplinary approach and follow-up being essential.

Data availability statement

The original contributions presented in the study are included in the article/supplementary material. Further inquiries can be directed to the corresponding author.

Ethics statement

The studies involving humans were approved by Hospital General Universitario Morales Meseguer. The studies were conducted in accordance with the local legislation and institutional requirements. The participants provided their written informed consent to participate in this study. Written informed consent was obtained from the individual(s) for the publication of any potentially identifiable images or data included in this article.

Author contributions

AL: Writing – original draft, Writing – review & editing, Visualization, Methodology, Supervision, Validation, Conceptualization, Investigation. CN: Investigation, Visualization, Conceptualization, Validation, Writing – original draft. JM: Investigation, Methodology, Writing – review & editing, Visualization, Validation. JB: Writing – review & editing, Conceptualization, Visualization, Validation. LL: Visualization, Validation, Writing – review & editing, Supervision. MS: Supervision, Visualization, Writing – review & editing. MN: Validation, Conceptualization, Writing – review & editing, Visualization. MM: Visualization, Methodology, Writing – review & editing, Validation. IV: Visualization, Writing – review & editing, Supervision. AC: Visualization, Supervision, Validation, Writing – review & editing.

Funding

The author(s) declare that no financial support was received for the research and/or publication of this article.

Conflict of interest

The authors declare that the research was conducted in the absence of any commercial or financial relationships that could be construed as a potential conflict of interest.

Generative AI statement

The author(s) declare that no Generative AI was used in the creation of this manuscript.

Any alternative text (alt text) provided alongside figures in this article has been generated by Frontiers with the support of artificial intelligence and reasonable efforts have been made to ensure accuracy, including review by the authors wherever possible. If you identify any issues, please contact us.

Publisher's note

References

1. National Cancer Institute. Surveillance, epidemiology and end results program. In: *Cancer Stat Facts: Lung and Bronchus*. Available online at: https://seer.cancer.gov/statfacts/html/lungb.html (Accessed February 5, 2025).

2. Sociedad Española de Oncología Médica. Las cifras del cáncer en España(2024). Available online at: https://www.seom.org/images/LAS_CIFRAS_2024.pdf (Accessed March 16 2025).

3. Bade BC, Dela Cruz CS. Lung cancer 2020: epidemiology, etiology, and prevention. *Clin Chest Med*. (2020) 41:1–24. doi: 10.1016/j.ccm.2019.10.001

4. Felip E, Altorki N, Zhou C, Vallières E, Martínez-Martí A, Rittmeyer A, et al. Overall survival with adjuvant atezolizumab after chemotherapy in resected stage II-IIIA non-small-cell lung cancer (IMpower010): a randomised, multicentre, open-label, phase III trial. *Ann Oncol*. (2023) 34:907–19. doi: 10.1016/j.annonc.2023.07.001

5. Frey C, Etminan M. Immune-related adverse events associated with atezolizumab: insights from real-world pharmacovigilance data. *Antibodies (Basel)*. (2024) 13:56. doi: 10.3390/antib13030056

6. Hercun J, Vincent C, Bilodeau M, Lapierre P. Immune-mediated hepatitis during immune checkpoint inhibitor cancer immunotherapy: lessons from autoimmune hepatitis and liver immunology. *Front Immunol*. (2022) 13:907591. doi: 10.3389/fimmu.2022.907591

7. Velarde-Ruiz Velasco JA, Tapia Calderón DK, Cerpa-Cruz S, Velarde-Chávez JA, Uribe Martínez JF, García Jiménez ES, et al. Hepatitis inmunomediada: conceptos básicos y tratamiento. *Rev Gastroenterología México*. (2024) 89:106–20. doi: 10.1016/j.rgmx.2023.12.003

8. Kim H, Shin YE, Yoo HJ, Kim JY, Yoo JJ, Kim SG, et al. Atezolizumab-induced ulcerative colitis in patient with hepatocellular carcinoma: case report and literature review. *Medicina (Kaunas)*. (2024) 60:1422. doi: 10.3390/medicina60091422

9. European Association for the Study of the Liver. EASL clinical practice guidelines: liver transplantation. *J Hepatol*. (2016) 64:433–85. doi: 10.1016/j.jhep.2015.10.006

10. Saik RP, Greenburg AG, Farris JM, Peskin GW. Spectrum of cholangitis. *Am J Surg*. (1975) 130:143–50. doi: 10.1016/0002-9610(75)90362-1

11. Acetaminophen. *En LiverTox: Clinical and Research Information on Drug-Induced Liver Injury*. Bethesda (MD: National Institute of Diabetes and Digestive and Kidney Diseases (2016).

12. Metronidazole. *En LiverTox: Clinical and Research Information on Drug-Induced Liver Injury*. Bethesda (MD: National Institute of Diabetes and Digestive and Kidney Diseases (2016).

13. Mesalamine. *En LiverTox: Clinical and Research Information on Drug-Induced Liver Injury*. Bethesda (MD: National Institute of Diabetes and Digestive and Kidney Diseases (2016).

14. Gordon SC, Reddy KR, Schiff L, Schiff ER. Prolonged intrahepatic cholestasis secondary to acute hepatitis A. *Ann Intern Med*. (1984) 101:635–7. doi: 10.7326/0003-4819-101-5-635

15. Chau TN, Lai ST, Tse C, Ng TK, Leung VK, Lim W, et al. Epidemiology and clinical features of sporadic hepatitis E as compared with hepatitis A. *Am J Gastroenterol*. (2006) 101:292–6. doi: 10.1111/j.1572-0241.2006.00416.x

16. Almanza-Hurtado AJ, Tomás Rodríguez-Yánez MC, Martínez-Ávila JD, Rodríguez- Blanco, Imbeth-Acosta PL. Artículo de revisión: colangitis esclerosante primaria. *Hepatología*. (2021) 2:325–40. doi: 10.52784/issn.2711-2330

17. Parés A. Colangitis esclerosante primaria: diagnóstico y pronóstico. *Gastroenterol Hepatol*. (2011) 34:41–52. doi: 10.1016/j.gastro-hep.2010.02.006

18. Pariente A. Colangitis (ex-cirrosis) biliar primaria. In: *Tratado de medicina*, vol. 25. Paris, France: Elsevier (2021). p. 1–8.

19. Thompson JA, Schneider BJ, Brahmer J, Zaid MA, Achufusi A, Armand P, et al. NCCN guidelines® insights: management of immunotherapy-related toxicities, Version 2.2024. *J Natl Compr Canc Netw*. (2024) 22(9):582–92. doi: 10.6004/jnccn.2024.0057

20. Córdoba Iturriagagoitia A, Iñarrairaegui Bastarrica M, Pérez de Equiza E, Zozaya Urmeneta JM, Martínez-Peñuela JM, Beloqui Pérez R. Recuperación ductular en el síndrome de los conductillos biliares evanescentes en paciente con linfoma de Hodgkin. *Gastroenterol Hepatol*. (2005) 28:275–8. doi: 10.1157/13074061

21. Zhao Z, Bao L, Yu X, Zhu C, Xu J, Wang Y, et al. Acute vanishing bile duct syndrome after therapy with cephalosporin, metronidazole, and clotrimazole: A case report. *Med (Baltimore)*. (2017) 96:e8009. doi: 10.1097/MD.0000000000008009

22. Reau NS, Jensen DM. Vanishing bile duct syndrome. *Clin Liver Dis*. (2008) 12:203–17. doi: 10.1016/j.cld.2007.11.007

23. Trejo Estrada R, Aguirre García J. Caso anatomoclínico: síndrome de los conductos biliares evanescentes. *Rev Fac Med UNAM*. (1996) 39:25–8.

24. Vanishing Bile Duct Syndrome. *En LiverTox: Clinical and Research Information on Drug-Induced Liver Injury*. Bethesda (MD: National Institute of Diabetes and Digestive and Kidney Diseases (2019).

25. Gemelli M, Carbone M, Abbate MI, Mancin M, Zucchini N, Colonese F, et al. Vanishing bile duct syndrome following pembrolizumab infusion: case report and review of the literature. *Immunotherapy*. (2022) 14:175–81. doi: 10.2217/imt-2021-0078

26. Masseti C, Pugliese N, Rimassa L, Finocchiaro G, Di Tomaso L, Lancelloti C, et al. Pembrolizumab-induced vanishing bile duct syndrome: a case report. *SN Compr Clin Med*. (2021) 3:906–8. doi: 10.1007/s42399-021-00803-9

27. Thorsteindottir T, Loitergard T, Reims HM, Porojnicu AC. Fatal cholestasic liver injury during treatment with PD1 immune checkpoint inhibitor for Malignant melanoma: a case report. *Case Rep Oncol*. (2020) 13:659–63. doi: 10.1159/000507695

28. Doherty GJ, Duckworth AM, Davies SE, Mells GF, Brais R, Harden SV, et al. Severe steroid-resistant anti-PD1 T-cell checkpoint inhibitor-induced hepatotoxicity driven by biliary injury. *ESMO Open*. (2017) 2:e000268. doi: 10.1136/esmoopen-2017-000268

29. Ludwig J, Wiesner RH, LaRusso NF. Idiopathic adulthood ductopenia. A cause of chronic cholestatic liver disease and biliary cirrhosis. *J Hepatol*. (1988) 7:193–9. doi: 10.1016/S0168-8278(88)80482-3

30. Bakhit M, McCarty TR, Park S, Njei B, Cho M, Karagozian R, et al. Vanishing bile duct syndrome in Hodgkin's lymphoma: A single center experience and clinical pearls. *J Clin Gastroenterol*. (2016) 50:688. doi: 10.1097/MCG.0000000000000548

31. Sorin M, Prosty C, Ghaleb L, Nie K, Katergi K, Shahzad MH, et al. Neoadjuvant chemoimmunotherapy for NSCLC: A systematic review and meta-analysis. *JAMA Oncol*. (2024) 10:621–33. doi: 10.1001/jamaoncol.2024.0057

32. Ladjevardi CO, Skribek M, Koliadi A, Rydén V, El-Naggar AI, Digkas E, et al. Differences in immune-related toxicity between PD-1 and PD-L1 inhibitors: a retrospective cohort study in patients with advanced cancer. *Cancer Immunol Immunother*. (2024) 74:14. doi: 10.1007/s00262-024-03869-1

33. Remon J, Soria JC, Peters S, on behalf of the ESMO Guidelines Committee. Early and locally advanced non-small-cell lung cancer: an update of the ESMO Clinical Practice Guidelines focusing on diagnosis, staging and systemic and local therapy. *Ann Oncol*. (2021) 32:1637–42. doi: 10.1016/j.annonc.2021.08.1994

34. Riely GJ, Wood DE, Ettinger DS, Aisner DL, Bauman JR, Bharat A, et al. Non-small cell lung cancer, version 7.2025, NCCN clinical practice guidelines in oncology. *J Natl Compr Canc Netw*. (2025), 1–287.

frontiers | Frontiers in Immunology

TYPE Case Report
PUBLISHED 11 December 2025
DOI 10.3389/fimmu.2025.1631953

OPEN ACCESS

EDITED BY
Ashraf A. Tabll,
National Research Centre, Egypt

REVIEWED BY
Sridhar Vemulapalli,
University of Nebraska Medical Center, United States
Meng-Yao Li,
Shanghai Jiao Tong University, China
Wenya Tian,
IQVIA Laboratories, United States

*CORRESPONDENCE
Bin Zhang
Zhangbin_dlmu@163.com
Weiguo Zhang
zhangwg0158@sina.com

†These authors have contributed equally to this work

RECEIVED 20 May 2025
REVISED 24 November 2025
ACCEPTED 25 November 2025
PUBLISHED 11 December 2025

CITATION
Zhang X, Zhang X, Yin H, Zhang W and Zhang B (2025) Case report of acute hepatorenal failure induced by third-line treatment with tislelizumab in a patient with cholangiocarcinoma: was influenza virus the culprit?
Front. Immunol. 16:1631953.
doi: 10.3389/fimmu.2025.1631953

Case report of acute hepatorenal failure induced by third-line treatment with tislelizumab in a patient with cholangiocarcinoma: was influenza virus the culprit?

Xuebing Zhang[1†], Xia Zhang[1,2†], Hang Yin[1], Weiguo Zhang[1*] and Bin Zhang[1*]

[1]Department of Oncology, The First Affiliated Hospital of Dalian Medical University, Dalian, Liaoning, China, [2]Department of Oncology, Dalian Fifth People's Hospital, Dalian, Liaoning, China

A 72-year-old male diagnosed with cholangiocarcinoma was initiated on third-line therapy comprising Tislelizumab and Anlotinib. Within four days of treatment, he developed fulminant hepatic injury concurrent with acute kidney injury. Despite aggressive management with high-dose glucocorticoids, hepatoprotective agents, comprehensive supportive care, and subsequent anti-infective therapy, his clinical status declined rapidly. In view of the grave prognosis and the family's decision to decline intensive interventions such as plasma exchange, the patient ultimately succumbed to multiorgan failure. This case highlights a potential synergistic interaction between concomitant infection (e.g.,influenza virus) and immune checkpoint inhibitor(ICI) therapy, possibly mediated through enhanced antigenic stimulation and loss of immunoregulatory control, culminating in exaggerated immune activation. This mechanism may have profoundly amplified ICI-related toxicity, leading to fatal multiorgan irAEs. Regarding the issue of immune storms, it is challenging for clinical practice to provide favorable outcomes for patients, and we need to remain highly vigilant.

KEYWORDS

immune-related adverse events, tislelizumab, H1N1 influenza A virus (IAV), immune storm, intrahepatic cholangiocarcinoma (ICC)

Introduction

Intrahepatic cholangiocarcinoma (ICC) is the second most common primary liver tumor,with a global incidence of 0.3-6/100,000 and a higher incidence in China (>6/100,000). The global mortality rate is 1-6/100,000, while in China,it is >4/100,000. Most patients (70%) are diagnosed at an advanced stage, with a 5-year survival rate of 7-20%. Approximately 20%-30% of patients are eligible for surgery, which is the only potentially

curative treatment; adjuvant capecitabine after surgery has a median survival of 53 months. For the 70%-80% of patients with locally unresectable or metastatic disease,systemic therapy may delay progression,but survival is limited to approximately 1 year (1). For the past decade, doublet chemotherapy with gemcitabine and cisplatin has been considered the most effective first-line regimen, but the results of ICI therapy may shift this paradigm for the first time (2). For patients who have not received ICI therapy initially, second-line treatment with the addition of immunotherapy may improve patient prognosis. However, the adverse reactions of ICI are still unpredictable, and events leading to death have occurred in both clinical studies and the real world, although the proportion is extremely low, it is still a problem that we need to pay close attention to. Cytokine storm is the main cause of death, but it is sometimes difficult to detect clinically. This article reports a case of a patient with influenza virus infection during ICI therapy, who developed severe liver damage and eventually died of unknown causes, hoping to raise clinical vigilance.

It is worth noting that the bottleneck of the therapeutic effect of cholangiocarcinoma is partly due to its complex tumor microenvironment and the lack of specific targeting methods. In order to overcome this limitation, A study revealed that that single-cell multi-omics is helpful to discover new therapeutic targets for cholangiocarcinoma (3). Rishabha et al. have reviewed how to exploit the unique electrical, optical and magnetic properties of cancer cells to develop new therapies. By intervening these physical parameters, strategies such as magnetic field-assisted therapy play an important role in improving the effectiveness and safety of cancer diagnosis and treatment (4). At the same time, the rise of nanotechnology has brought another powerful impetus to achieve precision medicine. As multifunctional therapeutic and diagnostic platforms, novel photoactivated nanomaterials have shown great potential in the field of cancer. Although it is not yet mature from laboratory research to large-scale clinical application, such cutting-edge technologies undoubtedly lay an innovative foundation for overcoming the dilemma of solid tumor treatment, including cholangiocarcinoma (5).

Case data

In December 2022,a 72-year-old male presented to the Second Affiliated Hospital of Dalian Medical University with abdominal distension and scleral icterus. He had no history of smoking and drinking. He did not have a medical history of hypertension, diabetes, kidney disease, or hepatitis. and no family members had a tumor history.

Imaging revealed thickening of the mid-common bile duct wall, raising suspicion of malignancy. On February 3,2023, the patient underwent radical resection of the hilar bile duct carcinoma, retroperitoneal lymph node dissection, and complex adhesion release under general anesthesia. Pathology confirmed moderately to poorly differentiated extrahepatic cholangiocarcinoma, T2N0Mx.

The immunohistochemical examination indicated pMMR, CK7 (+), Muc-1(+), CK20(+), CDx2(-), Muc-5(+)Ki67(35%+), PMS2(+), HER-2(-). Genetic testing revealed microsatellite stability (MSS), TMB 0.53 Muts/Mb,PD-L1(-), absence of ERBB-2 amplification, and strong VEGFR expression. Postoperative radiotherapy was initiated in March 2023,concurrently with capecitabine 1000mg po bid. The patient received four cycles of single-agent tegafur in May 2023,followed by three cycles of gemcitabine plus cisplatin due to disease progression in September. The patient went to our hospital on March 28,2024,due to further disease progression. Based on previous findings, the diagnosis was cholangiocarcinoma with peritoneal lymph node metastasis. A third-line treatment regimen of tislelizumab combined with anlotinib was planned. The patient's ECOG score was 2 before treatment, and the patient's laboratory results on admission are summarized in Table 1.

The patient developed a fever on the night of March 29,the day of toripalimab initiation, with a peak temperature of 39.5°C,

TABLE 1 The patient's laboratory results on admission.

Laboratory test	Patient's value	Reference range	Unit
WBC(White blood cell)	3.17	3.5-9.5	10^9/L
LYMPH(Lymphocyte percentage)	16.1	20-50	%
MONO(Monocyte percentage)	12.60	3-10	%
RBC(Red blood cell)	3.06	4.3-5.8	10^12/L
HB(Hemoglobin)	101	130-175	G/L
PLT(Blood platelet)	94	125-350	10^9/L
ALT(Alanine Aminotransferase)	30	9-50	U/L
AST(Aspartate Aminotransferase)	55	15-46	U/L
T-BIL(Total Bilirubin)	13.7	3-22	μmol/L
CK-MB(Creatine Kinase)	0.45	<5	μg/L
MYO(Myoglobin)	47.27	<110	ng/ml
Hs-TnI(High-sensitivity troponin I)	0.003	0-0.057	μg/L

accompanied by mild catarrhal symptoms. Upper respiratory tract infection was suspected,and symptomatic treatment was administered, resulting in a decrease in temperature. However,the fever recurred. On the fourth day of medication (April 1) the patient experienced another high fever. A comprehensive etiologic workup was performed on April 2nd during the acute phase of his clinical deterioration.Respiratory pathogen testing was performed,and the COVID-19 antigen test was negative.

Laboratory results from a 6:00 AM blood draw revealed a neutrophil count of 8.09×10*9,a platelet count of 28×10*9, hemoglobin of 147g/L, and WBC:4.63×10*12. The neutrophil percentage was 78%, and the lymphocyte percentage was 14.4%.

Liver function:ALT:353U/L, AST:1095U/L, T-BIL:33.3μmol/L, Creatinine(CRE):43umol/L(normal:58-110umol/L), procalcitonin (PCT): 6.68 ng/ml(normal:0-0.5ng/ml), C-reactive protein(CRP): 104.68 mg/L(normal:0-6mg/L), which was suggestive of immune checkpoint inhibitor-related hepatitis. Intravenous infusion of methylprednisolone (160mg per day) and glutathione (2.4mg per day) and diphenhydramine (20mg once) as well as oral bicyclol (25mg once) were immediately administered.

Repeat liver function tests at 9:00 AM showed ALT: 467 U/L, AST: 1501 U/L,ALP: 231 U/L,T-BIL: 36 μmol/L,and conjugated bilirubin 8.3 μmol/L; Albumin: 24.5 g/L,indicating rapidly deteriorating liver function.CK-MB: 12.84 μg/L,hs-tnI: 0.165 μg/L, MYO: 1238.55 ng/ml,which was suggestive of myositis,with a potential for myocardial injury,hypoalbuminemia,and thrombocytopenia. Treatment included liver protective,pulse hormone therapy (methylprednisolone 340mg per day), anti allergic (diphenhydramine 20mg once),platelet transfusion,and albumin supplementation.

Physical examination showed that the jaundice of the patient's skin worsened rapidly in a short period of time, with poor appetite, extreme fatigue, irritability, abdominal distension, and no nausea or vomiting. The patient could not cough up phlegm and was given phlegm and cough relieving treatment. The patient had dysuria, and diuretic therapy was intensified. The family was informed,and liver replacement therapy was recommended,but they opted for pharmacological treatment due to financial constraints.

On the April 2th the patient's condition worsened,with 24-hour urine output <500 ml. Repeat tests revealed CRP: 83.82 mg/L, WBC:12.93 10^9/L, LYMPH: 18.30%, MONO:17.90%, CK-MB:34.19 μg/L, hs-TnI:0.431 μg/L, MYO:1080.17 ng/ml, ALT: 743 U/L, AST: 2752 U/L, ALP: 225 U/L, T-BIL: 381 μmol/L, CRE:168 μmol/L. The patient presented with liver failure,renal insufficiency, and oliguria, suggestive of Multiple Organ Dysfunction Syndrome (MODS). Plasma exchange was again recommended but declined by the family. Concurrently, pathogen reports indicated positive IgM antibodies for influenza A virus, influenza B virus, and Legionella pneumophila. The patient was treated with antiviral therapy and anti-inflammatory therapy with marbasalovir following consultation with the intensive care unit.

Intravenous infusion of Shenkang injection (100ml per day), fluid replacement, intravenous injection human immunoglobulin (10mg iv), compound amino acid injection (500ml per day), and levofloxacin (500mg per day), pheresis leucopenic platelets(iv), oral mabasalovir (40mg once), Anuria persisted despite repeated use of diuretics. However, the patient's condition rapidly progressed, with the development of jaundice and anuria, ultimately leading to clinical death on the April 3. The timeline of symptoms, diagnosis, and treatment was summarized in Figure 1.

Discussion

Analysis of the cause of death indicated that the underlying fatal event was fulminant,lethal immune-related adverse events (irAEs) induced by combined ICI therapy and antiangiogenic therapy. Subsequent serologic testing revealed positive IgM antibodies against influenza virus and Legionella species,which suggesting recent coinfection as potential contributory factors. Anlotinib, a multitargeted tyrosine kinase inhibitor (TKI), is associated with hepatotoxic effects—including elevated transaminases and hyperbilirubinemia—as described in its instruction. The hepatotoxicity profile of anlotinib monotherapy is generally characterized by low-grade, asymptomatic elevations in transaminases, triglycerides, total cholesterol, and bilirubin (6). Mechanistically, anlotinib may alter the tumor immune microenvironment by inhibiting vascular endothelial growth factor receptor (VEGFR) signaling or downregulating PD-L1 expression on vascular endothelial cells (7). When combined with immune checkpoint inhibitors (ICIs), these effects may synergistically enhance systemic T-cell activation, thereby amplifying on-target, off-tumor toxicity in normal tissues such as the liver. However, the current clinical trials of ICI + TKI combination therapy have not reported a higher incidence of immune-related adverse events (irae), especially hepatitis, than that of anlotinib monotherapy (8). According to the known clinical data, the side effects of immunotherapy combined with anti-angiogenesis therapy can not be prevented, but are basically controllable. Thus, while anlotinib monotherapy is unlikely to fully account for the fulminant hepatic failure observed in this case, it may have acted as a "toxicity amplifier,"potentiating the immune-related toxicity of tislelizumab. An acute influenza infection may have served as a third insult, further exacerbating this dysregulated immune response. The Naranjo Adverse Drug Reactions Probability Scale was used for monitoring adverse drug reactions (9), the patient's score of 6 points showed that the causal relationship between tislelizumab and irAE was 'probable' (Table 2). We speculate that acute influenza virus infection may have acted as a powerful catalyst in this process.

The patient had no underlying conditions for cirrhosis or acute liver failure. Acute progression of cholangiocarcinoma itself was ruled out as highly unlikely and because the patient's imaging studies on admission did not show progression.

Although sepsis can also present with high fever, markedly elevated PCT, and subsequent positive pathogen serology, the timing of symptoms is too strongly correlated with Immunotherapy (within hours), and sepsis rarely causes injury in

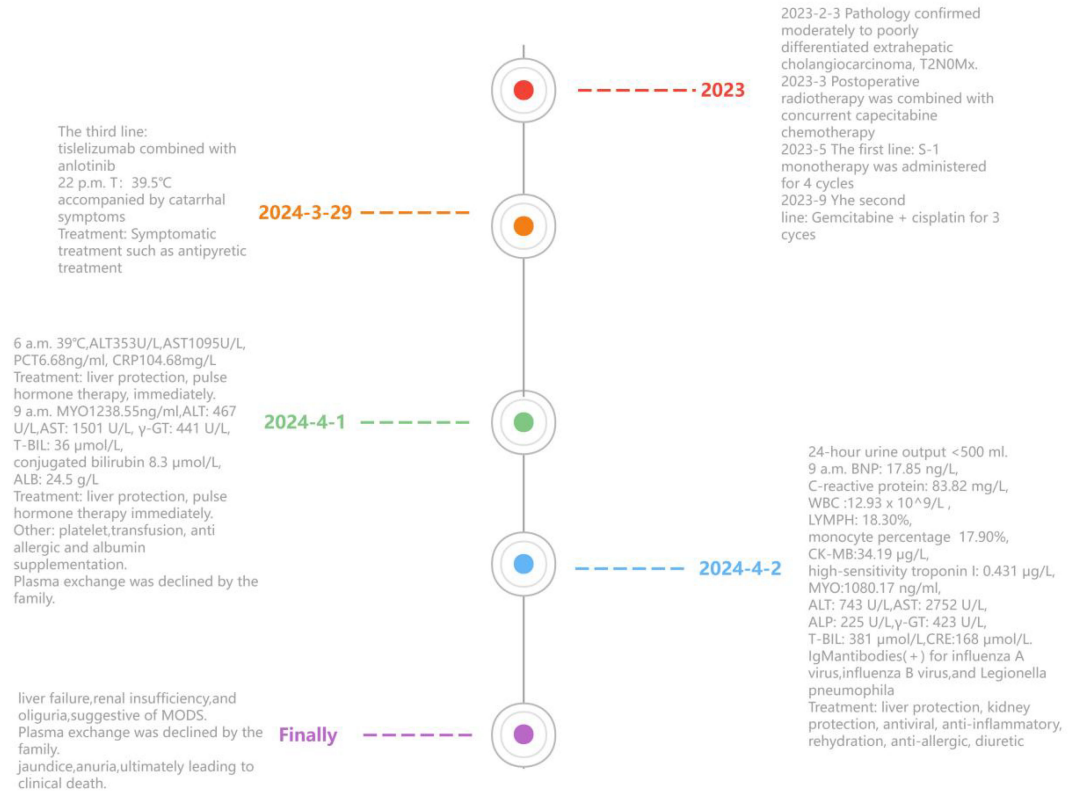

FIGURE 1
The timeline of the patient's symptom, diagnosis and treatments.

TABLE 2 Naranjo scale score of fulminant multiorgan failure caused by tislelizumab.

Are there previous conclusive reports on this reaction?	Yes, +1
Did the adverse event appear after the suspected drugs was given?	Yes, +2
Did the adverse reaction improve when the drug was discontinued or when a specific antagonist was given?	Not known or not done, 0
Did the adverse reaction appear when the drugs was readministered?	Not known or not done, 0
Are there alternative caused the reaction?	Yes, +2
Did the reaction reappear when a placebo was given?	Not known or not done, 0
Was the drug detected in any body fluid in toxic concerntrations?	Not known or not done, 0
Was the reaction more serve when the dose was increased, or less serve when the dose was decreased?	No, 0
Did the patient have a similar reaction to the same or similar drugs in any previous explorsure?	No, 0
Was the adverse event confirmed by any objective evidence?	Yes, +1
Total	6

the pattern of AST >2000 U/L and myoglobin >1000 ng/mL, the condition continues to worsen after high-dose steroid pulse. It is also not completely consistent with typical sepsis. We do not dispute the diagnosis of sepsis, but it is not the underlying cause of this fatal event. We believe that sepsis is more like an integral part of the disease process, with the underlying driver being a lethal immune storm triggered by immunotherapy. Influenza virus infection may act as an immune adjuvant, exacerbating this process.

Previous reports have associated tislelizumab with adrenal insufficiency, psoriasis, liver injury, and diabetic ketoacidosis, as well as severe thyrotoxicosis, cytokine release syndrome, toxic epidermal necrolysis-like skin reactions, steroid-refractory immune checkpoint inhibitor-related pneumonitis, acetylcholine receptor-binding antibody-associated myasthenia gravis, myocarditis, rhabdomyolysis, and pancytopenia. There have been no reported fatalities associated with tislelizumab (Table 3).

The pathophysiological mechanism of this fatal event involves the synergy between ICI therapy and viral infection: influenza virus can upregulate PD-L1 expression (27), which can regulate the host immune response during infection by this mechanism (28), as an adaptive immune resistance mechanism to inhibit T cell responses. ICI treatment,by blocking PD-1/PD-L1,a key immunosuppressive checkpoint,reversed depletion of cytotoxic T lymphocytes (CTLS) and

TABLE 3 Tislelizumab-related adverse events in available case reports.

Malignancies	Grender	Age	Diagnosis	Reference
Lung cancer	M	72	cytokine release syndrome	(10)
urothelial carcinoma	M	58	Adrenal crisis	(11)
thymic carcinoma	M	27	ureteritis/cystitis	(12)
dual organs dysfunction	M	74	acute kidney injury (grade 3) and acute liver injury (grade 4)	(13)
bladder cancer	M	67	adrenal hypofunction and Psoriasisby induced by tislelizumab	(14)
Liver cancer	M	49	Severe thyrotoxicosis	(15)
Bladder Cancer and Prostate Cancer	M	72	Hypophysitis	(16)
Chronic nonspecific cheilitis	F	36	Chronic nonspecific cheilitis	(17)
lung adenocarcinoma	M	66	Life-threatening pancytopenia	(18)
metastatic lung cancer	F	75	Lichen planus pemphigoides	(19)
metastatic Lung Squamous cell Carcinoma (LUSC)	M	75	Toxic Epidermal Necrolysis and Agranulocytosis	(20)
Esophageal cancer	M	63	Exfoliative esophagitis	(21)
pulmonary sarcomatoid carcinoma	M	59	Fatal hemoptysis	(22)
thymic epithelial tumors	M	42 and 52	Severe cardiotoxicity	(23)
Non-Small Cell Lung Cancer	M	71	multiple-organs irAEs (lung,muscle,myocardium,liver,and pituitary)	(24)
Lung cancer	M	74	THSD7A-Positive Membranous Nephropathy	(25)
colon cancer	M	65	Acetylcholine receptor binding antibody-associated myasthenia gravis, myocarditis,and rhabdomyolysis	(26)

promoted their proliferation and activation (29). During acute infection, upregulation of PD-1 on $CD8^+$ T cells serves as a host feedback inhibitory mechanism to prevent excessive immunopathology. Meanwhile,hepatic sinusoidal endothelial cells constitutively express high levels of PD-L1,which promotes immune tolerance and protects hepatic tissue from immune damage through activation of the PD-1/PD-L1 checkpoint pathway (30). ICI therapy abrogates this protective mechanism,leading to severe immune-related adverse events (irAEs) through disinhibition of regulatory signaling and enhanced immune activation.

In this case, immune-mediated hepatitis was the primary clinical manifestation. Within four days of treatment, he developed fulminant hepatic injury concurrent with acute kidney injury(KDIGO stage 3). The patient also developed bone marrow suppression, myositis, and renal impairment, culminating in fatal multisystem organ failure. The particular nature and high severity of these irAEs have not been previously reported in clinical trials of tislelizumab.

We speculate that influenza virus infection may have served as a critical trigger. During viral infection, upregulated PD-1 expression on $CD8^+$T cells functions to suppress excessive immune activation. The excessive immune response is caused by the suppression of PD-1-mediated immune tolerance by ICI treatment, which eventually leads to liver failure. Although liver replacement therapy might have been the only potential rescue intervention, it was not feasible in this case.

Limitations

In this case report, influenza virus PCR testing on respiratory samples was not performed. As this is a retrospective analysis, clinical management during the acute presentation was primarily focused on stabilizing the patient's rapidly deteriorating condition (e.g. fulminant hepatic failure). Thus, the patient had severe thrombocytopenia and coagulopathy, and a liver biopsy was not performed because it was considered to be a very high risk of bleeding. Furthermore, a postmortem examination (autopsy) was not performed, as it was declined by the family. Serologic antibody testing and routine biochemical and inflammatory markers were prioritized to facilitate rapid diagnosis and guide urgent treatment decisions. When the patient developed hyperpyrexia and respiratory symptoms,clinicians strongly suspected viral infection based on the clinical presentation (e.g. high fever, catarrhal symptoms) and epidemiological context. Although PCR confirmation was unavailable,empirical treatment with the antiviral agent baloxavir marboxil was promptly initiated in accordance with the principle of "clinical diagnosis first". This approach aligns with standards of care for critically ill patients, where in treatment should not be delayed pending definitive laboratory results. But in future research, it is also advised that respiratory samples undergo influenza PCR testing and liver biopsy to elucidate the role of influenza virus infections in the patients' prognosis.

Conclusion

This case report describes a 72-year-old male with postoperative cholangiocarcinoma who developed fulminant multiorgan immune-related adverse events (irAEs) shortly after initiating treatment with tislelizumab combined with anlotinib. Although immune-mediated hepatitis associated with tislelizumab has been reported, it is rarely fatal. In this patient, concomitant influenza virus infection may have contributed to a fulminant course through immune hyperactivation. Clinicians should be aware of this potentially life-threatening toxicity. Further research is needed to determine how to use ICI in patients with concurrent viral infections and to minimize risks.

Data availability statement

The raw data supporting the conclusions of this article will be made available by the authors, without undue reservation.

Ethics statement

The studies involving humans were approved by The First Affiliated Hospital of Dalian Medical University. The studies were conducted in accordance with the local legislation and institutional requirements. The participants provided their written informed consent to participate in this study. Written informed consent was obtained from the individual(s) for the publication of any potentially identifiable images or data included in this article. Written informed consent was obtained from the participant/patient(s) for the publication of this case report.

Author contributions

XBZ: Formal analysis, Methodology, Writing – original draft. XZ: Investigation, Writing – review & editing. HY: Investigation, Software, Supervision, Writing – review & editing. WZ: Supervision, Funding acquisition, Resources, Writing – review & editing. BZ: Funding acquisition, Project administration, Resources, Validation, Visualization, Writing – review & editing.

Funding

The author(s) declared financial support was received for the research and/or publication of this article. The funding for the design, collection, analysis and writing of the manuscript was provided by CHEN XIAO-PING FOUNDATION FOR THE DEVELOPMENT OF SCIENCE AND TECHNOLOGY OF HUBEIPROVINCE (CXPJJH124001-2488), the Dalian Municipal Science and Technology Bureau Life and Health Guidance Program(0122023103), and the Beijing Medical and Health Public Welfare Foundation(BU1-N24001).

Conflict of interest

The authors declare that the research was conducted in the absence of any commercial or financial relationships that could be construed as a potential conflict of interest.

Generative AI statement

The author(s) declared that Generative AI was not used in the creation of this manuscript.

Any alternative text (alt text) provided alongside figures in this article has been generated by Frontiers with the support of artificial intelligence and reasonable efforts have been made to ensure accuracy, including review by the authors wherever possible. If you identify any issues, please contact us.

Publisher's note

References

1. Moris D, Palta M, Kim C, Allen PJ, Morse MA, Lidsky ME. Advances in the treatment of intrahepatic cholangiocarcinoma: An overview of the current and future therapeutic landscape for clinicians. *CA Cancer J Clin.* (2023) 73:198–222. doi: 10.3322/caac.21759

2. Burris HA 3rd, Okusaka T, Vogel A, Lee MA, Takahashi H, Breder V, et al. Durvalumab plus gemcitabine and cisplatin in advanced biliary tract cancer (TOPAZ-1): patient-reported outcomes from a randomised,double-blind,placebo-controlled, phase 3 trial. *Lancet Oncol.* (2024) 25:626–35. doi: 10.1016/S1470-2045(24)00082-2

3. Tang N, Li J, Gu A, Li M-Y, Liu Y. Single-cell multi-omics in biliary tract cancers: decoding heterogeneity, microenvironment, and treatment strategies. *Mol Biomedicine.* (2025) 6:82. doi: 10.1186/s43556-025-00330-2

4. Yadav D, Malviya R. Novel nanomaterials as photo-activated cancer diagnostics and therapy. *Med Adv.* (2023) 1:190–209. doi: 10.1002/med4.36

5. Sharma R, Malviya R. Modifying the electrical, optical, and magnetic properties of cancer cells: a comprehensive approach for cancer management. *Med Adv.* (2024) 2:3–19. doi: 10.1002/med4.51

6. Han B, Li K, Wang Q, Zhang L, Shi J, Wang Z, et al. Effect of anlotinib as a third-line or further treatment on overall survival of patients with advanced non-small cell lung cancer: the ALTER 0303 phase 3 randomized clinical trial. *JAMA Oncol.* (2018) 4:1569–75. doi: 10.1001/jamaoncol.2018.3039

7. Liu S, Qin T, Liu Z, Wang J, Jia Y, Feng Y, et al. anlotinib alters tumor immune microenvironment by downregulating PD-L1 expression on vascular endothelial cells. *Cell Death Dis.* (2020) 11:309. doi: 10.1038/s41419-020-2511-3

8. Yuan M, Fang J, Zhu Z, Mao W, Wang H, Liu W. The clinical activity and safety of anlotinib combined with anti-PD-1 antibodies in patients with advanced solid

tumors. *J Clin Oncol*. (2020). ASCO meeting abstract (189701) 38:e15081. doi: 10.1200/JCO.2020.38.15_suppl.e15081

9. Naranjo CA, Busto U, Sellers EM, Sandor P, Ruiz I, Roberts EA, et al. A method for estimating the probability of adverse drug reactions. *Clin Pharmacol Ther*. (1981) 30:239–45. doi: 10.1038/clpt.1981.154

10. Yin H, Diao Y, Zheng Z, Dong Q, Zhang J. Tislelizumab-induced cytokine release syndrome: the first case report and review of the literature. *Immunotherapy*. (2024) 16:1113–22. doi: 10.1080/1750743X.2024.2422814

11. Wei H, Zuo A, Chen J, Zheng C, Li T, Yu H, et al. Adrenal crisis mainly manifested as recurrent syncope secondary to tislelizumab: a case report and literature review. *Front Immunol*. (2024) 14:1295310. doi: 10.3389/fimmu.2023.1295310

12. Zhou Q, Qin Z, Yan P, Wang Q, Qu J, Chen Y. Immune-related adverse events with severe pain and ureteral expansion as the main manifestations: a case report of tislelizumab-induced ureteritis/cystitis and review of the literature. *Front Immunol*. (2023) 14:1226993. doi: 10.3389/fimmu.2023.1226993

13. Yang B, Gou W, Lan N, Shao Q, Hu W, Xue C, et al. Tislelizumab induced dual organs dysfunction in a patient with advanced esophageal squamous cell carcinoma: a case report. *Front Oncol*. (2024) 14:1347896. doi: 10.3389/fonc.2024.1347896

14. Deng Y, Huang M, Deng R, Wang J. Immune checkpoint inhibitor-related adrenal hypofunction and Psoriasisby induced by tislelizumab: A case report and review of literature. *Med (Baltimore)*. (2024) 103:e37562. doi: 10.1097/MD.0000000000037562

15. Huo L, Wang C, Ding H, Shi X, Shan B, Zhou R, et al. Severe thyrotoxicosis induced by tislelizumab: a case report and literature review. *Front Oncol*. (2023) 13:1190491. doi: 10.3389/fonc.2023.1190491

16. Zhang N, Qu X, Zhang X, Sun X, Kang L. Immunotherapy-induced hypophysitis following treatment with tislelizumab in an elderly patient with bladder cancer and prostate cancer: A case report. *Cureus*. (2023) 15:e51015. doi: 10.7759/cureus.51015

17. Yu H, Ruan Q, Jiang L. Chronic nonspecific cheilitis associated with tislelizumab treatment in a patient with a history of tongue squamous cell carcinoma: a case report. *BMC Oral Health*. (2024) 4:906. doi: 10.1186/s12903-024-04683-y

18. Gu HY, Zhao JW, Wang YS, Meng ZN, Zhu XM, Wang FW, et al. Case Report: Life-threatening pancytopenia with tislelizumab followed by cerebral infarction in a patient with lung adenocarcinoma. *Front Immunol*. (2023) 14:1148425. doi: 10.3389/fimmu.2023.1148425

19. Kerkemeyer KLS, Lai FYX, Mar A. Lichen planus pemphigoides during therapy with tislelizumab and sitravatinib in a patient with metastatic lung cancer. *Australas J Dermatol*. (2020) 61:180–2. doi: 10.1111/ajd.13214

20. Zhou Y, Xue H, Lu C, Zhang Y, Wu Q, Zhang J, et al. Treatment of tislelizumab-induced toxic epidermal necrolysis and agranulocytosis: A case report and literature review. *Curr Drug Saf*. (2024) 20:361-65. doi: 10.2174/0115748863297885240604111018

21. Wang M, Sun Q, Dong W. Exfoliative esophagitis secondary to tislelizumab: a case report. *Front Oncol*. (2024) 14:1498253. doi: 10.3389/fonc.2024.1498253

22. Pu CW, Ma YF, Peng JJ, Wang ZZ. Case report: Fatal hemoptysis after effective treatment with tislelizumab and anlotinib in pulmonary sarcomatoid carcinoma. *Front Oncol*. (2024) 14:1445358. doi: 10.3389/fonc.2024.1445358

23. Liu S, Ma G, Wang H, Yu G, Chen J, Song W. Severe cardiotoxicity in 2 patients with thymoma receiving immune checkpoint inhibitor therapy: A case report. *Med (Baltimore)*. (2022) 101:e31873. doi: 10.1097/MD.0000000000031873

24. Deng C, Yang M, Jiang H, Wang R, Yang Z, Sun H, et al. Immune-related multiple-organs injuries following ICI treatment with tislelizumab in an advanced non-small cell lung cancer patient: A case report. *Front Oncol*. (2021) 11:664809. doi: 10.3389/fonc.2021.664809

25. Chen M, Zhang L, Zhong W, Zheng K, Ye W, Wang M. Case report: THSD7A-positive membranous nephropathy caused by tislelizumab in a lung cancer patient. *Front Immunol*. (2021) 12:619147. doi: 10.3389/fimmu.2021.619147

26. Wang S, Peng D, Zhu H, Min W, Xue M, Wu R, et al. Acetylcholine receptor binding antibody-associated myasthenia gravis,myocarditis,and rhabdomyolysis induced by tislelizumab in a patient with colon cancer: A case report and literature review. *Front Oncol*. (2022) 12:1053370. doi: 10.3389/fonc.2022.1053370

27. Ning H, Chiu SH, Xu X, Ma Y, Chen JL, Yang G. The immunosuppressive roles of PD-L1 during influenza A virus infection. *Int J Mol Sci*. (2023) 24:8586. doi: 10.3390/ijms24108586

28. Valero-Pacheco N, Arriaga-Pizano L, Ferat-Osorio E, Mora-Velandia LM, Pastelin-Palacios R, Villasís-Keever MÁ,Alpuche-Aranda C, et al. PD-L1 expression induced by the 2009 pandemic influenza A(H1N1) virus impairs the human T cell response. *Clin Dev Immunol*. (2013) 2013:989673. doi: 10.1155/2013/989673

29. David P, Drabczyk-Pluta M, Pastille E, Knuschke T, Werner T, Honke N, et al. Combination immunotherapy with anti-PD-L1 antibody and depletion of regulatory T cells during acute viral infections results in improved virus control but lethal immunopathology. *PloS Pathog*. (2020) 16:e1008340. doi: 10.1371/journal.ppat.1008340

30. Naidoo J, Page DB, Li BT, Connell LC, Schindler K, Lacouture ME, et al. Toxicities of the anti-PD-1 and anti-PD-L1 immune checkpoint antibodies. *Ann Oncol*. (2015) 26:2375–91. doi: 10.1093/annonc/mdv383

Frontiers in Immunology

Explores novel approaches and diagnoses to treat immune disorders.

The official journal of the International Union of Immunological Societies (IUIS) and the most cited in its field, leading the way for research across basic, translational and clinical immunology.

Discover the latest Research Topics

See more →

Frontiers

Avenue du Tribunal-Fédéral 34
1005 Lausanne, Switzerland
frontiersin.org

Contact us

+41 (0)21 510 17 00
frontiersin.org/about/contact